UNIVERSITÀ
DEGLI STUDI
DI PADOVA

Sede Amministrativa: Università degli Studi di Padova

Dipartimento di Medicina Molecolare

CORSO DI DOTTORATO DI RICERCA IN MEDICINA MOLECOLARE
CURRICOLO: BIOMEDICINA
CICLO XXX

Protein kinase A in human glioblastoma non-stem and stem like cells: from transient interference to stable lentiviral-mediated downregulation of the regulatory subunit R2A

Coordinatore: Ch.mo Prof. Stefano Piccolo
Supervisore: Ch.ma Prof.ssa Carla Mucignat

Dottorando : Maira Zorzan

Index

Riassunto

I gliomi sono i più frequenti tumori cerebrali a livello mondiale. Il glioblastoma è classificato dall'Organizzazione Mondiale della Sanità come glioma ad alto grado con prevalente differenziazione astrocitica ed è caratterizzato da elevata eterogeneità intratumorale, proliferazione microvascolare e grande capacità infiltrativa. Il glioblastoma è la forma più comune di glioma ed è attualmente associato ad una sopravvivenza media di soli 14 mesi dalla diagnosi. La terapia standard per questo tipo di tumore prevede la resezione chirurgica della massa tumorale, radioterapia e chemoterapia con l'agente alchilante temozolomide. Nonostante questo approccio aggressivo, il gliobastoma è ad oggi ancora considerato un tumore incurabile e meno del 5% dei pazienti sopravvive a cinque anni dalla diagnosi. Nei pazienti affetti da glioblastoma, le ricadute si verificano frequentemente e sono probabilmente dovute alla presenza di una sottopopolazione di cellule staminali tumorali, che rappresentano uno dei maggiori ostacoli alla terapia. È infatti noto che queste cellule sono resistenti a radioterapia e chemioterapia grazie alla loro plasticità, un'elevata capacità di riparare i danni al DNA, un'elevata espressione di proteine checkpoint che controllano la progressione del ciclo cellulare in risposta a danni genetici e di proteine che sono in grado di espellere all'esterno della cellula diverse molecole tra cui i farmaci. Proprio per queste caratteristiche di resistenza alle terapie convenzionali, le colture cellulari di cellule staminali tumorali sono oggi un modello in vitro riconosciuto per lo studio del glioblastoma e per l'identificazione di nuovi target terapeutici. Le cellule staminali tumorali vengono mantenute in particolari condizioni di coltura, che ne permettono la crescita selettiva sottoforma di aggregati sferici (sfere) in sospensione. Grazie alla ricerca scientifica, la conoscenza dell'eziopatogenesi dei gliomi è recentemente cresciuta e l'introduzione di marcatori molecolari, oltre ai criteri istologici per la classificazione dei gliomi, rappresenta un avanzamento verso una terapia molecolare personalizzata. Negli ultimi vent'anni, sono state sviluppate molte strategie terapeutiche innovative e sono stati identificati potenziali nuovi target tra i componenti delle vie di segnalazione intracellulari specificamente alterate nel glioblastoma. La maggior parte di questi nuovi approcci terapeutici è attualmente in fase di valutazione preclinica e clinica, i risultati sembrano promettenti, ma la complessità e l'eterogeneità dei gliomi sottolineano la necessità di cercare continuamente nuovi bersagli terapeutici. Proprio in questa direzione, la proteina chinasi A (PKA) è recentemente emersa per il suo coinvolgimento in molte caratteristiche distintive delle cellule tumorali e per le sue peculiarità nelle cellule di glioblastoma rispetto al parenchima cerebrale. PKA è un enzima che svolge molte funzioni all'interno della cellula e la cui attivazione dipende dal secondo messaggero cAMP. Nella sua forma inattiva PKA è un tetramero costituito da due subunità catalitiche e un

dimero di subunità regolatorie. Fino ad oggi sono state identificate tre isoforme catalitiche e quattro isoforme regolatorie. Ciascuna subunità, sia catalitica che regolatoria, presenta un pattern di espressione specifico tra i diversi tipi cellulari e i diversi tessuti dell'organismo. La via mediata da cAMP/PKA regola una vasta gamma di processi cellulari, tra i quali il metabolismo, la progressione del ciclo cellulare, la proliferazione cellulare, la differenziazione cellulare, la trascrizione genica e l'apoptosi. La distribuzione isoforma-specifica di PKA e la sua regolazione spazio-temporale permettono un fine controllo dei segnali mediati dalla via di cAMP/PKA, che risulta essere di primaria importanza per il mantenimento di uno stato cellulare fisiologico. Infatti, molte alterazioni di PKA, come una sbilanciata espressione delle sue isoforme, una disregolazione della sua attività chinasica e la delocalizzazione dell'enzima stesso, sono state associate a molte malattie umane, compresi diversi tumori. In particolare, nel glioblastoma umano PKA è dieci volte più abbondante rispetto al cervello sano. Inoltre, nelle cellule di glioblastoma di roditore e umane la subunità regolatoria R2A di PKA presenta una peculiare localizzazione intracellulare sottoforma di cluster perinucleari co-localizzati con l'apparato di Golgi. Questa particolare distribuzione della subunità R2A non è stata riscontrata nel parenchima cerebrale, dove invece sono stati individuati aggregati delle subunità R1A e R2B. Il significato funzionale della proteina chinasi A associata all'apparato di Golgi non è ancora chiara, ma questa osservazione indica un potenziale ruolo della subunità R2A come marcatore tumorale o come nuovo target terapeutico.

Sulla base di quanto esposto finora, questo progetto di dottorato ha lo scopo di approfondire il ruolo della proteina chinasi A, ed in particolare della subunità R2A, nel glioblastoma umano. Per questo motivo, lo studio della localizzazione intracellulare di R2A è stato esteso, per la prima volta, alle cellule staminali tumorali di glioblastoma. Esperimenti di immunofluorescenza hanno dimostrato che anche in queste cellule la subunità R2A presenta la stessa distribuzione intracellulare che era stata precedentemente descritta in linee cellulari e colture primarie non staminali di glioblastoma umano. Questa osservazione rafforza ulteriormente la peculiarità di R2A rispetto al parenchima sano e sottolinea la necessità di caratterizzare lo specifico ruolo funzionale di questa subunità. Al fine di sviluppare nuovi strumenti molecolari per lo studio di PKA, è stato generato un set di plasmidi ricombinanti per l'espressione delle subunità di PKA in fusione alla proteina verde fluorescente (EGFP). Questi plasmidi sono stati validati in cellule di glioblastoma umano e, nonostante la bassa efficienza di trasfezione, si sono rivelati degli utili strumenti per studi funzionali di PKA in vari modelli cellulari. Nella prima parte del progetto di ricerca sono inoltre stati analizzati in cellule di glioblastoma umano gli effetti di una interferenza transiente con la via di PKA. Alterazioni dell'attività, dell'espressione e della distribuzione intracellulare della proteina chinasi A sono state indotte mediante diversi approcci, come il trattamento con agenti chimici, la

trasfezione con small interfering RNA (siRNA), l'overespressione di forme wild type e mutate delle subunità di PKA e l'espressione di peptidi inibitori che causano la delocalizzazione di PKA. Coerentemente con quanto riportato in letteratura, questi esperimenti hanno dimostrato che l'interferenza transiente con PKA può avere effetti diversi sulle cellule di glioblastoma umano, in particolare sulla loro vitalità e capacità migratoria. Come già riportato in altre linee cellulari umane, si è osservato che la ridotta espressione di PKA R2A indotta dalla trasfezione con siRNA induce la frammentazione dell'apparato di Golgi e la dispersione di R2A nel citoplasma delle cellule di glioblastoma, un effetto che deve essere ulteriormente approfondito. Per studiare più a fondo la relazione tra PKA R2A e apparato di Golgi, sono stati anche analizzati gli effetti indotti dall'interferenza con l'apparato di Golgi sulle cellule di glioblastoma e in particolare sulla localizzazione intracellulare di R2A. Il trattamento con brefeldina A, che distrugge la funzione dell'apparato di Golgi, causa un aumento della mortalità cellulare, riduce la motilità e induce la ridistribuzione della subunità R2A nel citosol delle cellule di glioblastoma. Questi risultati sono a sostegno dell'importante relazione tra PKA R2A e l'apparato di Golgi, ma ulteriori studi sono necessari per comprenderne meglio il significato funzionale.

La seconda parte del progetto di ricerca riguarda lo sviluppo di un sistema basato su vettori lentivirali di terza generazione per la riduzione dell'espressione della subunità R2A di PKA mediante short hairpin RNA (shRNA). Sono quindi stati generati dei vettori lentivirali per l'espressione di shRNA aventi come bersaglio diversi esoni del gene di R2A, per la co-espressione degli stessi shRNA e del gene reporter EGFP e per l'espressione di uno shRNA scrambled per la valutazione di eventuali effetti off-target. Tutti i vettori sono stati validati sia in cellule non staminali che in cellule staminali di glioblastoma umano, dimostrandosi in grado di indurre un silenziamento efficiente e stabile dell'espressione di R2A in entrambi i tipi di colture cellulari. Esperimenti preliminari hanno inoltre valutato gli effetti del silenziamento della subunità R2A sulla proliferazione e sulla morte cellulare. Per quanto riguarda le cellule non staminali di glioblastoma umano, i dati ottenuti sono controversi a causa di una possibile citotossicità della sequenza scrambled, che non era stata rilevata dalla precedente validazione bioinformatica e che è tuttora in fase di studio. Al contrario, nelle cellule staminali di glioblastoma la stessa sequenza scrambled non risulta essere tossica in quanto non induce una riduzione della vitalità cellulare rispetto alle cellule non trasdotte. Ancora più interessante è l'osservazione che le cellule staminali di glioblastoma con una ridotta espressione di R2A dovuta alla trasduzione con il vettore recante la sequenza shRNA contro il gene di R2A, presentano una distribuzione di cellule vive/morte significativamente diversa, nello specifico un aumento della morte cellulare, rispetto alle cellule trasdotte con il vettore scrambled. Questi risultati suggeriscono quindi una potenziale relazione tra il silenziamento della

subunità R2A e la sopravvivenza delle cellule staminali di glioblastoma, un aspetto che merita di essere ulteriormente approfondito.

In conclusione, questo progetto di dottorato ha indagato le molteplici funzioni di PKA nel glioblastoma umano, attraverso approcci tra loro complementari e diversi modelli in vitro. È stato dimostrato che l'interferenza transiente con la via di PKA può avere effetti anti-tumorali sulle cellule di glioblastoma. Dati preliminari indicano anche una possibile relazione tra la riduzione dell'espressione della subunità R2A e la crescita delle cellule staminali di glioblastoma. Inoltre, è stato messo a punto un sistema lentivirale per il silenziamento efficiente e stabile di PKA R2A. Questo strumento è stato validato con successo nelle cellule di glioblastoma umano e può essere considerato uno strumento promettente per futuri studi della proteina chinasi A in diversi modelli cellulari.

Summary

Gliomas are the most frequent brain tumors worldwide. Glioblastoma is classified by the World Health Organization as a high-grade glioma with predominantly astrocytic differentiation and is characterized by large intratumoral heterogeneity, microvascular proliferation and high infiltrative capacity. This brain tumor represents the most common form of glioma and is currently associated with a median survival of only 14 months from diagnosis. The standard therapy for glioblastoma patients include surgical resection of the tumor mass, radiotherapy and chemotherapy with the alkylating agent temozolomide. Despite this aggressive treatment, glioblastoma is still considered an incurable cancer and less than 5% of patients survive after five years. Tumor relapse is frequently observed and is probably related to the presence of a subpopulation of cancer stem cells, which represent one of the major obstacle to glioblastoma therapy. Indeed, cancer stem cells are known to be resistant to radiotherapy and chemotherapy thanks to their recently described plasticity, a strong DNA repair capacity, overexpression of DNA checkpoints and drug efflux proteins. Based on these characteristics, cell cultures of cancer stem cells as gliomaspheres are a recognized in vitro model for the study of glioblastoma and for identification of new therapeutic targets. Recent advancement in glioma etiopathogenesis allowed introduction of molecular markers in addition to histological criteria for glioma classification, pointing to a future personalized molecular therapy. In the last decades, many innovative therapeutic strategies and potential targets among molecules of signaling pathways specifically altered in glioblastoma have been investigated. Most of these therapeutic options are currently under preclinical and clinical evaluation showing promising results, but the high complexity and heterogeneity of glioma tumors underlie the continuous need for novel therapeutic targets. In this direction, protein kinase A (PKA) has recently emerged due to its involvement in many distinctive features of cancer cells and to its peculiarities in glioblastoma cells compared to brain parenchyma. PKA is a multifunctional enzyme, whose activation depends on binding of cAMP molecules. In its inactive form PKA is a tetramer consisting of two catalytic subunits and a regulatory subunit dimer. Up to now three catalytic isoforms and four regulatory isoforms have been identified and all of them present a specific expression pattern among different cell types and tissues. The cAMP/PKA pathway regulates a wide range of cellular processes, such as metabolism, gene transcription, cell cycle progression, cell proliferation, cell differentiation and apoptosis. The isoform-specific, spatio-temporal regulated PKA distribution allows a fine control of PKA signaling and is of primary importance for maintenance of physiological state. Indeed, several alterations of protein kinase A, including unbalanced expression of its subunits, dysregulation of the kinase activity and PKA delocalization, have been associated with many human diseases, including

cancer. In particular, in human glioblastoma PKA is ten-times more abundant than normal brain. What is more, in rodent and human glioblastoma cells the regulatory subunit R2A presents a peculiar intracellular localization. In these cells perinuclear clusters of R2A co-localized with the Golgi apparatus have been described, whereas they have not been reported in the brain parenchyma, where R1A and R2B aggregates are instead detected. The functional significance of Golgi-associated PKA is still unknown, but this observation points to a potential role of R2A subunit as a tumor marker or a novel therapeutic target.

Based on these considerations, the present PhD project aimed at providing additional insights into the role of protein kinase A, particularly R2A subunit, in human glioblastoma. For this purpose, the study of PKA R2A intracellular localization was extended to human glioblastoma stem like cells, as up to now no data are reported as regard to R2A localization in cancer stem cells. Immunofluorescence experiments were performed on human gliomaspheres, confirming in glioblastoma stem like cells the same peculiar R2A intracellular distribution that had been previously described in non-stem glioblastoma cell lines and primary cell cultures. This observation further supports the peculiarity of R2A subunit in human glioblastoma compared to brain parenchyma, as well as the need to further characterize the specific functional role of this peculiarity. In order to develop new molecular tools for study of PKA, a set of recombinant plasmids for expression of PKA subunits fused to EGFP fluorescent protein were generated and preliminarily validated in human glioblastoma cells. Despite a low transfection efficiency, these plasmids proved to be useful tools for functional studies of PKA in different cellular models. Moreover, in the first part of the research project, effects of transient interference with PKA pathway were analyzed in human glioblastoma cells through multiple approaches. Alterations of PKA activity, expression and intracellular distribution were induced by drug treatments, small interfering RNA (siRNA) transfection, overexpression of wild type and mutant PKA isoforms and expression of peptide inhibitors for PKA dislocation. Consistently with other scientific studies, these experiments demonstrated that transient interference with PKA differentially affects human glioblastoma cells, particularly cell viability and cell motility. In addition, as previously reported in other human cell lines, siRNA-mediated downregulation of PKA R2A expression proved to induce Golgi fragmentation and dispersion of R2A in the cell cytoplasm of glioblastoma cells, an effect that deserves further investigation. As a complementary approach, to investigate the relationship between PKA R2A and Golgi apparatus, effects of disrupted Golgi function on human glioblastoma cells and R2A intracellular localization were also analyzed. Increased cell death, reduced cell motility and redistribution of R2A subunit in the cell cytosol were observed in glioblastoma cells following treatment with the Golgi disruptor brefeldin A. These results support the relevant

relationship between R2A subunit and Golgi complex in glioblastoma cells, but future studies are needed to better understand its functional meaning.

The second part of the PhD project was focused on the development of a third-generation lentiviral system for downregulation of PKA R2A expression through short hairpin RNA (shRNA) delivery. Lentiviral vectors for expression of shRNA targeting different exons of R2A gene, their co-expression with EGFP reporter protein, as well as expression of a scrambled shRNA were thus generated and validated in non-stem and stem like glioblastoma cells. In both cell cultures PKA R2A gene silencing lentiviral vectors proved able to induce an efficient and stable downregulation of R2A expression. Preliminary experiments also evaluated the effects of PKA R2A knockdown on glioblastoma cell proliferation and cell death. As regard to non-stem glioblastoma cells, data from cell growth assays are still controversial due to a possible cytotoxicity of the scrambled shRNA sequence, not detected by previous bioinformatic validation of the shRNA and that is currently under investigation. Conversely, in glioblastoma stem like cells the scrambled vector did not affect cell viability compared to untransduced cells. Moreover, a significantly different distribution between viable and dead cells, particularly an increase in dead cells, was reported for glioblastoma stem like cells with downregulated PKA R2A expression compared to scrambled transduced cells. These results thus point to a potential relationship between PKA R2A silencing and cell survival of glioblastoma stem like cells, an interesting aspect that should be further investigated.

In conclusion, the present PhD project investigated the multiple functions of PKA in human glioblastoma by means of many complementary approaches and different in vitro models. PKA transient interference exhibited some anti-tumor effects and preliminary data indicated a potential relationship between PKA R2A downregulation and glioblastoma stem like cell growth. What is more, a lentiviral system for efficient R2A silencing was developed and successfully validated, proving to be a promising tool for future study of PKA in several cellular models.

1. Introduction

1.1 Gliomas

Gliomas are tumors with glial-like histological features and represent the most common central nervous system (CNS) cancers, with around 20,000 new cases every year in the United States (Mesfin and Al-Dhahir 2017) and six cases per 100,000 individuals worldwide (Weller et al. 2017). Four grades of increasing malignancy (from grade I to IV) are distinguished depending on the proliferation activity, that is related to the mitotic index and the presence or absence of necrosis (Mesfin and Al-Dhahir 2017). In the 2016 World Health Organization (WHO) classification of CNS tumors, gliomas are classified according to both histological criteria and molecular parameters. The previous histological classification was based on the similarity of tumor cells with CNS cells (astrocytes, oligodendrocytes, ependymal cells) and their level of differentiation, evaluated through microscopic observation of hematoxylin and eosin-stained sections and immunohistochemistry for lineage-specific proteins. In 2016 WHO classification, histology is still used to define the major category of brain tumors, but genetic and epigenetic information are applied to define different glioma subsets (Komori 2017). This combination of phenotypic and genotypic markers is expected to facilitate prognostic, clinical and experimental studies and thus to improve future treatment of glioma patients (Louis et al. 2016). Introduction of the molecular classification of brain tumors points to a deeper knowledge of glioma etiopathogenesis and represents an important step forward for the personalized molecular therapy (Zorzan et al. 2015).

Glioblastoma (GBM) is the most malignant (grade IV) and also most common form of glioma, with an incidence of around 12,000 cases every year in the United States (Mesfin and Al-Dhahir 2017). It is defined by 2016 WHO classification as a high-grade glioma with predominantly astrocytic differentiation, characterized by nuclear atypia, cellular pleomorphism, microvascular proliferation and/or necrosis (Louis et al. 2016). Depending on genetic testing of IDH1/IDH2 mutations, GBMs have been divided into 3 categories: GBM, IDH-wildtype, which corresponds to primary or *de novo* GBM and accounts for approximately 90% of cases; GBM, IDH-mutant, which corresponds to secondary GBM deriving from prior lower grade diffuse glioma and accounts for approximately 10% of cases; GBM, not otherwise specified (NOS), for tumors with IDH testing not possible or inconclusive (Louis et al. 2016; Komori 2017). IDH-wildtype GBM includes giant cell GBM, gliosarcoma and the new variant epithelioid GBM (Louis et al. 2016). Main characteristics of IDH-wildtype and IDH-mutant GBMs are reported in Table 1.1. Common GBM features are a remarkable intratumoral heterogeneity, the presence of areas of vascular proliferation and/or

necrosis and a high infiltrative capacity (Bageritz et al. 2014; Brat and Van Meir 2004; Ng et al. 2014).

	IDH-wildtype GBM	**IDH-mutant GBM**
Synonym	Primary GBM, IDH-wildtype	Secondary GBM, IDH-mutant
Precursor lesion	Not identifiable; develops de novo	Diffuse astrocytoma Anaplastic astrocytoma
Proportion of GBMs	~90%	~10%
Median age at diagnosis	~62 years	~44 years
Male-to-female ratio	1.42:1	1.05:1
Mean length of clinical history	4 months	15 months
Median overall survival Surgery+radiotherapy Surgery+radiotherapy+chemotherapy	 9.9 months 15 months	 24 months 31 months
Location	Supratentorial	Preferentially frontal
Necrosis	Extensive	Limited
TERT promoter mutations	72%	26%
TP53 mutations	27%	81%
ATRX mutations	Rare	71%
EGFR amplification	35%	Rare
PTEN mutations	24%	Rare

Table 1.1 - Main characteristics of IDH-wildtype and IDH-mutant GBMs (modified from Louis et al. 2016).

Characterization of the molecular signature of individual tumors is important for diagnosis, prognosis and treatment of glioma patients. In 2008, the Cancer Genome Atlas (TGCA) consortium analyzed the expression profile and the genetic data of 500 primary untreated GBM specimens collected worldwide and identified three common alterations of key signaling pathways: activation of the receptor tyrosine kinase pathway, inactivation of the p53 and retinoblastoma (Rb) tumor suppressor pathway (TCGA Research Network, 2008; TCGA Research Network, 2013). This large-scale analysis greatly increased our knowledge on molecular profile of GBM but also defined new potential targets for development of future therapies. In 2016 WHO classification four molecular biomarkers gained a central role for glioma diagnosis and treatment choice: IDH mutation, 1p/19q

co-deletion and histone H3-K27M mutation are new criteria for classification of different glioma entities, whereas methylation status of O6-methylguanine DNA methyltransferase (MGMT) is evaluated as relevant indicator for chemotherapy use (Weller et al. 2017). Moreover, IDH mutations, 1p/19q co-deletion and MGMT promoter methylation are recognized as positive prognostic factors for improved survival of glioma patients (Weller et al. 2017; Delgado-Lopez and Corrales-Garcia 2016).

Cellular origin of gliomas has been largely discussed in the past years. Gliomas have been traditionally thought to arise from dedifferentiation of a parenchymal differentiated glial cell following genetic alterations (Jellinger 1978). More recently, neural stem cells (NSCs) and glial progenitor cells have been increasingly evaluated as putative glioma cells of origin (Ligonet al. 2007; Noble and Dietrich 2002; Pardal et al. 2003; Hadjipanayis and Van Meir 2009A; Hadjipanayis and Van Meir 2009B). NSCs have been isolated from multiple regions of the adult brain, including the subventricular zone, the lining of the lateral ventricles, the dentate gyrus, the hippocampus and the subcortical white matter (Doetsch et al. 1997; Fukuda et al. 2003; Gage 2000; Kim and Morshead 2003). They can proliferate and migrate extensively and are characterized by self-renewal, being able to generate identical daughter cells as well as cells of multiple lineages. According to the stochastic or clonal evolution model of tumorigenesis, during early stages of tumor formation a single or very few cells gain unlimited proliferative capacity thanks to genetic pro-survival mutations. As a result of the clonal expansion of these transformed cells, various subpopulations of cancer cells coexist in the heterogeneous tumor mass and any of them can participate in tumor progression and develop resistance to therapy (Chen et al. 2010; Li et al. 2007A; Shackleton et al.2009). This model has been countered by the hierarchical model, also known as cancer stem cell hypothesis (Reya et al. 2001; Rich 2008; Sanai et al. 2005). According to this theory, only a small subpopulation of tumor cells, termed cancer stem cells (CSCs), are able to self-renew and extensively proliferate. These cells give rise to multi-differentiated progeny, that is responsible for the heterogeneity of the tumor, whereas most cancer cells are differentiated tumor cells, with no ability to proliferate and self-renew and that does not contribute to tumor growth and recurrence (Reya et al. 2001). Thus, CSCs and NSCs share important functional features, such as sustained proliferation, self-renewal and multilineage potential (Schonberg et al. 2014). Furthermore, they are maintained in vitro in the same growth conditions. Isolated NSCs are grown in serum-free media supplemented with basic Fibroblast Growth Factor (bFGF) and Epidermal Growth Factor (EGF). These culture conditions allow the proliferation of NSCs as floating spheres (neurospheres or spheres) of undifferentiated, multipotent, self-renewing cells (Reynolds et al. 1992; Reynolds and Weiss 1992; Reynolds and Weiss 1996). The same sphere culture system

allows isolation of glioma CSCs (Van Meir et al. 2010), that have a much higher tumor initiation capacity compared to non-stem cancer cells transplanted into the brain of immunodeficient mice (Rahman et al. 2011; Modrek et al. 2014). Gliomaspheres represent nowadays a recognized model for the study of many aspects of GBM biology and a potential opportunity to identify new malignancy determinants and new therapeutic targets (Laks et al. 2016; Balvers et al. 2017).

1.2 Current standard GBM therapies and their failure

GBM is the most lethal brain tumor, associated with an average 27% survival after two years (Gilbert et al. 2013) and a 5-year survival of <5% (www.braintumourresearch.org). Only very minor improvements were provided by the most recent therapeutic advances (Seymour et al. 2015) and despite current aggressive treatments, overall median survival for GBM patients is still as modest as 14 months (Stupp et al. 2009). The standard of care for newly diagnosed GBM in adults consists of maximal surgical tumor resection, followed by radiotherapy and concomitant temozolomide (TMZ) chemotherapy over 6 weeks and up to 6 months of adjuvant TMZ (Stupp et al. 2010; Lawrence et al. 2012; Bauchet et al. 2010).

The most frequent symptoms reported by glioma patients are due to mass effects, resulting from tumor growth in the brain: headaches, nausea, vomiting and seizures. Other presenting symptoms might include weakness, difficult ambulation, tingling sensations and altered mental status (Mesfin and Al-Dhahir 2017). The main imaging diagnostic tools for brain cancers are Computed Tomography (CT) and Magnetic Resonance Imaging (MRI) of the head, whereas chest X-Ray and CT body scan are used for metastatic monitoring (Mesfin and Al-Dhahir 2017).

Surgical intervention is aimed at the so-called maximum safe resection, meaning gross total resection of the tumor without new neurological deficits (Delgado-Lopez and Corrales-Garcia 2016). Surgery is critical to reduce tumor mass effects, but also for histological diagnosis and molecular analysis of the tumor, that guide the choice for proper therapeutic approach (Van Meir et al. 2010; Weller et al. 2017). Achievement of total tumor resection depends mainly on tumor location. However, due to the highly infiltrative nature of GBM, recurrence for this type of tumor is reported in the vast majority of cases (Wallner et al. 1989). Extent of tumor resection is an important prognostic factor for patients with glioma, even if it remains unclear whether resectable tumors are associated with a less aggressive pattern (Weller et al. 2017). Radiotherapy also increases survival of glioma patients. Different radiation protocols are applied depending on tumor diagnosis and prognostic factors. Modern focused radiotherapy techniques are expected to further

reduce irradiation of surrounding healthy tissue (Stieberand and Mehta 2007; Weller et al. 2017). TMZ (Figure 1.1) is the most widely used chemotherapeutic agent for treatment of malignant gliomas. It is an oral alkylating agent that methylates the O6 position of guanine in DNA: these methyl adducts lead to the introduction of errors during DNA transcription and thus to the death of cancer cells (Liu et al. 2006).

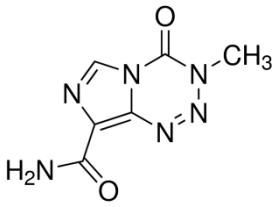

Figure 1.1 - Representation of the temozolomide chemical structure.

TMZ has good penetration of the blood-brain barrier and favorable safety profile, with hematologic toxicity reported in only 10-20% of patients (Weller et al. 2017; Delgado-Lopez and Corrales-Garcia 2016). Compared to radiation alone, concomitant and adjuvant TMZ has increased median survival of GBM patients from 12.1 to 14.6 months (Stupp et al. 2009). The stronger predictor of benefit for TMZ therapy is the methylation status of the promoter of the MGMT gene, coding a repair enzyme that removes methyl residues from DNA. Indeed, a better response to alkylating agents has been associated with methylation of the MGMT promoter, leading to inactivation of the gene (Hegi et al. 2005; Beier et al. 2011; Sorensen et al. 2015). Bevacizumab is a monoclonal antibody against human endothelial growth factor (VEGF), it is the only anti-angiogenic drug approved for recurrent GBM in the United States, Canada, Switzerland and several other countries outside the European Union (Weller et al. 2017). The use of bevacizumab for newly diagnosed GBM is still under evaluation as some randomised trials reported a longer progression-free survival but no effect on overall survival (Gilbert et al. 2014; Chinot et al. 2014; Poulsen et al. 2014). In most European countries nitrosoureas, such as lomustine and carmustine, are the second choice after TMZ for treatment of glioma, but they usually have a higher hematologic toxicity compared to TMZ and their efficacy is still to be evaluated in large comparative trials (Weller et al. 2017).

The extremely high mortality associated with GBM reveals the failure of all current therapies and prompts research to investigate novel targeted therapeutic approaches and new treatment options. In 2011, the Food and Drug Administration (FDA) approved tumor-treating fields (TTF) for treatment of recurrent GBM. This technique delivers alternating electric fields to the brain to induce mitotic arrest and apoptosis of tumor cells by interfering with mitotic spindle formation (Stupp et al. 2012; Stupp et al. 2015). In a phase III trial TTF was demonstrated to have equivalent efficacy to

chemotherapy but minor cytotoxic side effects, improving the quality of life of patients with recurrent GBM (Stupp et al. 2012). The use of TTF for newly diagnosed GBM has also been evaluated: a phase III trial reported a modest improvement of both progression-free and overall survival in patients treated with TTF in combination with standard maintenance TMZ compared to patients treated with standard maintenance TMZ alone (Stupp et al. 2016; Stupp et al. 2015). However, the mode of action, effects on quality of life and cost-effectiveness of TTF therapy are still under discussion (Wick et al. 2016; Bernard-Arnoux et al. 2016).

The cure of GBM is still today an open challenge in biomedical research. The high infiltrative nature of GBM limits the efficacy of surgical intervention (Delgado-Lopez and Corrales-Garcia 2016), while the presence of the blood-brain barrier limits the dose of systemic therapeutic agent that reaches cells infiltrating the normal brain parenchyma (Auffinger et al. 2015). Elucidation of therapy resistance mechanisms is crucial for the development of new therapeutic approaches aimed to reduce GBM recurrence and increase the survival of GBM patients. In the last years, different molecular mechanisms responsible for resistance of CSCs to radiotherapy and chemotherapy have been described. First of all, CSCs are characterized by a stronger DNA repair capacity compared to non-stem glioma cells (Annovazzi et al. 2017). Indeed, they present an increased MGMT expression compared to differentiated GBM cells (Liu et al 2006), as well as aberrant activity of mismatch repair (MMR) system (Ropolo et al. 2009) and base excision repair (BER) system (Bobola et al. 2001). Dysregulation of these DNA repair mechanisms not only allows replication of tumor cells with genetic changes that usually prevent cell cycle progression, but also creates a subpopulation of cells that could benefit from genetic damage induced by radiation and chemotherapeutic agents (Van Meir et al. 2010; Auffinger et al. 2015). Resistance to therapies that target proliferating tumor cells is further increased by the ability of CSCs to suspend the proliferative state and enter in a transitory state of quiescence (Eramo et al. 2006). DNA checkpoints, specifically Chk1 and Chk2 kinases, present an increased activity in CSCs isolated from GBM even in absence of treatment, and contribute to therapy resistance by inducing a cell cycle delay that gives sufficient time to repair DNA damage induced by radio- and chemotherapy (Bao et al. 2006; Frosina 2010). Compared to differentiated tumor cells, CSCs also present an increased expression of ATP-binding cassette (ABC) transporter channels, such as ABCG2, that are involved in the active efflux of chemotherapeutic drugs (Li et al. 2010; Jovčevska et al. 2013). Another important mechanism of chemoresistance recently described is the plasticity of CSCs, a new concept that raised questions on the hierarchical model and the cancer stem cell hypothesis. Many studies have reported that the conversion of differentiated tumor cells to CSCs might occur spontaneously or might be induced by TMZ therapy, radiation and niche factors such as hypoxia

and acidic stress (Auffinger et al. 2014; Seidel et al. 2010; Pistollato et al. 2010; Hjelmeland et al. 2011; Dahan et al. 2014). CSC plasticity is thus responsible for continuous replenishing of CSC population, that represents the most difficult target of glioma therapies.

In summary, CSCs are currently considered responsible for the high recurrence rate of GBM (Bageritz et al. 2014) and many research studies focused on the design of new therapies targeting the aggressive CSC subpopulation. Despite this, the most promising approach could be the combination of conventional radio- and chemotherapy with completely novel therapeutic strategies. In this sense, various targeted therapies, immunological therapies and gene therapy approaches are now being explored and are gaining more and more attention.

1.3 Novel therapeutic approaches

In the last two decades, the need to design new GBM therapies based on specific molecular targets emerged. Many novel therapeutic strategies have been proposed, including administration of small drugs or monoclonal antibodies, RNA-based strategies, immunotherapies and gene therapy approaches. The new targets have been identified among the components of signaling pathways specifically altered in brain cancers, such as IDH, PTEN, PI3K/Akt/mTOR, EGF, Notch, VEGF, PDGF, SHH and TGF-β (Zorzan et al. 2015). The literature of the last five years presents a series of studies pointing to this direction.

Molecular targeted therapies

About ten years ago, receptor tyrosine kinase, p53 and retinoblastoma were first identified as commonly altered signaling pathways in gliobastoma. Since then, several research studies pointed out a highly intricate and interconnected signaling network involving even other signaling molecules and partially revealed the role of their alteration in cancer cells. Many molecular targeted therapies were thus designed based on this recently increased knowledge and are currently under preclinical and clinical evaluation.

IDH. The most common mutated form of the isocitrate dehydrogenase 1 is IDH1-R132H (Olarand and Aldape 2014), a mutant protein that catalyzes the conversion of α-ketoglutarate to the oncometabolite 2-hydroxyglutarate (Sasaki et al. 2012). A selective IDH1-R132H inhibitor, called AGI-5198, has been developed by Rohle and colleagues (Rohle et al. 2013), who demonstrated a dose-independent reduction of tumor growth in human glioma xenograft models. More recently it was demonstrated that AGI-5198 protects IDH1-mutated cancer cells from radiation, probably

through altered oxidative stress responses. This suggests that coadministration of IDH1-R132H inhibitors with radiotherapy might limit radiation efficacy and thus abolish the prolonged survival of patients with IDH-mutated glioma (Molenaar et al. 2015).

PTEN. The tumor suppressor protein PTEN can sensitize glioma cells to chemotherapy and radiotherapy. Mutations in the PTEN gene have been reported in 15-40% of primary GBM (Ohka et al. 2012). A subset of high grade gliomas presents overexpression of the oncogenic miR-26a, that reduces PTEN levels and facilitates glioma formation in murine models (Huse et al. 2009; Wang et al. 2012). This observation suggests miR-26a as a potential therapeutic target still to be evaluated. Another glioma gene therapy approach has been recently proposed by Nan and colleagues, who demonstrated that a combination of adenoviral-mediated PTEN and the PI3K inhibitor LY294002 reduces the growth of GBM cells both in vitro and in tumor xenografts (Nan et al. 2017).

PI3K/Akt/mTOR. The PI3K/Akt/mTOR pathway is involved in cell growth and proliferation and is frequently activated in GBM. Several PI3K inhibitors have been tested in preclinal studies, such as LY294002, wortmannin and GDC-0941 (Workman et al. 2010). The PI3K inhibitor buparlisib (NVP-BKM120) demonstrated anticancer effects in GBM cellular and xenograft models (Netland et al. 2016) and is now being evaluated in a phase II clinical trial (NCT01339052; www.clinicaltrials.gov). The phospholipid perifosine, that interferes with the association of Akt with PIP3, is currently undergoing phase II clinical trials (Calvo et al. 2009) and perifosine administration in combination with bevacizumab has been proposed as a new GBM treatment to be clinically evaluated (Ramezani et al. 2017). In a recent study the dual PI3K/mTOR inhibitor DS7423 exhibited potent antitumor activity in both in vitro and in vivo preclinical GBM models and enhanced TMZ cytotoxicity in glioma xenografts (Koul et al. 2017).

EGFR pathway. Overexpression of the epidermal growth factor receptor (EGFR) or amplification of the EGFR gene have been reported in 40-60% of GBM (Ohgaki et al. 2004). Monoclonal antibodies against wildtype and mutant EGFR, such as cetuximab, panitumumab and nimotuzumab, have proved effective against GBM in preclinical studies (Blesaet al. 2012; Taylor and Gercel-Taylor 2011; Hegi et al. 2012). More recently, RNA based strategies, including antisense oligonucleotides, RNA interference and ribozymes, targeting the EGFR and the mutant form EGFRvIII, have proved successful in vitro and in xenograft GBM models (Shir and Levitzki 2002; Kang et al. 2006; Halatsch et al. 2009) and are currently under evaluation in a clinical setting. A completely new strategy for GBM treatment has also been proposed by Hicks and colleagues, who demonstrated that delivery and expression of the anti-EGFR antibody cetuximab mediated by an adeno-associated virus vector resulted in reduced tumor growth and increased survival in xenograft GBM models (Hicks et al. 2016).

Notch pathway. The Notch pathway is activated in GBM and increases migration and hypoxic response of tumor cells. Elevated Notch1 signaling seems to be responsible for chemotherapy resistance and recurrence of GBM (Yu et al. 2016). Downregulation of Notch1 by siRNA transfection inhibits growth and invasion of GBM cells and induces apoptosis in vivo. Similar effects are induced by Notch2 upregulation (Xu et al. 2013), suggesting that the Notch signaling pathway may provide multiple new targets for glioma therapy. Inhibition of Notch pathway by γ-secretase inhibitors causes an impairment of cell growth and sensitizes CSCs to radiation (Pannuti et al. 2010). The combination of the NOTCH/γ-secretase inhibitor RO4929097 with standard radiotherapy and TMZ chemotherapy has an anti-glioma stem cell effect in vitro (Yahyanejad et al. 2016). This combined treatment also proved to be well-tolerated in a phase 0/I trial conducted in patients with newly diagnosed GBM or anaplastic astrocytoma (Xu et al. 2016). Moreover, the combination of RO4929097 with bevacizumab in patients with recurrent malignant glioma has already been tested in a phase I clinical trial proving to be a well-tolerated treatment that deserves further clinical evaluation (Pan et al. 2016).

VEGF signaling. Anti-angiogenic therapy has been shown to increase GBM cell invasiveness (Norden et al. 2008; Plate et al. 2012; de Groot et al. 2010; Narayana et al. 2012) as a consequence of local hypoxic status through activation of Src family kinases (SFKs) (Zagzag et al. 2000; Keunen et al. 2011; Lu et al. 2012). However, some studies indicate that combined inhibition of angiogenesis and tumor cell invasion may represent a more effective glioma treatment (Huveldt et al. 2013; Navis et al. 2013). The novel monoclonal antibody D16F7 against the vascular endothelial growth factor receptor-1 (VEGFR-1) was demonstrated to inhibit GBM cell migration and invasion, suggesting VEGFR-1 as potential target for synergistic GBM therapies (Atzori et al. 2017). In addition, siRNA-mediated inhibition of both mesenchymal-epithelial transition factor (MET) and VEGF exhibits therapeutic effects in vitro and in murine GBM models (Okuda et al. 2017), thus representing a new approach to be further investigated.

PDGF signaling. Gliomagenesis is sustained by platelet-derived growth factor (PDGF) signaling (Pannuti et al. 2010). Many PDGF receptor inhibitors, such as imatinib (Reardon et al. 2012), sunitinib (Czabanka et al. 2013), sorafenib (Den et al. 2013) and vandetanib (Kreisl et al. 2012; Lee et al. 2015) have been evaluated in several clinical trials showing only limited or no significant activity. Combination of sorafenib and TMZ results in potent apoptosis induction in GBM cells (Jakubowicz-Gil et al. 2017); however the poor results of a previous phase I clinical trial evaluating sorafenib combined with radiotherapy and TMZ chemotherapy (Hottinger et al. 2014) make this approach not convincing for treatment of glioma patients.

SHH signaling. The SHH pathway is involved in glioma growth, CSC survival and proliferation (Clement et al. 2007). Several inhibitors of the membrane protein SMO, leading to inhibition of the SHH pathway, have been developed and their antitumor activity is being investigated in different types of cancers, including brain cancers. Among these, Vismodegib, a derivative of the alkaloid cyclopamine, is currently being tested for treatment of newly diagnosed MGMT unmethylated-GBM in a phase I/IIa clinical trial (NCT03158389; www.clinicaltrials.gov). A recent in vitro study also demonstrated that the combination of micellarized cyclopamine and TMZ exhibits a synergistic cytotoxic effect in human GBM cells through increased SHH-mediated downregulation of Gli1 (Liu et al. 2017).

TGF-β. The TGF-β pathway is involved in invasion, proliferation and therapy resistance of GBM. Agents targeting the TGF-β signaling, such as the inhibitors of the TGF-β type1 receptor SD-208 and LY364947, exhibited antitumor activity in preclinical studies (Joseph et al. 2013). The TGF-β receptor I and II kinase inhibitor LY2157299 is currently under evaluation in phase I and phase II clinical trials in patients with recurrent malignant glioma and recurrent GBM, respectively (NCT01682187, NCT01582269; www.clinicaltrials.gov). A recent study demonstrated that the TGF-β inhibitor peptide P144 reduces GBM cell proliferation and migration in vitro and impairs in vivo tumor growth, suggesting a therapeutic potential of this new drug for treatment of GBM (Gallo-Oller et al. 2016). In addition, integrin inhibition through neutralizing antibodies, RNA interference or pharmacological inhibition with cilengitide, has been proposed as a new promising approach to block TGF-β signaling in GBM (Roth et al. 2013).

Despite the great number of molecular targeted therapies that have been proposed and promising results exhibited by some of them in early clinical evaluation, these therapies are expected to give just a contribution to GBM treatment, without making the cure of gliomas really effective. For this reason, completely different therapeutic approaches are being explored for future combination into highly innovative multi-targeted therapies.

Immunotherapies

Modulating the host immune system to generate an anti-tumor response provides a long-lasting treatment against cancer (Tivnan et al. 2016; Rajesh et al. 2017) and is currently considered one of the most promising approaches for eradication of brain tumors (Miranda et al. 2017). Indeed, the central nervous system is not anymore considered an immune-privileged site (Galea et al. 2007; Klein et al. 2017; Savarin et al. 2013; Davies 2002) as low levels of antigen presenting cells are present in the normal brain (D'Agostino et al. 2012) and the blood-brain barrier is permeable to

immune cells in case of inflammation (Perng and Lim 2015). Main immunotherapeutic strategies against brain tumors include peptide and cellular vaccines, adoptive cell transfer and immune checkpoint inhibitors (Rajesh et al. 2017).

Peptide vaccines are developed through combination of either tumor isolated or synthetic antigens with carrier protein adjuvants. This approach is potentially highly specific, but the lack of homogeneous GBM antigens is a central challenge for development of anti-GBM vaccines, limiting antigen identification to in vitro assessment (Tivnan et al. 2016).

Dendritic cell vaccination consists in ex vivo priming of dendritic cells with tumor biopsy, followed by their reintroduction in the patient. Primed dendritic cells present in vivo tumor antigens and thus promote activation of cytotoxic T lymphocytes, resulting in destruction of cancer cells (Miranda et al. 2017). Some dendritic cell-based vaccines have proved successful in GBM patients in several clinical trials (Polyzoidis et al 2015; Ladomersky et al. 2016) and give high expectation for the future.

In the adoptive cell transfer therapy, lymphocytes isolated from patient blood are expanded ex vivo, genetically modified by adding T cell receptors (TCRs) or chimeric antigen receptors (CARs) specifically targeting tumor antigens, and finally reinfused in the patient (Tivnan et al. 2016; Rajesh et al. 2017). Several GBM-specific CARs have been developed (Genßler et al. 2015) with positive results in first clinical testing.

Immune checkpoint proteins are surface and secreted molecules made by some immune system cells, such as T cells, and some cancer cells. They act as checks on the immune response (Tivnan et al. 2016) and their upregulation allows tumor cells to avoid detection by immune system, for instance preventing T cell-mediated destruction of cancer cells. The most widely studied immune checkpoint proteins include CTLA-4 (Cytotoxic T-lymphocye-associated protein 4) and PD-1 (Programmed cell death protein 1). Immune checkpoint inhibitors result in enhanced anti-cancer immune responses and may represent an effective glioma immunotherapy (Grossauer et al. 2015; Kim et al. 2016), as immune checkpoints are often upregulated in the serum of patients with high grade glioma (Rajesh et al. 2017).

Factors that may limit the efficacy of GBM immunotherapeutic strategies include the great inter- and intra-tumor heterogeneity and immunosuppression induced by glioma cells through expression of immunosuppressive checkpoints, secretion of immunosuppressive proteins (i.e. TGFβ, IL-10, VEGF) and other molecules recruiting immunosuppressive cells (Chandran et al. 2017). Single immunotherapies effective in preclinical studies may also induce selection of poorly immunogenic tumor cells, able to evade the immune system. Despite this, combination of multiple immunotherapies as well as combination of immunotherapeutic approaches with gene therapy

strategies are very promising in both preclinical and clinical settings (Chandran et al. 2017) and may really improve the efficacy of current glioma treatments.

Gene therapy approaches

Many different gene therapy strategies have been designed to target glioma cells and specifically glioma cells resistant to conventional treatments. Stem cells and viral vectors have been used as gene therapy vehicles in order to overcome the low specificity and the inefficiency of therapeutic drug delivery to tumor sites (Wang et al. 2015; Rajesh et al. 2017). Stem cells, including NSCs (Muller et al. 2006g) and mesenchymal stem cells (MSCs) derived from embryonic stem cells, bone marrow, peripheral blood or adipose tissues (Shah 2012; Jones and McTaggart 2008; Nakamizo et al. 2005; Kim et al. 2008; Hu et al. 2012; Bak et al. 2011), can migrate to tumor site, probably guided by cytokines and other factors secreted in the tumor microenvironment and acting as chemoattractants (An et al. 2009; Beckermann et al. 2008; Chamberlain et al. 2007). Stem cells can be loaded with anticancer drugs, cytotoxic genes or immune stimulatory genes, to induce cancer cell death, enhance the immune response against tumor antigens and cause disruption of the tumor microenvironment (Castro et al. 2011; Assi et al. 2012; Samaranayake et al. 2010; Wang et al. 2015). Several gene therapy approaches based on viral vectors have also been proposed. In the oncolytic viral therapy, tumor cell lysis is induced by replication of oncolytic viruses, such as HSV, conditionally-replicating adenovirus and poliovirus (Miranda et al. 2017). Suicide gene therapy is based on the viral mediated delivery of a prodrug activating enzyme together with administration of the nontoxic prodrug (Miranda et al. 2017). For instance, in the Herpes simplex virus-thymidine kinase (HSV-TK)/ganciclovir (GCV) system, the enzyme thymidine kinase derived from HSV converts the nontoxic GCV to its cytotoxic form. Immunomodulatory therapy is instead aimed at the stimulation of an immune response against glioma cells through viral mediated transfer of cytokine genes (Rajesh et al. 2017). Gene therapy approaches have been implemented in different viral settings, such as herpesvirus (Grandi et al. 2009; Joseph et al. 2017), retrovirus (Pizzato et al. 1998) and adenovirus (Sandmair et al. 2000). They have been tested in preclinical studies demonstrating significant therapeutic effects and some of them also gained clinical attention (Palù et al. 1999; Colombo et al. 2005; Barzon et al. 2009; Patel et al. 2016; Westphal et al. 2013; Ji et al. 2016). Gene-silencing viral vectors, engineered to achieve stable downregulation of relevant genes in target cells through expression of small interfering RNA (siRNA) or other RNA interference (RNAi) molecules, represent another important approach that may reach clinical application in the next future. Lentiviral vectors have been widely used in this field of research thanks to several attractive characteristics, including stable vector integration in the genome of transduced cells, the

ability to transduce both dividing and non-dividing cells, a broad tissue-tropism, the absence of viral proteins expressed by last generation viral vectors and the possibility to deliver complex genetic elements (Sakuma et al. 2012). From earliest replication-competent viruses carrying transgenes, lentiviral vectors have been optimized up to third-generation lentiviral vectors, consisting of replication-deficient self-inactivating recombinant HIV-1 based vectors. Last generation lentiviral vectors also present a highly safer profile compared to previous generations as regard to the possible production of replication-competent recombinant HIV-like viruses and the potential for insertional activation of cellular oncogenes by viral promoter activities (Sakuma et al. 2012). Third-generation gene silencing lentiviral vectors were recently used to successfully sensitize human GBM cells to TMZ treatment by stable downregulation of HIF-1a expression (Tang et al. 2016). Another recent study demonstrated that lentivirus-mediated silencing of human protein phosphatase 1D magnesium dependent (PPM1D) gene enhances TMZ induced GBM cell apoptosis and cell cycle arrest (Wang et al. 2016). A relevant aspect of viral gene therapy approaches is the selectivity of the vector to target specific cell subpopulations, such as CSCs. In this direction, multiple efforts are ongoing and lentiviral vectors engineered with an anti-CD133 antibody on their envelope have been proposed for the specific transduction of CD133-expressing CSCs (Sumru Bayin et al. 2014).

To summarize, the recently increased understanding of glioma molecular pathogenesis allowed a great number of innovative therapeutic approaches to be designed and developed. Most of these novel strategies are currently under preclinical and clinical evaluation, showing significant potential to improve patient outcome. Nevertheless, the identification of new therapeutic targets is always in progress, prompted by the high molecular complexity of glioma tumors and the compelling need for more effective treatments. In this scenario, protein kinases, particularly protein kinase A, have emerged as promising targets for novel anti-cancer therapies, including anti-glioma therapies (Caretta and Mucignat-Caretta 2011; Sapio et al. 2014).

1.4 Protein kinase A

The cAMP-dependent Protein Kinase (PKA or protein kinase A) is a second messenger dependent serine-threonine kinase involved in a wide range of biological events. It was the second protein kinase to be discovered, in 1968 after phosphorylase kinase (Walsh et al. 1968), and it is conserved also in fungi and even single-cell pathogen like *Plasmodium falciparum* (Haste et al. 2012). PKA is ubiquitously expressed in all mammalian cells and regulates many cellular processes, including

transcription, metabolism, cell proliferation, cell differentiation and apoptosis. The intracellular concentration of cAMP (cyclic 3', 5'-Adenosine Monophosphate) is regulated by the activity of two enzymes with opposite functions: adenylyl cyclases (AC), that catalyze the synthesis of cAMP starting from ATP, and phosphodiesterases (PDEs), that are responsible for cAMP degradation. Changes in cAMP levels are related to the selective activation of PKA isoforms (Taylor et al. 2013). The PKA holoenzyme is a tetrameric complex of two catalytic (C) subunits and a regulatory (R) subunit dimer. Different isoforms of PKA subunits have been identified, in particular four regulatory subunits (R1A, R1B, R2A, R2B) and three catalytic subunits (CA, CB, CG) have been reported (Boettcher et al. 2011). Both regulatory and catalytic subunits present a differential distribution among mammalian tissues, that is peculiar for each isoform (Taskén et al. 1997). R1A and R2A subunits are ubiquitously expressed, whereas R1B is predominantly present in the brain and R2B is mainly expressed in brain, adrenal and adipose tissues (Mantovani et al. 2009). PKA CA is the predominant catalytic subunit and shares 93% of homology with PKA CB. The CG subunit has been identified in the human genome and its expression has been reported also in primates (Foss et al. 1992). PKA regulatory subunit isoforms are functionally non-redundant, but they have the same domain organization, that includes an N-terminal dimerization and docking domain (D/D domain), a flexible linker and two cyclic nucleotide-binding (CNB) domains in tandem (CNBA and CNBB) at the C terminus. The linker contains an inhibitor site resembling a peptide substrate, whose function is to dock to the active site cleft of the catalytic subunit in the PKA holoenzyme. The CNB is a universal binding domain for cAMP, conserved from bacteria to humans (Taylor et al. 2012). PKA catalytic subunits have a conserved catalytic core comprising an N-terminal lobe (N-lobe or small lobe) and a C-terminal lobe (C-lobe or large lobe). The active site cleft, which binds an ATP molecule and transfers the ATP γ-phosphate on PKA substrates, is located between the N- and the C-lobe (Taylor et al. 2012). Tetrameric PKA is commonly anchored to subcellular structures through binding of the regulatory subunits to A kinase anchoring proteins (AKAPs; Tröger et al. 2012). Catalytic subunits can also be targeted to intracellular sites through interaction with specific proteins, such as A kinase interacting protein 1 (AKIP1), which binds the catalytic subunit promoting its nuclear retention (Gao et al. 2008; King et al. 2011). PKA function must be tightly regulated inside the cell as the cAMP signaling is involved in many fundamental cellular processes (Søberg et al. 2017). The tight spatiotemporal control of PKA activity is achieved thanks to the cell type-specific expression of regulatory and catalytic isoforms, different PKA substrates and specific intracellular localization of PKA tetramers (Taylor et al. 2012). PKA holoenzyme is usually inactive as the regulatory subunits bind to the catalytic subunits suppressing their activity. Traditionally it was thought that binding of two cAMP molecules to each regulatory

subunit induces a conformational change in the regulatory dimer, resulting in the release of active catalytic subunits that can phosphorylate specific target proteins (Sjoberg et al. 2010; Lefkimmiatis and Zaccolo 2014). However, increasing evidence indicates that upon cAMP stimulation some catalytic subunits may not fully dissociate from the regulatory dimer and phosphorylate their substrates in close proximity (Smith et al. 2013). Recently it was demonstrated that within the cell cytoplasm physiological concentrations of cAMP promote minimal release of catalytic subunits from the anchored holoenzyme, despite cAMP binding to CNB sites. In this conditions PKA holoenzyme is catalytically active but remains intact, indicating that dissociation of the holoenzyme is not necessary for anchored PKA activation. As the action of anchored PKA is restricted to substrates within the immediate proximity, in this new model compartmentalization of PKA by AKAPs is the primary determinant for the substrate selectivity (Smith et al. 2017). PKA nuclear signaling, that is mediated by PKA phosphorylation of cAMP response element-binding protein (CREB) leading to transcriptional events, may represent an exception as it requires supraphysiological levels of cAMP, that normally induce PKA dissociation (Smith et al. 2017). Although the second messenger cAMP is the major PKA activator, protein kinase A can be activated independently of cAMP through different mechanisms. Among these, phosphorylation and degradation of NF-kappa-B inhibitor alpha (NFKBIA) and NF-kappa-B inhibitor beta (NFKBIB) in response to vasoactive peptides, result in the release of a pool of active PKA catalytic subunits, that under basal conditions are retained in their inactive form by NFKBIA and NFKBIB (Zhong et al. 1997; Dulin et al. 2001). In addition, cAMP-independent activation of PKA can be induced by the TGFβ signaling through phosphorylation and activation of SMAD3 and SMAD4 proteins (Zhang et al. 2004; Yang et al. 2008). The PKA pathway mediates a great variety of cellular functions through phosphorylation of many different substrates. PKA phosphorylation of class C L-type Ca^{2+} channels is involved in the regulation of membrane excitability and synaptic plasticity (Davare et al. 2000). Another relevant PKA target is the proapoptotic protein BAD (Bcl2-Antagonist of Cell Death), whose phosphorylation determines blockade of apoptosis and consequently cell survival (Harada et al. 1999; Tan et al. 2000). PKA modulation of RhoA (ras homolog gene family; member A; Rho family GTPase) activity is an important mechanism for regulation of cytoskeletal organization and cellular morphology (Dong et al. 1998), whereas regulated PKA-dependent phosphorylation of the small G protein Rap1 is involved in cell adhesion and migration (Lerosey et al. 1991; Takahashi et al. 2013). PKA substrates also include several transcription factors, such as the cAMP response element-binding protein (CREB; Fiol et al. 1987; Delghandi et al. 2005), high-mobility-group N (HMGN) proteins (Prymakowska-Bosak et al. 2001) and the Gli3 protein (Gli-Kruppel Family Member-3) in the SHH pathway (Tempe et al. 2006).

PKA regulation of cell metabolism is mediated by phosphorylation of glycogen synthase kinase 3 (GSK-3) isoforms GSK-3α and GSK-3β (Fang et al. 2000), glycogen synthase (Palm et al. 2013) and hormone-sensitive lipase (HSL; Donsmark et al. 2004). In addition, a relation between PKA and the glucose transporter 3 (GLUT3) has also been reported (Reddy et al. 2010; Yu et al. 2014). Finally, PKA is differently involved in the control of cell cycle progression, for instance through regulation of cyclin D1 (Justin et al. 2000) and the cyclin-dependent kinase PCTAIRE kinase 3 (PCTK3; Matsuda et al. 2014), as well as through association with centrosome and the anaphase-promoting complex/cyclosome (ACP/C; Matyakhina et al. 2002).

The fundamental key role of protein kinase A in such a wide range of cellular functions is based on a strict, precise and rigorous control of its activity. Alterations of this fine signaling network can have dramatic consequences on cellular status, leading to multiple pathological conditions. Understanding the pathophysiological role of PKA is thus important and could significantly contribute to future treatment of several human diseases.

1.5 Pathological implications of protein kinase A

The scientific literature provides many studies demonstrating the relation between impaired PKA pathway and several pathological conditions (Gold et al. 2013). Investigation of the molecular basis of this relationship can give a deeper insight into human pathologies and consequently lead to improvements of current therapies. Diseases that have been associated with PKA dysregulation include obesity (Cummings et al. 1996; Czyzyk et al. 2008), asthma (Gerthoffer et al. 2013), neurodegenerative and behavioral disorders (Bernstein et al. 2013; Millar et al. 2005; Reissner 2013; Renthal et al. 2009; Richter et al. 2011). Type 2 diabetes is characterized by reduced insulin secretion, an event that is mediated by the cAMP/PKA signaling in β-pancreatic cells (Gao et al. 1997; Lester et al. 1997). Based on this observation, anti-diabetic drugs have been associated to modulation of cAMP levels (Miller et al.2013). The cAMP/PKA signaling cascade is also involved in stress responses of heart muscular cells and thus in many cardiovascular diseases (Carnegie et al. 2008; Kim et al. 2011). Moreover, the relationship between PKA and cancer has been deeply investigated revealing multiple alterations of the cAMP/PKA pathway in many different types of tumors. The alterations of the cAMP/PKA network in cancer cells are related to variations of the intracellular cAMP levels, but also to altered expression, distribution and activity of different PKA regulatory and catalytic isoforms (Neary et al. 2004). PKA is involved in proliferation signals mediated by the mitogen-activated protein kinase (MAPK) cascade, that is usually upregulated in

tumor cells (Burgering et al. 1993; Cook and McCormick 1993; Wu et al. 1993; Dumaz and Marais 2005), and direct phosphorylation of specific MAPK-related proteins is indeed dependent on AKAPs-mediated PKA intracellular localization (Smith et al. 2010). In several tumors, including GBM (Sugimoto et al. 2013) and bladder cancer (Zheng et al. 2014), the cAMP pathway induces a reduction of tumor cell growth by acting on MAPK cascade in a PKA-dependent manner. Genetic alterations of PKA coding genes have also been associated to human cancers. Heterozygous inactivating mutations of the PKA R1A gene are the most common genetic cause of Carney complex, an autosomal dominant multiple neoplasia syndrome (Papanastasiou et al. 2016). In this genetically heterogeneous disease, only the wild type allele of the PKA R1A gene is translated, resulting in a 50% reduction of R1A protein levels and consequently in the increase of PKA catalytic subunit activity (Kirschner et al. 2000). Recently, microinsertions in the PKA CA gene have been reported in cardiac myxoma, the most frequent tumor of the heart. In this case, mutated PKA catalytic subunits are not able to bind R1A subunits and the PKA pathway results constitutively activated (Tseng et al. 2017). In lung cancer cells, hypoxia induces the upregulation of PKA CA, R1A and R2B subunits expression; the consequent increase in PKA activity is involved in hypoxia-mediated epithelial-mesenchymal transition, tumor cell migration and invasion (Shaikh et al. 2012). In prostate carcinoma cells, PKA R2B overexpression inhibits tumor growth, whereas overexpression of R1A and CA subunits induces upregulation of genes associated with cell transformation and proliferation (Neary et al. 2004). Additionally, overexpression of either PKA R2A or truncated forms of the same subunit increases survival of prostate cancer cells treated with taxanes, probably through inhibition of the kinase activity (Zynda et al. 2014). Recent data also indicate that the splice variant CB2 of PKA catalytic subunit is upregulated in prostate cancer and it has been proposed as a biomarker to better predict the aggressiveness of this type of tumor (Moen et al. 2017). In breast cancer, PKA R1 overexpression has been associated with poor prognosis and resistance to antiestrogens, whereas reduced R1 mRNA levels are potentially predictive of successful antiestrogen therapy. This suggests PKA R1 as a novel candidate target for breast cancer treatment (Miller 2002). In epithelial ovarian cancers, an increased expression of PKA R1A subunit is associated with advanced tumor stage (McDaid et al. 1999). PKA activity and AKAP-mediated PKA anchoring are both required for migration and invasion of ovarian tumor cells, pointing to a potential role of PKA in ovarian cancer metastasis (McKenzie et al. 2011). Human melanomas are characterized by high expression of R1A subunit, with a consequently high R1/R2 ratio. Reversion of this unbalanced expression by pharmacological and genetic manipulations has significant antiproliferative and proapoptotic effects in melanoma cells, which could be exploited for melanoma treatment (Mantovani et al. 2008A). Cortisol-producing adrenocortical adenomas present

reduced protein levels of PKA R2B compared to normal adrenal gland and the defective expression of this subunit is related to tumor cell survival (Mantovani et al. 2008B; Weigand et al. 2017). Moreover, genetic alterations of the PKA CA gene have been associated with different adrenal diseases. In particular, germline duplications of the PKA CA gene result in bilateral adrenal hyperplasia, whereas somatic mutations result in unilateral cortisol-producing adrenal adenomas (Beuschlein et al. 2014). All somatic mutations identified so far, the most frequent being L205R, lie at the interface between catalytic and regulatory subunit and prevent formation of the PKA tetramer, resulting in constitutive activation of mutant catalytic subunits (Sato et al. 2014; Beuschlein et al. 2014; Goh et al. 2014; Calebiro et al. 2015; Calebiro et al. 2017). Interestingly, germline duplications of the PKA CA gene in bilateral adrenal hyperplasia cause an increase in PKA CA protein levels, leading again to increased PKA activity (Beuschlein et al. 2014). The expression pattern of PKA regulatory isoforms was recently analyzed in thyroid tumors, showing high expression of R2B subunit in benign lesions, malignant differentiated and undifferentiated lesions and high expression of R1A subunit in follicular adenomas and undifferentiated thyroid carcinomas (Ferrero et al. 2015). Future studies will elucidate the relation between this peculiar expression pattern and the different clinical outcomes (Del Gobbo et al. 2016). A few years ago, a novel and previously unknown PKA genetic alteration was discovered in fibrolamellar hepatocellular carcinoma, a rare variant of hepatocellular carcinoma occurring in young patients without underlying liver disease. These tumors present a deletion in chromosome 9 leading to fusion of the genes encoding a heat shock protein (DNAJB1) and PKA CA subunit (Honeyman et al. 2014). Cancer cells express both the chimeric protein (DNAJB1-PKA CA) and the wild-type catalytic subunit, resulting in enhanced PKA activity in response to cAMP compared to normal liver (Riggle et al. 2016).

In summary, breakthroughs in our understanding of cancer molecular pathogenesis have revealed a crucial role of the cAMP/PKA pathway in the initiation and progression process of many types of tumors. Several evidences suggest PKA as a potential useful target for both cancer diagnosis and therapy (Caretta and Mucignat-Caretta 2011). Many efforts have been done and many others are still needed to uncover the function and regulatory mechanisms of such a complicated signaling network. This knowledge is fundamental to develop new therapeutic options and achieve a real clinical benefit for cancer patients. In this view, the laboratory of Neurophysiology, University of Padova, has being investigating since many years the relation between PKA and brain tumors (Mucignat-Caretta et al. 2008; Mucignat-Caretta et al. 2010; Caretta and Mucignat-Caretta 2011; Mucignat-Caretta et al. 2018). Interestingly, relevant peculiarities as regard to PKA isoform

expression and PKA intracellular distribution in glioblastoma cells point to a potential therapeutic role for this kinase to be further elucidated.

1.6 Protein kinase A and brain: from the physiological function to disease

Protein kinase A regulatory and catalytic isoforms present differential expression patterns in many mammalian tissues, such as adrenal gland (Weigand et al. 2017) and brain (Mucignat-Caretta and Caretta 2001; Mucignat-Caretta and Caretta 2002; Mucignat-Caretta and Caretta 2004; Ilouz et al. 2017). Variations of both PKA tetramer composition and intracellular localization have been described in several physiological processes, including development and ageing. The isoform-specific, spatio-temporal regulated PKA distribution allows a fine control of cAMP/PKA signaling and thus of cellular responses elicited by stimulation of this pathway (Mucignat-Caretta and Caretta 2002). As a consequence, balanced expression of PKA subunits, tight regulation of kinase activity and proper PKA localization should be always guaranteed to avoid deviations from physiological cellular states. On the other hand, elucidation of the molecular mechanisms driving these pathological deviations could be the basis for development of novel therapies. These considerations find particular applications in the pathophysiology of the central nervous system, including brain diseases and high grade gliomas.

The expression patterns of PKA subunits have been deeply investigated in rodent brain, showing switching between different regulatory isoforms in various brain areas at different ages, during pre- and postnatal development (Mucignat-Caretta and Caretta 2002; Mucignat-Caretta and Caretta 2004). A similar PKA distribution has been reported in the CNS of other animal species (Mucignat-Caretta and Caretta 2007; Mucignat-Caretta and Caretta 2011), pointing to a common mechanism of regulation of PKA-mediated events in brain development. PKA subcellular compartmentalization has also been demonstrated to have a functional relevance in rat developing hippocampal neurons. In these cells cAMP forms a gradient, that changes according to the developmental stage, depends on AKAP-anchored PKA activity and is crucial for proper axonal development (Gorshkov et al. 2017). As regard to the adult rodent brain, the differential expression between PKA regulatory isoforms has been described. R1A subunit is neuronal and restricted to some brain nuclei (Mucignat-Caretta and Caretta 2002), whereas R1B is present in the olfactory bulb mitral cells, the cerebellar Purkinje cells, the lateral thalamic neurons and the superior olivary complex neurons (Mucignat-Caretta and Caretta 2001). R2A is localized only at the base of the cilia of ependymal cells lining the ventricles, while R2B is present in most neural and glial cells (Mucignat-Caretta and

Caretta 2004). A recent study further analyzed the patterns of cellular and subcellular distribution of R1B and R2B subunits in mouse brain, reporting significant differences between these two regulatory isoforms (Ilouz et al. 2017). R1B is predominant in the pyramidal neurons of the hippocampus, consistently with its known role in synaptic plasticity (Brandon et al 1995), as well as in the dentate gyrus and hilus neuron. On the contrary, R2B is concentrated in the striatum and it is not expressed in the hippocampus. At the subcellular level, R2B is concentrated in axons, whereas R1B is present in mitochondria and in dendrites, where it co-localizes with MAP2, an AKAP protein that anchors PKA to microtubules. R1B is also localized in the nucleus in different brain regions. Consistently with this observation, downregulation of R1B, but not of R2B, decreases CREB phosporylation, indicating an important functional distinction between R1B and R2B subunits (Ilouz et al. 2017). Interestingly, alterations of the normal brain PKA distribution have been reported in several pathological conditions affecting the CNS. For example, a dysregulated expression of R1A and R1B subunits has been described in animal models of depression induced by traumatic or chemical lesions (Mucignat-Caretta et al. 2004). Recently, a missense mutation in the gene coding for PKA R1B has been associated with a new hereditary neurodegenerative disease, characterized by dementia, Parkinsonism and abundant accumulation of R1B in neuronal inclusions. This point mutation lies in the D/D domain of R1B and potentially impairs the regulatory binding to AKAP proteins and PKA catalytic subunit, thus resulting in subcellular dislocation of PKA activity (Wong et al. 2014). Moreover, several alterations of PKA have been reported in brain tumors. In particular, PKA is ten-times more abundant in human GBM compared to normal brain (Frattola et al. 1983), whereas the catalytic subunit is reduced in human high grade gliomas (Odreman et al. 2005). Mouse and rat GBM cells present a peculiar perinuclear cluster of R2A co-localized with the Golgi apparatus. This intracellular localization is not observed in the healthy brain parenchyma, where R1A and R2B aggregates are detected, and allows identification of the tumor margin in rodent glioma models (Mucignat-Caretta et al. 2008). The peculiar distribution of R2A subunit has been confirmed also in human GBM cell lines and human primary GBM cell cultures (Mucignat-Caretta et al. 2008; Mucignat-Caretta et al. 2018). Some evidences indicate that PKA activity is involved in the assembly of Golgi complex and maintenance of its structural organization, but the functional significance of Golgi-associated PKA is still unclear (Bejarano et al. 2006). Despite this, the peculiar localization of R2A in GBM cells suggests a potential role of this subunit as a tumor marker or a novel therapeutic target. Differently from GBM cells, in human medulloblastoma PKA R2A is organized in large single dots (Mucignat-Caretta et al. 2010). In mouse neuroblastoma, tumors of ectodermal origin derived from the autonomic nervous system, PKA R2A expression is regulated in the presence of estrogen by a feedback

mechanism involving the transcriptional coregulators E6-associated protein (E6ap) and the estrogen receptor alpha (Erα; Obeid et al. 2017). All these observations might indicate a differential role of R2A in different tumors of the nervous system. Understanding the molecular mechanisms underlying PKA R2A peculiarities in brain tumors and other nervous system pathologies is thus of major interest for future clinical applications.

Apart from PKA, other components of the cAMP pathway often dysregulated in brain tumors include AKAP1, which docks PKA to cytoskeleton, and the cAMP-degradating enzyme PDE1A, that are both upregulated in GBM (Hoelzinger et al. 2005). Some studies on glioma molecular pathogenesis report alterations on chromosomes 7 and 17, carrying PKA R1A, R1B and R2B genes (Ichimura et al. 2004), that could be related to PKA subunits unbalance. Consistently, an altered degradation rate of PKA subunits could explain the differentiation and apoptosis of glioma cells induced by activation of the cAMP pathway through PKA R2 (Chen et al. 1998). In addition, the cAMP/PKA signaling can exert its effects on glioma cells by modifying transcription of several genes, such as the proto-oncogene c-Jun (Lee et al. 1999) and the GFAP gene, which encodes one of the major intermediate filament proteins of mature astrocytes (Anciaux et al. 1997; Oh-hashi et al. 2006). As an example, cholera toxin, an inducer of cAMP accumulation, causes differentiation of glioma cells by increasing the expression of GFAP and cell-cycle inhibitory proteins and by reducing the expression of cyclin D1 and the cyclin-dependent kinase Cdk2 (Li et al. 2007B). Also, activation of the PKA pathway is reported to inhibit invasion and migration of glioma cells through transcriptional upregulation of microtubule-associated protein 2 (MAP2), suggesting that PKA may be targeted in anti-invasion glioma therapy (Zhou et al. 2015). Recently it was demonstrated that the cAMP responsive transcription factor CREB1 positively regulates the expression of the glucose transporter protein GLUT1 in human GBM cells. This indicates a potential mechanism for cAMP pathway to stimulate tumor progression by activating glucose uptake of glioma cells (Chen et al. 2017).

Apparently, multiple mechanisms may mediate the involvement of the cAMP/PKA signaling in CNS cancers. Dysregulation of PKA can differently impair nervous cell biology, even with dramatic consequences leading to neoplasm transformation and persistent tumor cell growth. Many distinctive features of brain cancer cells are dependent on PKA-mediated events and altered PKA signaling. In GBM a peculiar role may be played by the regulatory subunit R2A of PKA, whose specific distribution on Golgi complex is not observed in the normal brain tissue. It is believed that PKA dysregulations in glioma cells may be exploited for therapeutic purposes, thus a deep investigation of these defects is a primary issue in brain cancer research. Based on these considerations, further studies are needed to better understand the function of PKA, in brain tumors.

Taking advantage of this knowledge could finally give a significant improvement of currently ineffective glioma treatments. In this direction, the present PhD project aimed to give additional insights into the multiple roles of PKA pathway and particularly R2A subunit in human glioblastoma by investigating their complex functions in different cellular models.

2. Aim of the study

The aim of the present PhD project is to investigate the role of the protein kinase A in human glioblastoma cells and evaluate the PKA signaling pathway as a potential candidate target for the development of novel glioma therapies. Particular attention was focused on the regulatory subunit R2A of PKA, due to the remarkable peculiarity of its intracellular distribution in GBM cells. Indeed, R2A subunit is specifically present as a perinuclear cluster co-localized with the Golgi apparatus in rodent and human GBM cells, whereas this peculiar distribution is not detected in the healthy brain parenchyma (Mucignat-Caretta et al. 2008; Mucignat-Caretta et al. 2018). Based on these observations, investigation of PKA intracellular localization was extended to human GBM stem like cell cultures, that in recent years emerged as a major obstacle in GBM treatment. In addition, new molecular tools for functional studies of PKA were developed. Through standard cloning techniques recombinant plasmids for expression of PKA subunits in fusion with EGFP protein were generated and preliminarily tested in human GBM cells, opening the way to a deeper investigation of PKA subunits in several cellular models.

In order to further elucidate the role of the cAMP/PKA signaling pathway in human GBM cells, the first part of the present study analyzed the effects induced by a transient interference with PKA activity, expression and intracellular localization. Multiple approaches, including drug treatment, plasmid and small interfering RNA (siRNA) transfection, were adopted to differentially interfere with PKA function. Effects on GBM cell viability and motility were then analyzed, showing an anti-tumor potential of PKA interference. Moreover, the relation between PKA and Golgi apparatus was further investigated by evaluating the effects of disrupted Golgi function on PKA R2A intracellular distribution. In particular, cell viability, cell migration and PKA localization were analyzed following treatment of human GBM cells with brefeldin A (BFA), a well known inhibitor of intracellular protein transport to Golgi complex.

Based on the results of the first part of the project, silencing of PKA R2A expression emerged as the most promising approach, showing significant effects on GBM cell viability, proliferation, migration and Golgi structure. For this reason, the second part of the research study was focused on the development of a third-generation lentiviral system for the efficient delivery of short hairpin RNA (shRNA) targeting PKA R2A subunit in human GBM cells. Lentiviral vectors were thus tested for their ability to efficiently transduce human non-stem and stem like GBM cell cultures. Then, two shRNA sequences against PKA R2A and the same shRNA sequences in fusion with EGFP gene were separately cloned in the selected lentiviral vector to generate a set of four recombinant gene-silencing lentiviral vectors for downregulation of PKA R2A expression. A

scrambled shRNA was also designed, cloned in the same lentiviral vector and preliminarily tested to evaluate off-target effects induced by lentiviral vectors carrying PKA R2A shRNA sequences. All generated lentiviral particles were tested for efficient silencing of PKA R2A expression in human non-stem and stem like GBM cells. Finally, effects of reduced R2A expression on GBM cell viability and cell proliferation were also investigated.

3. Materials and methods

3.1 Cell cultures

The experiments reported in the present study were performed on human GBM cell lines and human GBM tumor-like stem cell cultures.

The following human GBM cell lines were used:

- U87MG (U87): mutated in PTEN, CDKN2A and CDKN2C genes (ATCC, Pontén 1975);
- D-423:homozygously deleted in 1p36, with deletion spanning CAMTA1, VAMP3, PER3, UTS2, TNFRSF9, PARK7, ERRFI1, SLC45A1, RERE, ENO1, CA6, SLC2A5, GPR157, MIR34A, H6PD, SPSB1 and SLC25A33 genes (Duncan et al. 2010);
- GLI56: deleted in UTS2, TNFRSF9, PARK7, ERRFI1, SLC45A1, RERE, ENO1, CA6, SLC2A5, GPR157, MIR34A, H6PD, SPSB1, SLC25A33, TMEM201, C1orf200, PIK3CD, CLSTN1, CTNNBIP1, LZIC, NMNAT1, RBP7 and UBE4B loci (Mueller et al. 2007).

The reported cell lines were grown as adherent cells in Dulbecco's modified Eagle's medium nutrient mixture (DMEM, Gibco™, cat. n° 41965-039) supplemented with 10% fetal bovine serum (FBS, Gibco™, cat. n° 10082147). The medium formulation is referred in the text as complete DMEM.

The following human GBM stem cell like cultures were also studied:

- NCH421K: glioblastoma from 66-years-old man, tumorigenic and highly CD133 positive (CLS Cell Lines Service GmbH, Campos et al. 2010);
- GBM2: glioblastoma from 58-years-old man patient (available at the Department of Molecular Medicine, University of Padova);
- GBM5: glioblastoma from 63-years-old woman patient (available at the Department of Molecular Medicine, University of Padova).

GBM stem cell like cultures were grown as cell clusters (spheres) in suspension in Neurobasal medium (Life Technologies Italia, cat. n° 21103049) supplemented with 3 mmol/l L-Glutamine (Sigma-Aldrich Chemie GmbH, cat. n° G6392-1VL), 1X B27 supplement (Life Technologies Italia, cat. n° 17504044), 0.5X N2 supplement (Life Technologies Italia, cat. n° 17502048), 2 μg/ml heparin (STEMCELL Technologies, cat. n° 07980), 20 ng/ml recombinant human EGF (Merck

Millipore, cat. n° 01-407), 20 ng/ml recombinant human FGF-basic (Peprotech, cat n° 100-18B-50UG), 1% Penicillin/Streptomycin (Thermo Fisher Scientific, cat. n° 15140-122), 1% Tetracycline (CellBio™, cat. n° ECB3003D) and 1% Plasmocin® (InVivogen™, cat. n° ant-mpp). This formulation is referred in the text as complete Neurobasal medium. NCH421K cell line is a phenotypically and genetically characterized GBM tumor-like stem cell line (CLS Cell Lines Service GmbH). GBM2 and GBM5 cell cultures had been previously established from human GBM surgical specimens according to published protocols (Wakimoto et al. 2009; Sgubin et al. 2012). GBM2 and GBM5 cells were grown as spheres in complete Neurobasal medium, thus in culture conditions that had originally been designed for selective expansion of neural stem cells (Wakimoto et al. 2009). Characterization of GBM2 and GBM5 cells is not yet complete, but expression of nestin, a marker for neural stem/progenitor cells, and Sox2, another marker for neural stem cells, has been reported in both cell cultures (Moschioni 2014). In addition, GBM2 cells express βIII-tubulin, a marker for mature neurons, and the astrocytic marker GFAP. Expression of CD133, a putative GBM stem like cell marker (Zeppernick et al. 2008) is still to be evaluated.

For production and titration of lentiviral vectors as well as preliminary testing of recombinant plasmid vectors, human embryonic kidney 293T cell line was used. These cells constitutively express the Simian Virus 40 (SV40) T-antigen, which allows efficient replication of vectors carrying the SV40 origin of replication. 293T cells were grown in adhesion in complete DMEM.

All cell cultures were grown in humidified incubator at 37°C and 5% CO_2.

3.2 Set up and maintenance of cell cultures

3.2.1 Adherent cell lines

GBM cell lines growing in adhesion (U87, D-423, GLI56) were set up from aliquots stored at -80°C or in liquid nitrogen according to the following protocol:

- the cellular suspension was heated at 37°C and added to 5 ml of DMEM 10% FBS;
- cells were centrifuged at 1400 rpm for 5 minutes;
- cell pellet was resuspended in 3 ml of DMEM 10% FBS;
- the cellular suspension was put in a sterile T-75 flask containing 10 ml of DMEM 10% FBS.

After 24 hours the medium was discarded to remove cellular debris and detached cells and replaced with fresh DMEM 10% FBS. The same operation was performed every 48-72 hours according to the status of the culture. Cells were routinely monitored by observation with a direct light inverted microscope (Leica DMIL LED) and passaged when in confluent or semi-confluent status.

Standard procedure for cell passaging of adherent GBM cell lines was as follows:

- cell monolayer was washed three times with 3 ml of Phosphate-Buffered Saline (PBS, Gibco™, cat. n° 14190-094) to remove dead cells and residual FBS growth factors;
- 3 ml of 0.05% trypsin-EDTA solution (Gibco™, cat n° 25300-054) were added to the cell monolayer and the cell flask was put in incubator for 1 minute to allow cell detachment;
- 7 ml of DMEM 10% FBS were added to inactivate trypsin solution;
- cells were collected and centrifuged at 1400 rpm for 5 minutes;
- cell pellet was resuspended in a proper volume (3-8 ml) of DMEM 10% FBS, cells were counted with a Burker chamber (par. 3.18) and cellular suspension was split into flasks according to the desired cellular density.

293T cell cultures were set up from aliquots stored in liquid nitrogen and maintained as previously described for adherent GBM cells, in DMEM 10% FBS. For cell passaging of confluent cell cultures, only one PBS wash was performed before addition of trypsin-EDTA solution and after cell detachment and trypsin inactivation, cells were put into new flasks without previous centrifugation of the cellular suspension.

3.2.2 GBM stem cell like cultures

Human GBM stem cell like cultures growing as spheres (NCH421K, GBM2 and GBM5) were set up in complete Neurobasal medium from aliquots stored at -80°C or in liquid nitrogen, according to the protocol previously reported for adherent GBM cell lines. After centrifugation, cell pellet was resuspended in 5 ml of complete Neurobasal medium and the cellular suspension was put in a T-25 flask.

Culture feeding was performed every 48-72 hours, by changing the culture medium as follows:

- cell flasks were left in vertical position for 3-5 minutes, to let the GBM spheres precipitate;
- according to the cellular density, 1/2 or 1/3 of the cell culture volume was removed and replaced with freshly prepared complete Neurobasal medium.

GBM sphere cultures were routinely observed with a direct light inverted microscope (Leica DMIL LED) to monitor sphere formation and growth in diameter, as well as the possible presence of differentiating cells attached to the bottom of the flask. When adherent cells were observed, the entire volume of the cell culture was placed in a new flask to avoid contact with differentiated cells. Passaging of GBM spheres was performed by mechanical dissociation when most of the spheres in the flask reached a diameter of at least 30 cells and according to the experimental requirements and timetable. The GBM sphere cell culture was centrifuged at 1200 rpm for 5 minutes, the cell pellet was resuspended in 1 ml of complete Neurobasal medium and dissociated by prolonged pipetting. Fragmentation of GBM spheres led to a cell suspension containing single cells, small spheres and cell clusters, in addition to cell debris derived from dead cells. This procedure thus allowed to increase the number of growing GBM spheres in the culture.

3.3 Cryopreservation of cell cultures

Culture medium added with dimethyl sulfoxide (DMSO) was used for cryopreservation of cell cultures. GBM cells growing in adhesion were detached by trypsinization as previously described and centrifuged at 1400 rpm for 5 minutes. Cell pellet was resuspended in a small volume of DMEM 10% FBS and 1 million cell aliquots were prepared in cryovials as follows:

- 60% cell suspension;
- 20% FBS;
- 20% DMSO.

GBM sphere cell cultures were centrifuged at 1200 rpm for 5 minutes and cell pellet was then resuspended in Neurobasal medium supplemented with 3 mmol/l L-Glutamine, 1% Penicillin/Streptomycin, 1% Tetracycline, 1% Plasmocin® and 15% DMSO.

Cryovials were put overnight at -80°C and transferred in liquid nitrogen the following day.

3.4 Treatment of GBM cells with chemical agents

To investigate the role of PKA and its association with Golgi apparatus in human GBM cells, interference with either Golgi function or PKA activity were induced in U87 cells by treatments

with different chemical agents. Cell viability, cell motility and PKA intracellular distribution were then evaluated in U87 cells with disrupted Golgi function or disregulated PKA activity.

The fungal metabolite brefeldin A (BFA, Sigma-Aldrich™, cat. n° B7651-5MG) is commonly used to disrupt Golgi structure and function through inhibition of the anterograde transport to the Golgi apparatus (Klausner et al. 1992). For the experiments reported in the present study, a stock solution of BFA 10 mg/ml in DMSO was properly diluted from 10 μg/ml up to 0.01 μg/ml and treated U87 cells were evaluated at different time points.

Interference with PKA activity was induced in human GBM cells by treatments with the PKA activator 8Br-cAMP and the PKA inhibitor H89 (N-(2-(4-Bromocinnamylamino)ethyl)-5-isoquinolinesulfonamide). 8Br-cAMP is an analogue of the signalling molecule cAMP in which the hydrogen in position 8 of the heterocyclic nucleobase has been replaced by bromide. This compound has a higher membrane permeability compared to cAMP and is resistant to degradation by phosphodiesterases. H89 competitively binds to the ATP binding site of multiple cellular kinases, resulting in inhibition of their activities. Despite not selective, H89 is widely used as a PKA inhibitor in many experimental studies (Lochner and Moolman 2006). Treatments with 8Br-cAMP and H89 were performed at selected concentrations (8Br-cAMP 50 μM and 500 μM; H89 1.25 μM and 12.5 μM) for 24 hours (Mucignat-Caretta et al. 2008; Mucignat-Caretta et al. 2018).

3.5 Interference with PKA through plasmids and siRNA transfection

In order to interfere with PKA activity, expression and intracellular localization, the following plasmids were used for transfection of U87 cells:

- **pLX303**: Gateway destination vector (Yang et al. 2011) used for generation of recombinant pLX303 plasmids for overexpression of specific PKA subunits
- **pLX303-PRKACG**, for overexpression of PKA CG subunit
- **pLX303-PRKACA**, for overexpression of PKA CA subunit
- **pLX303-PRKAR2A**, for overexpression of PKA R2A subunit
- **pLX303-PRKAR2B**, for overexpression of PKA R2B subunit
- **pMC36-PRKACAwt**, encoding the wild type PKA CA subunit
- **pMC36-PRKACAmut**, encoding a mutant isoform of PKA CA subunit, that carries two mutations preventing inactivation by regulatory subunits without compromising catalytic

activity. Expression of mutant PKA CA thus induces PKA hyperactivation (Orellana and McKnight 1992; Clegg et al. 1988).

- **pMT-REV$_{AB}$-neo**: expression vector that encodes a dominant negative form of PKA R1A (R1a-DN) containing point mutations in both cAMP binding sites, which prevent cAMP binding and catalytic subunit activation. Expression of this construct thus results in repression of PKA activity (Hayashida et al.2006).
- **pEGFP-sAKAPis**: plasmid encoding EGFP fused to the PKA type-II anchoring inhibitor sAKAPis, that specifically displaces PKA R2A subunit by binding to the AKAP binding site of PKA (McKenzie et al. 2011)
- **pEGFP-sAKAPis-SCR**: plasmid encoding EGFP fused to the scrambled peptide of sAKAPis (McKenzie et al. 2011)
- **pmCherry-sAKAPis**: plasmid encoding the mCherry protein fused to the sAKAPis peptide (McKenzie et al. 2011)
- **pmCherry-sAKAPis-SCR**: plasmid encoding the mCherry protein fused to the scrambled peptide of sAKAPis (McKenzie et al. 2011)
- **pEGFP-RIAD**: plasmid encoding EGFP fused to the PKA type-I anchoring disrupter RIAD, that specifically displaces PKA R1A subunit by binding to the AKAP binding site of PKA (McKenzie et al. 2011)
- **pEGFP-RIAD-SCR**: plasmid encoding EGFP fused to the scrambled peptide of RIAD (McKenzie et al. 2011).

Cloning details for generation of recombinant pLX303 plasmids are reported in Zorzan 2014 (see Appendix A1). The expression vectors pMC36-PRKACAwt and pMC36-PRKACAmut vectors were kindly provided by Professor G. Stanley McKnight (University of Washington, Seattle, United States of America). The pMT-REV$_{AB}$-neo plasmid was provided by Professor Pyong Woo Park (Baylor College of Medicine, Houston, Texas, United States of America). Plasmids coding EGFP or mCherry fused to RIAD, sAKAPis and their scrambled controls were a kind gift from Professor Alan K. Howe (University of Vermont College of Medicine, Burlington, Vermont, United States of America).

All described plasmids were managed in RbCl competent *E. coli* XL-gold bacterial cells according to standard procedures (par. 3.7 and 3.8) and using proper antibiotic (ampicillin or kanamycin) selection system.

Downregulation of PKA expression was induced through transfection of U87 cells with siRNA targeting specific PKA subunits:

- **siRNA-PRKAR2A** (Santa Cruz Biotechnology™, cat. n° sc-39165), for silencing of PKA R2A expression;
- **siRNA-PRKACA** (Sigma-Aldrich™, cat. n° EHU132541), for silencing of PKA CA expression.

Transfection of U87 cells with PKA interfering plasmids and siRNA was performed using lipofectmine reagents, as described in par. 3.12. Time lapse and immunofluorescence experiments were carried out 72 hours post-transfection to evaluate cell motility and PKA intracellular distribution in transfected cells.

3.6 Preparation of chemically competent *E. coli* bacterial cells

Bacterial *E. coli* cells, XL Gold and DH5α strains, were made chemically competent through either Rubidium Cloride (RbCl) or Calcium Chloride ($CaCl_2$) methods.

To prepare RbCl competent XL Gold cells, a single bacterial colony was inoculated into 5 ml of LB medium and grown overnight at 37°C with shacking at 118 rpm. The following day 1 ml of bacterial culture was added to two separate flasks with 100 ml of LB each and grown to an optical density of 0.6 at the wavelength of 600 nm. The bacterial culture was chilled on ice for 20 minutes and centrifuged at 5100 rpm for 5 minutes at 4°C. The pellet was resuspended in 60 ml of cold TFB I solution (30 mM KOAc, 50 mM $MnCl_2$, 100 mM RbCl, 10 mM $CaCl_2$, 15% (v/v) glycerol; pH 5.8) and shaked on ice for 20 minutes. Cell suspension was centrifuged again at 5100 rpm for 5 minutes at 4°C and gently resuspended in 8 ml of cold TFB II solution (10 mM NaMOPS pH 7.0, 75 mM $CaC1_2$, 10 mM RbC1, 15% (v/v) glycerol; pH 7.0). After incubation on ice for 30 minutes, RbCl competent cells were aliquoted and stored at -80°C.

For preparation of $CaCl_2$ competent DH5α cells, a single bacterial colony was inoculated into 3 ml of LB medium added with $MgCl_2$ (15 mM), and grown for 16 hours at 37°C with shaking at 118 rpm. The obtained bacterial suspension was used to inoculate 200 ml of the same LB medium and then incubated at 37°C until reaching an optical density of 0.4-0.6 at the wavelength of 600 nm. The bacterial culture was rapidly put on ice to stop cell growth and centrifuged at 3500 rpm for 15 minutes at 4°C. The pellet was resuspended in 50 ml of a cold solution containing $MnCl_2$-$4H_2O$ (10 mM), $CaCl_2$ (50 mM), MES [2-(N-morpholino)ethanesulfonic acid] (10 mM, pH 6.3), and

centrifuged again as previously. The bacterial pellet was resuspended in 5 ml of the same cold solution added with 15% (v/v) glycerol, finally aliquoted and stored at -80°C.

3.7 Transformation of chemically competent *E. coli* bacterial cells

Bacterial transformation was performed through heat shock treatment according to the following standard protocol:

- chemically competent *E. coli* XL Gold or DH5α cells stored at -80°C were thawed on ice for a few minutes;
- 50-100 ng of plasmid DNA were added to 50 µl of competent cells;
- the competent cells/DNA mixture was gently mixed by flicking the bottom of the tube with finger a few times and then placed on ice for 30 minutes;
- heat shock was induced by incubation of bacterial cells in 37°C water bath for 4 minutes, immediately followed by incubation on ice;
- 200 µl of LB medium without antibiotics were added to transformed cells and bacteria were then incubated in 37°C water bath for 45 minutes in order to allow the synthesis of proteins responsible for antibiotic resistance;
- 40-80 µl of transformed cells were finally plated on 10 cm LB 1.5% agar Petri dishes containing the appropriate antibiotic (50 µg/ml kanamicine or 100 µg/ml ampicillin) and incubated at 37°C for 16 hours.

For transformation of bacterial cells with ligation products, the entire volume of the ligation reaction was used and all transformed cells were plated on LB agar plates.

3.8 Plasmid preparation

Single bacterial colonies grown on LB agar plates were inoculated into 3 ml of LB medium containing the appropriate antibiotic and grown for 16 hours at 37°C with shaking at 118 rpm. For screening of a high number of colonies, plasmid DNA was extracted according to the following alkaline lysis miniprep protocol:

- 1.5 ml of bacterial culture was centrifuged at 13000 rpm for 5 minutes at 4°C;

- the bacterial pellet was resuspended in 100 µl of cold GTE solution (50 mM glucose; 25 mM Tris-HCl, pH 8.0; 10 mM EDTA, pH 8.0);
- 200 µl of lysis buffer (0.2 M NaOH, 1% sodium dodecyl sulfate (SDS)) were added to induce solubilisation of bacterial cell proteins and membranes and DNA denaturation;
- 150 µl of cold 5 M potassium acetate were added to induce precipitation of chromosomal DNA, proteins and cell debris;
- the mixture was centrifuged at 13000 rpm for 10 minutes at 4°C;
- the supernatant was transferred to a clean tube and 1 ml of 96% (v/v) ethanol was added to induce precipitation of plasmid DNA;
- the mixture was centrifuged again at 13000 rpm for 20 minutes at 4°C;
- DNA pellet was washed in 200 µl of 70% (v/v) ethanol and dried at 65°C for 3-5 minutes;
- plasmid DNA was resuspended in 20 µl of TE buffer (10 mM Tris-HCl; 1 mM EDTA, pH 7.4) containing 20 µg/ml RNase A.

Plasmid preparation was then incubated at 37°C for 30 minutes to allow RNA degradation by RNase A and finally stored at -20°C.

When higher plasmid purity was required (ex. cloning, Sanger sequencing, eukaryotic cell transfection), QIAGEN Plasmid Mini Kit (Qiagen, cat. n° 12123) or QIAGEN Plasmid Maxi Kit (Qiagen, cat. n° 12162) were used according to the manufacturer's instructions, to extract plasmid DNA from 3 ml or 200 ml of bacterial cultures, respectively. Concentration and purity of plasmid preparations were then determined by Nanodrop™ analysis.

3.9 Generation of recombinant plasmids for expression of fluorescently-tagged PKA subunits

A set of recombinant plasmids for expression of PKA subunits (R1A, R2A, R2B, CA and CB) in fusion with fluorescent EGFP protein was generated. The obtained plasmids are useful to investigate the intracellular localization of tagged subunits in live and fixed cells, as well as for functional study of PKA in many cellular models. For this purpose, cDNA coding human PKA subunits was cloned in the eukaryotic expression plasmid pEGFP-C1, that allows expression of cloned proteins fused to the C-terminal of EGFP under the control of human Cytomegalovirus (hCMV) promoter. In the present study, recombinant pEGFP-C1-PRKAR1A, pEGFP-C1-PRKACA and pEGFP-C1-PRKACB plasmids for expression of, respectively, EGFP-fused PKA R1A, CA and CB subunits, were generated and cloning details are reported in the following sections.

Recombinant pEGFP-C1-PRKAR2A and pEGFP-C1-PRKAR2B plasmids, for expression of EGFP-fused PKA R2A and R2B respectively, had been previously generated according to the same protocols (Zorzan 2014).

3.9.1 RNA extraction, RT-PCR and PCR

Total RNA was first extracted from HeLa cells using the commercial kit Quick-RNA™ MiniPrep (Zymo Research, cat. n° R1054) according to the manufacturer's instructions. Extracted RNA was stored at -80°C and quantified by Nanodrop™ (NanoDrop 1000 Spectophotometer, Thermo Scientific) analysis.

For cDNA synthesis, RNA was incubated at 70°C for 5 minutes with 3 µM oligo(dT) primers (Invitrogen, cat. n° 18418-020), stretches of 20 deoxythymidines that anneal to poly(A) tails of eukaryotic mRNAs. After a brief incubation on ice to prevent the super-folding of the annealed structures, deoxynucleotide triphosphates (dNTPs) and reverse transcriptase M-MLV RT (Promega, cat. n° M1701) were added. The reaction was incubated at 42°C for 60 minutes and then at 92°C for 10 minutes. Synthesized cDNA was stored at -20°C and quantified by Nanodrop™ analysis.

The cDNA coding for human PKA R1A, CA and CB subunits was amplified by PCR with TopTaq DNA Polymerase (Qiagen, cat. n° 200205) and specific primers (Table 3.1) inserting XhoI and BamHI restriction sites.

Primer	**Sequence (5'-3')**
PKA R1A XhoI forward	TAAGCA**CTCGAG**GCATGGAGTCTGGCAGTA
PKA R1A BamHI reverse	TGCTTA**GGATCC**TCAGACAGACAGTGACAC
PKA CA XhoI forward	TAAGCA**CTCGAG**GCATGGCTTCCAACTCCA
PKA CA BamHI reverse	TGCTTA**GGATCC**CTAAAACTCAGAAAACT
PKA CB XhoI forward	TAAGCA**CTCGAG**GCATGGGGAACGCGGCGA
PKA CB BamHI reverse	TGCTTA**GGATCC**TTAAAATTCACCAAATTC

Table 3.1 - Forward and reverse primers used for PCR amplification of cDNA coding for human PKA R1A, CA and CB subunits. Restriction sites sequences are reported in bold red.

PCR protocol for amplification of PKA R1A, CA and CB cDNA was as follows:

- 94°C for 3 minutes
- 33 cycles:
  94°C for 30 seconds
  58°C for 30 seconds
  72°C for 1 minute 30 seconds
- 72°C for 10 minutes.

Following amplification, PCR products were verified on 0.8% agarose gel, based on expected amplicon length of 1172, 1059 and 1083 nucleotides (nt) for PKA R1A, CA and CB subunits respectively.

3.9.2 Restriction, ligation and plasmid verification

PCR products and the eukaryotic expression plasmid pEGFP-C1 were submitted to digestion by XhoI (Invitrogen, cat. n° 15231-012) and BamHI (Invitrogen, cat. n° 15201-023) restriction enzymes. The reactions were set up in proper restriction buffer and incubated at 37°C for 3 hours. Restriction products were then analyzed on 0.8% agarose gel and DNA fragments of interest were extracted and purified using QIAquick Gel Exctraction Kit (Qiagen, cat. n° 28704) according to the manufacturer's instructions.

Ligation reactions between purified PKA R1A, CA or CB insert and digested pEGFP-C1 plasmid were set up in specific ligation ATP buffer with 2 units of T4 DNA Ligase (Invitrogen, cat. n° 15224-041). The reaction was incubated for 10 minutes at room temperature and 15 minutes at 4°C. Ligation products were then used for transformation of competent *E. coli* XL-Gold cells (par. 3.7) and transformed cells were plated on LB agar plates containing 50 μg/ml kanamicine.

The following day liquid cell cultures were started from single colonies grown on the plates. DNA plasmids were purified (par. 3.8) from bacterial cultures resulting positive to PCR for amplification of cloned PKA subunits. Restriction reactions, PCR and Sanger sequencing (par. 3.11) were performed to verify correct recombination of pEGFP-C1 plasmid with PKA R1A, CA and CB cDNA.

3.10 Third-generation lentiviral vectors

Third-generation replication-defective lentiviral particles may represent an efficient strategy for targeting human GBM cells (Sumuru Bayin et al. 2014; Tang et al. 2016; Wang et al. 2016). In the present study recombinant lentiviral vectors carrying shRNA sequences were generated in order to induce downregulation of PKA R2A expression in GBM cells.

The lentiviral transfer vector used for delivery of shRNA sequences was **cPPT.hCMV.eGFP**. This is an HIV-1 based *Self-Inactivating* (SIN) lentiviral vector, which presents the RSV U3 region in the 5' LTR and a partially deleted 3'-LTR U3 region. It contains the EGFP gene, that was previously cloned in the multiple cloning site of the vector under the control of a hCMV promoter. The plasmid is further characterized by PBS (Primer Binding Site) and *cis*-acting cPPT (central polypurine tract) sequences for increased vector transduction efficiency, a part of *gag* gene, the RRE (Rev Responsive Element) sequence and the WPRE (Woodchuck Hepatatis C Virus Post-transcriprional Regulatory Element) sequence for increased transgene expression in target cells. The presence of the SV40 origin of replication allows the efficient replication of the plasmid in cells constitutively expressing the SV40 T-antigen.

The lentiviral transfer vector **pLentiLox.7** (**pLL3.7**) was also tested for transduction of human GBM cells. It is a *Self-Inactivating* (SIN) lentiviral vector, based on HIV-1, presenting a hybrid 5' LTR in which the U3 region is replaced with the CMV promoter and enhancer sequences. The construct contains the mouse U6 promoter upstream of a multiple cloning site for transgene insertion and a CMV-EGFP expression cassette (Rubinson et al. 2003). The plasmid is also characterized by packaging signal (ψ), *cis*-acting cPPT (central polypurine tract) sequence for increased vector transduction efficiency, central termination sequence (CTS), a part of *gag* gene, the RRE (Rev Responsive Element) sequence and the WPRE (Woodchuck Hepatatis C Virus Post-transcriprional Regulatory Element) sequence for increased transgene expression in target cells. The presence of the SV40 origin of replication allows the efficient replication of the plasmid in cells constitutively expressing the SV40 T-antigen.

The packaging system for both lentiviral transfer vectors includes the following plasmids:

- **pMDL**, containing the *gag* and *pol* genes of HIV-1 placed under the control of the hCMV promoter. The RRE sequence and the polyadenylation signal from the human β-globin gene are also present.

- **pVSV$_G$**, containing the VSV-G (Vesicular Stomatitis Virus envelope glycoprotein G) gene under the control of the hCMV promoter and the polyadenylation signal from the human β-globin gene.
- **pRSVREV**, containing the HIV-1 *rev* gene under the control of the CMV promoter and the polyadenylation signal from the human β-globin gene.

The transfer vectors and the packaging plasmids contain the bacterial origin of replication ColE1 and the ampicillin resistance gene. For amplification of plasmids $CaCl_2$ competent *E. coli* DH5α bacterial cells were used according to standard protocols (par. 3.7 and 3.8).

3.10.1 Cloning of shRNA targeting PKA R2A in cPPT.hCMV.eGFP vector

Lentiviral vectors can be engineered for stable and efficient delivery of short hairpin RNAs (shRNAs) in a wide variety of cells (Sakuma et al. 2012). In gene-silencing lentiviral vectors, shRNAs can be expressed from a RNA Polymerase III promoter (Pol-III; i.e. U6 promoter in pLL3.7) or as a part of an miRNA-like structure from RNA Polymerase II promoters (Pol-II; i.e. hCMV promoter in cPPT.hCMV.eGFP). In the latter case, synthetic shRNA are embedded into the context of endogenous microRNAs (miRNAs) and mimic the pri-miRNAs in the endogenous RNA interference (RNAi) pathway. Once transcribed, the resulting hairpin-like structures are recognized and processed first by the Drosha/DGCR8 microprocessor complex and then in the cell cytoplasm by the Dicer/TRBP complex, which releases mature small RNA duplexes. The guide strand of the RNA duplex acts as guide to downregulate the expression of complementary mRNA transcripts. In the present study oligonucleotides coding for shRNAs targeting PKA R2A were cloned under the control of Pol-II hCMV promoter of cPPT.hCMV.eGFP vector for the subsequent production of recombinant lentiviral particles.

3.10.1.1 PCR amplification of PKA R2A shRNA sequences and cloning strategies

In a recent work Fellmann and colleagues identified an optimized miRNA backbone, termed "miR-E", which strongly increases knockdown efficacy through enhanced pri-miRNA processing and consequent higher mature small RNA levels (Fellmann et al. 2013). For all human and mouse coding genes they also provided a list of ten 97-mer oligonucleotides for shRNA predicted to target all known transcript variants (Fellmann et al. 2013). In the present study, top-ranked

oligonucleotides Temp1 and Temp2 for PKA R2A shRNA were selected for generation of recombinant gene-silencing lentiviral particles.

PKA R2A Temp1 and Temp2 shRNA were PCR amplified using the primers miRE-Xho-fw and miRE-EcoOligo-rev, 0.05 ng oligonucleotide template and the PfuUltra™ HF DNA polymerase (Agilent Technologies, cat. n° 600380-51). Temp1 and Temp2 oligonucleotides and primer sequences are reported in Table 3.2.

97-mer oligonucleotide or primer	**Sequence (5'-3')**
PKA R2A Temp1 shRNA	TGCTGTTGACAGTGAGCGC**AGCAGATTTAATAGACGAGTA** TAGTGAAGCCACAGATGTA**TACTCGTCTATTAAATCTGCT** **A**TGCCTACTGCCTCGGA
PKA R2A Temp2 shRNA	TGCTGTTGACAGTGAGCGA**CCGCTCTGTTGGTCAATATGA** TAGTGAAGCCACAGATGTA**TCATATTGACCAACAGAGCGG** **G**TGCCTACTGCCTCGGA
miRE-Xho-fw	TGAA**CTCGAG**AAGGTATATTGCTGTTGACAGTGAGCG
miRE-EcoOligo-rev	TCTC**GAATTC**TAGCCCCTTGAAGTCCGAGGCAGTAGGC

Table 3.2 - 97-mer oligonucleotides for PKA R2A shRNAs, forward and reverse primer sequences, from Fellmann et al. 2013. Guide and passenger strands of PKA R2A shRNA are reported in bold blue and bold green, respectively. XhoI and EcoRI restriction sites, inserted by forward and reverse primers respectively, are reported in bold red.

PCR protocol for amplification of PKA R2A Temp1 and Temp2 shRNA sequences was as follows:

- 95°C for 5 minutes
- 30 cycles:
  95°C for 25 seconds
  56°C for 25 seconds
  72°C for 30 seconds
- 72°C for 7 minutes.

Following amplification, the 125 nt shRNA fragments Temp1 and Temp2 were XhoI/EcoRI cloned into the eukaryotic expression plasmid pEGFP-C1. Recombinant pEGFP-C1-shTemp1 and pEGFP-C1-shTemp2 were verified by PCR and restriction reactions.

Two parallel cloning strategies were then followed to generate recombinant cPPT.hCMV.eGFP vectors for expression of either transcripts coding PKA R2A shRNAs or polycistronic transcripts for both EGFP synthesis and PKA R2A shRNA biogenesis:

1. **cPPT.hCMV.shTemp1 and cPPT.hCMV.shTemp2 vectors:**
   recombinant pEGFP-C1-shTemp1 and pEGFP-C1-shTemp2 were submitted to BglII/SalI restriction reactions and shRNA fragments Temp1 and Temp2 were cloned into BamHI/SalI digested cPPT.hCMV.eGFP vector. The obtained constructs express PKA R2A shRNA Temp1 or Temp2 under the control of hCMV promoter and do not express the green fluorescent protein as the eGFP gene was deleted by BamHI/SalI restriction of the lentiviral vector.

2. **cPPT.hCMV.EGFP.shTemp1 and cPPT.hCMV.EGFP.shTemp2 vectors:**
   recombinant pEGFP-C1-shTemp1 and pEGFP-C1-shTemp2 were submitted to NheI restriction, blunting of overhangs by DNA Polymerase I Large (Klenow) Fragment and SalI restriction to generate fragments including the EGFP gene and the Temp1 or Temp2 shRNA sequence. These fragments were then cloned into the cPPT.hCMV.eGFP vector previously submitted to BamHI restriction, DNA Polymerase I Large (Klenow) Fragment-mediated blunting of overhangs and SalI restriction. The generated recombinant constructs express transcripts coding both the EGFP and the PKA R2A shRNA Temp1 or Temp2. As a consequence, in cells transduced with these recombinant lentiviral vectors, part of the polycistronic transcripts are recognized and processed in the RNA interference pathway, whereas another fraction of the transcripts is available for reporter EGFP protein expression.

All recombinant cPPT.hCMV.eGFP-based lentiviral vectors carrying PKA R2A shRNA sequences were verified as reported in the following section.

3.10.1.2 Restriction, ligation and plasmid verification

Restriction reactions were performed with restriction enzymes from New England Biolabs (BamHI cat. n° R0136S, BglII cat. n° R0144S, NheI cat. n° R0131S, SalI cat. n°R0138S) in proper restriction buffers and were incubated at 37°C in humidified environment for 1-3 hours, depending on quantity of DNA to be digested. When necessary, DNA blunting of overhangs was achieved using DNA Polymerase I Large (Klenow) Fragment (New England Biolabs, cat n° M0210S) in proper reaction buffer and incubating the reaction at 37°C for 30 minutes and then at 75°C for 20 minutes to inactivate the enzyme. DNA fragments were analyzed on 1% agarose gel, extracted and purified using QIAquick Gel Exctraction Kit according to the manufacturer's instructions.

Ligation reactions were set up with T4 DNA Ligase (New England Biolabs, cat. n° M0202S) in proper ligation buffer. Quantities of insert and vector DNA were determined according to the following formula:

$$insert\ (ng) = \frac{insert\ (bp) \times vector\ (ng)}{vector\ (bp)}$$

In each ligation reaction around 150 ng of vector DNA were used, with a vector/insert ratio ranging from 1:3 to 1:8. Ligation reactions were incubated overnight at 16°C in thermocycler and the following day ligation products were used for transformation of $CaCl_2$ competent *E. coli* DH5α bacterial cells. Transformed cells were plated on LB agar plates containing proper antibiotic (50 μg/ml kanamicine for recombinant pEGFP-C1 plasmids, 100 μg/ml ampicillin for recombinant cPPT.hCMV.eGFP vectors).

Single colonies grown on the plates were inoculated into LB medium supplemented with kanamicine or ampicillin and screened for correct DNA recombination. For this purpose, plasmid DNA was extracted from all bacterial cultures using the alkaline lysis miniprep protocol (par. 3.8) and subsequently submitted to restriction reaction to verify the presence of the DNA insert. Sanger sequencing was then performed to finally confirm the correct sequence of selected recombinant plasmids.

Primer	Sequence (5'-3')
CMV Forward	CGCAAATGGGCGGTAGGCGTG
WPRE-R	CATAGCGTAAAAGGAGCAACA

Table 3.3 - Primers used for Sanger sequencing of recombinant cPPT.hCMV.eGFP-based vectors.

CMV Forward and WPRE-R reverse primers (Table 3.3), annealing respectively to the CMV promoter and the WPRE sequence of cPPT.hCMV.eGFP plasmid, were used for Sanger sequencing of generated recombinant lentiviral vectors (par. 3.11).

3.10.2 Cloning of scrambled shRNA in cPPT.hCMV.eGFP vector

Parallel to the construction of PKA R2A gene-silencing lentiviral vectors, a scrambled control vector was also generated in order to investigate off-target effects induced by PKA R2A shRNAs. For this aim, the scrambled sequence of PKA R2A Temp1 shRNA was designed and cloned under the control of Pol-II hCMV promoter of cPPT.hCMV.eGFP vector using a cloning strategy similar to those previously described for cloning of PKA R2A Temp1 and Temp2 shRNAs.

3.10.2.1 Scrambled design

The GenScript program (https://www.genscript.com/ssl-bin/app/scramble) was used to create a negative control for PKA R2A shRNA. The guide sequence of PKA R2A Temp1 shRNA was inserted as input sequence in the GenScript software, which returned a scrambled sequence having the same nucleotide composition as the guide strand of Temp1 shRNA and no match with any mRNA in the mRNA pool of human species. The absence of cellular targets was further verified by use of the SpliceCenter/siRNACheck software (http://projects.insilico.us/SpliceCenter/siRNACheck.jsp), which confirmed that no human gene splice variants were targeted by the designed scrambled sequence nor its complementary passenger strand, even with one or two mismatches allowed. In addition, Nucleotide BLAST 2.7.0+ program (https://blast.ncbi.nlm.nih.gov/Blast.cgi?PROGRAM=blastn&PAGE_TYPE=BlastSearch&LINK_LOC=blasthome; Stephen et al. 1997) was interrogated with the designed scrambled guide and passenger strands, producing no significant alignments with human gene transcripts in NCBI Transcript Reference Sequence (RefSeq) database. The guide and passenger strands of Temp1

shRNA were thus replaced by the designed scrambled guide and passenger strands, respectively, generating a 97-mer oligonucletotide that coded for a scrambled shRNA, named shSCR.

3.10.2.2 PCR amplification of scrambled shRNA sequence and cloning strategies

Scrambled shRNA (Table 3.4) was PCR amplified using the primers miRE-Xho-fw and miRE-EcoOligo-rev (Table 3.2), 0.05 ng scrambled oligonucleotide template and EconoTaq® PLUS GREEN 2X Master Mix (Lucigen, cat. n° 30033-0).

97-mer oligonucleotide	**Sequence (5'-3')**
Scrambled shRNA	TGCTGTTGACAGTGAGCGC**TAATTAACGAGACAGGTTAAT** TAGTGAAGCCACAGATGTA**ATTAACCTGTCTCGTTAATTA** **C**TGCCTACTGCCTCGGA

Table 3.4 - Designed 97-mer oligonucleotide for scrambled shRNA. Scrambled guide and passenger strands are reported in bold blue and bold green, respectively.

PCR protocol for amplification of scrambled shRNA sequence was as follows:

- 95°C for 5 minutes
- 30 cycles:
  95°C for 30 seconds
  56°C for 30 seconds
  72°C for 1 minute
- 72°C for 7 minutes.

Following amplification, the 125 nt scrambled shRNA fragment was verified on 1% agarose gel and cloned in the pCR®2.1-TOPO® vector using the TOPO TA Cloning kit (Invitrogen, cat. n° K4500-01). For this purpose, addition of 3' adenine-overhangs to amplified shSCR DNA was previously performed by adding EuroTaq DNA Polymerase (Euroclone, cat. n° EME010250) and dATP (deoxyadenosine triphosphate) 10 mM directly to the PCR products and incubating the reaction at 72°C for 10 minutes. The TOPO® cloning reaction was then set up using 4 µl of PCR products with 3' adenine-overhangs, 1 µl of salt solution (1.2 M NaCl, 0.06 M $MgCl_2$) and 1 µl of TOPO® vector. The reaction mix was incubated for 1-2 hours at room temperature and transformed into $CaCl_2$ competent *E. coli* DH5α bacterial cells. Transformed bacteria were plated on LB agar plates

containing 100 μg/ml ampicillin and spread with 40 mg/ml X-gal (5-Bromo-4-chloro-3-indolyl-β-D-galactopyranoside) for visual analysis of bacterial colonies based on α-complementation of the β-galactosidase gene (*lacZ*). The following day, white and light blue colonies grown on the plates were inoculated into LB medium supplemented with ampicillin and screened for correct shSCR sequence-containing clones. Thus, plasmid DNA was extracted from bacterial cultures by alkaline lysis miniprep protocol (par. 3.8), submitted to restriction reaction and Sanger sequencing using M13 Forward (-20) and M13 Reverse primers provided by TOPO TA Cloning kit (par. 3.11).

The scrambled shRNA insert from selected recombinant pCR®2.1-TOPO® vector was then XhoI/EcoRI cloned into the eukaryotic expression plasmid pEGFP-C1, generating the pEGFP-C1-shSCR, which was verified by PCR and restriction reactions. Similarly to previous cloning of PKA R2A shRNAs, recombinant pEGF-C1-shSCR was submitted to BglII/SalI restriction reaction and shSCR fragment was cloned into BamHI/SalI digested cPPT.hCMV.eGFP vector. The obtained cPPT.hCMV.shSCR vector expresses the designed scrambled shRNA under the control of hCMV promoter and does not express the green fluorescent protein as the eGFP gene was deleted by BamHI/SalI restriction of the lentiviral vector.

3.10.2.3 Restriction, ligation and plasmid verification

Restrictions, ligation reactions and plasmid verification were performed as previously reported for cloning of PKA R2A shRNAs (par. 3.10.1.2). In addition to recombinant pCR®2.1-TOPO® sequencing, Sanger sequencing of purified cPPT.hCMV.shSCR vectors was also performed using primers reported in Table 3.3, as final confirmation of correct recombination of scrambled shRNA sequence with the lentiviral vector.

3.10.3 Secondary structure prediction of shRNA

The 'mfold web server' software (version 3.5; Zuker 2003; http://unafold.rna.albany.edu/?q=mfold) was used to predict folding of PKA R2A Temp1 and Temp2 shRNA sequences. As an independent indication of proper scrambled design, the secondary structure predicted for scrambled shRNA was also compared to PKA R2A shRNAs secondary structure predictions.

3.11 Sanger sequencing

In order to verify the correct sequence of all generated recombinant plasmids, Sanger sequencing was performed using the BigDye® Terminator v3.1 Cycle Sequencing Kit (Applied Biosystems, cat. n° 4337455) according to the manufacturer's instructions. Each sequencing reaction included 200-250 ng of plasmid DNA as template, 1 µl of 1 µM primer, 1 µl of 5X buffer (Tris-HCl 200 mM, pH 9, MgCl2 5 mM), 1 µl of Big Dye® mix, containing AmpliTaq® DNA polymerase, dNTPs and dideoxynucleotide triphosphates (ddNTPs) for DNA chain termination, and diethylpyrocarbonate (DEPC) water to a final volume of 10 µl.
Cycling parameters of sequencing PCR reactions were as follows:

- 95°C for 10 minutes
- 35 cycles:
  95°C for 10 seconds
  50°C for 10 seconds
  62°C for 4 minutes
- 62°C for 7 minutes.

Products of sequencing reactions were purified by precipitation first in 50 µl of ethanol 96% (v/v) and 2 µl of sodium acetate (3 M, pH 5.2) and secondly in 150 µl of ethanol 70% (v/v). Samples were then resuspended in 15 µl of formamide and denatured at 95°C for 4 minutes. Capillary electrophoresis of DNA extension fragments was finally performed in the automated sequencer ABI PRISM 3100 Genetic Analyzer (Applied Biosystems).

3.12 Human cell transfection

Transfection of human cells with plasmids or siRNA was performed using, respectively, Lipofectamine® 2000 (Thermo Fisher Scientific, cat. n° 11668027) and Lipofectamine® RNAiMAX (Thermo Fisher Scientific, cat. n° 13778030) according to manufacturer's instructions. Briefly, 24 hours before transfection cells (2.5×10^4 U87 cells/well in 24-well plates or 2.5×10^5 293T cells/well in 6-well plates) were seeded to be 60-80% confluent at transfection. Cells were then transfected with 5 pmol of siRNA or 500-1500 ng (depending on well plate format) of plasmid DNA, properly diluted in DMEM medium without FBS. For transfection of 293T cells with PKA R2A gene-silencing lentiviral vectors, 500 ng of pRSV-Rev plasmid were used together with 1500 ng of

lentiviral transfer vector. Cell medium containing transfection reagents was finally replaced with DMEM 10% FBS 4 hours after transfection.

3.13 Production of recombinant lentiviral particles

Lentiviral particles were produced in 293T cells through co-transfection of transfer vector and packaging plasmids pVSVG, pMDL and pRSVREV, using Calcium Phosphate reagents. Briefly, 24 hours before transfection, 12×10^6 293T cells were plated in 20 ml of DMEM 10% FBS medium in T-150 flasks. The following day, one transfection mix per flask was prepared as follows:

- 1.75 ml TE (Tris-HCl 10 mM pH 8, EDTA 1 mM pH 8) 1:10
- 10 µl pVSVG plasmid 1 µg/µl
- 10 µl pMDL plasmid 1 µg/µl
- 10 µl pRSVREV plasmid 1 µg/µl
- 20 µl lentiviral transfer vector 1 µg/µl
- 200 µl $CaCl_2 \cdot H_2O$ 2.5 M.

Then, 2 ml of 2X HPB pH 7.1 (5 M NaCl, 0.5 M HEPES pH 7.1, 0.15 M $Na_2HPO_4 \cdot 2\ H_2O$) were added dropwise to each transfection mixture and bubbles were produced with a Pasteur pipette for 15-22 seconds before adding the transfection mixture dropwise all over the cell flask. Around 3.5-4 hours after transfection, cells were washed twice with PBS and 20 ml of DMEM 10% FBS were added. Lentiviral particles were collected in the supernatant 48 hours post-transfection: culture supernatants were centrifuged at 700 rpm for 10 minutes at 4°C, passed through 0.45-µm filters, aliquoted and stored at -80°C. When required, recovered lentiviral particles were concentrated through ultracentrifugation (Optima™ L-90K Ultracentrifuge Beckman) at 27000 rpm for 2 hours at 4°C and then resuspended in DMEM 10% FBS or Neurobasal medium. Viral titre was determined by reverse transcriptase activity assay (par. 3.14.3) and p24 assay (par. 3.14.2). Lentiviral vectors carrying EGFP reporter gene were also titrated through transduction of 293T cells with serial dilutions of lentivirus and subsequent flow-cytometry analysis (par. 3.14.1).

3.14 Titration of recombinant lentiviral particles

For quantification of recombinant lentiviral particles, different methods were used: flow cytometry analysis, p24 assay and reverse transcriptase (RT) activity assay.

3.14.1 Flow cytometry analysis

Viral titre of lentiviral vectors carrying EGFP reporter gene was determined through transduction of 293T cells with serial dilutions of lentiviral particles and subsequent flow cytometry analysis. Briefly, 24 hours before transduction, 2.5×10^5 293T cells/well were plated in 2 ml of DMEM 10% FBS medium in 6-well plates. The following day, lentiviral vectors were thawed on ice and serial dilutions of lentiviral particles in DMEM 10% FBS medium were prepared. 293T cells were transduced by removing the old medium and adding 1 ml per well of diluted lentiviral vector. Around 8 hours later, 1 ml of DMEM 10% FBS was added to each well. Transductions were performed in duplicate, with at least two non-transduced control wells. 72 hours post-transduction cell samples were prepared for flow cytometry analysis: transduced and control non-transduced cells were detached with 1 ml of cold PBS and centrifuged at 1200 rpm for 7 minutes at 4°C. Cell pellets were washed again two times in 500 µl of cold PBS, centrifuged as above and finally resuspended in 500 µl of cold PBS. Cells were analyzed for EGFP expression using a FACScalibur™ (BD Biosciences). For titer calculations dilutions yielding 1% to 20% EGFP-positive cells were considered and viral titre was calculated using the following equation:

$$titre\ (transducing\ unit/ml) = \frac{number\ of\ transduced\ cells \times dilution\ factor \times \left[\frac{\%\ of\ EGFP-positive\ cells}{100}\right]}{volume\ of\ transducing\ supernatant\ in\ ml}$$

The number of EGFP-positive cells may not be reliably determined below 1% as the FACS may not be accurate enough. Conversely, above 20% the number of transducing particles could be underestimated because the chance for each EGFP-positive cell to be transduced twice significantly increases.

3.14.2 p24 assay

Total particle concentration of all recombinant lentiviral vectors was determined using INNOTEST® HIV Antigen mAb (Fujirebio, cat. n° INX88020), an enzyme immunoassay for qualitative and quantitative detection of HIV-1 core antigen p24. The assay was performed according to manufacturer's instructions in multiwell plates coated with human polyclonal antibodies to HIV. Briefly, proper dilutions of lentiviral vector preparations were incubated in coated test wells together with a mixture of biotinylated anti-p24 monoclonal antibodies. After biotin binding to peroxidase-conjugated streptavidin, peroxidase chromogen substrate was added to test wells producing a blue color, which turned yellow when the reaction was stopped with sulfuric acid. Absorbance at 450 nm was finally measured for each test well with a Tecan Sunrise™ absorbance microplate reader. Interpolation of absorbance values of lentiviral samples with a standard curve allowed determination of p24 antigen concentration. This assay is important to monitor the efficiency of vector production and packaging, but does not evaluate the transduction capability of lentiviral vectors as high p24 concentrations can be measured from viral particles devoid of genomic RNA or envelope protein.

3.14.3 Reverse transcriptase (RT) activity assay

The RT assay was used for the quantitative determination of viral RT activity as previously described by Rho and colleagues (Rho et al. 1981). Briefly, lentiviral particles in 500 µl of filtered culture supernatant or 25 µl of concentrated viral preparation were precipitated by centrifugation at 13000 rpm for 2 hours at 4°C. The precipitate was resuspended in 10 µl of a buffer containing 50 mM Tris-HCl pH 7.5, 1mM dithiothreitol (DTT), 20% glycerol, 250 mM KCl and 0.25% Triton X-100, transferred in dry ice and lysed through three cycles of freezing and thawing. The sample was added to a reaction mixture containing 50 mM Tris-HCl pH 7.5, 7.5 mM MgCl2, 0.05% Triton X-100, 5 mM DTT, 100 µg/ml polyA, 10 µg/ml oligo-dT and 74 KBq of 3H-dTTP (2.934 TBq/mmol) in a final volume of 50 µl and incubated for 1 h at 37°C. The sample was then transferred on HYBOND-N+ membranes (GE Healthcare Life Science, cat. n° RPN119B), which were immediately washed three times in SSC 2X (0.3 M NaCl, 0.03 M sodium citrate pH 7.2) for 10 minutes each, twice in absolute ethanol for 10 seconds each, and finally dried. The radioactivity was measured by using a scintillator counter (Tri-Carb 2810 TR, PerkinEmer) and expressed in counts per minute (cpm).

3.15 Cell transduction

Adherent cells (10^5 U87 cells/well or 2.5×10^5 293T cells/well in 6-well plates) were grown for 24 hours and then incubated with 1 ml of lentiviral vector-containing medium or proper dilutions of concentrated lentiviral preparations. An additional 1 ml of DMEM 10% FBS was added 8 hours later and cells were evaluated at least 72 hours post-transduction. For human GBM spheres, proper dilutions of concentrated lentiviral vectors in complete Neurobasal medium were incubated with either GBM spheres or GBM cells immediately after mechanical dissociation of the spheres. In all experiments mock transduction was performed with DMEM 10% FBS.
All transduced cells were routinely observed under a direct light or fluorescent inverted microscope (Leica DMIL LED) to evaluate eventual effects on cell morphology and proliferation and to monitor EGFP expression.

3.16 Immunofluorescence

Immunofluorescence was performed to investigate the intracellular localization of PKA subunits in human GBM cells and human gliomaspheres of stem cell like cells. For adherent cell cultures, immunofluorescence was performed as previously described (Mucignat-Caretta et al. 2008). Cells grown on 9 mm diameter coverslips were washed in PBS, fixed in paraformaldehyde 4% for 20 minutes and washed three times for 10 minutes in PBS. Cell membranes were permeabilized by incubation in 0.01% Triton X-100 in PBS for 5 minutes. After two additional washes in PBS, cells were incubated overnight at 4°C with the primary antibody properly diluted in PBS. The following day, three washes in PBS were performed before incubating cells for 45 minutes at room temperature with the secondary antibody properly diluted in PBS. Cells were washed again for 10 minutes in PBS and nuclear staining was performed with bisbenzimide (DAPI, 100 nM in PBS, 15 minutes; Sigma-Aldrich™, cat. n° D9542) or DRAQ5 (1:1250 in PBS, 30 minutes; Cell Signaling Technology, cat. n° 4084) for epifluorescence and confocal microscope observation, respectively. Cells were finally washed three times in PBS before microscope observation.
For GBM spheres growing in suspension, immunofluorescence protocol was adapted by Weiswald et al. 2010 and Sasaki et al. 2010. GBM spheres in suspension were transferred to a small centrifuge tube and precipitated by gravity for 5 minutes before aspirating the culture medium by the pipette. GBM spheres were then fixed and permeabilized for 3 hours at 4°C in PBS containing 4% paraformaldehyde and 1% Triton X-100. After washing three times for 10 minutes in PBS, GBM

spheres were incubated with the primary antibody properly diluted in 0.1% Triton X-100 in PBS at 4°C for 48 hours and regularly shaken by inversion of the centrifuge tube. GBM spheres were then rinsed four times for 30 minutes in 0.1% Triton X-100 in PBS and incubated with the secondary antibody in 0.1% Triton X-100 in PBS for 24 hours, regularly shaking the sphere suspension by inversion of the centrifuge tube. GBM spheres were washed again three times for 10 minutes in PBS, incubated with DRAQ5 1:1250 in PBS for 40 minutes at room temperature in order to stain cell nuclei, and finally washed three times in PBS. Before confocal microscope observation, GBM spheres were resuspended in a small volume (10-20 µl) of PBS and mounted using VECTASHIELD® Mounting Medium for Fluorescence (Vector Laboratories, cat. n° H-1000) in a chamber assembled from a glass slide and two coverslips, as shown in Figure 3.1.

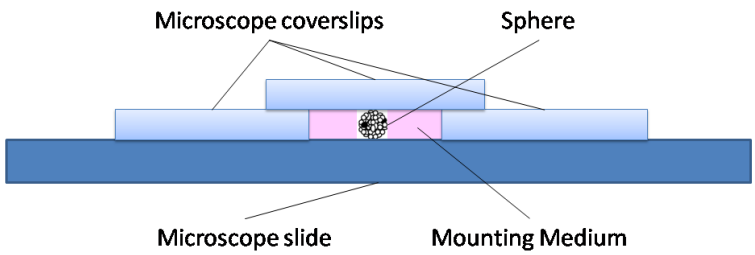

Figure 3.1 - Assembling of GBM sphere suspension in a microscope slide chamber for confocal microscope observation.

For immunofluorescence experiments, the following primary antibodies were used:

- PKA R2A (rabbit, 1:250; Santa Cruz Biotechnology™, cat. n° sc-908)
- PKA R1B (rabbit, 1:250; Santa Cruz Biotechnology™, cat. n° sc-907)
- PKA CA (rabbit, 1:500; Santa Cruz Biotechnology™, cat. n° sc-909)
- GRASP65 (goat, 1:250; Santa Cruz Biotechnology™, cat. n° sc-19481).

The following secondary antibodies were used:

- anti-rabbit Alexa Fluor 594 (donkey, 1:250; Life technologies, cat. n° A-21207)
- anti-rabbit Alexa Fluor 488 (donkey, 1:250; Life technologies, cat. n° A-21206)
- anti-goat Alexa Fluor 488 (donkey, 1:250; Invitrogen, cat. n° A-11055).

Microscope observation was performed on Leica Epifluorescence DC100 or on a Leica TCS confocal microscope (Leica Microsystems AG, Wetzlar, Germany). Digital images were elaborated with ImageJ 1.50b.

3.17 Morphological analysis

Morphological analysis through Wright staining evaluates the cytotoxicity of a treatment based on the number of necrotic and apoptotic cells, identified by specific morphological characteristics. Cells (2.5×10^4 U87 cells/well in 24-well plates) were grown on sterile coverslips and then transfected with PKA plasmids or treated with different chemical agents (8Br-cAMP, H89, BFA). At 72 hours post-transfection or after 24 hour-chemical treatment, cells were washed two times with PBS, fixed in methanol for 5 minutes and stained with 250 µl/well of 0.22 µm filtered Wright stain. Cells were then washed with milliQ water and air dried before stable mounting on a microscope slide with Eukitt (Sigma-Aldrich™, cat. n° 03989). Observation of stained cells was performed at least 24 hours later under a light microscope. Around 600 cells were counted for each slide, evaluating cell death based on morphological criteria. Necrotic cells are characterized by swelling and intracellular organelle dilatation, nucleus disintegration and loss of plasma membrane integrity leading to leakage of cytosol into extracellular space. In contrast, apoptotic cells are typically shrunken and present intact plasma membrane and cellular organelles, chromatin condensation and fragmentation. They develop blebs and eventually divide into apoptotic bodies containing organelles and nuclear debris (Ziegler and Groscurth 2004; Rello et al. 2005). Morphological analysis for evaluation of glioma cell death has already been reported (Mucignat-Caretta et al. 2008; Redaelli et al. 2012; Mucignat-Caretta et al. 2018).

3.18 Cell counting of trypan blue stained cells

Cell counting of trypan blue stained cells was performed as preliminary proliferation assay on U87 and NCH421K cells transduced with PKA R2A and scrambled shRNA lentiviral vectors. After cell detachment through trypsinization, cell suspension was properly diluted in a solution of 10% trypan blue (Sigma-Aldrich™, cat. n° T8154) in PBS and transferred in a Burker chamber. Cells in at least five main squares of the Burker chamber were counted and the total amount of cells per ml was calculated according to a standard procedure. Use of the vital stain trypan blue allowed to

distinguish between live and dead cells as the dye is absorbed only by cells with damaged cell membrane and not by healthy viable cells.

3.19 MTT assay

MTT assays were performed to evaluate cell viability of U87 cells treated with chemical agents (8Br-cAMP, H89, BFA) and U87 and NCH421K cells transduced with PKA R2A and scrambled shRNA lentiviral vectors.

For experiments with chemical agents, U87 cells (5.0×10^3 cells/well in 96-well plates) were grown for 24 hours, treated for 24 or 72 hours and then incubated for 3 hours with MTT (3-[4,5-dimethylthiazol-2-yl]-2,5-diphenyltetrazolium), which is converted to blue/purple formazan salt by mitochondrial dehydrogenase in live cells. DMSO was used to ensure solubilization of formazan and optical density was measured at 570 nm with a VICTOR PerkinElmer Plate Reader.

MTT assay was also performed on U87 and NCH421K cells transduced with PKA R2A and scrambled shRNA lentiviral vectors using Cell Proliferation Kit I (MTT) (Roche, cat. n° 11465007001) according to manufacturer's instructions. Briefly, cells (1.0×10^3 cells/well in 96-well plates) were grown for 24 hours in a final volume of 100 µl culture medium per well and then transduced with lentiviral vectors. At defined time points, 10 µl of the MTT labelling reagent were added to each well and cells were returned to incubator. After 4 hours incubation, 100 µl of the solubilization solution was added into each well. The well plate was allowed to stand overnight in the incubator for complete solubilization of formazan crystals and the absorbance of the samples at 620 nm was finally measured with a Tecan Sunrise™ absorbance microplate reader.

3.20 Cell motility assays

Three complementary approaches were used to investigate cell motility of BFA treated U87 cells as well as U87 cells with differently interfered PKA pathway: wound healing assay was performed to estimate cell invasion after monolayer scratching, cell migration assay to evaluate cell motility following cell growth in silicon circles and time lapse experiments to measure the distance travelled by cells in a fixed time.

3.20.1 Wound healing assay

Cells were grown in 24-well plates until semi-confluence and the cell monolayer was scratched with a sterile micropipette 1000 µl tip before incubation with 8Br-cAMP, H89 or BFA for 24 hours. After treatment removal, cells were allowed to grow for other 72 hours in complete DMEM, then fixed in methanol for 5 minutes and stained with Wright staining. Scratched areas were photographed under a direct light microscope (5x objective) and cells in the scratched areas were counted by using ImageJ Cell Counter. Experiments were performed in triplicate.

3.20.2 Cell migration assay

Cells were seeded inside silicone circles with a 5 mm diameter, adhered to sterile microscope slides. Semi-confluent cells were treated with BFA for 24 hours and then allowed to migrate for 72 hours after both treatment and silicone circles removal. Cells on microscope slides were then fixed in methanol for 5 minutes and stained with Wright staining. Pictures of circular areas covered by cells were acquired with a low magnification microscope and migration was quantified by measuring with ImageJ the diameter in pixels of the circular area covered by cells, out of silicone circles margins. The assay was performed in triplicates.

3.20.3 Time lapse experiments

Effects of BFA treatment and PKA interference on U87 cell motility was evaluated through an online monitoring system in time lapse experiments. For this purpose, cells (3.0×10^4 cells/well in 24-well plates) were allowed to grow while monitored under a Leica DM6000 B light microscope. Photos of cell cultures were taken at 15 or 20 minutes intervals, for a time lapse of 17 hours, starting 2 hours after chemical treatment set up or 72 hours after siRNA or plasmid transfection. All images were processed into video sequences with the software ImageJ 1.50b and cells were tracked by using ImageJ Manual Tracking tool. For BFA experiments, 10 cells were tracked in each cell culture and total travelled distance was compared between BFA treated and control untreated cells. For PKA interference experiments, either total distance travelled by cells in 17 hours or the median distance travelled in 15 minutes was compared between chemically treated, siRNA or plasmid transfected U87 cells and relative control cells.

3.21 Preparation and quantification of cell lysates

Cell lysates of lentiviral transduced cells were prepared and quantified for subsequent analysis on Sodium Dodecyl Sulphate - PolyAcrylamide Gel Electrophoresis (SDS-PAGE) and western blot.
At defined time points transduced cells were detached trough trypsinization and centrifuged at 1800 rpm for 8 minutes at 4°C. Cell pellets were washed two times in cold PBS, centrifuged as above, resuspended in a proper volume (50-220 µl) of RIPA buffer (in milliQ water, 10% PBS 10X, 1% IGEPAL CA-630, 0.5% sodium deoxycholate, 0.05% SDS) supplemented with protease inhibitor cocktail (cOmplete™ Protease Inhibitor Cocktail, Sigma-Aldrich™, cat. n° 000000011697498001) and incubated on ice for 30 minutes to enable cell lysis and extraction of cellular proteins. Cell lysates were then centrifuged at 13000 rpm for 30 minutes at 4°C and the collected supernatants were stored at -80°C.
Quantification of protein extracts was performed through a bicinchoninic acid (BCA) protein assay (Micro BCA™ Protein Assay Kit, Thermo Scientific™, cat. n° 23235) for colorimetric detection of total proteins. The assay was performed in a 96-well plate and each sample was analyzed in triplicate according to manufacturer's instructions. Briefly, 3 µl of sample replicate were first diluted in 100 µl of water. Then, 100 µl of Micro BCA Working Reagent were added to diluted samples before incubating the plate at 37°C for 2 hours. During incubation Cu^{+2} ions contained in the Micro BCA Working Reagent are reduced by protein in an alkaline environment leading to formation of cuprous ions Cu^{+1}. Chelation of two molecules of BCA with one Cu^{+1} ion produces a purple water-soluble complex exhibiting a strong absorbance at 562 nm, that is linear with increasing protein concentrations (Figure 3.2).

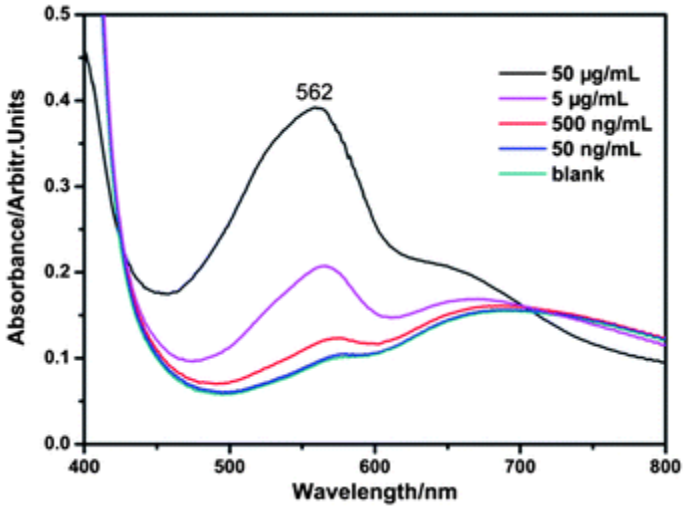

Figure 3.2 - Example of full absorbance spectrum of BCA assay.

Absorbance at 492 nm was measured for all test wells with a Tecan Sunrise™ absorbance microplate reader and a standard curve was prepared using BSA standards with increasing concentration. Finally, interpolation of sample absorbance values with BSA standard curve allowed determination of protein concentration of cellular extracts.

3.22 SDS-PAGE and western blot

Protein extracts were separated on SDS-PAGE and transferred on nitrocellulose membrane for chemiluminescenct detection of interest proteins through specific antibodies.
For SDS-PAGE, 15-40 µg of protein extracts were properly diluted in RIPA buffer and mixed 1:1 with Laemmli loading buffer 2X (Table 3.5). After incubation at 100°C for 5-10 minutes, protein samples were run on a 4.5% polyacrilamide stacking gel (Table 3.5) and a 10% polyacrilamide separating gel (Table 3.5) in running buffer SDS-PAGE (running buffer 1X containing 0. 1% SDS; Table 3.5). The electrophoretic run was performed as follows: 75 V for 10 minutes, 95 V for 10 minutes, 105 V for 10 minutes, 115 V for 90 minutes. Separated proteins were then blotted on nitrocellulose membrane (Amersham™ Protran™ Premium 0.45 µm NC, GE Healthcare Life Science, cat. n° 10600003) after incubation of both polyacrilamide gel and nitrocellulose membrane in transfer buffer (Table 3.5) for at least 10 minutes. Protein transfer was performed in transfer buffer, on ice, for 2 hours at 50 V. The nitrocellulose membrane was then incubated for 30-120 minutes with a blocking solution of 5% (w/v) dry milk (Blotting-Grade Blocker, Bio-Rad, cat. n° 170-6404) in PBS + 0.1% (v/v) Tween 20 in order to saturate aspecific binding sites on the membrane. The incubation with the primary antibodies, properly diluted in blocking solution, was performed on shaking overnight at 4°C. The nitrocellulose membrane was washed three times with PBS + 0.1% (v/v) Tween 20 for 10 minutes and incubated 1 hour at room temperature with secondary antibodies in blocking solution. The membrane was washed again three times with PBS + 0.1% (v/v) Tween 20 for 10 minutes and finally with PBS for 10 minutes. Proteins were revealed through chemiluminescence using ECL reagents (Amersham™ ECL™ Western Blotting Detection Reagents, cat. n° RPN2106) according to manufacturer's instructions.

The following primary antibodies were used in western blot applications:

- PKA R2A (rabbit, 1:1000; Santa Cruz Biotechnology™, cat. n° sc-908)
- GAPDH (rabbit, 1:7500; Sigma-Aldrich™, cat. n° G9545).

The following peroxidase-conjugated secondary antibody was used for chemiluminescent detection of interest proteins: anti-rabbit HRP conjugated (goat, 1:1000; Abcam, cat. n° ab6721-1)

When necessary, following first chemiluminescent detection of interest proteins, primary and secondary antibodies were removed from nitrocellulose membrane by incubation with hot (60°C) stripping solution (100 mM β-mercaptoethanol, 2% SDS, 62.5 mM Tris-Cl pH 6.8; two times for 15 minutes each). Nitrocellulose membrane was then washed three times with PBS + 0.1% (v/v) Tween 20, incubated with blocking solution as previously and again with properly diluted primary and secondary antibodies for chemiluminescent protein detection.

Laemmli loading buffer 2X	
0.5 M Tris-Cl, pH 6.8	6.25 ml
Deionized water	10.03 ml
Glycerol	2.25 ml
10% SDS	5 ml
1% bromphenol blue	0.25 ml
β-mercaptoethanol	1.22 ml
total volume	*25 ml*
4.5% polyacrilamide stacking gel	
0.5 M Tris-Cl, pH 6.8	4 ml
Deionized water	9.4 ml
30% Acrilamide/Bis Solution	2.4 ml
10% SDS	160 µl
10% APS	160 µl
TEMED	40 µl
total volume	*16.06 ml*
10% polyacrilamide separating gel	
1.5 M Tris-Cl, pH 8.8	6.25 ml
Deionized water	9.98 ml
30% Acrilamide/Bis Solution	8.3 ml
10% SDS	0.25 ml

10% APS	200 µl
TEMED	40 µl
total volume	*25.02 ml*
Running buffer 10X	
Tris	30.2 g
Glycine	144 g
total volume	*1 L*
Running buffer SDS-PAGE	
Running buffer 10X	100 ml
10% SDS	10 ml
Deionized water	890 ml
total volume	*1 L*
Transfer buffer	
Running buffer 10X	100 ml
Methanol	200 ml
Deionized water	700 ml
total volume	*1 L*

Table 3.5 - Recipes for western blot buffers and polyacrilamide gels. All reagents for western blot were from Bio-Rad (30% Acrilamide/Bis Solution cat. n° 161-0158; APS, Ammonium Persulfate, cat. n° 161-0700; TEMED cat. n° 1610800).

3.23 Data elaboration and statistical analysis

For elaboration of flow cytometry data, WinMDI 2.8 and Flowing Software 2 were used. ImageJ 1.50b was used for elaboration of microscope digital images, as well as data from wound healing assays, cell migration assays and time lapse experiments. Statistical analysis (t-test and chi-square test) were performed with the software GraphPad Prism 5 (GraphPad Software Inc., USA).

4 Results

4.1 Intracellular localization of PKA in human GBM

In GBM cells, the regulatory subunit R2A of PKA is present in perinuclear clusters co-localized with the Golgi apparatus. This peculiar intracellular distribution has been demonstrated in several mouse, rat and human GBM cell lines as well as in primary human GBM cell cultures (Mucignat-Caretta et al. 2008; Zorzan 2014, see Appendix A1, Figure S1a; Mucignat-Caretta et al. 2018). In rodent glioma models, PKA R2A distribution also defines the margin of the tumor. Indeed in rodent brain, R2A aggregates are detected only at the base of the cilia of ependymal cells but not in the rest of the normal brain parenchyma, where R1A and R2B aggregates are instead observed (Mucignat-Caretta et al. 2004). Co-localization of PKA R2A subunit with Golgi apparatus has been demonstrated by immunofluorescence and immunoelectron microscopy using the trans-Golgi network marker golgin 97 (Mucignat-Caretta et al. 2008; Mucignat-Caretta et al. 2018) and further confirmed using the cis-Golgi network marker GRASP65 in immunofluorescence experiments. In the present study, investigation of PKA intracellular distribution was extended to different human GBM cell cultures, including adherent GBM cell lines and GBM stem like cell cultures.

4.1.1 D-423 and GLI56 human GBM cell lines

Intracellular localization of PKA R2A subunit was investigated in two additional adherent human GBM cell lines, D-423 and GLI56. As shown in Figure 4.1 and 4.2, both cell cultures presented perinuclear clusters of R2A subunit.

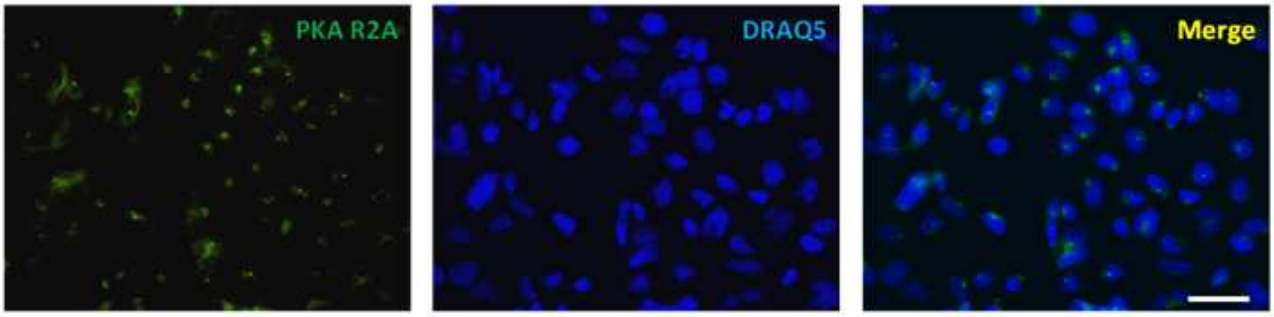

Figure 4.1 - Immunofluorescence on D-423 cells. Green: PKA R2A; blue: DRAQ5 nuclear staining. Confocal 63x, bar 200 μm.

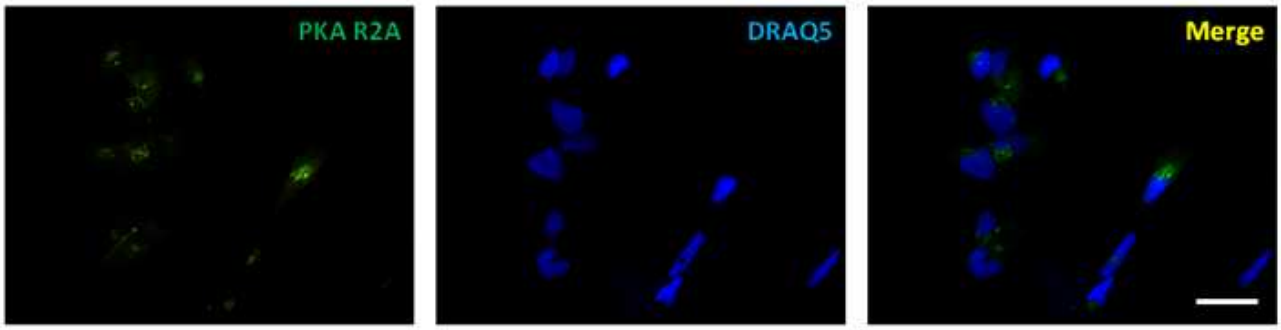

Figure 4.2 - Immunofluorescence on GLI56 cells. Green: PKA R2A; blue: DRAQ5 nuclear staining. Confocal 63x, bar 100 μm.

Moreover, double immunolabeling of D-423 cells with anti-PKA R2A and anti-GRASP65 antibodies demonstrated co-localization between perinuclear PKA R2A clusters and Golgi apparatus (Figure 4.3).

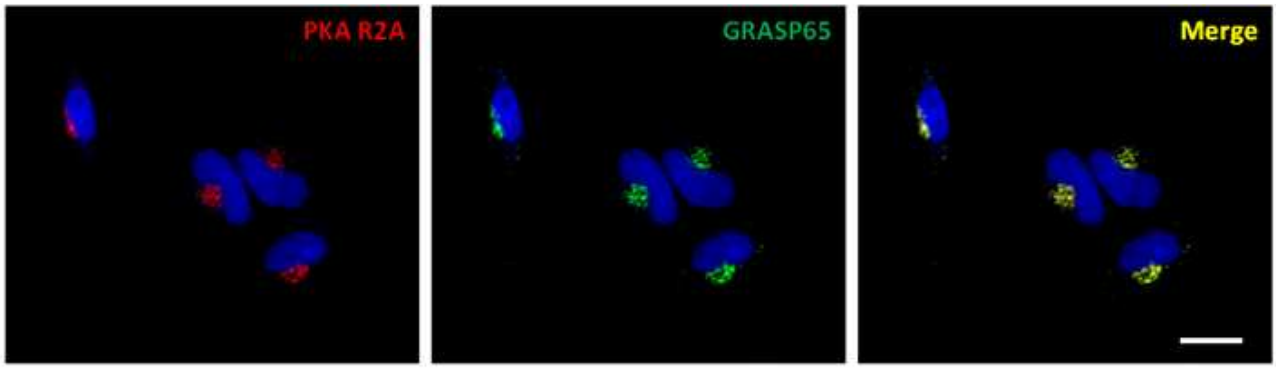

Figure 4.3 - Immunofluorescence on D-423 cells. Red: PKA R2A; green: GRASP65; blue: DRAQ5 nuclear staining. Confocal 63x, bar 50 μm.

This observation thus confirmed the peculiar R2A distribution previously described in rodent and other human GBM cell lines (Mucignat-Caretta et al. 2008; Mucignat-Caretta et al. 2018).

Localization of PKA CA subunit was also investigated in D-423 and GLI56 cells, showing a diffuse distribution, also in the area of the cell nucleus (Figure 4.4 and 4.5).

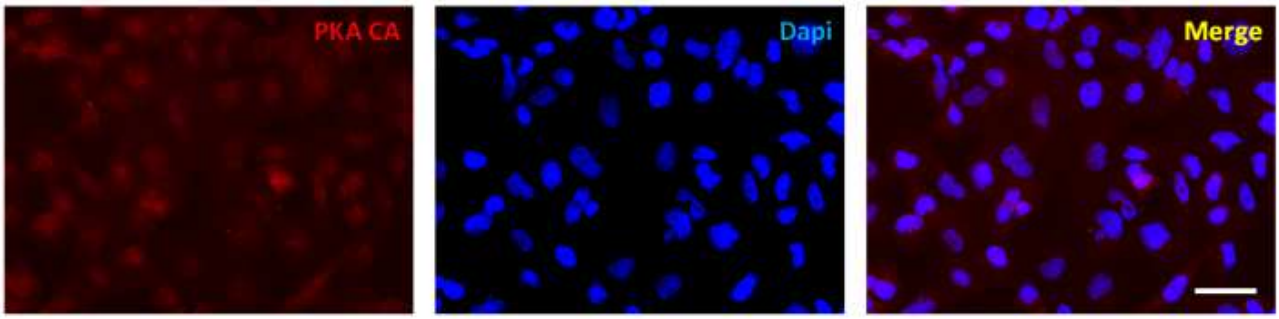

Figure 4.4 - Immunofluorescence on D-423 cells. Red: PKA CA; blue: DAPI nuclear staining. Epifluorescence 20x, bar 200 μm.

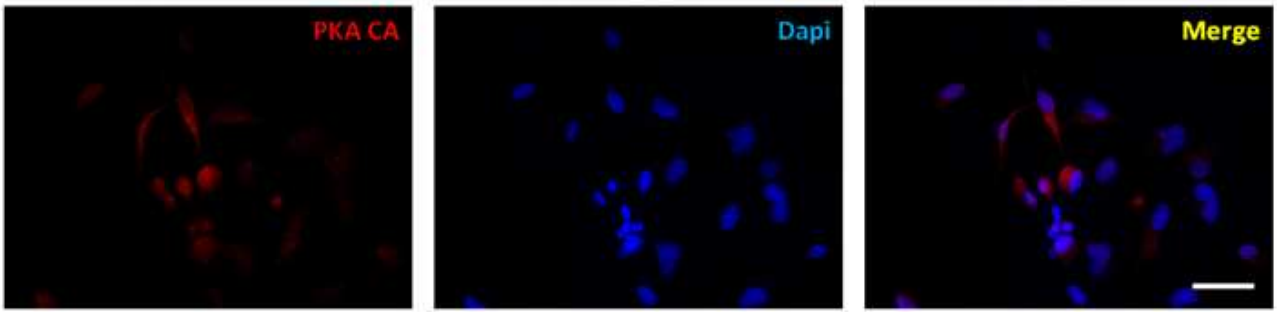

Figure 4.5 - Immunofluorescence on GLI56 cells. Red: PKA CA; blue: DAPI nuclear staining. Epifluorescence 20x, bar 200 μm.

The same diffuse intracellular distribution of PKA CA subunit had been previously observed in other human GBM cell lines presenting perinuclear clusters of PKA R2A (i.e. U87 cell line, Zorzan 2012).

4.1.2 GBM stem like cell cultures

Up to now, no data is provided by the literature as regard to the intracellular localization of PKA R2A subunit in stem like GBM cells. In the present study, NCH421K cells, a well-characterized human GBM stem like cell line, and two primary GBM cell cultures (GBM2 and GBM5) previously established from surgical specimens in our Department, were grown in stem cell selective growth conditions. Sphere formation was documented in all cell cultures, reporting differences in time required for cell cluster formation and growth in diameter (Figure 4.6).

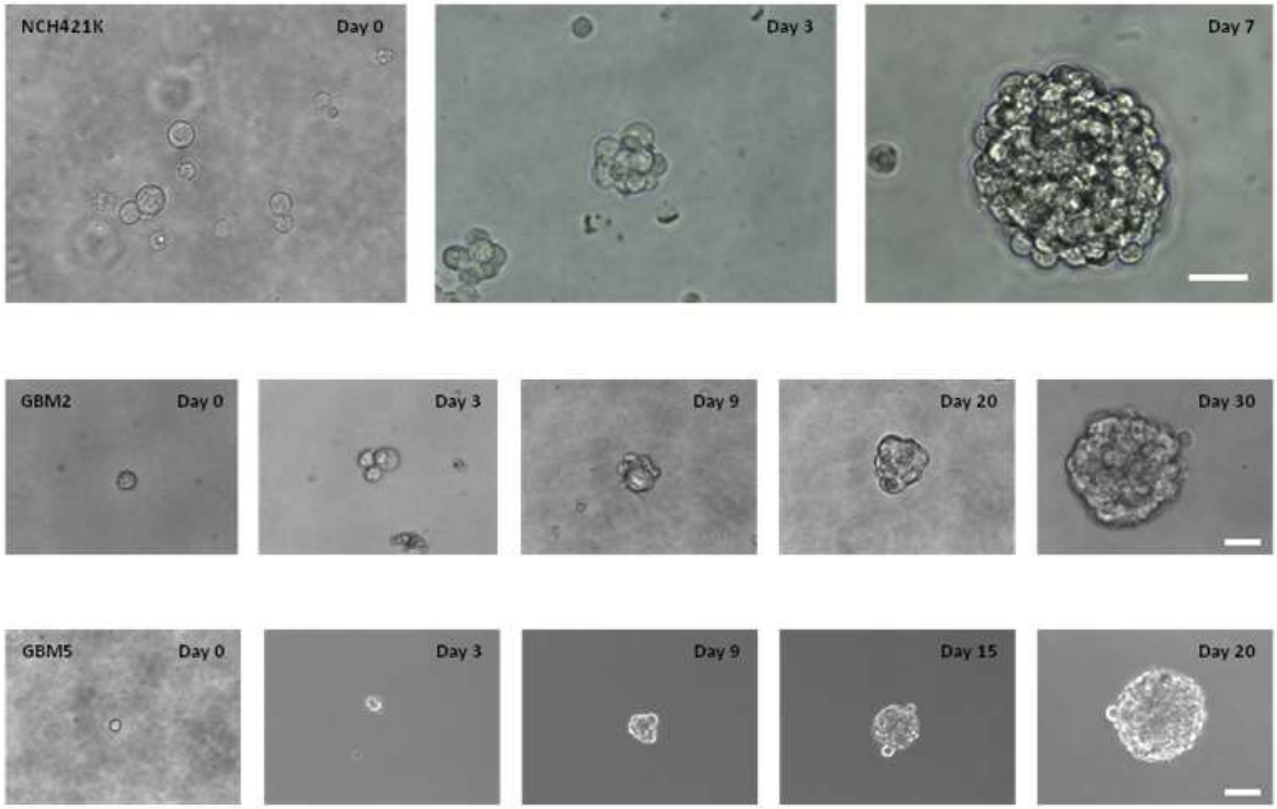

Figure 4.6 - Sphere formation process, from the top to the bottom: NCH421K, GBM2 and GBM5 GBM stem like cell cultures. Direct light; NCH421K: 40x, bar 250 µm; GBM2: 40x, bar 250 µm; GBM5: 20x, bar 500 µm.

Immunofluorescence for detection of R2A subunit was performed on GBM stem like spheres, revealing the presence of perinuclear PKA R2A clusters (Figure 4.7 and 4.8).

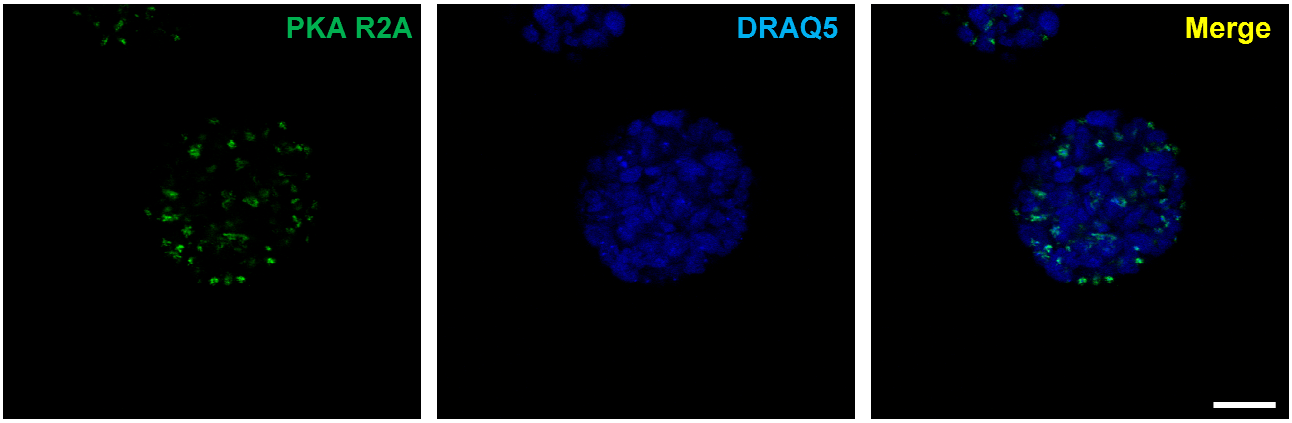

Figure 4.7 - Immunofluorescence on GBM2 spheres. Green: PKA R2A; blue: DRAQ5 nuclear staining. Confocal 63x, bar 250 µm.

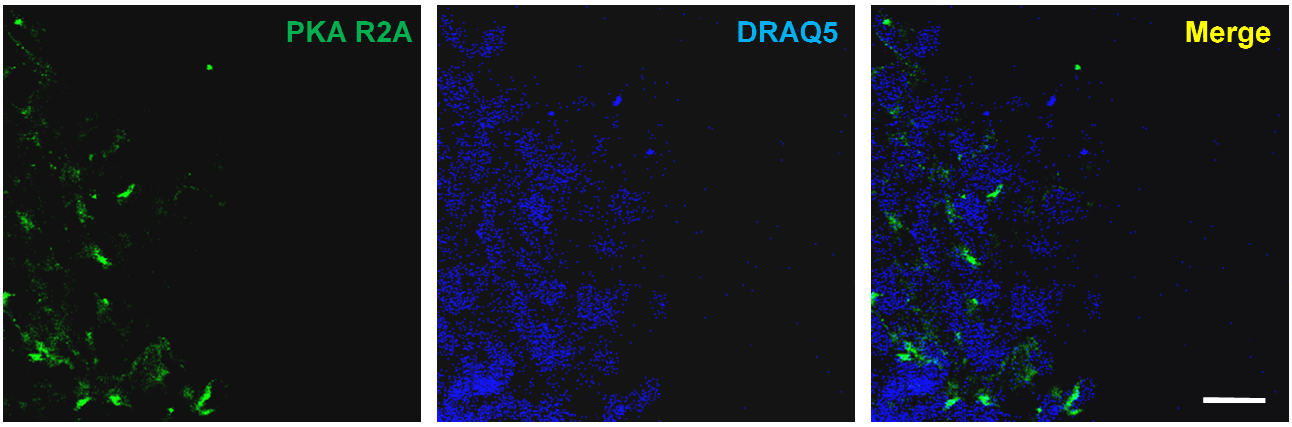

Figure 4.8 - Immunofluorescence on GBM5 spheres. Green: PKA R2A; blue: DRAQ5 nuclear staining. Confocal 63x, bar 50 µm.

Co-localization of R2A subunit with GRASP65 Golgi marker was also demonstrated in gliomaspheres of NCH421K and GBM2 cells (Figure 4.9 and 4.10).

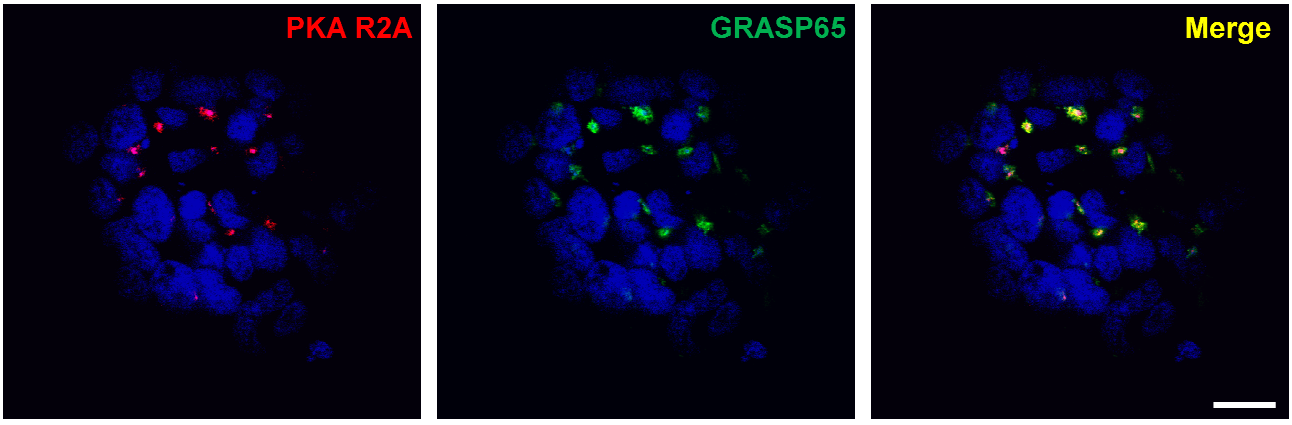

Figure 4.9 - Immunofluorescence on NCH421K spheres. Red: PKA R2A; green: GRASP65; blue: DRAQ5 nuclear staining. Confocal 63x, bar 100 µm.

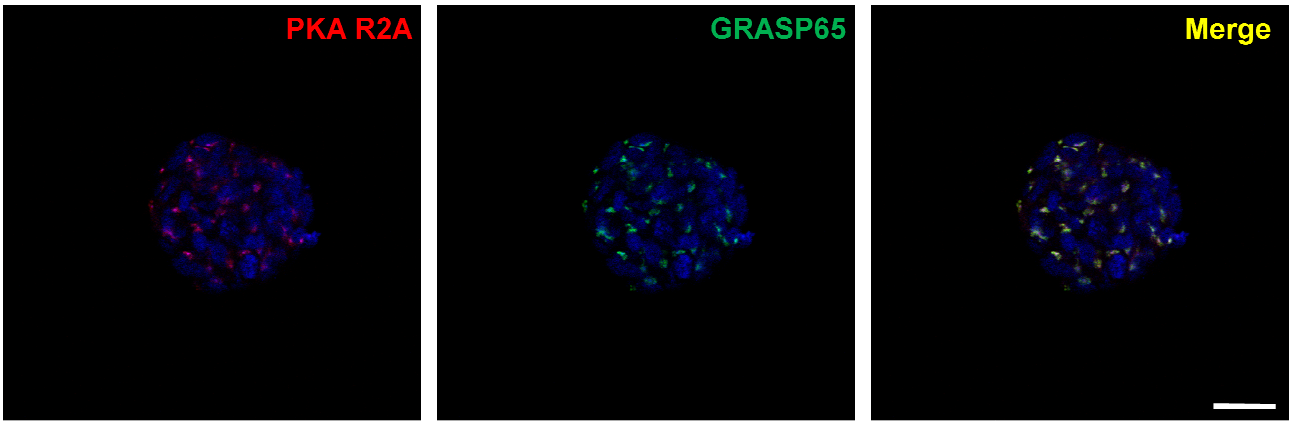

Figure 4.10 - Immunofluorescence on GBM2 spheres. Red: PKA R2A; green: GRASP65; blue: DRAQ5 nuclear staining. Confocal 63x, bar 250 µm.

These results confirmed the peculiar intracellular distribution of R2A subunit previously reported in non-stem human GBM cell lines and primary cell cultures (Mucignat-Caretta et al. 2008; Zorzan 2014; Mucignat-Caretta et al. 2018), further suggesting a specific role for this subunit in GBM cell biology.

4.2 Generation of recombinant plasmids for expression of EGFP-fused PKA subunits

In order to generate new potential tools for functional studies of PKA in several cellular models, recombinant plasmids for expression of EGFP-fused PKA R2A, R2B, R1A, CA and CB subunits were generated by cloning of human cDNA for PKA subunits in the eukaryotic expression plasmid pEGFP-C1. The obtained recombinant plasmids allowed visualization of fluorescently-tagged PKA subunits in live and fixed U87 cells.

4.2.1 Recombinant pEGFP-C1-PRKAR2A plasmid

U87 cells transfected with pEGFP-C1-PRKAR2A recombinant plasmid express human PKA R2A subunit fused to EGFP protein. Transfected cells were observed alive 72 hours post-transfection under an epifluorescent microscope, showing an EGFP signal spread in the whole cell body (Figure 4.11).

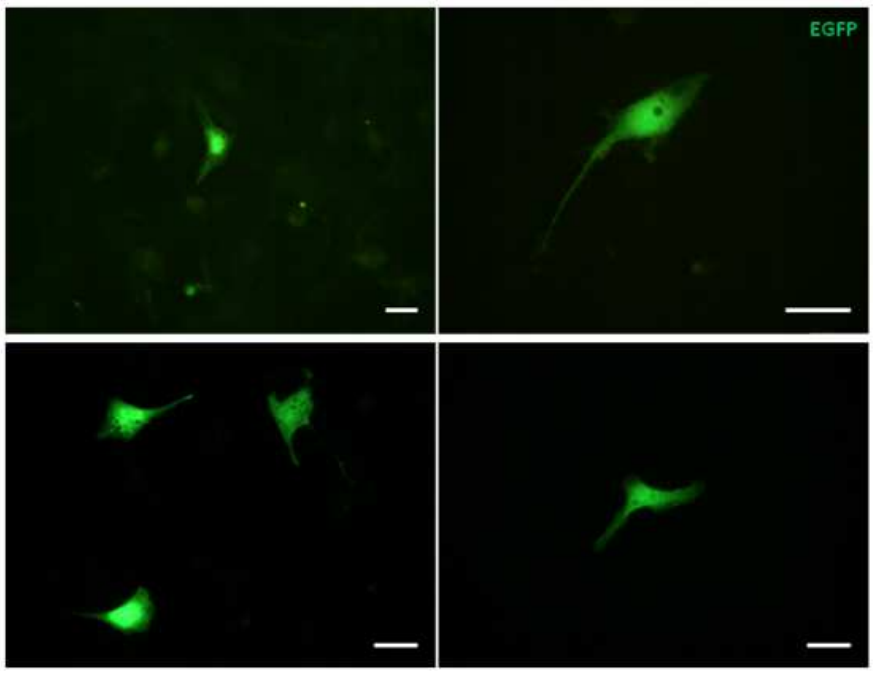

Figure 4.11 - EGFP signal from alive U87 cells, 72 hours post-transfection with pEGFP-C1-PRKAR2A. Epifluorescence 20x (upper left) and 40x (upper right and down), bar 50 μm.

The EGFP signal was very poorly preserved following cell fixation. However, in fixed transfected cells still presenting a green fluorescent signal, co-localization between EGFP and GRASP65 Golgi marker was not detected in all transfected cells (Figure 4.12).

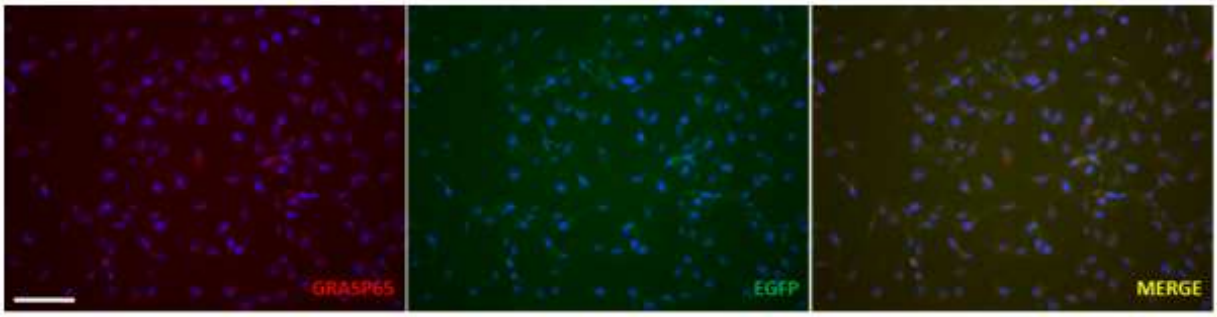

Figure 4.12 - Immunofluorescence on U87 cells transfected with pEGFP-C1-PRKAR2A. Red: GRASP65; green: EGFP-R2A; blue: DAPI nuclear staining. Epifluorescence 20x, bar 500 µm.

Immunofluorescence with anti-PKA R2A antibody was also performed on pEGFP-C1-PRKAR2A transfected cells. This analysis showed co-localization between EGFP and R2A signals, confirming the expression of EGFP-fused R2A subunit (Figure 4.13).

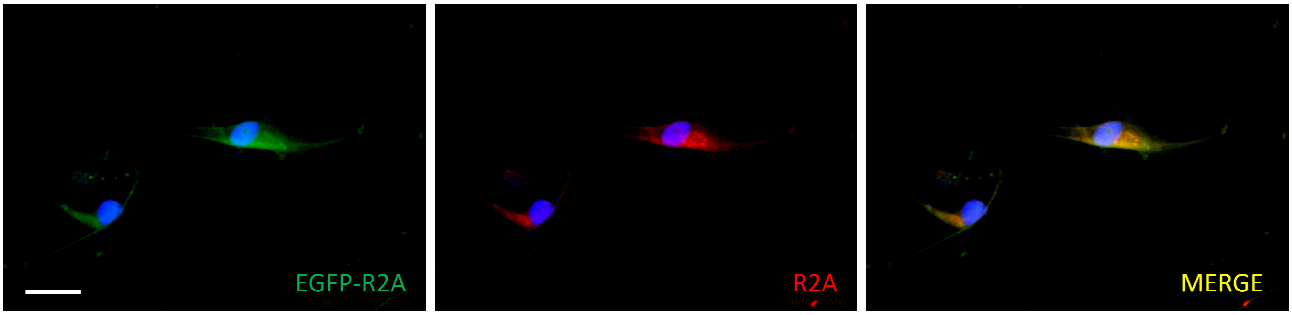

Figure 4.13 - Immunofluorescence on U87 cells transfected with pEGFP-C1-PRKAR2A. Left: green, EGFP-R2A; middle: red, PKAR2A; right: merge; blue, DAPI nuclear staining. Epifluorescence 40x, bar 50 µm.

Thus, in pEGFP-C1-PRKAR2A transfected cells a more diffuse intracellular distribution of EGFP-tagged R2A subunit was detected, compared to the intracellular localization of endogenous PKA R2A. This observation needs further investigation.

4.2.2 Recombinant pEGFP-C1-PRKAR2B plasmid

U87 cells were transfected with pEGFP-C1-PRKAR2B plasmid for expression of EGFP-fused PKA R2B subunit. In live transfected cells, observed 72 hours post-transfection under an epifluorescent microscope, EGFP signal was spread in the whole cell body (Figure 4.14).

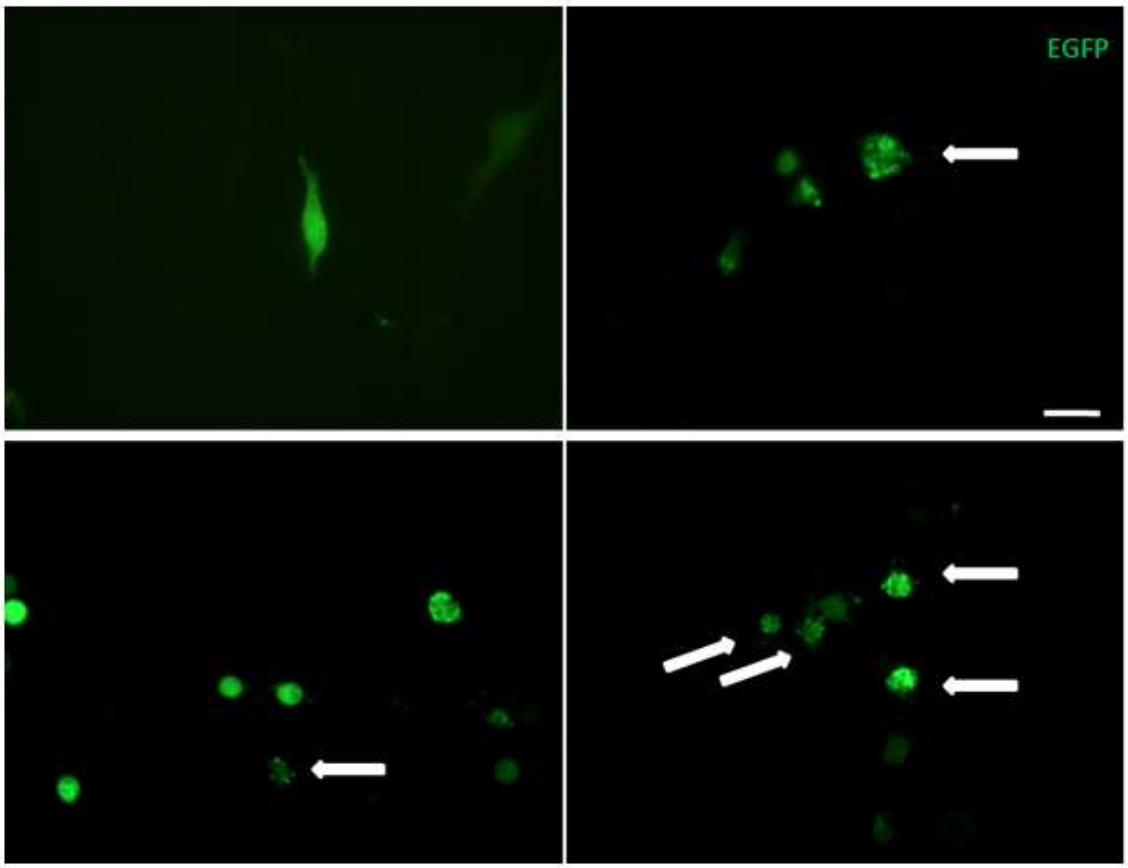

Figure 4.14 - EGFP signal from alive U87 cells, 72 hours post-transfection with pEGFP-C1-PRKAR2B. Many apoptotic EGFP-positive cells were observed (arrows).
Epifluorescence 40x, bar 100 μm.

Moreover, many apoptotic cells were detected (Figure 4.14). This observation is consistent with the cytotoxic effect of PKA R2B overexpression, previously demonstrated by morphological analysis of U87 cells transfected with pLX303-PRKAR2B plasmid (Zorzan 2014).

4.2.3 Recombinant pEGFP-C1-PRKAR1A plasmid

Distribution of EGFP-tagged PKA R1A subunit was analyzed in U87 cells transfected with pEGFP-C1-PRKAR1A plasmid. Confocal microscope observation was performed after cell fixation 72

hours post-transfection. EGFP-fused R1A appeared as multiple dots of variable size in the cytoplasm of transfected cells (Figure 4.15).

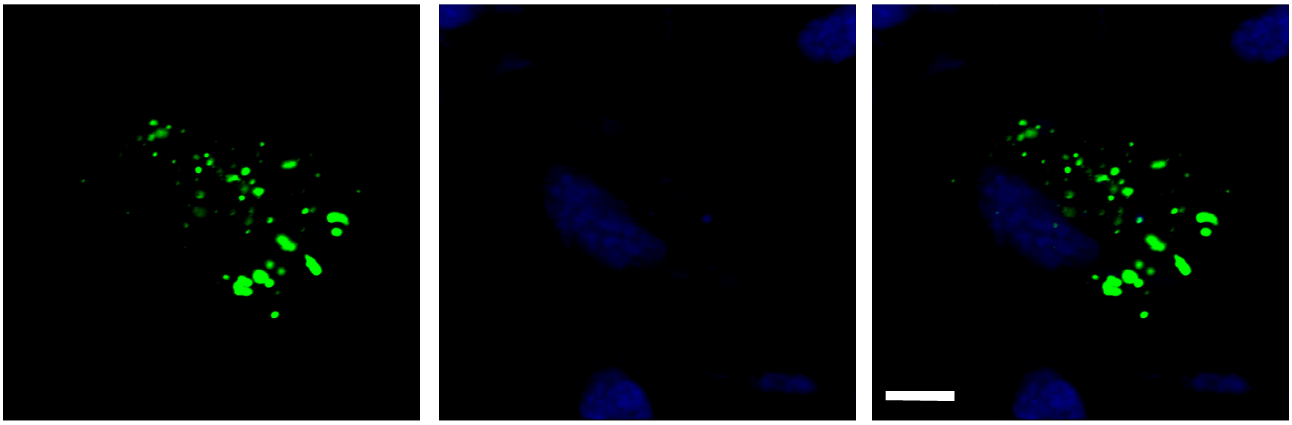

Figure 4.15 - EGFP signal from fixed U87 cells, 72 hours post-transfection with pEGFP-C1-PRKAR1A. Green: EGFP-R1A; blue: DRAQ5 nuclear staining. Confocal 63x, bar 50 µm.

Immunofluorescence was also performed on pEGFP-C1-PRKAR1A transfected cells using primary antibodies against PKA R1 and R2A subunits (Figure 4.16).

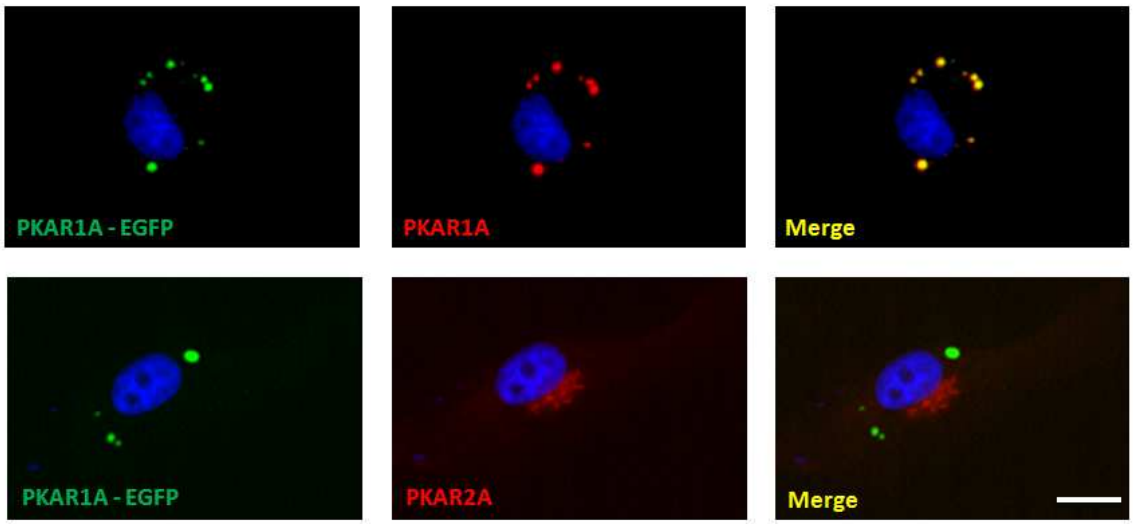

Figure 4.16 - Immunofluorescence on U87 cells transfected with pEGFP-C1-PRKAR1A recombinant plasmid. Left: green, PKAR1A-EGFP; middle: red, PKAR1A and PKAR2A; right: merge; blue, DAPI nuclear staining. Epifluorescence 40x, bar 50 µm.

The presence of PKA R1A subunit in the green dots (EGFP signal) of transfected cells was confirmed by labeling with the anti-R1 antibody, whereas this distribution was not detectable in non-transfectd cells. In addition, EGFP-tagged R1A subunit presented a completely distinct

intracellular localization compared to PKA R2A subunit, consistent with previous observations on endogenous R2A distribution.

4.2.4 Recombinant pEGFP-C1-PRKACA plasmid

U87 cells were transfected with pEGFP-C1-PRKACA plasmid for expression of PKA CA subunit fused to EGFP protein. Observation of live and fixed cells 72 hour post-transfection revealed a diffuse distribution of EGFP-tagged CA subunit in the whole cell body (Figure 4.17 and 4.18) and changes in the cellular morphology, compatible with unhealthy cellular state.

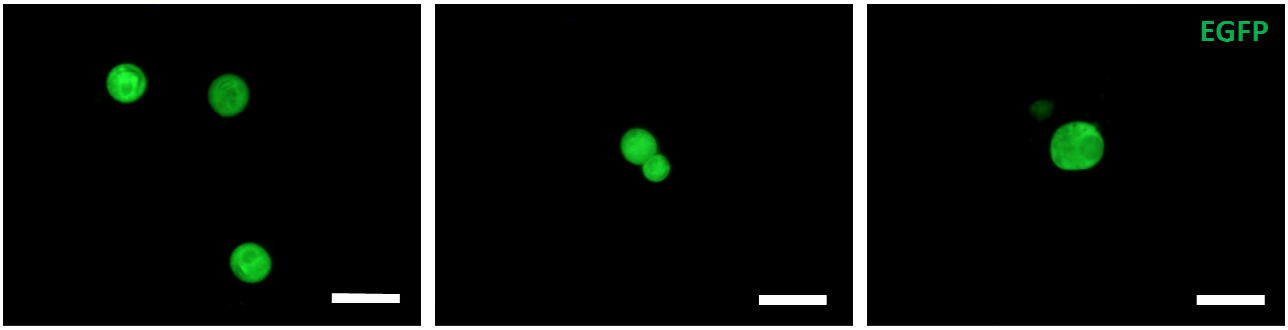

Figure 4.17 - EGFP signal from alive U87 cells, 72 hours post-transfection with pEGFP-C1-PRKACA. Epifluorescence 40x, bar 100 µm.

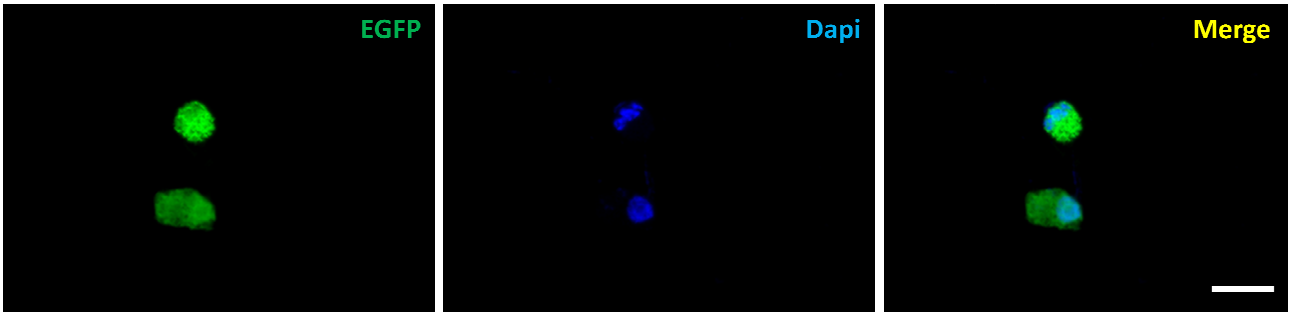

Figure 4.18 - EGFP signal from fixed U87 cells, 72 hours post-transfection with pEGFP-C1-PRKACA. Green: EGFP-CA; blue: DAPI nuclear staining. Epifluorescence 40x, bar 100 µm.

This distribution was consistent with the diffuse intracellular localization of endogenous PKA CA subunit in U87 cells (Zorzan 2012).

4.2.5 Recombinant pEGFP-C1-PRKACB plasmid

Similarly to EGFP-fused PKA CA subunit, U87 cells transfected with pEGFP-C1-PRKACB plasmid presented a diffuse intracellular distribution of EGFP-tagged CB subunit (Figure 4.19 and 4.20).

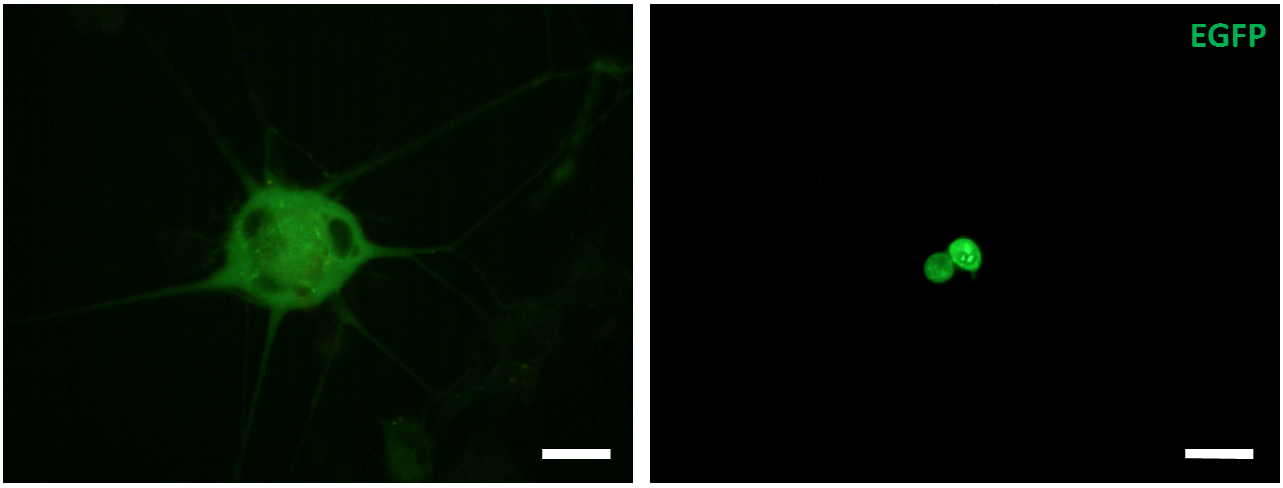

Figure 4.19 - EGFP signal from alive U87 cells, 72 hours post-transfection with pEGFP-C1-PRKACB. Epifluorescence 40x (left, bar 50 μm) and 20x (right, bar 100 μm).

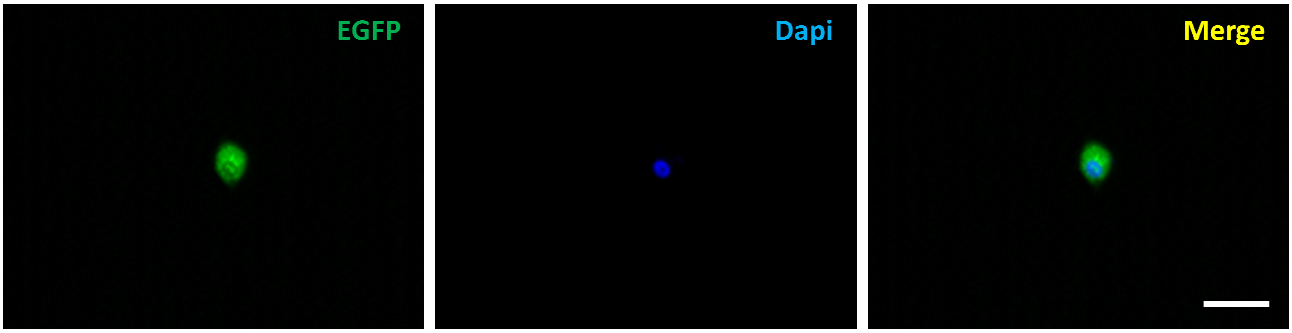

Figure 4.20 - EGFP signal from fixed U87 cells, 72 hours post-transfection with pEGFP-C1-PRKACB. Green: EGFP-CB; blue: DAPI nuclear staining. Epifluorescence 40x, bar 200 μm.

Thus, PKA CA and CB subunits in fusion with EGFP protein presented the same intracellular distribution, which was very similar to endogenous PKA CA localization in U87 cells (Zorzan 2012).

4.2.6 General considerations on EGFP-fused PKA plasmids

In vivo imaging of fluorescent fusion proteins is a useful method to get insights into protein cellular functions. Yet, some warnings about the above experiments on fluorescently-tagged PKA subunits should be mentioned. First, a very low efficiency in cell transfection emerged from experiments with all EGFP-fused PKA plasmids. This represented a relevant hurdle for the success of the experiments and the interpretation of the data. Indeed, any effect induced by exogenous expression of PKA subunits was made largely fainter by the presence of many non-transfected cells. Secondly, the start codon within PKA coding sequences was not removed when placing PKA subunits on the

C-terminal of EGFP. As a consequence, expression of some untagged form of the protein was still possible, that could partially contribute to the small rate of EGFP-expressing cells. Finally, some PKA subunits, such as PKA R1A and R2B, are usually not detected by immunohistochemistry in glioma cells, making it more difficult to understand if the N-terminal tag could in some way lead to mislocalization of the protein.

All considered, the generated PKA recombinant plasmids may potentially represent useful tools in different cellular models, provided an optimization of the fusion constructs and a higher cell transfection efficiency. Testing the fluorescent tag on both sides of PKA subunits could also be of help to uncover possible interference with the protein functionality and intracellular localization. What is more, optimized and validated PKA fusion constructs may be implemented in a much more efficient gene delivery system, such as lentiviral vectors, further increasing the potential applications for functional studies of protein kinase A.

4.3 Interference with PKA pathway

The laboratory of Neurophysiology, University of Padova, has been investigating since many years the effects of PKA interference on GBM cells (Mucignat-Caretta et al. 2008; Zorzan et al. 2013; Zorzan et al. 2014; Zorzan 2014; Mucignat-Caretta et al. 2018). Multiple approaches for modulation of PKA activity, expression and localization have been investigated, showing that PKA interfering treatments differently affect GBM cell biology. Part of the present PhD project was focused on investigating the functional effects induced by PKA interference, in the attempt to draw a more complete picture of the role of PKA pathway in human GBM cells.

4.3.1 Drug-mediated interference with PKA activity

Previous data of the laboratory of Neurophysiology, University of Padova, proved that treatment of mouse and human GBM cells with drugs that either induce (8Br-cAMP, 500 μM) or inhibit (H89, 12 μM) PKA activity result in increase of cell death (Mucignat-Caretta et al. 2008; Mucignat-Caretta et al. 2018). In the present study, human U87 cells were treated with the same substances. The effects of drug-induced PKA stimulation/inhibition on GBM cell viability and cell motility were analyzed.

MTT assay was performed to evaluate cell viability of U87 cells treated for 24 hours with increasing concentrations of PKA activator 8Br-cAMP and PKA inhibitor H89, ranging respectively from 5 to 500 µM and from 0.125 up to 12.5 µM (Figure 4.21).

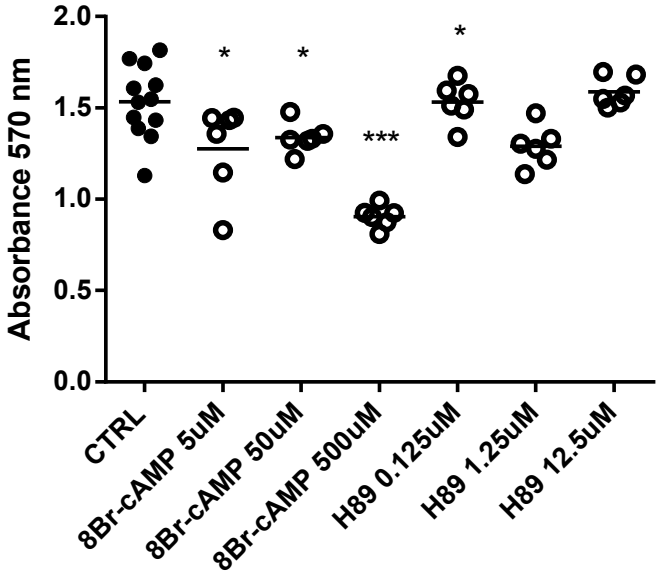

Figure 4.21 - MTT assay on U87 cells treated for 24 hours with increasing concentrations of 8Br-cAMP and H89. t-test, CTRL versus treatment. *p<0.05, **p<0.01, ***p<0.001.

Compared to H89, treatment with 8Br-cAMP proved to have a stronger effect, significantly reducing cell viability at all tested concentrations.

Morphological analysis through Wright staining evaluated cell death of U87 cells treated for 24 hours with either 8Br-cAMP 500 µM or H89 12.5 µM (Figure 4.22).

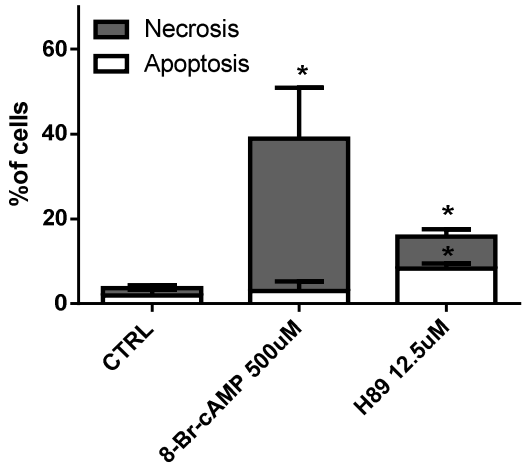

Figure 4.22 - Morphological analysis of U87 cells treated for 24 hours with 8Br-cAMP 500 µM or H89 12.5 µM. Percentages of cell necrosis and apoptosis were compared between treated and control untreated cells. t-test, CTRL versus 8Br-cAMP or H89. *p<0.05, **p<0.01, ***p<0.001.

As shown in Figure 4.22 and consistently with other literature data (Mucignat-Caretta et al. 2018), both treatments proved to significantly increase U87 cell death.

Effects of 8Br-cAMP and H89 treatments on U87 cell motility were investigated through a wound healing assay and a time lapse experiment. The wound healing assay evaluated cell migration for 72 hours, following 24 hours treatment with either 8Br-cAMP (50 and 500 µM) or H89 (2.25 and 12.5 µM) (Figure 4.23).

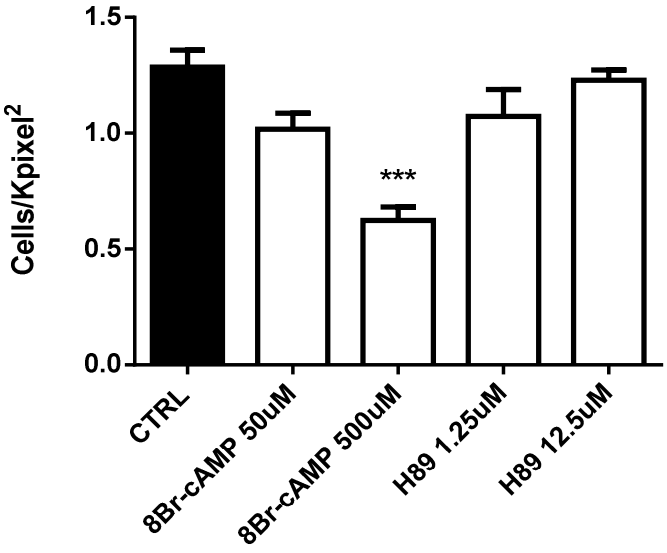

Figure 4.23 - Wound healing assay demonstrated a reduced cell invasion of U87 cells treated with 8Br-cAMP 500 µM for 24 hours compared to control untreated cells.
t-test, CTRL versus treatment. *p<0.05, **p<0.01, ***p<0.001.

U87 cells treated with 8Br-cAMP 500 µM exhibited a significant reduction in cell invasion compared to control untreated cells, whereas H89 treatment resulted not to affect U87 cell migration.

In a time lapse experiment, U87 cells treated with either PKA activator 8Br-cAMP (50 and 500 µM) or PKA inhibitor H89 (1.25 and 12.5 µM) were monitored for 17 hours. The travelled distance was compared between treated and untreated cells (Figure 4.24).

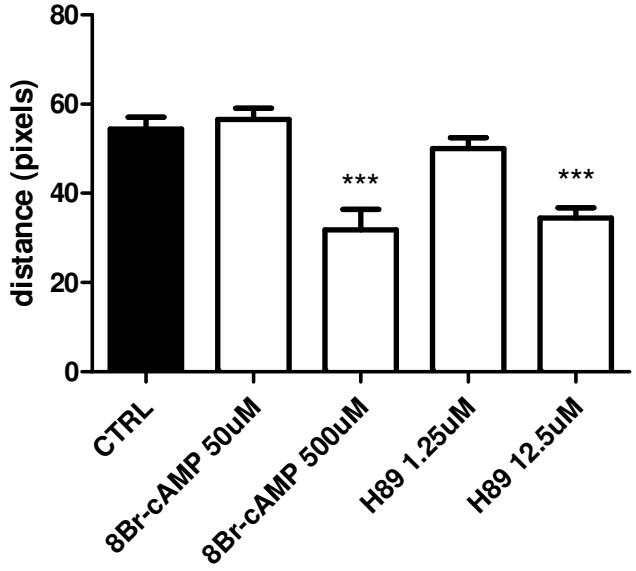

Figure 4.24 - Treatments with 8Br-cAMP 500 µM and H89 12.5 µM induced a significant reduction of travelled distance compared to control untreated cells.
t-test, CTRL versus treatment. *p<0.05, **p<0.01, ***p<0.001.

As shown in Figure 4.24, at the highest concentration both PKA activator 8Br-cAMP and PKA inhibitor H89 induced a significant reduction of GBM cell motility compared to control untreated cells.

4.3.2 Interference with PKA activity through plasmid transfection

U87 cells were transfected with plasmids inducing either PKA hyperactivation (pMC36-PRKACAwt and pMC36-PRKACAmut) or repression of PKA activity (pMT-REV$_{AB}$-neo; R1 DN). Previous experiments demonstrated that pMC36-PRKACAmut and pMT-REV$_{AB}$-neo transfection respectively increased and reduced U87 cell viability in MTT assay (Zorzan 2014). Also, morphological analysis of transfected cells revealed reduced and increased cell death in cells expressing mutant PKA CA and R1 DN subunit, respectively (Zorzan 2014). In the present study, cell migration of transfected cells was analyzed. In particular, median distance travelled by cells in 15 minutes was compared between cells transfected with plasmids for PKA activity interference and cells transfected with the pLX303 empty plasmid (Figure 4.25).

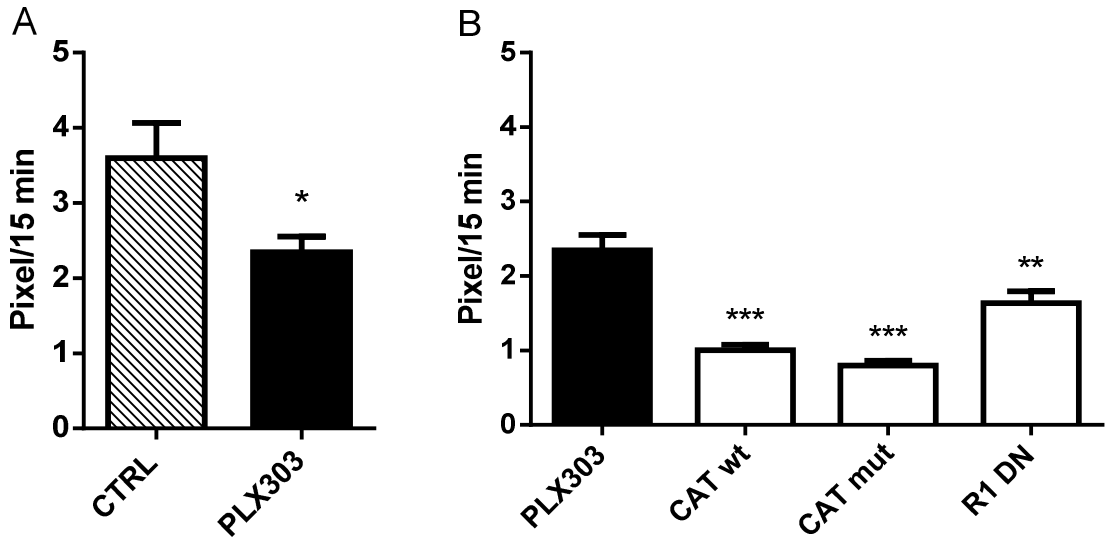

Figure 4.25 - Median distance travelled in 15 minutes by cells transfected with pMC36-PRKACAwt, pMC36-PRKACAmut, pMT-REV$_{AB}$-neo (R1 DN) or pLX303 empty plasmid. CTRL: non-transfected cells. A: t-test, CTRL versus pLX303. B: t-test, pLX303 versus CAT wt, CAT mut and R1 DN. *p<0.05, **p<0.01, ***p<0.001.

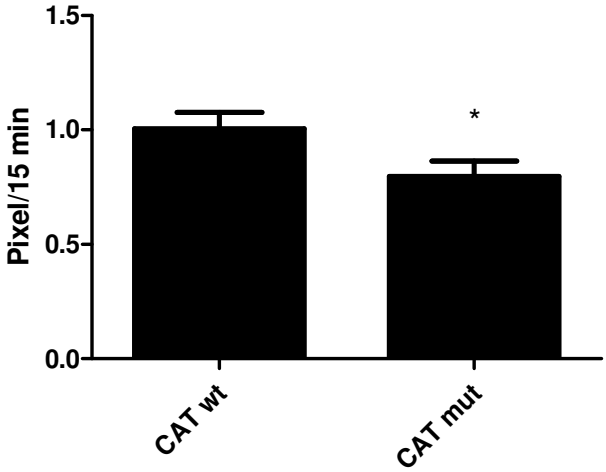

Figure 4.26 - Data from Figure 4.25 (relative control showed there), transfection with pMC36-PRKACAmut plasmid induced a reduction of cell motility compared to transfection with pMC36-PRKACAwt plasmid. t-test, *p<0.05.

As expected, empty plasmid transfection slightly reduced U87 median travelled distance compared to non-transfected cells (Figure 4.25 A). Despite this, PKA hyperactivation and repression of PKA activity through plasmid transfection both induced a significant reduction of U87 cell motility compared to pLX303-transfected cells (Figure 4.25 B). Moreover, PKA hyperactivation induced by

expression of mutant PKA CA subunit caused a larger reduction of median travelled distance compared to the expression of wild type PKA CA subunit (Figure 4.26).
These data thus point to the importance of PKA activity in glioma cell motility, consistently with other data from the literature on PKA-mediated glioma cell invasion (Feng et al. 2014; Zhou et al. 2015).

4.3.3 Disruption of PKA-AKAPs interaction

Delocalization of PKA type I and type II regulatory subunits through expression of the PKA-AKAPs inhibitors RIAD and sAKAPis, induced a reduction in GBM cell viability, associated with an increased cell death (Zorzan 2014). In the present study, cell motility of U87 cells transfected with RIAD and sAKAPis coding plasmids was analyzed in a time lapse experiment. Transfected cells were monitored for 17 hours, starting 72 hours post-transfection, and median distance travelled by cells in 15 minutes was then evaluated (Figure 4.27).

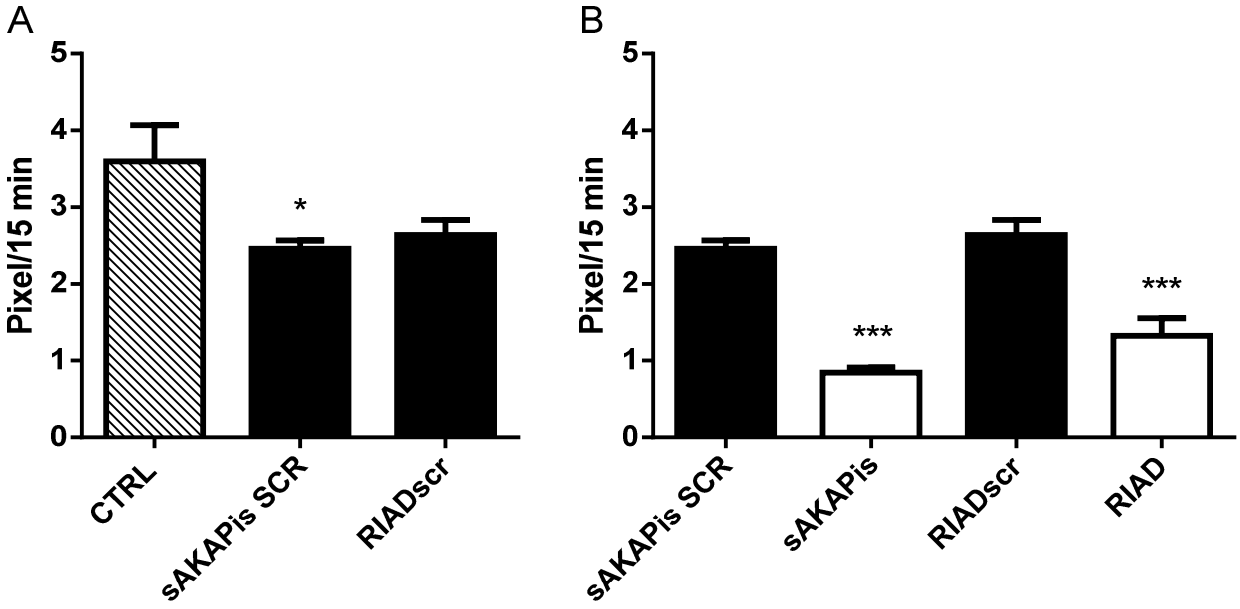

Figure 4.27 - Median distance travelled in 15 minutes by U87 cells expressing sAKAPis inhibitor, RIAD disrupter or their scrambled peptides. CTRL: non-transfected cells. A: t-test, CTRL versus SCR peptides. B: t-test, SCR versus sAKAPis or RIAD. *p<0.05, **p<0.01, ***p<0.001.

As expected, scrambled plasmid transfection slightly reduced median travelled distance compared to non-transfected cells. What is more, disruption of PKA-AKAPs interaction induced by sAKAPis inhibitor and RIAD disrupter caused a significant reduction of U87 cell motility compared to cells transfected with plasmids for expression of scrambled peptides. All together these data suggest that

not only PKA activity, but also PKA intracellular localization is involved in human GBM cell migration.

4.3.4 Dysregulation of PKA expression

The unbalance of PKA regulatory subunits may potentially drive the tumorigenic phenotype of GBM cells. A bioinformatic analysis on REMBRANDT database gene expression data demonstrated that PKA R2A subunit is significantly overexpressed in human GBM compared to non-tumor brain tissue, whereas PKA R1A, R1B and R2B subunits are downregulated in GBM specimens (Zorzan 2014). Also, patients with higher R2A expression appeared to have a shorter survival time compared to patients with lower R2A expression (Mucignat-Caretta et al. 2018). Based on these observations, in the present study the effects of PKA subunits overexpression and downregulation were analyzed, with a particular attention on PKA R2A gene silencing.

4.3.4.1 Overexpression of PKA subunits

Previous experiments with recombinant pLX303 plasmids for overexpression of PKA subunits revealed that PKA R2B and CG overexpression caused a reduction in U87 cell viability, whereas PKA R2A overexpression increased the viability of the cell culture (Zorzan 2014). The cytotoxic effect of PKA R2B expression was also confirmed by morphological analysis of pLX303-PRKAR2B transfected cells (Zorzan 2014) and microscope observation of live pEGFP-C1-PRKAR2B transfected cells (par. 4.2.1). Based on these data, effects of PKA overexpression on GBM cell motility was evaluated in a time lapse experiment. Median distance travelled by cells in 15 minutes was compared between cells overexpressing PKA subunits and cells transfected with the pLX303 plasmid backbone (Figure 4.28).

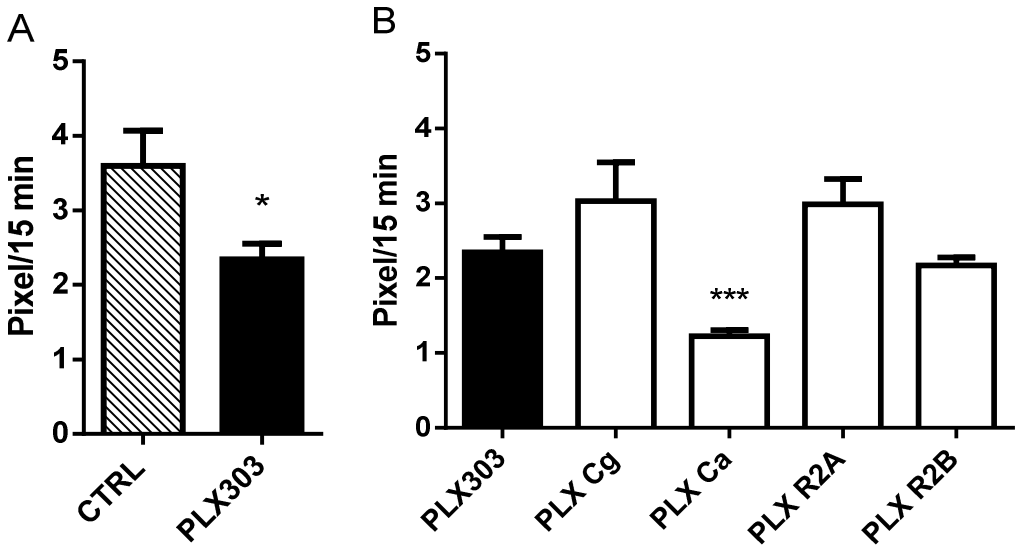

Figure 4.28 - Median distance travelled in 15 minutes by cells transfected with recombinant pLX303 plasmids for overexpression of specific PKA subunits. CTRL: non-transfected cells. A: t-test, CTRL versus pLX303 plasmid backbone. B: t-test, pLX303 versus pLX303-CG, pLX303-CA, pLX303-R2A, pLX303-R2B. *p<0.05, **p<0.01, ***p<0.001.

Overexpression of PKA CG, PKA R2A and PKA R2B subunits did not significantly affect U87 cell motility, whereas overexpression of PKA CA subunit induced a significant reduction of cell motility compared to cells transfected with the backbone plasmid. These data are consistent with the reduction in cell migration of U87 cells transfected with PKA hyperactivation plasmids pMC36-PRKACAwt and pMC36-PRKACAmut (par. 4.3.2).

4.3.4.2 Downregulation of PKA subunits expression

A reduced expression of different PKA subunits was induced in human GBM cells through transfection with pools of siRNA targeting either PKA CA or PKA R2A coding genes (siRNA-PRKACA and siRNA-PRKAR2A, respectively). Previous experiments demonstrated that both PKA CA and R2A gene silencing significantly reduced cell viability, without increasing cell death (Zorzan 2014). In addition, cytofluorimetric analysis revealed a reduction in the cell number of siRNA-PRKAR2A transfected cell population compared to control non-transfected cells. This was also confirmed by cell counting of Wright-stained siRNA-PRKAR2A transfected and control non-transfected cells (Zorzan 2014), suggesting a reduced cell proliferation of GBM cells with downregulated PKA R2A expression. In the present study, cell migration of U87 cells with siRNA-mediated PKA CA and PKA R2A downregulated expression was evaluated. A time lapse

experiment was performed to compare median distance travelled in 15 minutes by siRNA-transfected cells, control non-transfected and control siRNA scrambled (siRNA-SCR) transfected cells (Figure 4.29).

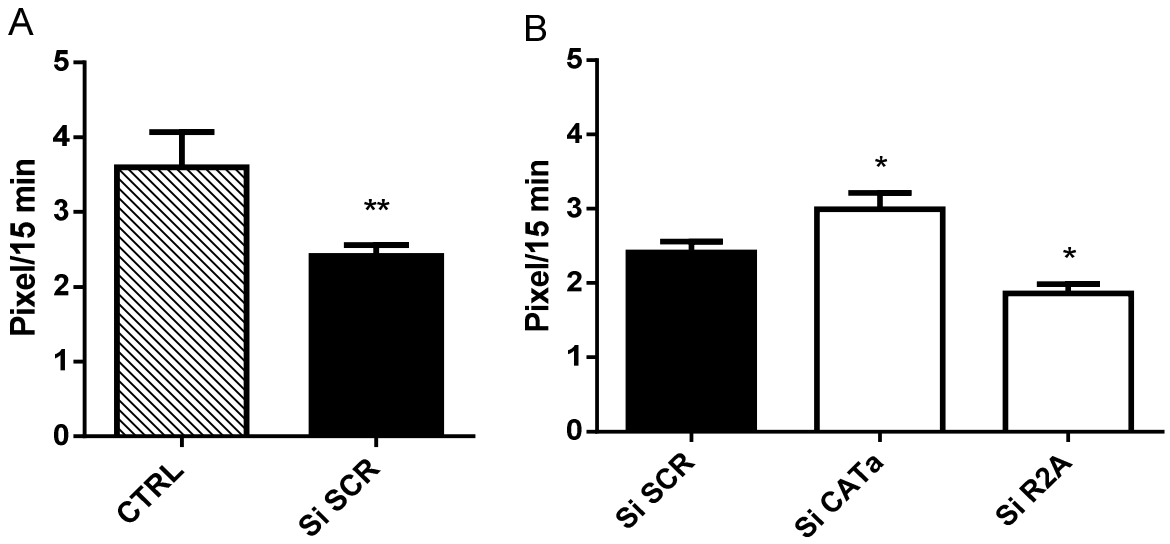

Figure 4.29 - Median distance travelled in 15 minutes by siRNA transfected U87 cells. CTRL: non-transfected cells. A: t-test, CTRL versus siRNA-SCR. B: t-test, siRNA-SCR versus siRNA-CA and siRNA-R2A. *p<0.05, **p<0.01, ***p<0.001.

As expected, siRNA-SCR transfection reduced U87 cell motility compared to non-transfected cells. However, downregulation of PKA CA expression induced a significant increase of median travelled distance compared to siRNA-SCR-transfected cells. On the contrary, silencing of PKA R2A expression significantly reduced cell motility of U87 cells compared to cells transfected with scrambled siRNA. As a decreased expression of PKA regulatory subunits is supposed to be associated with an increased PKA catalytic activity, this result is consistent with the reduction of GBM cell migration induced by 8Br-cAMP treatment (par. 4.3.1), transfection with PKA hyperactivation plasmids (pMC36-PRKACAwt and pMC36-PRKACAmut, par. 4.3.2) and transfection with PKA CA overexpression plasmid (pLX303-PRKACA, par. 4.3.4.1). To further support this observation, future experiments will include testing of different siRNA scrambled sequences, as well as double trasfection with scrambled and PKA siRNA sequences.

4.3.4.3 Effects of PKA R2A gene silencing on Golgi apparatus

Fragmentation of Golgi apparatus had been previously observed in U87 cells transfected with siRNA-PRKAR2A (Zorzan 2014). In these cells, R2A subunit was detectable by

immunofluorescence, even though the siRNA effect had been confirmed through RT-PCR. In siRNA-PRKAR2A-treated cells, PKA R2A was still co-localized with the trans-Golgi network marker golgin 97, but it appeared dispersed in the cell cytoplasm (Zorzan 2014). Moreover, this effect on Golgi complex was not observed in cells transfected with si-SCR and cells treated with transfection reagents. In the present study, immunofluorescence experiments on siRNA-PRKAR2A-transfected cells were replicated to evaluate co-localization of PKA R2A subunit with the cis-Golgi network marker GRASP65. For this purpose, transfected U87 cells were double immunolabeled 72 hours post-transfection with anti-PKA R2A and anti-GRASP65 antibodies (Figure 4.30).

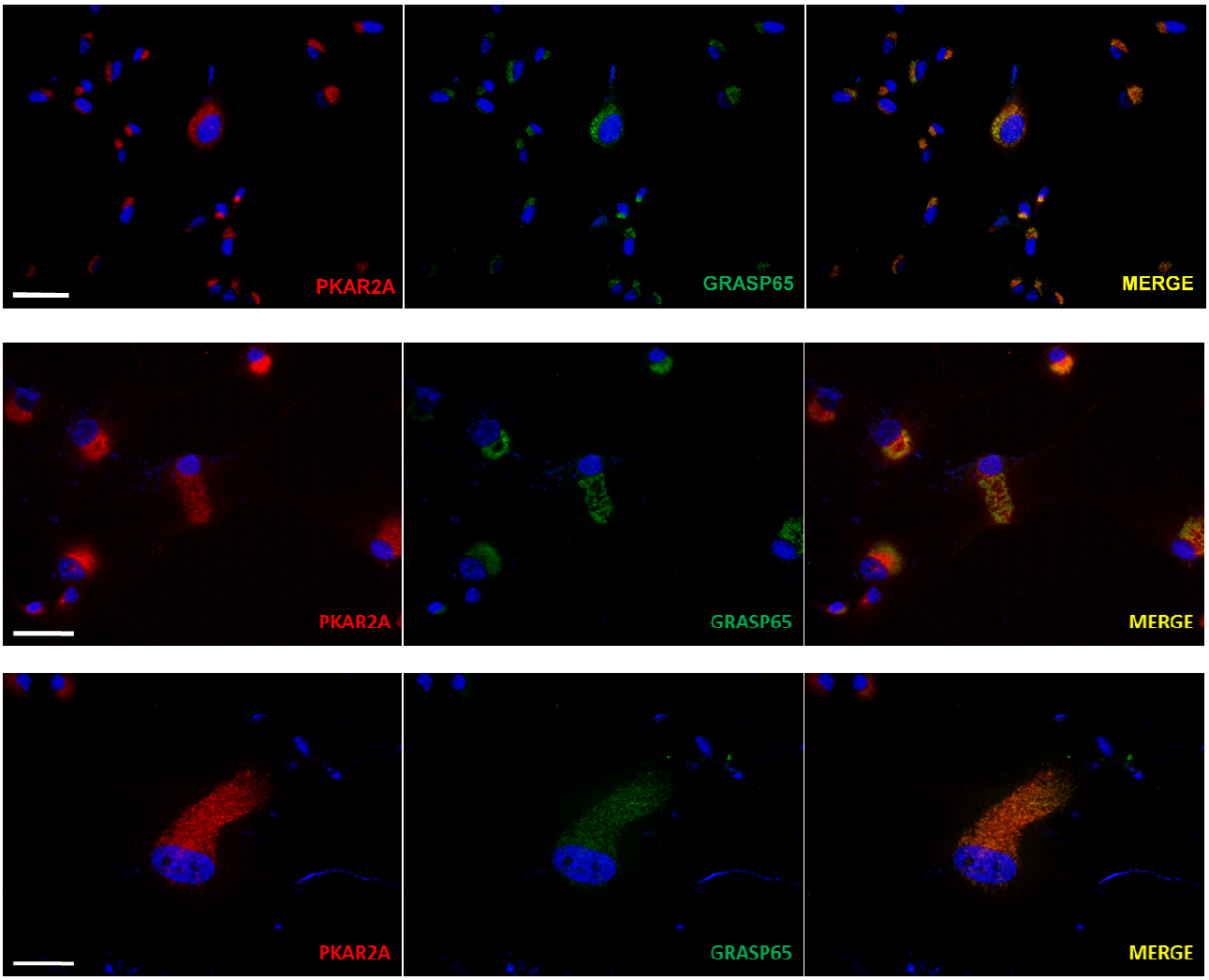

Figure 4.30 - Immunofluorescence on U87 cells transfected with siRNA-PRKAR2A. Upper panel: U87 cells treated with transfection reagents; middle and lower panel: U87 cells transfected with siRNA-PRKAR2A. Red: PKA R2A; green: GRASP65; blue: DAPI nuclear staining. Epifluorescence 40x, bar 100 µm.

As apparent in Figure 4.30, siRNA-PRKAR2A-transfected cell cultures presented some cells with a different PKA R2A distribution compared to cells treated with transfection reagents. In particular, in siRNA-PRKAR2A treated cells PKA R2A and GRASP65 co-localized signals appeared dispersed in the cytoplasm rather than clustered near the cell nucleus. This observation is consistent with previous experiments (Zorzan 2014) and other studies reporting disassembly of Golgi apparatus following PKA R2A depletion by siRNA treatment, PKA displacement and pharmacological inhibition of PKA (Bejarano et al. 2006). These results thus support the involvement of Golgi-associated PKA in the maintenance of Golgi integrity. This observation is still preliminary and further experiments are expected to better clarify PKA-Golgi relation, particularly if a higher efficiency in PKA R2A silencing could be provided.

4.4 Interference with Golgi function: brefeldin A

In order to investigate the relationship between PKA and Golgi apparatus, U87 human GBM cells were treated with BFA, a disrupter of Golgi structure and function. BFA inhibits the intracellular protein transport, particularly the anterograde membrane movement into the Golgi apparatus (Klausner et al. 1992), by inhibiting brefeldin A-inhibited guanine nucleotide-exchange factors 1 and 2 (BIG1 and BIG2). BIG proteins are implicated in Golgi membrane transport as they activate ADP-ribosylation factors (Arfs) by accelerating the replacement of bound GDP with GTP. Interestingly, BFA targets BIG1 and BIG2 contain AKAP sequences for PKA regulatory subunits, that act as scaffold for multimolecular assemblies including also PKA and phosphodiesterase 3A (PDE3A). Based on this known connection between BFA, Golgi apparatus and PKA (Puxeddu et al. 2009; Li et al. 2016), human U87 cells were treated with BFA and cell viability, cell motility, Golgi structure as well as PKA intracellular distribution were then analyzed.

4.4.1 Cell viability

Cell viability of U87 cells treated for 24 and 72 hours with BFA was first evaluated through MTT assays, showing a significant reduction in cell viability, even at the lowest concentration (0.01 µg/ml; Figure 4.31).

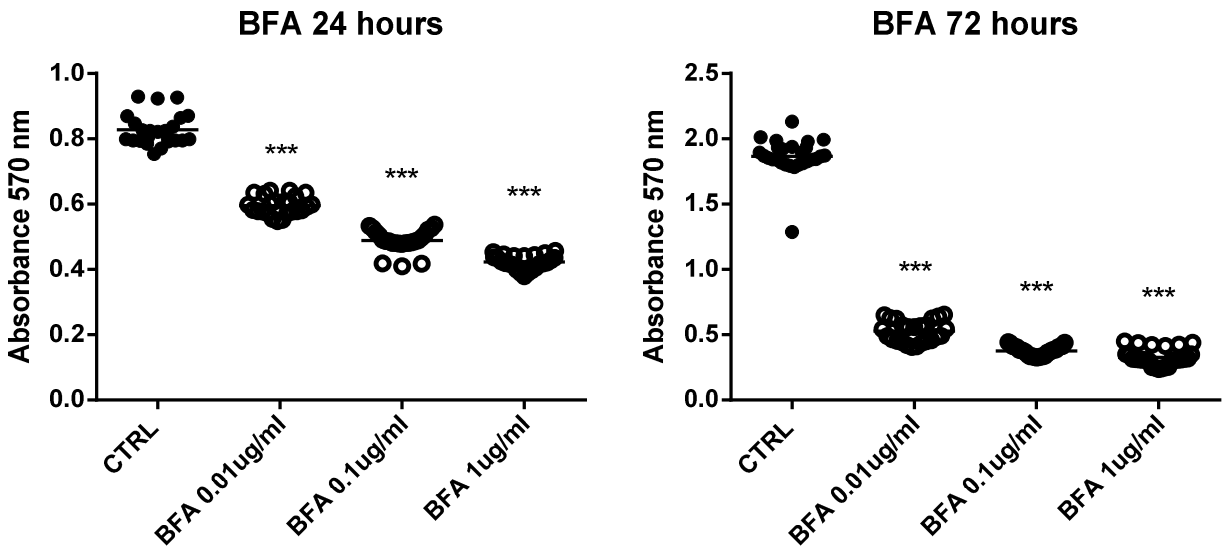

Figure 4.31 - MTT assay on U87 cells treated with BFA for 24 and 72 hours. A reduced cell viability was observed at all BFA tested concentrations. t-test, CTRL versus treatment. *p<0.05, **p<0.01, ***p<0.001.

Cell death was further evaluated through morphological analysis of Wright-stained BFA treated cells, confirming high BFA toxicity (Figure 4.32).

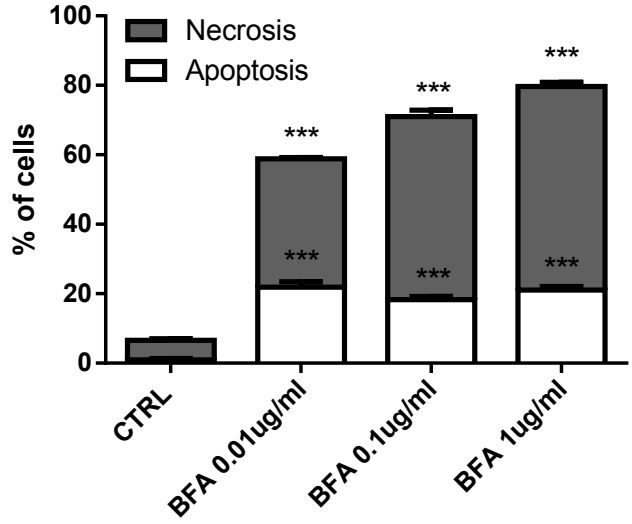

Figure 4.32 - Morphological analysis of U87 cells treated with BFA for 24 hours. Percentages of cell necrosis and apoptosis were compared between treated and control untreated cells. t-test, CTRL versus treatment. *p<0.05, **p<0.01, ***p<0.001.

BFA treated cells exhibited greatly increased mortality, including an increase in both cell necrosis and apoptosis. These data are consistent with the literature, reporting cell growth inhibition and induction of cell apoptosis in GBM cells treated with BFA (Pommepuya et al. 2003).

4.4.2 Cell motility

Cell motility of U87 cells with BFA-induced disrupted Golgi function was evaluated by three complementary approaches. First, a wound healing assay was performed to estimate cell invasion after 24 hour BFA treatment (Figure 4.33).

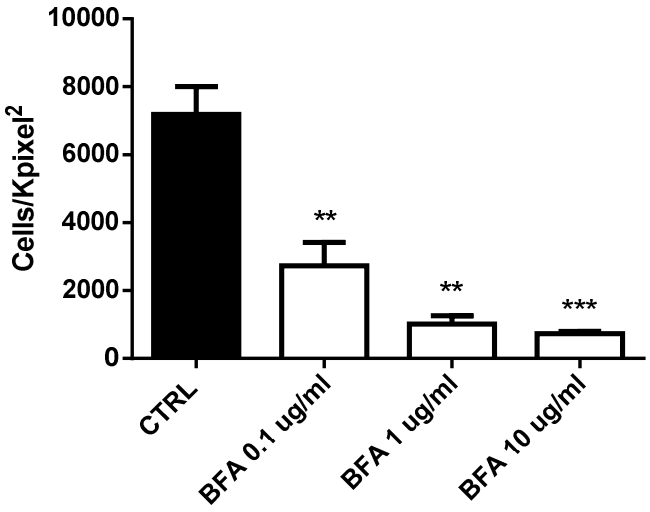

Figure 4.33 - Wound healing assay demonstrated a reduced cell invasion of U87 cells treated with BFA for 24 hours compared to control untreated cells. t-test, CTRL versus treatment. *p<0.05, **p<0.01, ***p<0.001.

Cellular invasion of the scratched areas was significantly reduced by treatment with BFA. Interestingly, BFA 0.1 µg/ml induced a reduction of U87 cell invasion without apparent changes in cell morphology.

Secondly, cell migration of BFA treated U87 cells grown in silicon circles was analyzed and compared to control untreated cells (Figure 4.34).

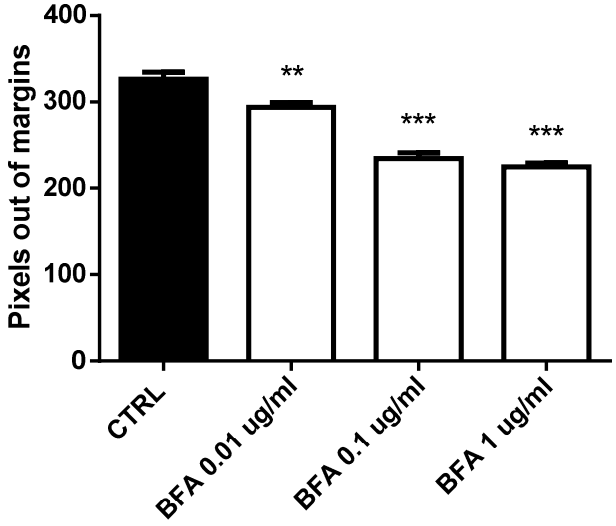

Figure 4.34 - Cell migration following silicon circles removal was reduced for U87 cells treated with BFA for 24 hours compared to control untreated cells. t-test, CTRL versus treatment. *p<0.05, **p<0.01, ***p<0.001.

All tested BFA concentrations significantly reduced U87 cell migration, confirming the decreased cell motility reported in the wound healing assay.

A time lapse experiment was also performed to monitor cell migration of live U87 cells under BFA treatment. Distance travelled by cells was compared between BFA treated and control untreated U87 cells (Figure 4.35).

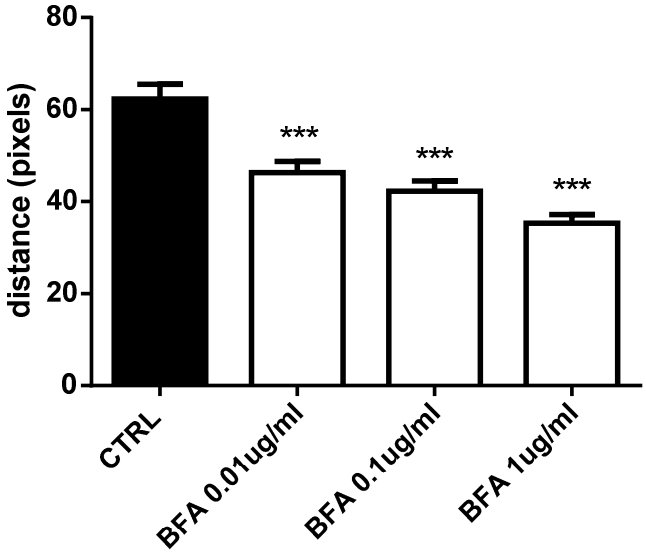

Figure 4.35 - Distance travelled by U87 cells treated with BFA was significantly reduced compared to control untreated cells. t-test, CTRL versus treatment. *p<0.05, **p<0.01, ***p<0.001.

As shown in Figure 4.35, distance travelled in 17 hours was significantly reduced by BFA treatment. These results further confirmed the reduced cell motility of GBM cells with disrupted Golgi function.

4.4.3 PKA intracellular distribution

Immunofluorescence was performed on U87 cells treated with increasing BFA concentrations to evaluate the integrity of Golgi apparatus and the intracellular distribution of PKA R2A subunit (Figure 4.36).

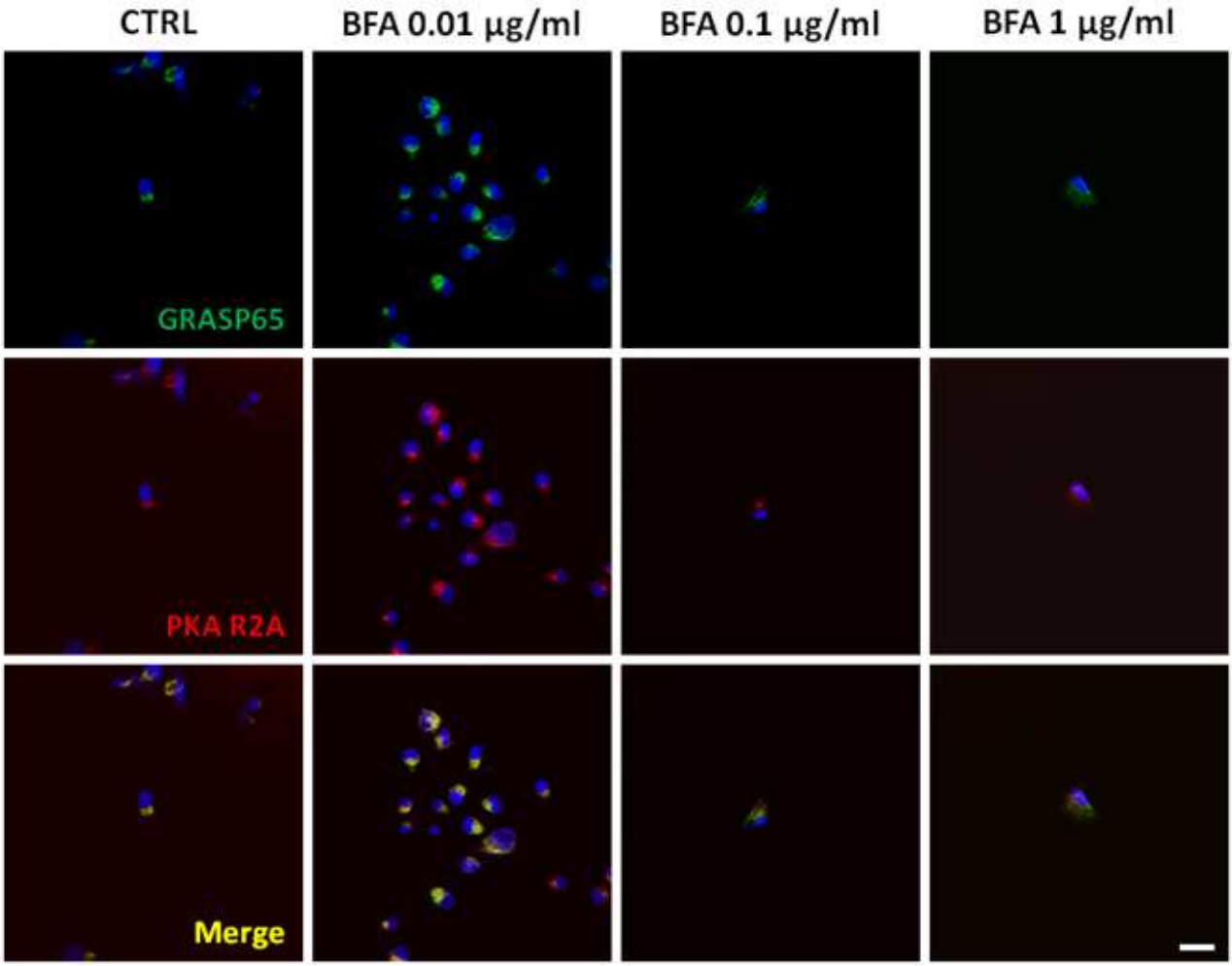

Figure 4.36 - Immunofluorescence on control untreated and BFA treated U87 cells.
Green: GRASP65; red: PKA R2A; blue: DRAQ5 nuclear staining. Confocal 63x, bar 100 µm.

No effect on Golgi apparatus and PKA R2A distribution was observed in cells treated with BFA 0.01 µg/ml, whereas following treatment with BFA 0.1 µg/ml GRASP65 Golgi marker appeared more diffuse than the perinuclear R2A signal, compared to control untreated cells. Treatment with

BFA 1 µg/ml clearly induced the redistribution of Golgi apparatus in the cell cytoplasm. What is more, a redistribution of PKA R2A was also observed in BFA 1 µg/ml treated cells: PKA R2A signal appeared not anymore clustered near the nucleus, but dispersed in the cytoplasm and partially not co-localized with GRASP65 Golgi marker.

4.4.4 BFA, Golgi apparatus and PKA R2A in human GBM cells

Dispersion of PKA subunits throughout the cytosol following BFA treatment has been reported in HeLa cellular model, in which Golgi-associated PKA is supposed to be involved in the Golgi assembly process and maintenance of its structural organization (Bejarano et al. 2006). The experiments above on BFA treated human GBM cells, together with data on the effects of siRNA-mediated PKA R2A gene silencing (Figure S1; par. 4.3.4.2 and 4.3.4.3), strongly support a relevant role for PKA R2A peculiar intracellular localization in GBM cells. Current results suggest the involvement of PKA R2A subunit in fundamental functions of GBM cells, including cell motility, cell proliferation and regulation of Golgi structure.

4.5 Focusing on PKA R2A subunit: development of a lentiviral-based system for efficient silencing of PKA R2A expression in human GBM cells

Transient interference with PKA pathway through chemical agents, plasmid transfection and siRNA treatment strongly affects human GBM cells. The experiments presented so far demonstrated the importance of PKA activity, regulated expression and peculiar intracellular localization for GBM cells, particularly for cell migration capability. Among all tested approaches, silencing of PKA R2A expression proved the most interesting and promising one. Indeed, this PKA subunit not only presents a peculiar intracellular distribution that is specific for GBM cells compared to non tumor brain tissue, but also may potentially have a critical role in the maintenance of Golgi structure. The specific PKA R2A intracellular localization was described also in GBM stem like spheres, adding further evidences on the opportunity to better define its cellular function. Moreover, preliminary data suggested a reduced cell proliferation of GBM cells with siRNA-induced PKA R2A downregulation, an effect that deserves further investigation and may find in the future a potential therapeutic application. Based on the results of this first section of the PhD project, the second part of the study was aimed at the development of a more powerful system to downregulate PKA R2A expression in human GBM cells. The first requirement for the intended gene-silencing system was

the ability to induce a reduction in PKA R2A expression in the great majority, potentially the entire population, of treated cells, in order to overcome the low transfection efficiency emerged in previous experiments with siRNA and PKA plasmids. In addition to the improved efficiency, the generated system was expected to allow investigation of acute as well as long-term effects induced by PKA R2A knockdown. For this purpose, third generation lentiviral vectors were designed, developed and tested for the efficient delivery of shRNA targeting PKA R2A subunit in human GBM cellular models.

4.5.1 Lentiviral transduction of human GBM cells

Two lentiviral vectors, cPPT.hCMV.eGFP and pLL3.7, were preliminarily tested for transduction of human GBM cells. The cPPT.hCMV.eGFP vector contains a hCMV promoter guiding the expression of the EGFP reporter gene, or other potential transgenes that might be cloned in the multiple cloning site downstream the promoter; the pLL3.7 vector contains a CMV-EGFP expression cassette and an additional mouse U6 promoter upstream of a multiple cloning site for transgene insertion. Both lentiviral vectors are suitable for expression of shRNAs, depending on the desired transgene promoter (Pol-II hCMV or Pol-III U6 promoter).

U87 cells were efficiently transduced by both cPPT.hCMV.eGFP and pLL3.7 lentiviral particles, showing high EGFP expression levels (Figure 4.37 and 4.38).

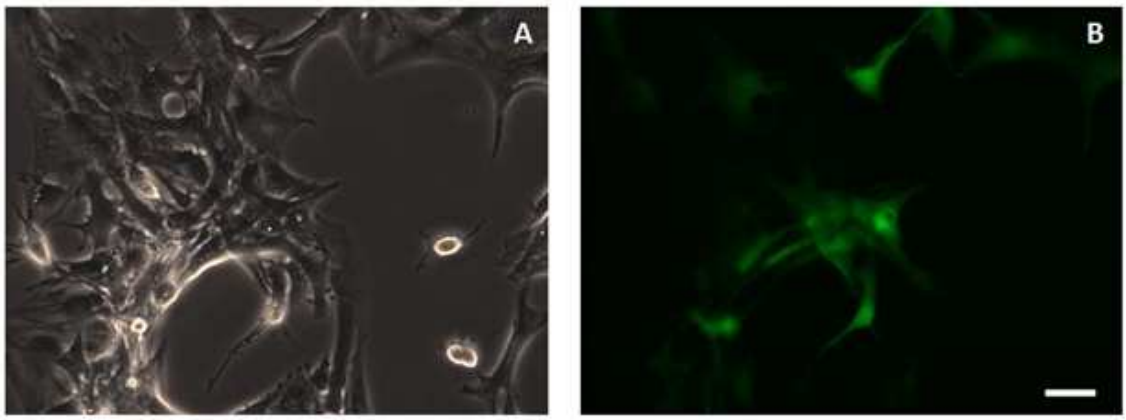

Figure 4.37 - U87 cells transduced with cPPT.hCMV.eGFP lentiviral particles. Direct light (A) and epifluorescence (B) 20x, bar 50 µm.

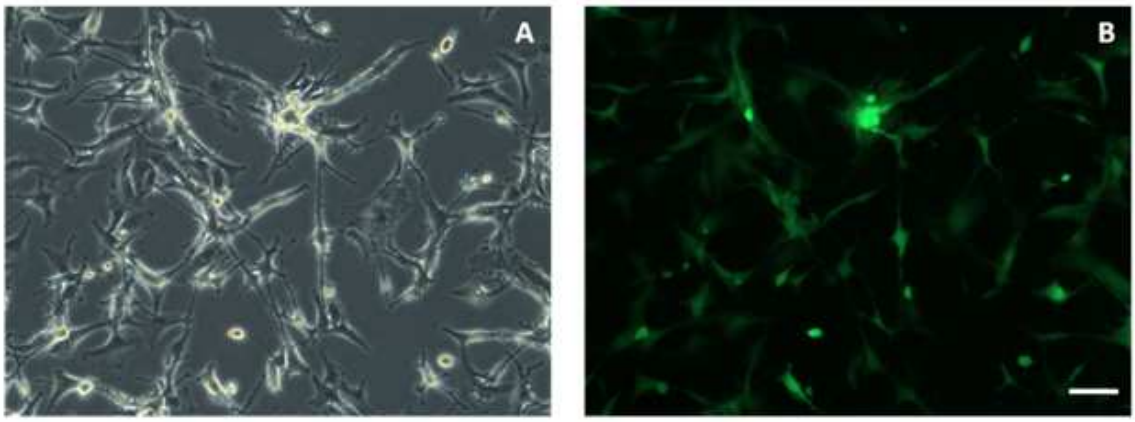

Figure 4.38 - U87 cells transduced with pLL3.7 lentiviral particles. Direct light (A) and epifluorescence (B) 10x, bar 100 µm.

Following cPPT.hCMV.eGFP transduction, U87 cells were monitored for more than 15 days: high expression of the EGFP reporter protein was maintained and no overt influence on cell growth was observed.

The cPPT.hCMV.eGFP lentiviral vector was also tested for transduction of human GBM stem like cell cultures, GBM2 and GBM5, proving able to efficiently transduce GBM spheres (Figure 4.39).

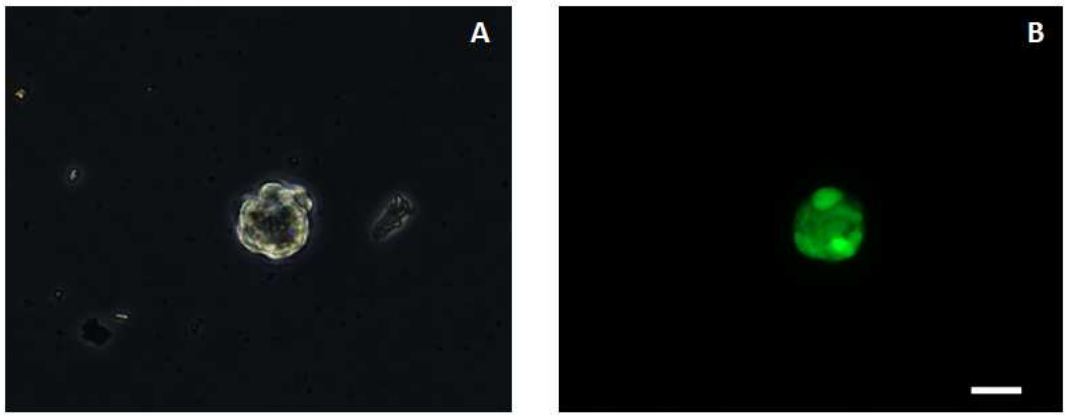

Figure 4.39 - GBM2 sphere transduced with cPPT.hCMV.eGFP lentiviral particles. Direct light (A) and epifluorescence (B) 20x, bar 50 µm.

EGFP expression was detected from most, but not all, cells forming GBM spheres. Moreover, transduced GBM stem like cells maintained both the expression of the reporter gene and the ability to form spheres after dissociation (Figure 4.40).

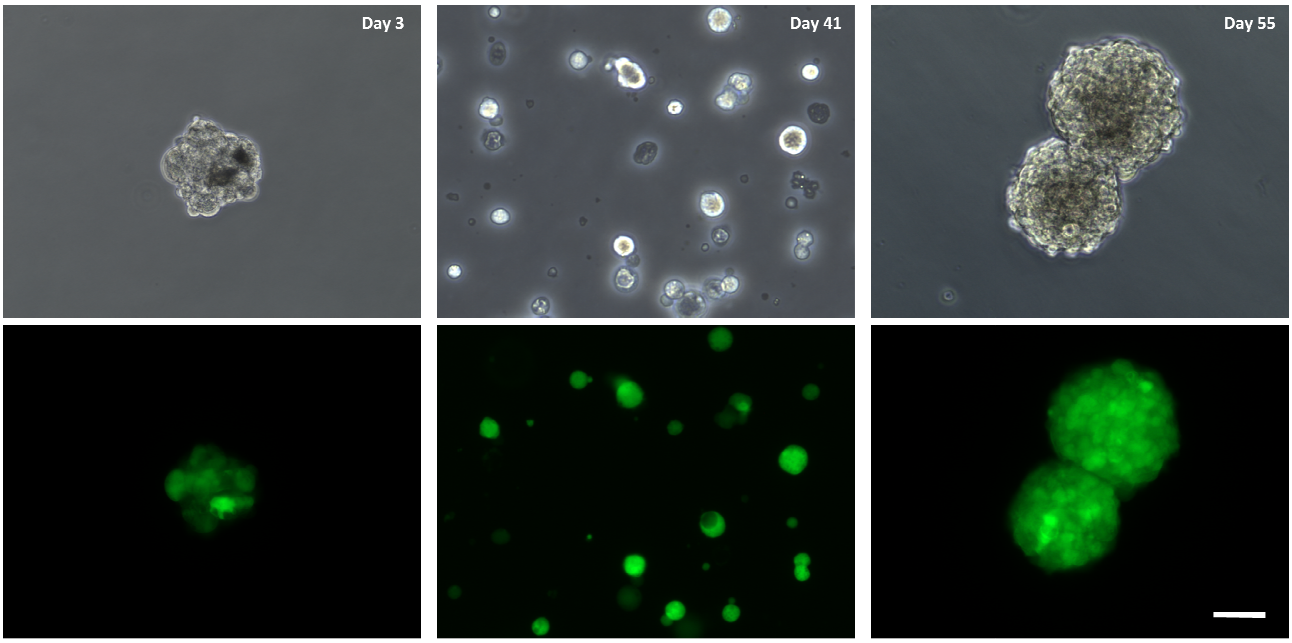

Figure 4.40 - GBM5 cells transduced with cPPT.hCMV.eGFP lentiviral particles: transduced sphere 3 days post-transduction (left); cells derived from dissociation of transduced spheres 41 days post-transduction (middle); new spheres formed 55 days post-transduction following dissociation of transduced spheres. Direct light (upper images) and epifluorescence (lower images) 40x, bar 250 µm.

Thus, transduction with lentiviral particles seemed not to affect glioma stem like cell growth and sphere formation.

4.5.2 Generation of PKA R2A shRNA lentiviral vectors and scrambled control vector

PKA R2A Temp1 and Temp2 shRNA sequences as provided by Fellman and colleagues (Fellmann et al. 2013) are suitable for direct cloning under the control of a Pol-II promoter, whereas expression of shRNAs from Pol-III promoters requires slightly different but precise sequence features in order to achieve production of shRNAs with optimal pre-miRNA-like structure. For this reason, PKA R2A Temp1 and Temp2 shRNA sequences were first cloned in the cPPT.hCMV.eGFP vector under the control of a Pol-II hCMV promoter, which is also associated with a reduced toxicity deriving from interference with endogenous miRNA processing compared to Pol-III promoters (Bofill-De Ros and Gu 2016).

As described above (par. 3.10.1), PKA R2A Temp1 and Temp2 shRNA sequences were subcloned in the eukaryotic expression plasmid pEGFP-C1 to generate recombinant pEGFP-C1-shTemp1 and

pEGFP-C1-shTemp2 vectors, that allowed expression of respectively EGFP-shRNA Temp1 and EGFP-shRNA Temp2 cassettes from a CMV promoter. Following plasmid verification, two parallel cloning strategies led to the generation of four gene-silencing cPPT.hCMV.eGFP-based lentiviral vectors (Figure 4.41):

- cPPT.hCMV.shTemp1, for expression of PKA R2A Temp1 shRNA;
- cPPT.hCMV.shTemp2, for expression of PKA R2A Temp2 shRNA;
- cPPT.hCMV.EGFP.shTemp1, for co-expression of EGFP reporter protein and PKA R2A Temp1 shRNA;
- cPPT.hCMV.EGFP.shTemp2, for co-expression of EGFP reporter protein and PKA R2A Temp2 shRNA.

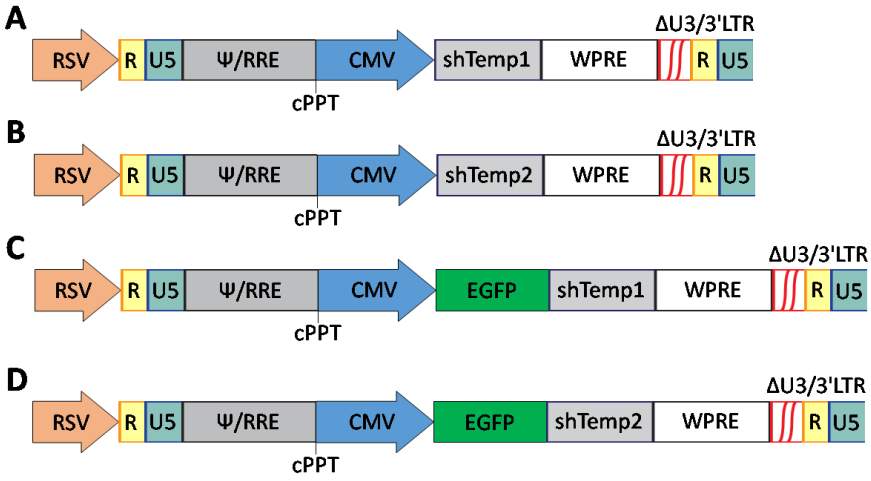

Figure 4.41 - Gene-silencing cPPT.hCMV.eGFP-based lentiviral vectors for silencing of PKA R2A expression. A: cPPT.hCMV.shTemp1; B: cPPT.hCMV.shTemp2; C: cPPT.hCMV.EGFP.shTemp1; D: cPPT.hCMV.EGFP.shTemp2.

All generated cPPT.hCMV.eGFP-based lentiviral vectors were properly verified (par. 3.10.1.2) prior to production of recombinant lentiviral particles. Lentiviral vectors carrying the EGFP reporter gene were titered through transduction of 293T cells and subsequent flow cytometry analysis (par. 3.14.1). A representative example of obtained biological titres for non concentrated EGFP-carrying lentiviral vectors is reported in Table 4.1.

	Transducing units/ml
cPPT.hCMV.eGFP	1.04×10^7
cPPT.hCMV.EGFP.shTemp1	1×10^5
cPPT.hCMV.EGFP.shTemp2	2.16×10^6

Table 4.1 - Biological viral titres of representative stocks of non concentrated lentiviral vectors carrying the EGFP reporter gene, as calculated after FACS analysis of transduced 293T cells.

FACS analysis of transduced cells revealed a progressive lower viral titre for cPPT.hCMV.EGFP.shTemp2 and cPPT.hCMV.EGFP.shTemp1 vectors compared to cPPT.hCMV.eGFP, consistently with data from Fellmann and colleagues (Fellmann et al. 2013). Indeed, single-copy expression of transcripts encoding EGFP and shRNA was expected to result in lower EGFP fluorescence levels compared to the backbone vector as a larger fraction of polycistronic transcripts was recognized and processed in the endogenous miRNA pathway and thus no longer available for reporter protein expression (Fellmann et al. 2013; Figure 4.42).

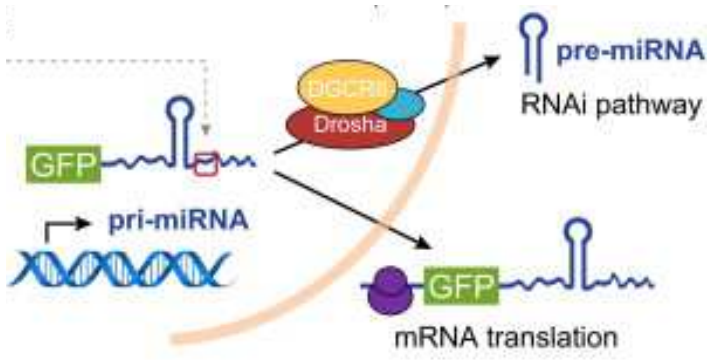

Figure 4.42 - Scheme from Fellmann et al. 2013, showing the dual use of polycistronic transcripts for both EGFP protein synthesis (mRNA translation) and shRNA biogenesis (RNA interference pathway).

Based on this, lower EGFP fluorescence levels detected by flow cytometry analysis for cPPT.hCMV.EGFP.shTemp2 and cPPT.hCMV.EGFP.shTemp1 vectors were not necessarily associated with a real lower biological viral titre. Instead, they indicated lower levels of mRNA translation and EGFP synthesis due to the biogenesis of PKA R2A shRNAs. For this reason, quantitative determination of viral p24 antigen (p24 assay) and viral RT activity (RT assay) were performed for all recombinant lentiviral vectors. For viral stocks reported in Table 4.1, the range of viral p24 antigen was 300-400 p24 ng/ml, whereas viral RT activity ranged between 67,000 and 128,000 cpm/500 µl.

In addition to the PKA R2A shRNA lentiviral vectors, a recombinant cPPT.hCMV.eGFP-based vector for expression of a scrambled shRNA was also generated. The scrambled vector cPPT.hCMV.shSCR contained the scrambled sequence of PKA R2A Temp1 shRNA, that was previously demonstrated to have no cellular targets, cloned under the control of the hCMV promoter in the cPPT.hCMV.eGFP vector (par. 3.10.2). The generated scrambled vector allowed expression only of the scrambled shRNA, with no co-expression of a reporter protein (Figure 4.43).

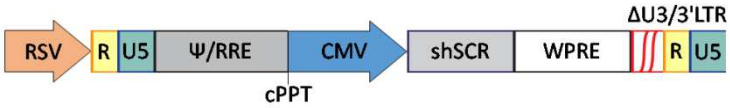

Figure 4.43 - Scrambled vector cPPT.hCMV.shSCR.

4.5.3 shRNA secondary structure: mfold predictions

Folding of PKA R2A and scrambled shRNA was predicted through the 'mfold web server' software (version 3.5; Zuker 2003; http://unafold.rna.albany.edu/?q=mfold). The predicted secondary structures are reported in Figure 4.44.

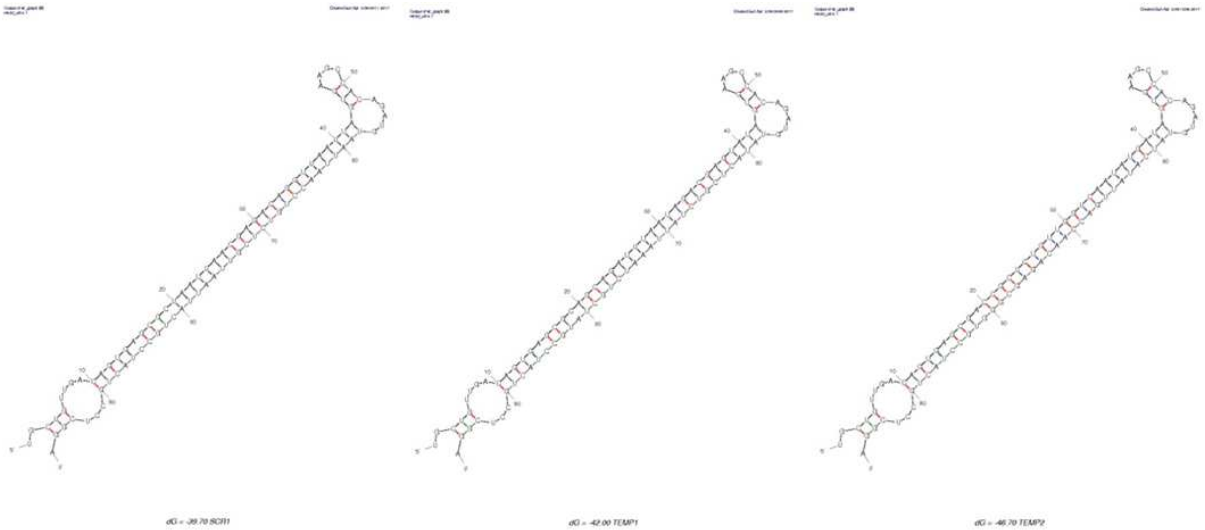

Figure 4.44 - mfold secondary structure predictions for PKA R2A Temp1 (shTemp1), PKA R2A Temp2 (shTemnp2) and scrambled (shSCR) shRNAs

As apparent in Figure 4.44, the same secondary structure was predicted for PKA R2A Temp1, PKA R2A Temp2 and scrambled shRNAs. This was an independent indication of proper scrambled design, as folding into an optimal hairpin-like structure is required for correct processing of the shRNA.

4.5.4 PKA R2A silencing in 293T cells

Gene silencing efficiency of the lentiviral vectors carrying PKA R2A shRNA sequences was tested in 293T cells in both transient and stable expression systems. First, 293T cells were transfected with the *cis*-elements of recombinant lentiviral vectors (cPPT.hCMV.eGFP, cPPT.hCMV.shTemp1, cPPT.hCMV.EGFP.shTemp1, cPPT.hCMV.shTemp2, cPPT.hCMV.EGFP.shTemp2) and PKA R2A expression was evaluated 3 days post-transfection (Figure 4.45).

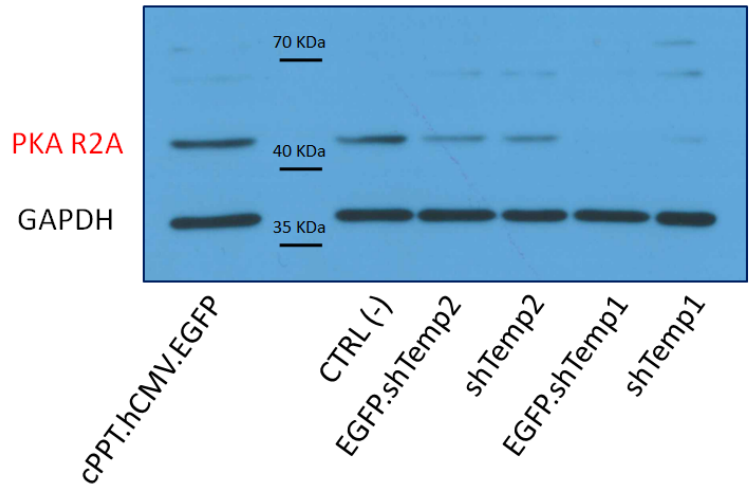

Figure 4.45 - Western blot analysis of 293T cells transfected with the *cis*-elements of recombinant lentiviral vectors, 72 hours post-transfection. Cells (2.5×10^5) were co-transfected with 500 ng of pRSV-Rev plasmid and 1500 ng of lentiviral transfer vector. CTRL (-): untransfected cells.

Transient expression of the *cis*-elements of recombinant lentiviral vectors induced downregulation of PKA R2A expression in 293T cells. In addition, PKA R2A Temp1 shRNA sequence proved more efficient in reducing R2A expression compared to PKA R2A Temp2 shRNA sequence.

As a second step, 293T cells were transduced with PKA R2A gene-silencing lentiviral vectors (cPPT.hCMV.shTemp1, cPPT.hCMV.EGFP.shTemp1, cPPT.hCMV.shTemp2, cPPT.hCMV.EGFP.shTemp2) and silencing efficiency was evaluated 3, 6 and 9 days post-transduction (Figure 4.46).

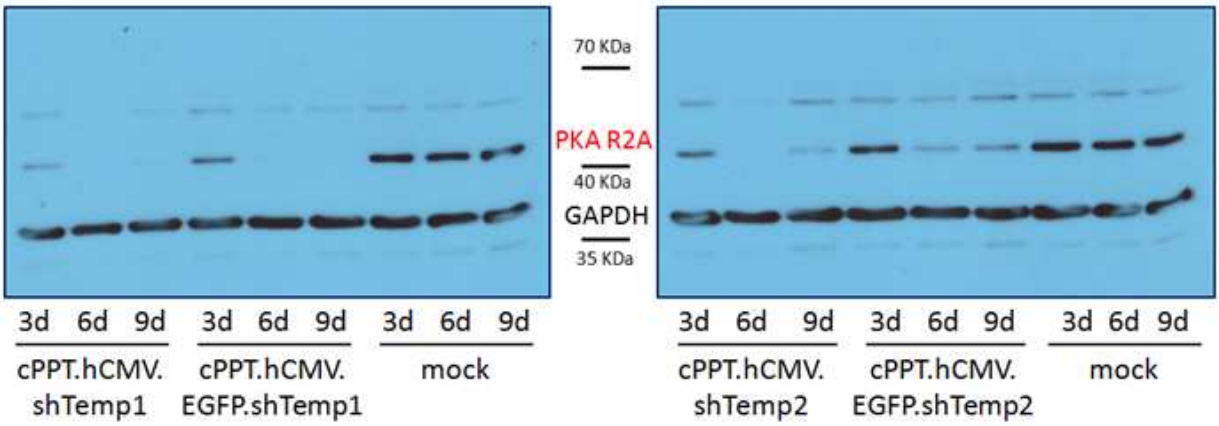

Figure 4.46 - Western blot analysis of 293T cells transduced with the recombinant lentiviral vectors 3, 6 and 9 days post-transduction. Cells (22.5×10^5) were transduced with 300 ng p24 of lentiviral vector (approximately 200,000 cpm of the viral stock used in this experiment).

As shown in Figure 4.46, all recombinant lentiviral particles for the expression of PKA R2A shRNAs induced a significant downregulation of R2A expression. Again, PKA R2A Temp1 shRNA sequence, with or without co-expression of EGFP protein, proved to be more efficient in silencing R2A expression compared to the Temp2 shRNA constructs.

4.5.5 PKA R2A silencing in U87 human GBM cells

In order to evaluate gene silencing efficiency of PKA R2A shRNA lentiviral vectors in human GBM cells, U87 cells were transduced with 300 ng p24 (approximately 200,000 cpm of the viral stock used in this experiment) of lentiviral vectors (cPPT.hCMV.shTemp1, cPPT.hCMV.EGFP.shTemp1, cPPT.hCMV.shTemp2, cPPT.hCMV.EGFP.shTemp2) and R2A expression was analyzed 3, 6 and 9 days post-transduction (Figure 4.47).

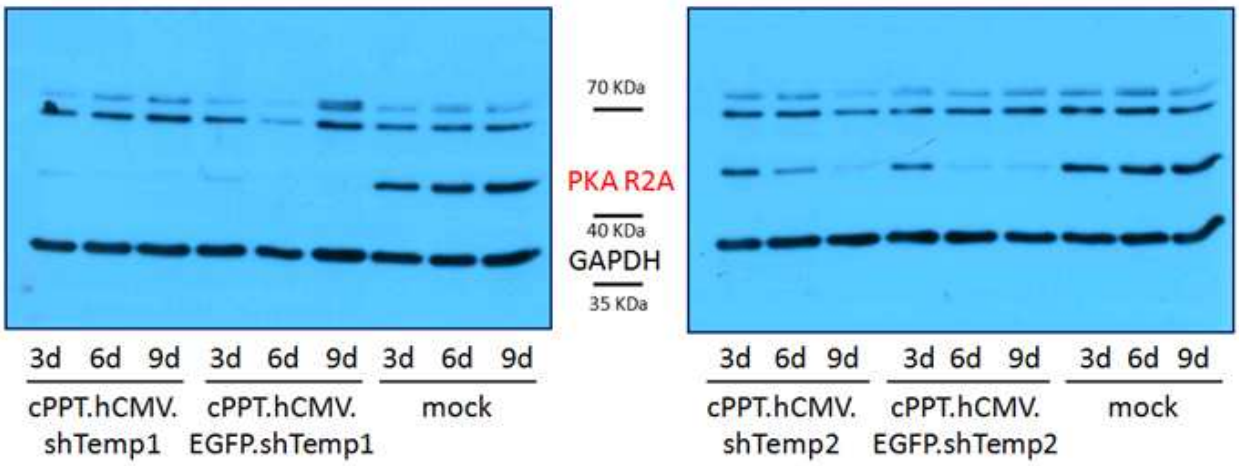

Figure 4.47 - Western blot analysis of U87 cells transduced with the recombinant lentiviral vectors 3, 6 and 9 days post-transduction. Cells (1.0×10^5) were transduced with 300 ng p24 of lentiviral vector (approximately 200,000 cpm of the viral stock used in this experiment).

An efficient silencing of PKA R2A expression was induced in U87 cells by shTemp1 vectors, starting 3 days post-transduction and also 6 and 9 days post-transduction. A progressive reduction in R2A expression was also reported in cells tranduced with shTemp2 vectors, even though with a minor efficiency compared to Temp1 shRNA sequence.

To verify the stability of PKA R2A downregulation, western blot analysis of transduced U87 cells was also performed 30 days post-transduction (Figure 4.48).

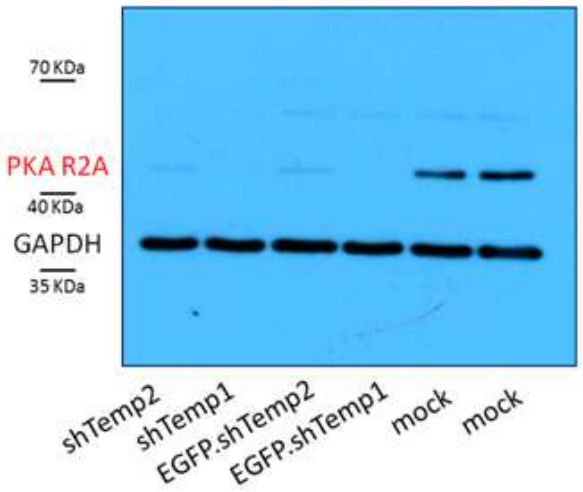

Figure 4.48 - Western blot analysis of U87 cells transduced with the recombinant lentiviral vectors 30 days post-transduction. Cells (1.0×10^5) were transduced with 300 ng p24 of lentiviral vector (approximately 200,000 cpm of the viral stock used in this experiment).

As shown in Figure 4.48, PKA R2A downregulation was maintained for at least 30 days in U87 human GBM cells transduced with shTemp1 and shTemp2 lentiviral vectors.

4.5.6 PKA R2A silencing in GBM5 human GBM stem like cells

PKA R2A silencing capability of PKA R2A shRNA lentiviral vectors was tested in human GBM stem like cells through transduction of GBM5 spheres with recombinant lentiviral particles (cPPT.hCMV.eGFP, cPPT.hCMV.EGFP.shTemp1, cPPT.hCMV.EGFP.shTemp2) and evaluation of PKA R2A expression 3 months post-transduction.
As expected, different EGFP expression levels were observed for cells transduced with cPPT.hCMV.eGFP and PKA R2A gene silencing lentiviral vectors (Figure 4.49).

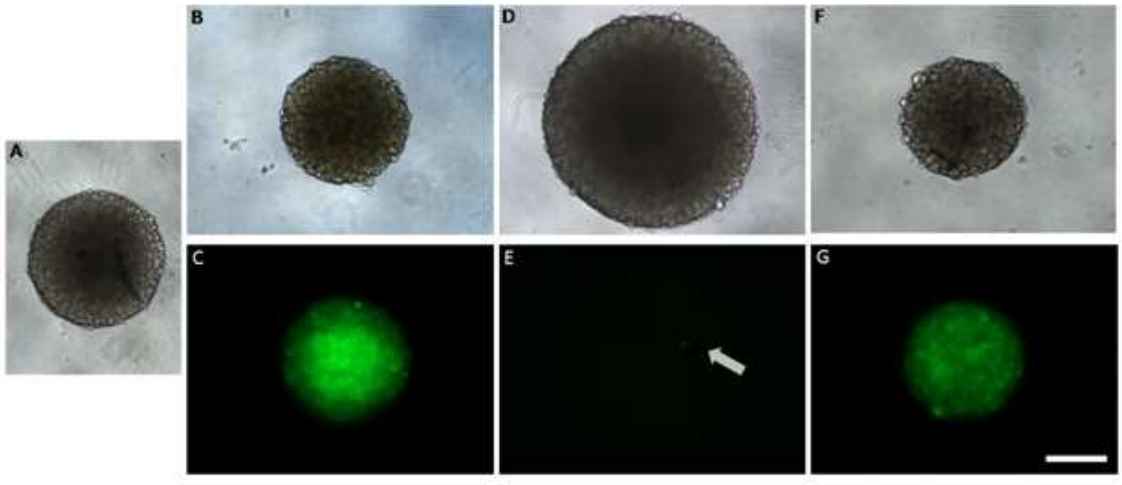

Figure 4.49 - GBM5 spheres transduced with the recombinant lentiviral particles 30 days post-transduction. A: mock transduced GBM5 sphere; B and C: cPPT.hCMV.eGFP; D and E: cPPT.hCMV.EGFP.shTemp1, weak EGFP signal is indicated in E (arrow); F and G: cPPT.hCMV.EGFP.shTemp2. Direct light (A, B, D, F) and epifluorescence (C, E, G) 10x, bar 200 µm.

Long-term PKA R2A downregulation was evaluated through western blot analysis of transduced GBM5 spheres (Figure 4.50).

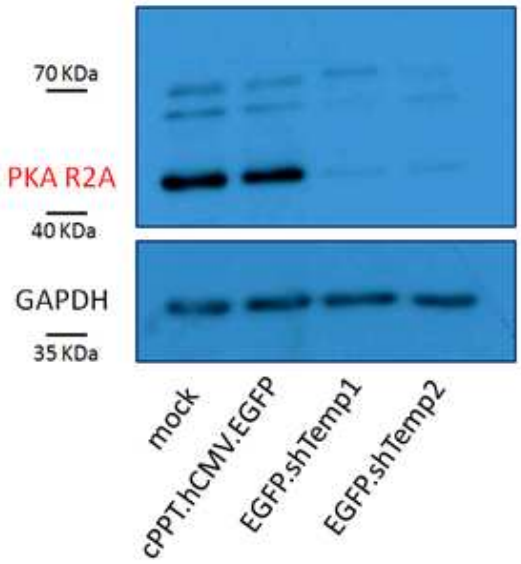

Figure 4.50 - Western blot analysis of GBM5 cells transduced with the recombinant lentiviral vectors 3 months post-transduction. GBM5 spheres were transduced with 20,000 cpm of the viral stock used in this experiment.

Western blot analysis demonstrated that both cPPT.hCMV.EGFP.shTemp1 and cPPT.hCMV.EGFP.shTemp2 lentiviral vectors induced an efficient and stable reduction in PKA R2A expression in GBM5 gliomaspheres.

4.5.7 Optimization of transduction and silencing efficiency in U87 human GBM cells

PKA R2A shRNA lentiviral vectors proved to be able to induce a stable and efficient downregulation of R2A expression in both human GBM non stem (U87, par. 4.5.5) and stem like (GBM5, par. 4.5.6) cells. However, in order to identify the lowest effective dose of shRNA vector, U87 cells were transduced with recombinant lentiviral particles at increasing multiplicities of infection. Lentiviral cPPT.hCMV.eGFP vector was used to monitor transduction efficiency by cytofluorimetric analysis of transduced U87 cells, whereas cPPT.hCMV.shTemp1 was preferentially used to monitor PKA R2A downregulation through western blot analysis, based on its higher silencing efficiency compared to lentiviral vectors carrying EGFP-shTemp1, shTemp2 and EGFP-shTemp2 cassettes. Assuming the same transduction capability for all cPPT.hCMV.eGFP-based vectors, multiplicity of infection was calculated based on the viral titre of cPPT.hCMV.eGFP, as determined through flow cytometry analysis of transduced 293T cells (par. 3.14.1).
Transduction of U87 cells with cPPT.hCMV.eGFP at low multiplicities of infection (<1) resulted in <50% transduction efficiency, whereas a higher multiplicity of infection (2.42) resulted in

approximately 80% of eGFP-positive cells, as assessed by flow cytometry analysis 3 days post-transduction. Transduction efficiency >99% was instead measured 4 days post-transduction for both 2.42 and 24.20 multiplicities of infection.

Silencing efficiency was also determined at several multiplicities of infection, starting from <1 and up to 24.20. U87 cells were transduced with cPPT.hCMV.shTemp1 vector at multiplicities of infection ranging from 0.04 to 0.42 and PKA R2A expression was evaluated 3 days post-transduction through western blot analysis, showing no reduction in R2A protein levels compared to mock transduced cells (Figure 4.51).

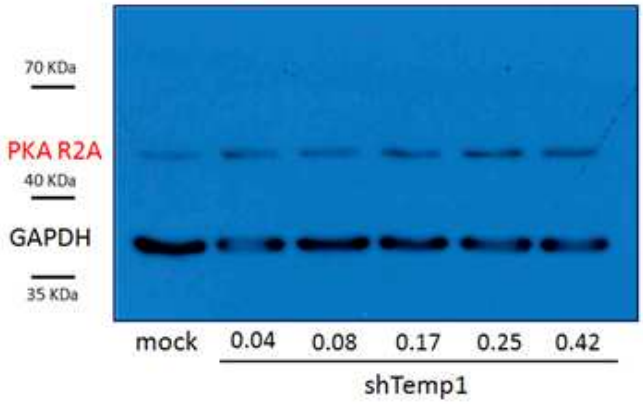

Figure 4.51 - Western blot analysis of U87 cells transduced with cPPT.hCMV.shTemp1 vector 3 days post-transduction. Transduction was performed at increasing multiplicities of infection: 0.04, 0.08, 0.17, 0.25 and 0.42.

Higher multiplicities of infection (2.42 and 7.26) similarly resulted in no appreciable PKA R2A downregulation, even when more extended time points were considered (Figure 4.52 and 4.53).

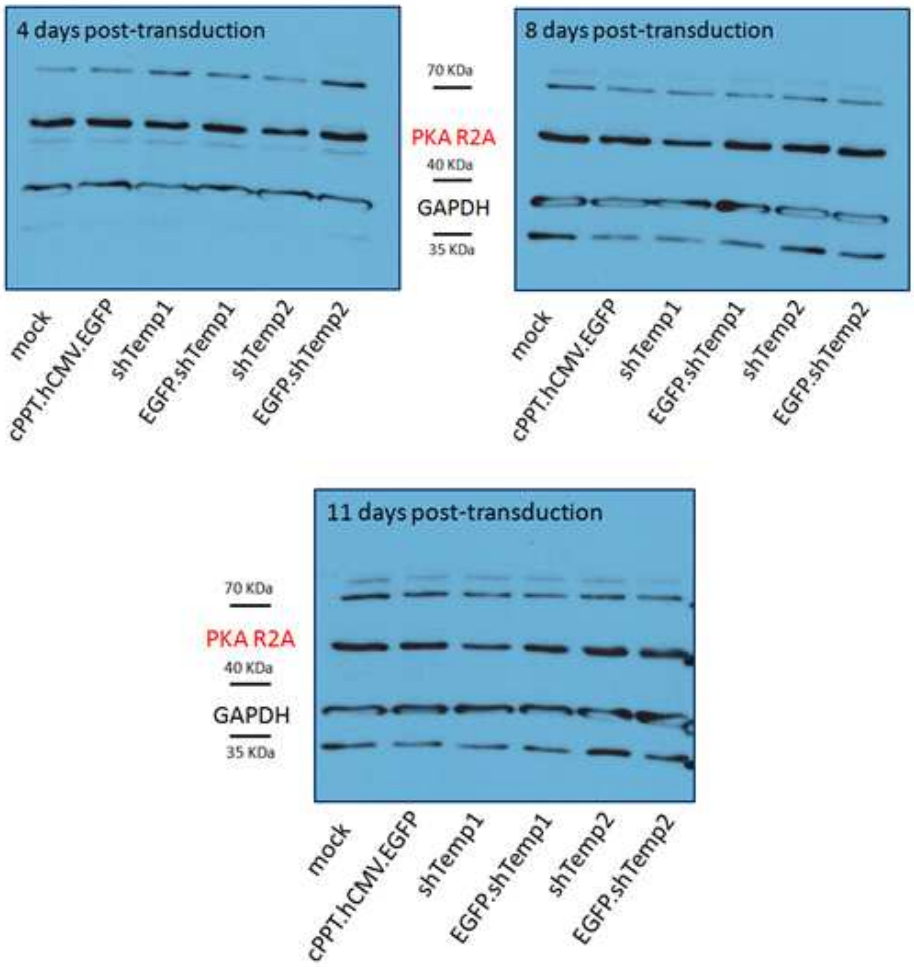

Figure 4.52 - Western blot analysis of U87 cells transduced with the recombinant lentiviral vectors (cPPT.hCMV.eGFP, cPPT.hCMV.shTemp1, cPPT.hCMV.EGFP.shTemp1, cPPT.hCMV.shTemp2, cPPT.hCMV.EGFP.shTemp2) at a multiplicity of infection of 2.42.

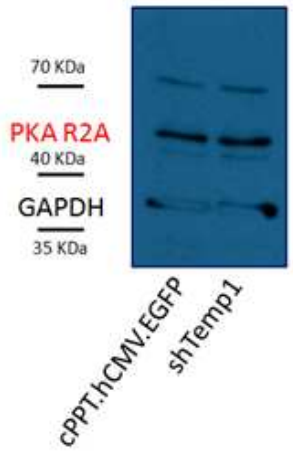

.

Figure 4.53 - Western blot analysis of U87 cells transduced with the recombinant lentiviral vectors cPPT.hCMV.eGFP and cPPT.hCMV.shTemp1 at a multiplicity of infection of 7.26. PKA R2A expression was evaluated 6 days post-transduction.

U87 cells were then transduced at a higher multiplicity of infection (24.20) and PKA R2A expression was assessed 6 and 10 days post-transduction (Figure 4.54).

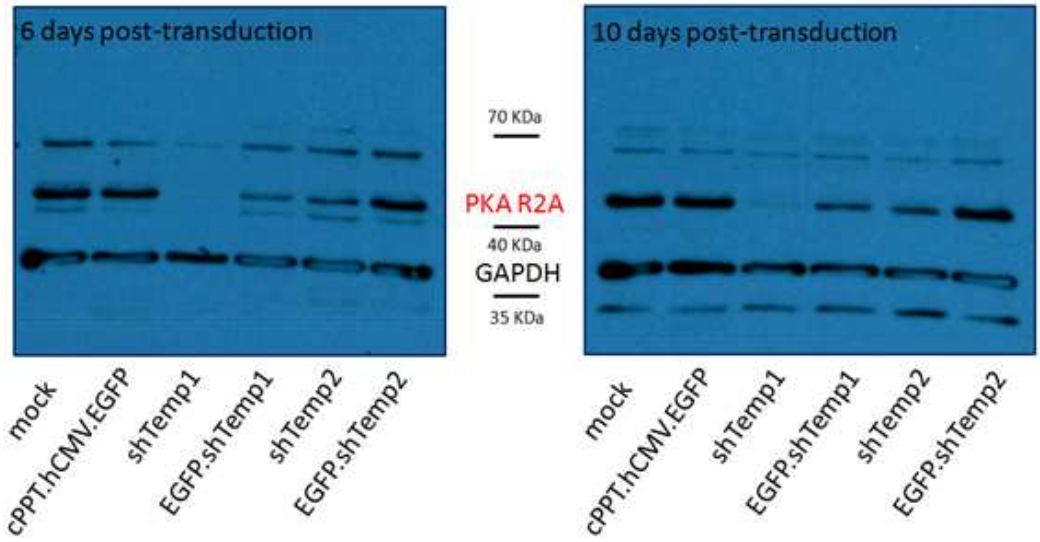

Figure 4.54 - Western blot analysis of U87 cells transduced with the recombinant lentiviral vectors (cPPT.hCMV.eGFP, cPPT.hCMV.shTemp1, cPPT.hCMV.EGFP.shTemp1, cPPT.hCMV.shTemp2, cPPT.hCMV.EGFP.shTemp2) at a multiplicity of infection of 24.20.

In these conditions an efficient PKA R2A downregulation was induced by the cPPT.hCMV.shTemp1 vector, whereas only a slight reduction in R2A expression was observed for cPPT.hCMV.EGFP.shTemp1 and cPPT.hCMV.shTemp2 vectors. Instead, no differences were reported between cPPT.hCMV.EGFP.shTemp2 and cPPT.hCMV.eGFP transduced cells.

Previous experiments on U87 cells (par. 4.5.5) had been performed at a multiplicity of infection as high as 104, in order to validate PKA R2A gene silencing capability of PKA R2A shRNA lentiviral vectors. The experiments reported above indicate that 24.20 is the lowest multiplicity of infection required for efficient R2A downregulation, corresponding to transduction of 1.0×10^5 cells with 100,000 cpm shRNA vector of the viral stock used in the above (Figure 4.54) and subsequent experiments. The same multiplicity of infection also resulted in transduction efficiency higher than 99%. These optimized transduction conditions were thus used in subsequent experiments, in order to limit the risk for off-target and other toxic effects associated with shRNA expression.

4.5.8 Transduction of U87 human GBM cells: PKA R2A expression, cell viability and cell growth

Following transduction of U87 cells with the lowest effective dose of shRNA vectors, cell viability and cell growth of GBM cells with downregulated PKA R2A expression were investigated through MTT assays and manual cell counting.

First, western blot analysis was performed to evaluate PKA R2A gene silencing 3, 6 and 10 days post-transduction, showing a progressive decrease in R2A protein levels induced by Temp1 shRNA and a minor reduction in R2A expression induced by Temp2 shRNA (Figure 4.55).

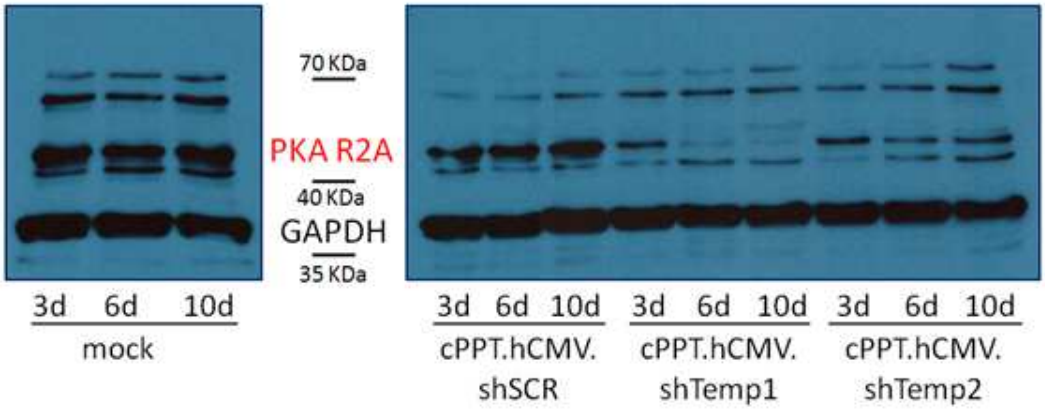

Figure 4.55 - Western blot analysis of U87 cells transduced with recombinant lentiviral vectors 3, 6 and 10 days post-transduction. Cells (1.0×10^5) were transduced with the lowest effective dose of lentiviral vector (100,000 cpm of the viral stock used in this experiment).

Cell viability was assessed through MTT assays 3, 6 and 10 days post-transduction. All data are reported in Figure 4.56, including cell viability of mock transduced cells.

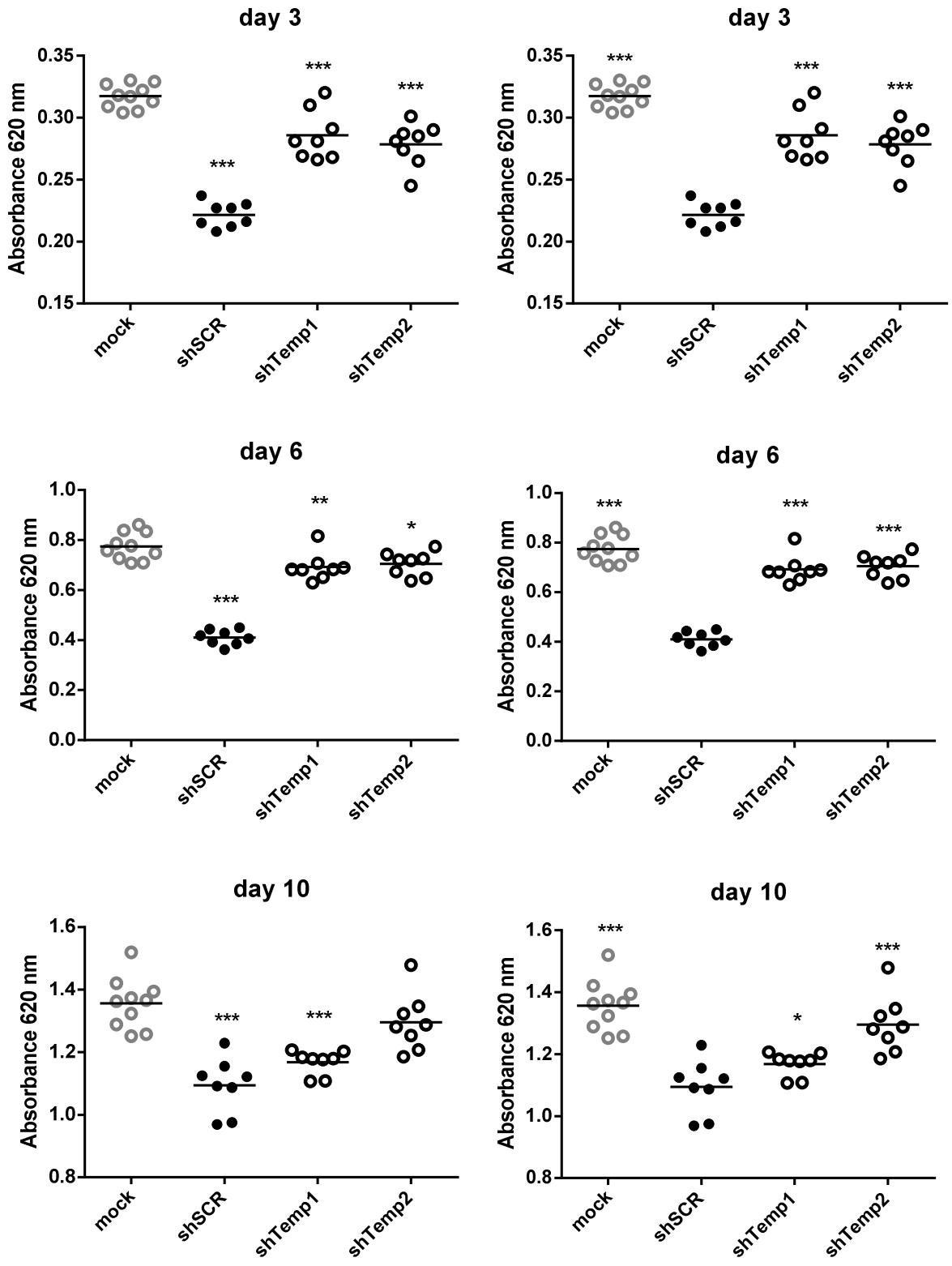

Figure 4.56 - MTT assays on U87 cells transduced with recombinant lentiviral particles 3, 6 and 10 days post-transduction. Cells (1.0×10^3 cells) were transduced with the lowest effective dose of lentiviral vector. The same graphs are shown in left and right columns with different statistical comparisons. Left: mock versus shSCR, shTemp1, shTemp2; right: shSCR versus mock, shTemp1, shTemp2. t-test, *p<0.05, **p<0.01, ***p<0.001.

MTT assays revealed a strongly significant reduction in cell viability of U87 cells transduced with cPPT.hCMV.shSCR lentiviral vector compared to mock transduced cells. This effect was highly unexpected based on previous experiments with cPPT.hCMV.eGFP lacking a shRNA cassette, which did not show such a cytotoxic effect on U87 cells. Also, cPPT.hCMV.shTemp1 and cPPT.hCMV.shTemp2 transduced cells exhibited a significantly reduced cell viability compared to mock transduced cells, which was consistent with previous data on siRNA-PRKAR2A transfected cells (Figure S1c), but a significantly increased cell viability compared to cells transduced with the scrambled vector.

Effects of shRNA expression on U87 cell growth were further investigated by manual cell counting of lentiviral transduced and mock transduced cells at defined time points. Total amounts of viable cells estimated based on cell culture volume and dilution factor, are reported in Figure 4.57.

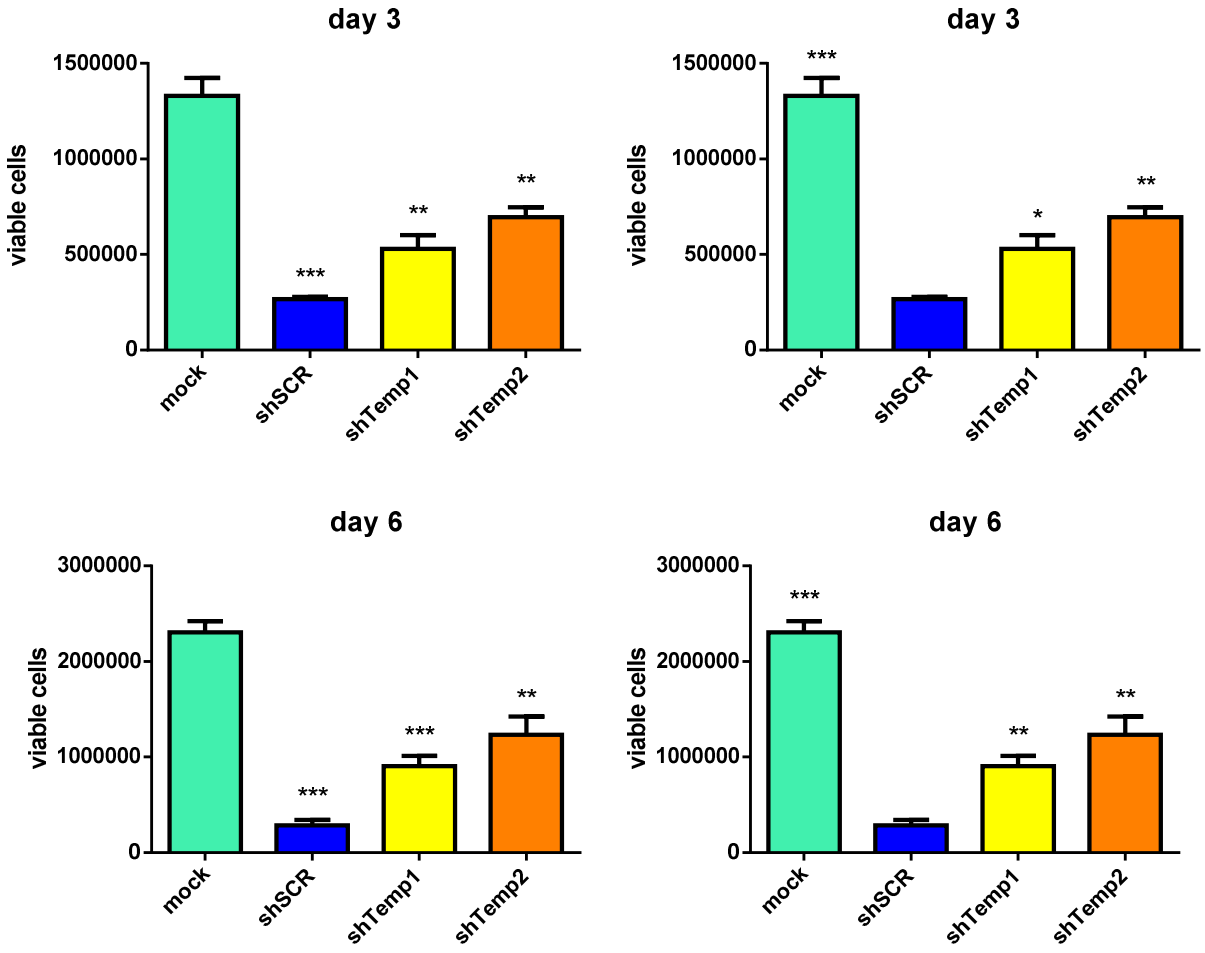

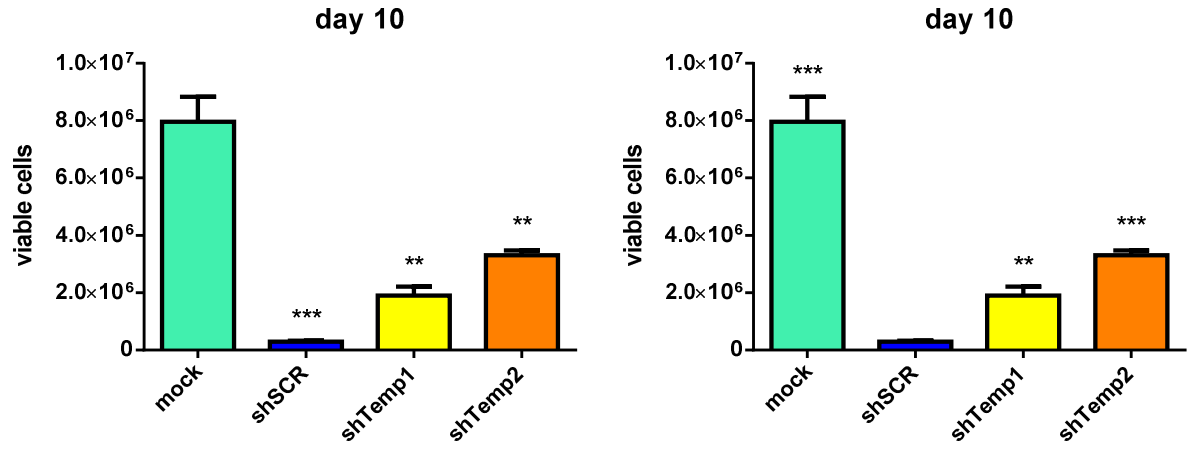

Figure 4.57 - Cell counting of U87 cells 3, 6 and 10 days post-transduction. Cells (1.0×10^5) were transduced with the lowest effective dose of lentiviral vector (100,000 cpm of the viral stock used in this experiment). The total amount of viable cells, as estimated by multiplying the average number of cells counted in the Burker chamber for dilution factor and cell culture volume, is reported. The same graphs are shown in left and right columns with different statistical comparisons. Left: mock versus shSCR, shTemp1, shTemp2; right: shSCR versus mock, shTemp1, shTemp2. t-test, *p<0.05, **p<0.01, ***p<0.001.

A significant reduction in the estimated amount of viable cells was reported for cPPT.hCMV.shSCR transduced cells compared to mock transduced cells at all time points. Consistently with results from MTT assays, estimated amounts of viable cells for cPPT.hCMV.shTemp1 and cPPT.hCMV.shTemp2 transduced cells were significantly higher than shSCR-expressing cells, but significantly reduced compared to mock transduced cells.

Observations on cell growth defects of U87 cells expressing scrambled and PKA R2A shRNAs raised a very controversial question about the effects of PKA R2A downregulation in human non-stem GBM cells. Based on data from scrambled and gene silencing transduced cells, a pro-growth effect might be hypothesized for PKA R2A downregulation. Indeed, a reduction in PKA R2A expression induced by either Temp1 or Temp2 shRNA was observed together with an increased cell proliferation compared to shSCR-expressing cells, as assessed by both MTT assay and manual cell counting. Despite this, the experiments presented above could not rule out a cytotoxic effect specifically associated with the scrambled shRNA sequence. Such scrambled cytotoxicity could also give an explanation for the great differences in cell viability and viable cell amounts between scrambled transduced and mock transduced cells. These differences were unexpected, based on preliminary testing of cPPT.hCMV.eGFP vector for transduction of U87 cells, showing no overt

effects on cell growth and maintenance of reporter gene expression for more than two weeks. According to the scrambled cytotoxicity hypothesis, a reduced PKA R2A expression might inhibit U87 cell proliferation or induce U87 cell death, resulting in a lower amount of viable cells in manual cell counting and lower absorbance in MTT assay for cPPT.hCMV.shTemp1 and cPPT.hCMV.shTemp2 transduced cells compared to mock transduced cells. In addition, a progressively reduced cell proliferation could be observed in shTemp2 and shTemp1-expressing cells respectively, parallel to a progressively reduced PKA R2A expression. Conversely, in case of the previous hypothesis about the pro-growth effect of PKA R2A downregulation, it remained unclear the higher proliferation of shTemp2-expressing cells, which presented a markedly higher expression of R2A subunit compared to shTemp1-expressing cells. However, it should be also noticed that when comparing shTemp1 and shTemp2 transduced cells with mock transduced cells, eventual side effects of lentiviral transduction are not discriminated from PKA R2A downregulation effects and could amplify the potential growth inhibition induced by PKA R2A gene silencing.
Further studies are ongoing to verify both hypothesis about functional effects of PKA R2A downregulation in U87 human GBM cells. Particularly, additional control lentiviral vectors and more sensitive cell growth assays are expected to give a contribution to the clarification of this controversial issue.

4.5.9 Transduction of NCH421K human GBM stem like cells: PKA R2A expression, cell viability and cell growth

In order to investigate the effects of PKA R2A gene silencing in human GBM stem like cells, NCH421K cells were transduced with recombinant lentiviral particles (cPPT.hCMV.shSCR, cPPT.hCMV.shTemp1, cPPT.hCMV.shTemp2) and cell viability and cell proliferation were then evaluated at defined time points, as well as PKA R2A expression.
Western blot analysis of transduced cells was performed 3, 6 and 10 days post-transduction, demonstrating a progressive reduction in PKA R2A expression induced by shTemp1 and no or minimal reduction in R2A expression induced by shTemp2 (Figure 4.58).

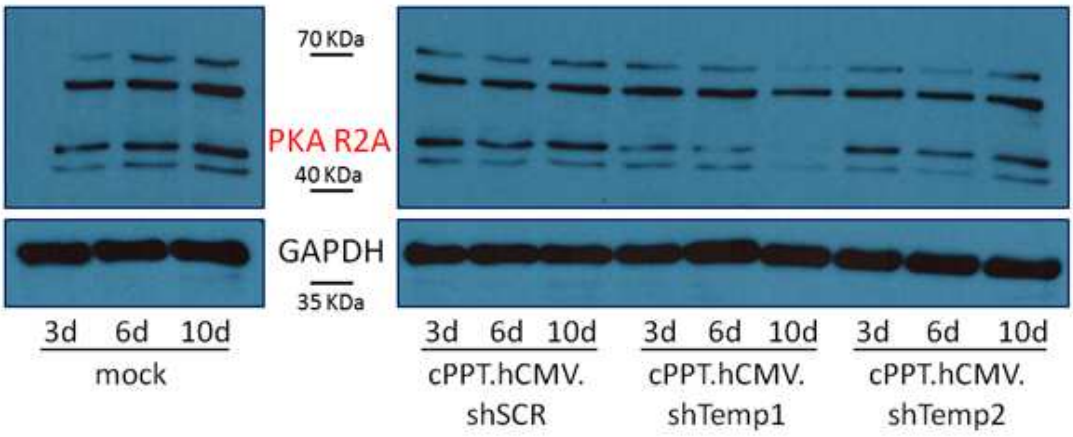

Figure 4.58 - Western blot analysis of NCH421K cells transduced with recombinant lentiviral vectors 3, 6 and 10 days post-transduction. Cells (1.0×10^5) were transduced with the lowest effective dose of lentiviral vector (100,000 cpm of the viral stock used in this experiment).

At the same time points MTT assays were performed to evaluate cell viability following lentiviral transduction and shRNA expression in NCH421K cells (Figure 4.59).

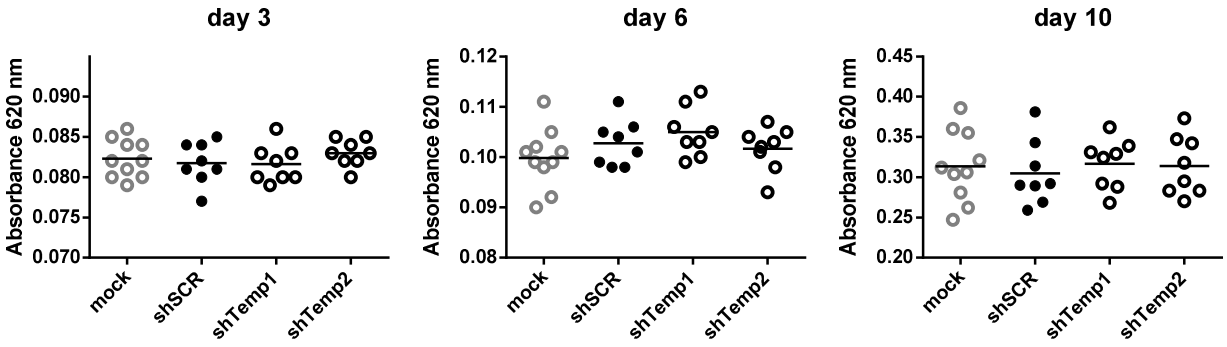

Figure 4.59 - MTT assays on NCH421K cells transduced with recombinant lentiviral particles 3, 6 and 10 days post-transduction. Cells (1.0×10^3 cells) were transduced with the lowest effective dose of lentiviral vector. t-test was performed to compare mock versus scrambled and gene silencing transduced cells and to compare shSCR versus shTemp1 and shTemp2 transduced cells, revealing no significant differences.

As shown in Figure 4.59, expression of PKA R2A Temp1 and Temp2 shRNAs did not affect cell viability of NCH421K cells compared to scrambled shRNA expression. Also, no significant differences were reported between mock transduced cells and cells transduced with either the scrambled vector or PKA R2A gene silencing vectors.

In addition, manual cell counting of trypan blue stained cells with a Burker chamber was performed 3, 6 and 10 days post-transduction to evaluate the effect of PKA R2A shRNA expression on NCH421K cell proliferation and cell death. During the whole experiment fresh complete medium was added to cell cultures without discarding the exhausted one, so that estimation of both viable and dead cells was possible at all time points. Preliminary data from a single experiment performed in duplicate are reported in Figure 4.60.

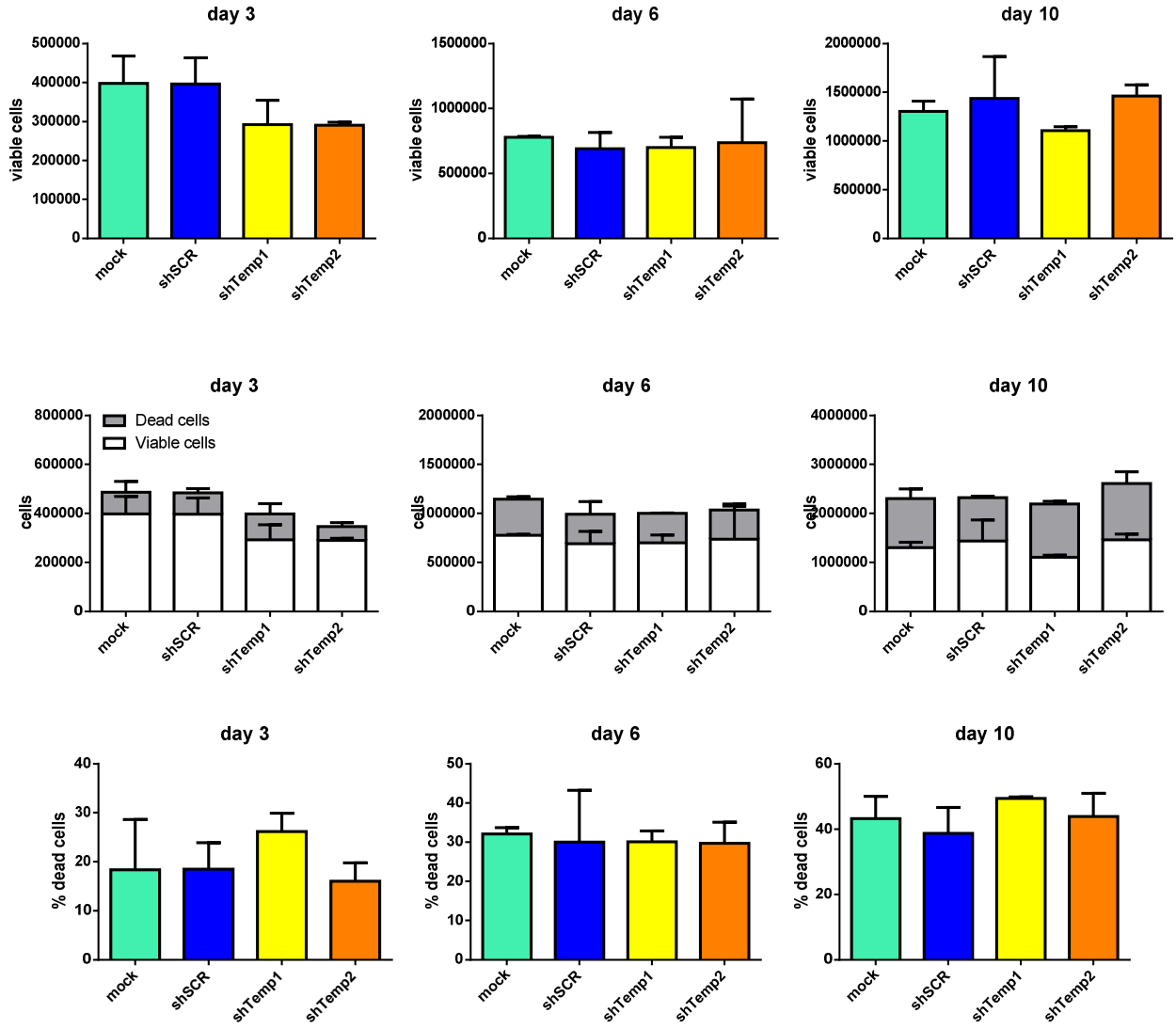

Figure 4.60 - Cell counting of NCH421K cells 3, 6 and 10 days post-transduction. Cells (1.0×10^5) were transduced with the lowest effective dose of lentiviral vector (100,000 cpm of the viral stock used in this experiment). Upper row: total amount of viable cells, as estimated by multiplying the average number of cells counted in the Burker chamber for dilution factor and cell culture volume; middle row: estimated amounts of viable and dead cells; lower row: percentage of estimated dead cells.

As shown in Figure 4.60, a decrease in the estimated amount of viable cells and an increase in dead cell percentage were observed 10 days post-transduction for NCH421K cells transduced with cPPT.hCMV.shTemp1 vector compared to cPPT.hCMV.shSCR transduced cells. Conversely, both the estimated amount of viable cells and the percentage of dead cells resulted similar for cPPT.hCMV.shTemp2 and cPPT.hCMV.shSCR transduced cells. Thus, a decrease in cell proliferation and an increase in cell death were reported together with reduced PKA R2A expression in cells expressing shTemp1, but not in shTemp2-expressing cells, which maintained high PKA R2A expression levels. Statistical analysis of variances was clearly not appropriate due to the low number of experimental replicates; instead, chi-square analysis was the most suitable statistical test to compare frequency distribution of viable/dead cells in different experimental conditions. For this purpose, raw viable and dead cell counts of mock, scrambled and gene silencing transduced cell cultures were compared in a chi-square analysis, pointing out a significantly different viable/dead cell distribution between cPPT.hCMV.shTemp1 and cPPT.hCMV.shSCR transduced cells (Figure 4.61).

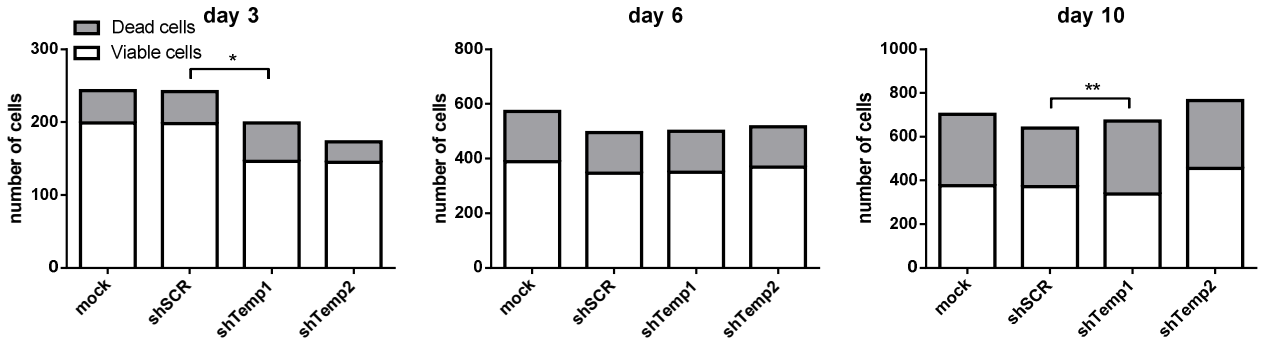

Figure 4.61 - Cell counting of NCH421K cells 3, 6 and 10 days post-transduction. Cells (1.0×10^5) were transduced with the lowest effective dose of lentiviral vector (100,000 cpm of the viral stock used in this experiment). Raw viable and dead cell counts are reported. Chi-square test, shSCR versus mock, shTemp1, shTemp2. *p<0.05, **p<0.01, ***p<0.001.

Indeed, 3 and 10 days post-transduction viable/dead cell distribution in the cPPT.hCMV.shTemp1 cell population proved to be significantly different compared to the scrambled cell culture. No significant differences were instead detected between cPPT.hCMV.shSCR transduced and mock transduced cell populations. As a consequence, a cytotoxic effect specifically associated with the scrambled shRNA sequence could reasonably be excluded in NCH421K cells. What is more, these data suggest a potential relationship between PKA R2A downregulation and induction of cell death in human GBM stem like cells. A reduced cell viability of cPPT.hCMV.shTemp1transduced cells compared to scrambled transduced cells was not detected by MTT tests, possibly due to the lower

sensitivity of the metabolic MTT assay in evaluation of cell growth compared to manual cell counting, as reported by Eekels and colleagues (Eekels et al. 2012). Therefore, the reported effect of PKA R2A gene silencing on GBM stem like cell survival is potentially promising and deserves further investigation.

5. Discussion

Glioblastoma is currently one of the most challenging problems in biomedical research. It is the most frequent form of glioma (around 12,000 cases every year in the United States; Mesfin and Al-Dhahir 2017) and is associated with a modest 27% survival after two year from diagnosis (Gilbert et al. 2013). Despite a very aggressive treatment including surgery, radiotherapy and chemotherapy (Stupp et al. 2010; Lawrence et al. 2012; Bauchet et al. 2010), overall median survival for GBM patients is still as poor as 14 months from diagnosis (Stupp et al. 2009). The remarkable intratumoral heterogeneity, the high infiltrative nature and the anatomical location of GBM, strongly limit the efficacy of conventional anti-tumor therapies and pose severe obstacles to the success of even the most recent therapeutic strategies. The presence of radio- and chemoresistant cancer stem cells and their known plasticity further contribute to the striking failure of current glioma treatments and make it necessary to develop new therapeutic options. Two complementary aims were primarily addressed: the design of innovative therapeutic strategies and the identification of new molecular targets. Novel approaches include the improved delivery of small drugs and monoclonal antibodies, RNA-based strategies, immunotherapies and viral gene therapies (Miranda et al. 2017; Rajesh et al. 2017). New targets have been identified among the components of the signaling pathways specifically altered in brain cancers (Zorzan et al. 2015). Several novel glioma therapies are currently under preclinical and clinical evaluation, showing significant therapeutic potential against GBM cells. However, a large number of aspects in GBM cell biology are still to be elucidated and investigation of glioma molecular pathogenesis is always in progress to fill up this gap. In this view, the present PhD project was focused on the study of a multifunctional enzyme, protein kinase A, which presents relevant peculiarities in GBM and recently emerged as a promising target for novel anti-cancer therapies (Caretta and Mucignat-Caretta 2011; Sapio et al. 2014). Particularly, the regulatory subunit R2A of PKA was previously demonstrated to be specifically present in perinuclear clusters co-localized with the Golgi apparatus in rodent and human GBM cells, whereas this peculiar distribution was not detected in the healthy brain parenchyma (Mucignat-Caretta et al. 2008; Mucignat-Caretta et al. 2018). The functional significance of Golgi-associated PKA in GBM cells and other cancer and non-cancer cell lines is still unclear (Bejarano et al. 2006) and needs further investigation to reveal potential applications in cancer treatment. For this reason, the study of PKA, particularly R2A subunit, was extended to human GBM stem like cells, that are commonly considered a major obstacle in the therapy of GBM (Bageritz et al. 2014). The multiple roles of PKA in glioma cells were investigated through

interference with PKA activity, expression and intracellular localization, but also, in a complementary approach, by evaluating the effects of disrupted Golgi function on PKA R2A subunit. Drug molecules and several molecular tools, such as siRNAs and eukaryotic expression plasmids, were used to transiently interfere with PKA pathway. Also, new molecular tools were de-novo generated and validated for the study of PKA in human GBM cells. Among these, a lentiviral system to efficiently and stably downregulate PKA R2A expression was developed and successfully used in both human GBM non-stem and stem like cell cultures, revealing intriguing potentialities for future studies of PKA in GBM models.

So far, the multiple roles of the cAMP/PKA pathway have been only partially elucidated due to the extremely high complexity of the signaling network, but PKA impairment has been associated with several pathological conditions (Gold et al. 2013). Expression of fluorescent fusion proteins is a widely used approach to study protein functions in cell biology as direct monitoring of the labeled protein in live cells can give information on its intracellular distribution, dynamics and interactions with other proteins (Snapp 2005). This approach has been exploited also for investigation of different functions of PKA isoforms in several cellular models. For instance, a doxycycline-inducible EGFP-fused PKA CA subunit overexpression system was used to overcome PKA agonist side effects in hippocampal progenitor cells, providing evidence for the direct involvement of PKA activation in neuronal differentiation of these cells in vitro (Kim et al. 2002). More recently, expression of fluorescent fusion PKA catalytic and regulatory subunits in endothelial cells revealed a reciprocal regulation between PKA and the Rac guanine nucleotide exchange factor P-Rex1, as well as the importance of this interaction for endothelial cell migration. Cell transfection with the EGFP-PKA constructs also allowed to describe an alternative mechanism of PKA signaling complex assembly that is different from the traditional AKAP-mediated one (Chávez-Vargas et al. 2016). In order to develop additional molecular tools for functional studies of PKA, in the present study recombinant plasmids for expression of EGFP-fused PKA regulatory (R1A, R2A, R2B) and catalytic (CA, CB) subunits were generated and preliminarily tested in U87 human GBM cells. EGFP-tagged PKA CA and CB subunits presented a diffuse intracellular distribution, very similar to endogenous PKA CA localization in U87 GBM cells. Conversely, following cell transfection with the EGFP-PKA R2A expression plasmid, the labeled subunit appeared to have a slightly more diffuse localization compared to the endogenous PKA R2A, an aspect that is still under investigation. Moreover, EGFP-PKA R1A subunit was present as multiple dots of variable size in the cytoplasm of GBM cells transfected with the recombinant construct, whereas endogenous R1A subunit was supposed to have a distributed localization, not detectable by immunohistochemistry (Mucignat-Caretta et al. 2008). Cytosolic discrete aggregates of GFP-tagged R1A had been

previously described in various cell types (Mavrakis et al. 2006; Mavrakis et al. 2007; Martin et al. 2007; Meoli et al. 2008) and these formations had been demonstrated to be associated with late endosomes and autophagosomes in HeLa and HEK293 cells (Mavrakis et al. 2006; Mavrakis et al. 2007). Further studies are needed to evaluate this association also in GBM cells expressing EGFP-fused PKA R1A subunit. Another relevant observation that emerged from fluorescent fusion PKA expression was a marked cell apoptosis of GBM cells transfected with the EGFP-fused PKA R2B overexpression plasmid. Aggregates of this regulatory subunit had been described in rodent normal brain parenchyma (Mucignat-Caretta et al. 2008), but they were not detected in glioma cells. Thus, it may be hypothesized a cytotoxic effect of R2B subunit in human GBM cells, as reported also for overexpression of the same non-tagged subunit (Zorzan 2014). All considered, fluorescent fusion PKA expression plasmids proved to be useful tools for imaging of PKA subunits inside cells. However, some tricky questions should be pointed out to avoid misleading conlusions. First, further studies are needed to evaluate the potential expression of both tagged and untagged PKA subunit from the recombinant expression plasmids due to the presence of two start codons downstream the promoter, within EGFP and PKA coding sequences. Secondly, it is recommended to test the functionality and correct intracellular localization of both N-terminal and C-terminal fusion proteins (Crivat and Taraska 2012). Indeed, GFP tagging on both sides is reported to adversely affects the localization of some proteins (Hanson and Ziegler 2004; Palmer and Freeman 2004), even if GFP family members are relatively small, chemically inert and minimally disruptive when attached to most proteins (Crivat and Taraska 2012). What is more, strong promoters such as CMV, can lead to a large increase in the protein cellular level, with potential dramatic effects on the localization and function of the fusion protein. For this reason, selection of cell types where promoters drive expression of low protein amount or use of promoters with tunable activity are some times suggested to reduce the effects of extreme fusion protein overexpression (Crivat and Taraska 2012). Based on these considerations, additional studies are ongoing for the optimization of the EGFP-fused PKA constructs and for the complete characterization of the fusion PKA subunits. Labeling proteins with a fluorescent tag allows to track them inside cells and tissues, as well as to monitor their cellular dynamics and association with other proteins, providing relevant information on the function of the tagged protein (Crivat and Taraska 2012). Thus, optimized fluorescent fusion PKA plasmids may contribute to functional studies of protein kinase A and implementation of these expression tools in a much more efficient gene delivery system, such as lentiviral vectors, may further increase their applications in several cellular models.

Trying to provide novel insights into the multiple roles of protein kinase A in human GBM, part of the research project analyzed the effects of transient interference with PKA activity, expression and

intracellular localization. Drug-mediated PKA stimulation and inhibition were induced by treatment of U87 human GBM cells with the cAMP analogue 8Br-cAMP and the PKA inhibitor H89, respectively. High concentrations of both chemical agents (8Br-cAMP 500 μM, H89 12 μM) proved to increase GBM cell death and to reduce GBM cell motility. This effect is consistent with other studies reporting 8Br-cAMP and H89 induction of apoptosis and cell death in mouse and human GBM cells respectively (Mucignat-Caretta et al. 2008; Mucignat-Caretta et al. 2018) and inhibition of human GBM cell proliferation by 8Br-cAMP through PKA and Epac-dependent suppression of MAPK (Sugimoto et al. 2013). Alteration of PKA basal activity was also induced by transient expression of wild type and mutant regulatory and catalytic PKA isoforms from eukaryotic expression plasmids transfected into U87 human GBM cells. A reduced cell motility was observed for U87 cells expressing a dominant negative form of PKA R1A subunit, that resulted in repression of PKA activity, as well as for U87 cells expressing wild type and mutant always active PKA CA subunit, that induced PKA hyperactivation. Different mechanisms for involvement of PKA activity in glioma cell migration have been described. Phosphorylation of the guanine nucleotide exchange factor Dock180 by PKA is important for PDGFRα-driven glioma cell migration in vitro and glioma cell invasion in vivo (Feng et al. 2014). PKA-mediated transcriptional upregulation of microtubule-associated protein MAP2 decreases the invasiveness of glioma cells, suggesting that PKA may be targeted in anti-invasion glioma therapy (Zhou et al. 2015).

In addition, effects of PKA delocalization on GBM cell motility were also investigated, demonstrating that disruption of either PKA type I or type II interaction with AKAP proteins caused a reduction in glioma cell migration. Several studies suggest that PKA is spatially regulated in migrating cells and controls signaling events critical for actin cytoskeletal dynamics (O'Connor et al. 1998; O'Connor and Mercurio 2001; Goldfinger et al. 2003; Howe 2004; Howe et al. 2005). For instance, PKA activity gradients have been demonstrated in migrating carcinoma cells, where they are mediated by both cAMP synthesis and PKA anchoring through specific AKAPs (Paulucci-Holthauzen et al. 2009). Moreover, AKAP anchoring of PKA and spatially regulated kinase activity are required for cell migration and invasion of epithelial ovarian cancer cells (McKenzie et al. 2011). Evidences for the involvement of PKA anchoring in GBM cell motility thus deserve further investigation, in order to evaluate a novel potential approach to reduce tissue invasion of GBM cells.

As regard to modulation of PKA expression, a balanced expression of type I and type II PKA regulates cell growth and differentiation, whereas loss of this balance may drive cell transformation and tumor progression (Cho-Chung and Nesterova 2005). In many cancer cells the PKA I/II ratio is reversed compared to their normal counterpart, thus PKA isozyme switching could provide a tumor-

targeted therapy by reversion of tumor cell malignant phenotype (Cho-Chung and Nesterova 2005). In agreement with this instance, reversion of the R1/R2 ratio has antiproliferative and proapoptotic effects on melanoma cells, that could be exploited for cancer treatment (Mantovani et al. 2008A). Unbalance of PKA regulatory subunits may also drive the tumorigenic phenotype of GBM as a consequence of genetic abnormalities involving PKA R1A, R1B and R2B genes on chromosomes 7 and 17 (Ichimura et al. 2004). R2A expression is increased in GBM compared to healthy brain tissue and patients with higher R2A expression have poorer survival, suggesting that reducing R2A levels could be desirable to induce other PKA subunits (Mucignat-Caretta et al. 2018). Previous data (Zorzan et al. 2014; Zorzan 2014) and the experiments reported in the present study indicate that GBM cell viability is increased by PKA R2A overexpression and reduced by downregulation of the same subunit through siRNA transfection. What is more, despite a low siRNA transfection efficiency, reduced cell motility and decreased cell number without increased cell death were observed in U87 human GBM cells with silenced PKA R2A expression, pointing to a possibly reduced cell proliferation. Following PKA R2A siRNA transfection, Golgi fragmentation and R2A redistribution in the cell cytoplasm were reported in some cells. This effect is consistent with a work by Bejarano and colleagues, who demonstrated that in HeLa cells integrity of the Golgi ribbon required both proper localization and activity of PKA. Indeed, disassembly of Golgi complex was caused by R2A depletion through siRNA treatment, PKA displacement from Golgi apparatus and prolonged pharmacological inhibition of PKA activity (Bejarano et al. 2006). Conversely, in retinal pigment epithelium RPE1 cells the activity of Golgi-associated PKA during activation of the cAMP pathway induced Golgi structural reorganization, resulting in collapse of the apparatus (Mavillard et al. 2010). Functional significance of PKA association with Golgi complex in mammalian cells is still largely unknown and may vary among different cell types. Thus, Golgi disruption in GBM cells transfected with PKA R2A siRNA could suggest a role for this subunit in maintenance of Golgi structure, but currently remains of challenging interpretation.

In a different yet complementary approach, the relationship between PKA and Golgi apparatus was investigated in U87 human GBM cells by interfering with Golgi function and evaluating the effects on PKA R2A subunit. In these experiments, brefeldin A was used to inhibit the endoplasmic reticulum-Golgi transport, resulting in disruption of Golgi structure and function. BFA treatment of U87 human GBM cells reduced cell viability and motility and increased cell death. Growth inhibition and induction of apoptosis by BFA had already been reported in various GBM cell lines (Pommepuya et al. 2003). Dispersion of PKA R2A in the cell cytoplasm was also observed in U87 cells treated with BFA, consistently with PKA redistribution in BFA-treated HeLa cells (Bejarano et al. 2006). Interestingly, BFA targets BIG1 and BIG2 contain AKAP sequences for PKA

regulatory subunits. Recently it was proposed that interaction of β-catenin-bound BIG1 with BIG2 and its associated PKA complex are required for PKA phosphorylation of β-catenin, resulting in transcriptional regulation (Li et al. 2016). β-catenin transcriptional activity can lead to uncontrolled cell proliferation and migration and is important in development and tumorigenesis (Valenta et al. 2012). Therefore, BFA targets, PKA and Golgi apparatus are connected through complex molecular mechanisms that so far have been only partially characterized. A deeper elucidation of this relationship in glioma cells could provide additional insights into the functional significance of Golgi-associated PKA.

To summarize, transient interference with PKA pathway proved to have some effects exploitable for anti-tumor potential in human GBM cells. These effects were confirmed through several approaches, including drug treatments, transient expression of PKA-AKAPs interaction peptide inhibitors, transient overexpression of wild type and mutant PKA isoforms and siRNA-mediated downregulation of specific PKA subunits. The present data are consistent with other studies performed in different cellular models and support the importance of PKA activity, balanced expression and peculiar intracellular localization for GBM cells. Particularly, these experiments suggest the involvement of PKA R2A subunit in fundamental functions of GBM cells, such as cell motility, cell proliferation and regulation of Golgi structure. Despite this, some limitations intrinsically related to the adopted approaches should be considered. First, chemical drugs always present some undesired side effects due to aspecific targeting through non-selective activity. For example, the cAMP analogue 8Br-cAMP is known to activate not only PKA but also Epac (Enserink et al. 2002; Christensen et al. 2003; Rehmann et al. 2003; Holz et al. 2008; Schmidt et al. 2013) and it is not possible to discriminate between the effects mediated by the two cAMP targets. H89 also has several PKA-independent effects due to inhibition of at least eight other cellular kinases (Lochner and Moolman 2006). What is more, plasmid and siRNA transfection efficiency of U87 cells was rather low (between 35 and 40% for siRNA, even lower for plasmid transfection), making it possible that some effects were masked by the large proportion of untransfected cells. In order to overcome these limitations and find further confirmation for the key-role of protein kinase A in human GBM, in the second part of the study the use of a lentiviral-based system was introduced. This lentiviral approach allowed to achieve a very high transduction efficiency, being able to target almost the entire population of cells. In addition, differently from plasmid and siRNA transfection, integration of the lentiviral vector into the host genome lead to a stable exploitation of the molecular machinery of the cell for transgene expression. Based on the peculiarity of PKA R2A subunit in GBM cells and previous results on R2A gene silencing, downregulation of R2A expression was selected for implementation in a lentiviral system. Third generation lentiviral

vectors were thus engineered for expression of short hairpin RNAs targeting PKA R2A subunit, as well as a scrambled short hairpin RNA with no cellular targets to evaluate off-target effects. These lentiviral vectors were then successfully used for induction of PKA R2A gene silencing in different GBM cellular models and to preliminarily evaluate the effects of the unbalanced PKA regulatory subunit expression.

The first GBM cellular model where lentiviral-mediated PKA R2A downregulation was evaluated, is U87 human GBM cell line. In these cells PKA R2A gene silencing lentiviral vectors induced an efficient and stable R2A downregulation, but effects of R2A dysregulation on cell growth were of difficult interpretation. Indeed, cells with silenced PKA R2A expression exhibited a significantly higher cell proliferation compared to scrambled transduced cells, but a significantly lower rate of cell growth compared to mock transduced cells. Therefore, PKA R2A downregulation may apparently have a pro-growth effect on U87 cells, contrarily to indications from PKA R2A siRNA experiments, if R2A silenced and scrambled transduced cells are compared. However, a correlation between the level of PKA R2A knockdown and the increase in cell growth could not be observed as cells with very low R2A protein levels had a reduced proliferation compared to cells with higher R2A expression. Moreover, cell viability and viable cell amounts were markedly reduced for scrambled transduced cells compared to mock transduced cells. These differences were unexpected as preliminary testing of the lentiviral vector carrying no shRNA sequences showed no toxic effect on U87 cells. As a consequence, a cytotoxic effect specifically associated with the scrambled shRNA sequence can be hypothesized and should be investigated in future experiments. Cytotoxicity of shRNAs has been largely discussed in the literature. Off-target, non-sequence specific effects can be elicited by shRNAs due to small regions of seed sequence homology to 3' untranslated region (UTR) of cellular miRNAs (Manjunath et al. 2009). Frequently shRNA can indeed induce downregulation of a large number of off-target transcripts, leading to unwanted toxic phenotypes (Fedorov et al. 2006; Seok et al. 2017). Additionally, shRNAs can potentially activate the innate immune system via induction of an interferone response through the cytosolic dsRNA-activated protein kinase PKR or binding to toll-like receptors (TLRs), such as TLR3, TLR7 and TLR8 (Sioud et al. 2005; Hornung et al. 2005; Jackson and Linsley 2010; Schlee and Hartmann 2016). High level expression of shRNA can also lead to saturation of the RNA interference machinery, that results in cytotoxicity or general perturbation of gene expression, including derepression of miRNA targets due to inhibited miRNA activities (Jackson and Linsley 2010; Khan et al. 2009). It should be noted that embedding of shRNA into an endogenous miRNA scaffold and expression from a Pol-II promoter, as for the shRNA sequences used in the present study, has been demonstrated to be less prone to cause toxicities by interference with the endogenous miRNA

pathway (Boudreau et al. 2009; Castanotto et al. 2007; McBride et al. 2008; Premsrirut et al. 2011; Maczuga et al. 2012). Despite this, the experiments performed so far cannot rule out a strong cytotoxicity of the scrambled vector, an aspect that is currently under investigation. Assuming a much higher cytotoxic effect of the scrambled sequence compared to PKA R2A shRNAs in U87 cells, downregulation of PKA R2A expression might either inhibit cell proliferation or induce cell death. Consistently with this hypothesis, a progressively reduced cell growth could be observed in U87 cells, parallel to a progressive reduction in PKA R2A expression. The potentially inhibitory effect of R2A silencing on U87 cell proliferation is also consistent with previous data on PKA R2A siRNA-transfected cells. Further experiments are ongoing to evaluate the side effects of lentiviral transduction on U87 cells and to verify the possible cytotoxicity of the scrambled shRNA sequence, in order to clarify the controversial question on the relationship between PKA R2A expression and U87 cell proliferation.

Moving to more recent GBM in vitro models, cell cultures of GBM spheres were introduced in this research project to extend the study of PKA to human GBM stem like cells. Gliomaspheres represent nowadays a recognized model for investigation of many aspects of GBM biology (Laks et al. 2016; Balvers et al. 2016); thus, study of PKA in these cells seems interesting to increase the consistency of previous results. Evidences indicate that the cAMP/PKA pathway is differently involved in cancer stem cell biology of several tumors. The role of PKA was recently explored in breast cancer cells, demonstrating that an increase in cAMP intracellular levels and the subsequent activation of PKA induce a mesenchymal-to-epithelial transition and promote differentiation of mammary tumor-initiating cells (Pattabiraman et al. 2016). PKA was also proposed as a novel potential target for anti-tumor therapy against colon cancer stem cells, based on the observation that PKA activation leads to cell cycle arrest and enhanced spheroid formation (Tsujii et al. 2009). What is more, induction of growth arrest and forced neural differentiation via cAMP/PKA/CREB signaling pathway in CD133-expressing GBM cancer stem cells was proposed as a new approach for brain tumor therapy (Kang et al. 2014).

Up to now, the intracellular localization of PKA R2A subunit has never been investigated in GBM stem like cells. In this study it was demonstrated in three different GBM sphere cultures that R2A subunit is present as perinuclear cluster co-localized with the Golgi apparatus, confirming in GBM stem like spheres the same peculiar intracellular distribution that had been previously described in non-stem GBM cell lines and primary adherent cell cultures (Mucignat-Caretta et al. 2008; Mucignat-Caretta et al. 2018). Moreover, lentiviral-mediated PKA R2A shRNA delivery proved able to induce an efficient and stable downregulation of R2A subunit also in GBM stem like cells. Interestingly, in contrast with what observed in U87 cells, in NCH421K GBM stem like cells no

cytotoxic effect of the scrambled vector was observed, as no significant difference in cell viability and proliferation was reported compared to mock transduced cells. This may point to a cell type-dependent cytotoxicity of the scrambled shRNA. In addition, transduction experiments of NCH421K cells with PKA R2A gene silencing lentiviral vectors suggested a possible relationship between PKA R2A knockdown and induction of GBM stem like cell death. Indeed, distribution of viable and dead cells in NCH421K cells with silenced PKA R2A expression proved significantly different compared to scrambled transduced cell population. Particularly, an increased proportion of dead cells was detected in the cell population with downregulated R2A expression, but not in gene silencing transduced cells that still presented elevated R2A protein levels. These results thus support a relevant and promising effect of PKA R2A downregulation on cell survival of GBM stem like cells. Future studies are needed to better elucidate this relationship and evaluate the potential applications for novel GBM therapies.

In conclusion, the present PhD project aimed at providing a deeper insight into to the multiple roles of protein kinase A in human GBM. Transient interference with PKA differentially affects GBM cells, indicating the importance of a precise and fine regulation of PKA signaling pathway. The regulatory subunit R2A of PKA presents a peculiar intracellular localization in both non-stem and stem like GBM cells. This characteristic is not observed in the healthy brain parenchyma, supporting a potential role for R2A as a tumor marker or a new target for anti-glioma therapies. In this direction, for the first time a lentiviral system for efficient silencing of PKA R2A has been developed and used to better investigate the function of this PKA subunit in human GBM cells. Preliminary data suggest an increase in cell death in GBM stem like cells with downregulated PKA R2A expression, pointing to a promising role for this lentiviral tool in cancer research. Different approaches have been adopted to study different aspects of PKA dysregulation. Drug treatments, plasmid and siRNA transfection experiments allowed to evaluate short-term effects induced by a transient acute interference with PKA pathway. Conversely, thanks to lentiviral transduction long-term effects of a stable gene knockdown could be investigated. Importantly, intrinsic characteristics of the lentiviral-mediated approach potentially give the cell the opportunity to compensate for transgene expression in a sort of homeostatic equilibrium. Indeed, compared to drug treatment and cell transfection where interfering molecules enter in the cell and are immediately available to sort out their effects, following lentiviral transduction and integration of the viral vector into the cellular genome, a gradual expression of the transgene is initiated, with a complete exploitation of the cellular machinery. Thus, a compensatory cellular response is reasonably more likely after lentiviral delivery of genetic material, whereas it seems more difficult in case of a shocking cell transfection

or drug treatment. In this view, the different approaches used in the research project can be considered complementary rather than alternative, and finally aimed at a more complete investigation of PKA in human glioblastoma.

6. References

Altschul, S.F., Madden, T.L., Schäffer, A.A., Zhang, J., Zhang, Z., Miller, W., and Lipman, D.J. (1997). Gapped BLAST and PSI-BLAST: a new generation of protein database search programs. Nucleic Acids Res. *25*, 3389–3402.

An, J.H., Lee, S.Y., Jeon, J.Y., Cho, K.G., Kim, S.U., and Lee, M.A. (2009). Identification of gliotropic factors that induce human stem cell migration to malignant tumor. J. Proteome Res. *8*, 2873–2881.

Anciaux, K., Van Dommelen, K., Nicolai, S., Van Mechelen, E., and Slegers, H. (1997). Cyclic AMP-mediated induction of the glial fibrillary acidic protein is independent of protein kinase A activation in rat C6 glioma. J. Neurosci. Res. *48*, 324–333.

Annovazzi, L., Mellai, M., and Schiffer, D. (2017). Chemotherapeutic Drugs: DNA Damage and Repair in Glioblastoma. Cancers (Basel) *9*.

Assi, H., Candolfi, M., Baker, G., Mineharu, Y., Lowenstein, P.R., and Castro, M.G. (2012). Gene Therapy for Brain Tumors: Basic Developments and Clinical Implementation. Neurosci Lett *527*, 71–77.

Atzori, M.G., Tentori, L., Ruffini, F., Ceci, C., Lisi, L., Bonanno, E., Scimeca, M., Eskilsson, E., Daubon, T., Miletic, H., Ricci Vitiani, L., Pallini, R., Navarra, P., Bjerkvig, R., D'Atri, S., Lacal, P.M., and Graziani, G. (2017). The anti-vascular endothelial growth factor receptor-1 monoclonal antibody D16F7 inhibits invasiveness of human glioblastoma and glioblastoma stem cells. J. Exp. Clin. Cancer Res. *36*, 106.

Auffinger, B., Tobias, A.L., Han, Y., Lee, G., Guo, D., Dey, M., Lesniak, M.S., and Ahmed, A.U. (2014). Conversion of differentiated cancer cells into cancer stem-like cells in a glioblastoma model after primary chemotherapy. Cell Death Differ. *21*, 1119–1131.

Auffinger, B., Spencer, D., Pytel, P., Ahmed, A.U., and Lesniak, M.S. (2015). The role of glioma stem cells in chemotherapy resistance and glioblastoma multiforme recurrence. Expert Rev Neurother *15*, 741–752.

Bageritz, J., Puccio, L., Piro, R.M., Hovestadt, V., Phillips, E., Pankert, T., Lohr, J., Herold-Mende, C., Lichter, P., and Goidts, V. (2014). Stem cell characteristics in glioblastoma are maintained by the ecto-nucleotidase E-NPP1. Cell Death Differ. *21*, 929–940.

Bak, X.Y., Lam, D.H., Yang, J., Ye, K., Wei, E.L.X., Lim, S.K., and Wang, S. (2011). Human embryonic stem cell-derived mesenchymal stem cells as cellular delivery vehicles for prodrug gene therapy of glioblastoma. Hum. Gene Ther. *22*, 1365–1377.

Balvers, R.K., Dirven, C.M.F., Leenstra, S., and Lamfers, M.L.M. (2017). Malignant Glioma In Vitro Models: On the Utilization of Stem-like Cells. Curr Cancer Drug Targets *17*, 255–266.

Bao, S., Wu, Q., McLendon, R.E., Hao, Y., Shi, Q., Hjelmeland, A.B., Dewhirst, M.W., Bigner, D.D., and Rich, J.N. (2006). Glioma stem cells promote radioresistance by preferential activation of the DNA damage response. Nature *444*, 756–760.

Barton, G.M., Kagan, J.C., and Medzhitov, R. (2006). Intracellular localization of Toll-like receptor 9 prevents recognition of self DNA but facilitates access to viral DNA. Nat. Immunol. *7*, 49–56.

Barzon, L., Pacenti, M., Franchin, E., Colombo, F., and Palù, G. (2009). HSV-TK/IL-2 gene therapy for glioblastoma multiforme. Methods Mol. Biol. *542*, 529–549.

Bauchet, L., Mathieu-Daudé, H., Fabbro-Peray, P., Rigau, V., Fabbro, M., Chinot, O., Pallusseau, L., Carnin, C., Lainé, K., Schlama, A., Thiebaut, A., Patru, M.C., Bauchet, F., Lionnet, M., Wager, M., Faillot, T., Taillandier, L., Figarella-Branger, D., Capelle, L., Loiseau, H., Frappaz, D., Campello, C., Kerr, C., Duffau, H., Reme-Saumon, M., Trétarre, B., Daures, J.-P., Henin, D., Labrousse, F., Menei, P., Honnorat, J., Société Française de Neurochirurgie (SFNC), Club de Neuro-Oncologie of the Société Française de Neurochirurgie (CNO-SFNC), Société Française de Neuropathologie (SFNP), and Association des Neuro-Oncologues d'Expression Française (ANOCEF) (2010). Oncological patterns of care and outcome for 952 patients with newly diagnosed glioblastoma in 2004. Neuro-Oncology *12*, 725–735.

Bayin, N.S., Modrek, A.S., Dietrich, A., Lebowitz, J., Abel, T., Song, H.-R., Schober, M., Zagzag, D., Buchholz, C.J., Chao, M.V., and Placantonakis, D.G. (2014). Selective lentiviral gene delivery to CD133-expressing human glioblastoma stem cells. PLoS ONE *9*, e116114.

Beckermann, B.M., Kallifatidis, G., Groth, A., Frommhold, D., Apel, A., Mattern, J., Salnikov, A.V., Moldenhauer, G., Wagner, W., Diehlmann, A., Saffrich, R., Schubert, M., Ho, A.D., Giese, N., Büchler, M.W., Friess, H., Büchler, P., and Herr, I. (2008). VEGF expression by mesenchymal stem cells contributes to angiogenesis in pancreatic carcinoma. Br. J. Cancer *99*, 622–631.

Beier, D., Schulz, J.B., and Beier, C.P. (2011). Chemoresistance of glioblastoma cancer stem cells--much more complex than expected. Mol. Cancer *10*, 128.

Bejarano, E., Cabrera, M., Vega, L., Hidalgo, J., and Velasco, A. (2006). Golgi structural stability and biogenesis depend on associated PKA activity. J. Cell. Sci. *119*, 3764–3775.

Bernard-Arnoux, F., Lamure, M., Ducray, F., Aulagner, G., Honnorat, J., and Armoiry, X. (2016). The cost-effectiveness of tumor-treating fields therapy in patients with newly diagnosed glioblastoma. Neuro Oncol *18*, 1129–1136.

Bernstein, H.-G., Dobrowolny, H., Schott, B.H., Gorny, X., Becker, V., Steiner, J., Seidenbecher, C.I., and Bogerts, B. (2013). Increased density of AKAP5-expressing neurons in the anterior cingulate cortex of subjects with bipolar disorder. J Psychiatr Res *47*, 699–705.

Beuschlein, F., Fassnacht, M., Assié, G., Calebiro, D., Stratakis, C.A., Osswald, A., Ronchi, C.L., Wieland, T., Sbiera, S., Faucz, F.R., Schaak, K., Schmittfull, A., Schwarzmayr, T., Barreau, O., Vezzosi, D., Rizk-Rabin, M., Zabel, U., Szarek, E., Salpea, P., Forlino, A., Vetro, A., Zuffardi, O., Kisker, C., Diener, S., Meitinger, T., Lohse, M.J., Reincke, M., Bertherat, J., Strom, T.M., and Allolio, B. (2014). Constitutive activation of PKA catalytic subunit in adrenal Cushing's syndrome. N. Engl. J. Med. *370*, 1019–1028.

Blesa, J.M.G., Mollá, S.B., Esparcia, M.F., Ortells, J.M.S., Godoy, M.P., Das, A.M., Magan, B.M., Pulla, M.P., Sanchez, J.L., Canales, J.B.L., and Candel, V.A. (2012). Durable Complete Remission of a Brainstem Glioma Treated with a Combination of Bevacizumab and Cetuximab. Case Rep Oncol *5*, 676–681.

Bobola, M.S., Blank, A., Berger, M.S., Stevens, B.A., and Silber, J.R. (2001). Apurinic/apyrimidinic endonuclease activity is elevated in human adult gliomas. Clin. Cancer Res. *7*, 3510–3518.

Boettcher, A.J., Wu, J., Kim, C., Yang, J., Bruystens, J., Cheung, N., Pennypacker, J.K., Blumenthal, D.A., Kornev, A.P., and Taylor, S.S. (2011). Realizing the allosteric potential of the tetrameric protein kinase A RIα holoenzyme. Structure *19*, 265–276.

Bofill-De Ros, X., and Gu, S. (2016). Guidelines for the optimal design of miRNA-based shRNAs. Methods *103*, 157–166.

Boudreau, R.L., Martins, I., and Davidson, B.L. (2009). Artificial microRNAs as siRNA shuttles: improved safety as compared to shRNAs in vitro and in vivo. Mol. Ther. *17*, 169–175.

Brandon, E.P., Zhuo, M., Huang, Y.Y., Qi, M., Gerhold, K.A., Burton, K.A., Kandel, E.R., McKnight, G.S., and Idzerda, R.L. (1995). Hippocampal long-term depression and depotentiation are defective in mice carrying a targeted disruption of the gene encoding the RI beta subunit of cAMP-dependent protein kinase. Proc. Natl. Acad. Sci. U.S.A. *92*, 8851–8855.

Brat, D.J., and Van Meir, E.G. (2004). Vaso-occlusive and prothrombotic mechanisms associated with tumor hypoxia, necrosis, and accelerated growth in glioblastoma. Lab. Invest. *84*, 397–405.

Burgering, B.M., Pronk, G.J., van Weeren, P.C., Chardin, P., and Bos, J.L. (1993). cAMP antagonizes p21ras-directed activation of extracellular signal-regulated kinase 2 and phosphorylation of mSos nucleotide exchange factor. EMBO J. *12*, 4211–4220.

Calebiro, D., Di Dalmazi, G., Bathon, K., Ronchi, C.L., and Beuschlein, F. (2015). cAMP signaling in cortisol-producing adrenal adenoma. Eur. J. Endocrinol. *173*, M99-106.

Calebiro, D., Bathon, K., and Weigand, I. (2017). Mechanisms of Aberrant PKA Activation by Cα Subunit Mutations. Horm. Metab. Res. *49*, 307–314.

Calvo, E., Bolós, V., and Grande, E. (2009). Multiple roles and therapeutic implications of Akt signaling in cancer. Onco Targets Ther *2*, 135–150.

Campos, B., Wan, F., Farhadi, M., Ernst, A., Zeppernick, F., Tagscherer, K.E., Ahmadi, R., Lohr, J., Dictus, C., Gdynia, G., Combs, S.E., Goidts, V., Helmke, B.M., Eckstein, V., Roth, W., Beckhove, P., Lichter, P., Unterberg, A., Radlwimmer, B., and Herold-Mende, C. (2010). Differentiation therapy exerts antitumor effects on stem-like glioma cells. Clin. Cancer Res. *16*, 2715–2728.

Caretta, A., and Mucignat-Caretta, C. (2011). Protein kinase a in cancer. Cancers (Basel) *3*, 913–926.

Castanotto, D., Sakurai, K., Lingeman, R., Li, H., Shively, L., Aagaard, L., Soifer, H., Gatignol, A., Riggs, A., and Rossi, J.J. (2007). Combinatorial delivery of small interfering RNAs reduces RNAi efficacy by selective incorporation into RISC. Nucleic Acids Res. *35*, 5154–5164.

Castro, M.G., Candolfi, M., Kroeger, K., King, G.D., Curtin, J.F., Yagiz, K., Mineharu, Y., Assi, H., Wibowo, M., Muhammad, A.G., Foulad, D., Puntel, M., and Lowenstein, P.R. (2011). Gene Therapy and Targeted Toxins for Glioma. Curr Gene Ther *11*, 155–180.

Chamberlain, G., Fox, J., Ashton, B., and Middleton, J. (2007). Concise review: mesenchymal stem cells: their phenotype, differentiation capacity, immunological features, and potential for homing. Stem Cells *25*, 2739–2749.

Chandran, M., Candolfi, M., Shah, D., Mineharu, Y., Yadav, V.N., Koschmann, C., Asad, A.S., Lowenstein, P.R., and Castro, M.G. (2017). Single vs. combination immunotherapeutic strategies for glioma. Expert Opin Biol Ther *17*, 543–554.

Chávez-Vargas, L., Adame-García, S.R., Cervantes-Villagrana, R.D., Castillo-Kauil, A., Bruystens, J.G.H., Fukuhara, S., Taylor, S.S., Mochizuki, N., Reyes-Cruz, G., and Vázquez-Prado, J. (2016). Protein Kinase A (PKA) Type I Interacts with P-Rex1, a Rac Guanine Nucleotide Exchange Factor: EFFECT ON PKA LOCALIZATION AND P-Rex1 SIGNALING. J. Biol. Chem. *291*, 6182–6199.

Chen, J., Zhang, C., Mi, Y., Chen, F., and Du, D. (2017). CREB1 regulates glucose transport of glioma cell line U87 by targeting GLUT1. Mol. Cell. Biochem.

Chen, R., Nishimura, M.C., Bumbaca, S.M., Kharbanda, S., Forrest, W.F., Kasman, I.M., Greve, J.M., Soriano, R.H., Gilmour, L.L., Rivers, C.S., Modrusan, Z., Nacu, S., Guerrero, S., Edgar, K.A., Wallin, J.J., Lamszus, K., Westphal, M., Heim, S., James, C.D., VandenBerg, S.R., Costello, J.F., Moorefield, S., Cowdrey, C.J., Prados, M., and Phillips, H.S. (2010). A hierarchy of self-renewing tumor-initiating cell types in glioblastoma. Cancer Cell *17*, 362–375.

Chen, T.C., Hinton, D.R., Zidovetzki, R., and Hofman, F.M. (1998). Up-regulation of the cAMP/PKA pathway inhibits proliferation, induces differentiation, and leads to apoptosis in malignant gliomas. Lab. Invest. *78*, 165–174.

Chinot, O.L., Wick, W., Mason, W., Henriksson, R., Saran, F., Nishikawa, R., Carpentier, A.F., Hoang-Xuan, K., Kavan, P., Cernea, D., Brandes, A.A., Hilton, M., Abrey, L., and Cloughesy, T. (2014). Bevacizumab plus radiotherapy-temozolomide for newly diagnosed glioblastoma. N. Engl. J. Med. *370*, 709–722.

Cho-Chung, Y.S., and Nesterova, M.V. (2005). Tumor reversion: protein kinase A isozyme switching. Ann. N. Y. Acad. Sci. *1058*, 76–86.

Christensen, A.E., Selheim, F., de Rooij, J., Dremier, S., Schwede, F., Dao, K.K., Martinez, A., Maenhaut, C., Bos, J.L., Genieser, H.-G., and Døskeland, S.O. (2003). cAMP analog mapping of Epac1 and cAMP kinase. Discriminating analogs demonstrate that Epac and cAMP kinase act synergistically to promote PC-12 cell neurite extension. J. Biol. Chem. *278*, 35394–35402.

Clegg, C.H., Cadd, G.G., and McKnight, G.S. (1988). Genetic characterization of a brain-specific form of the type I regulatory subunit of cAMP-dependent protein kinase. Proc. Natl. Acad. Sci. U.S.A. *85*, 3703–3707.

Clement, V., Sanchez, P., de Tribolet, N., Radovanovic, I., and Ruiz i Altaba, A. (2007). HEDGEHOG-GLI1 signaling regulates human glioma growth, cancer stem cell self-renewal, and tumorigenicity. Curr. Biol. *17*, 165–172.

Colombo, F., Barzon, L., Franchin, E., Pacenti, M., Pinna, V., Danieli, D., Zanusso, M., and Palù, G. (2005). Combined HSV-TK/IL-2 gene therapy in patients with recurrent glioblastoma multiforme: biological and clinical results. Cancer Gene Ther. *12*, 835–848.

Cook, S.J., and McCormick, F. (1993). Inhibition by cAMP of Ras-dependent activation of Raf. Science *262*, 1069–1072.

Crivat, G., and Taraska, J.W. (2012). Imaging proteins inside cells with fluorescent tags. Trends Biotechnol. *30*, 8–16.

Cummings, D.E., Brandon, E.P., Planas, J.V., Motamed, K., Idzerda, R.L., and McKnight, G.S. (1996). Genetically lean mice result from targeted disruption of the RII beta subunit of protein kinase A. Nature *382*, 622–626.

Czabanka, M., Bruenner, J., Parmaksiz, G., Broggini, T., Topalovic, M., Bayerl, S.H., Auf, G., Kremenetskaia, I., Nieminen, M., Jabouille, A., Mueller, S., Harms, U., Harms, C., Koch, A., Heppner, F.L., and Vajkoczy, P. (2013). Combined temozolomide and sunitinib treatment leads to better tumour control but increased vascular resistance in O6-methylguanine methyltransferase-methylated gliomas. Eur. J. Cancer *49*, 2243–2252.

Czyzyk, T.A., Sikorski, M.A., Yang, L., and McKnight, G.S. (2008). Disruption of the RIIbeta subunit of PKA reverses the obesity syndrome of Agouti lethal yellow mice. Proc. Natl. Acad. Sci. U.S.A. *105*, 276–281.

D'Agostino, P.M., Gottfried-Blackmore, A., Anandasabapathy, N., and Bulloch, K. (2012). Brain dendritic cells: biology and pathology. Acta Neuropathol. *124*, 599–614.

Dahan, P., Martinez Gala, J., Delmas, C., Monferran, S., Malric, L., Zentkowski, D., Lubrano, V., Toulas, C., Cohen-Jonathan Moyal, E., and Lemarie, A. (2014). Ionizing radiations sustain glioblastoma cell dedifferentiation to a stem-like phenotype through survivin: possible involvement in radioresistance. Cell Death Dis *5*, e1543.

Davare, M.A., Horne, M.C., and Hell, J.W. (2000). Protein phosphatase 2A is associated with class C L-type calcium channels (Cav1.2) and antagonizes channel phosphorylation by cAMP-dependent protein kinase. J. Biol. Chem. *275*, 39710–39717.

Davies, D.C. (2002). Blood-brain barrier breakdown in septic encephalopathy and brain tumours. J. Anat. *200*, 639–646.

Del Gobbo, A., Peverelli, E., Treppiedi, D., Lania, A., Mantovani, G., and Ferrero, S. (2016). Expression of protein kinase A regulatory subunits in benign and malignant human thyroid tissues: A systematic review. Exp. Cell Res. *346*, 85–90.

Delgado-López, P.D., and Corrales-García, E.M. (2016). Survival in glioblastoma: a review on the impact of treatment modalities. Clin Transl Oncol *18*, 1062–1071.

Delghandi, M.P., Johannessen, M., and Moens, U. (2005). The cAMP signalling pathway activates CREB through PKA, p38 and MSK1 in NIH 3T3 cells. Cell. Signal. *17*, 1343–1351.

Den, R.B., Kamrava, M., Sheng, Z., Werner-Wasik, M., Dougherty, E., Marinucchi, M., Lawrence, Y.R., Hegarty, S., Hyslop, T., Andrews, D.W., Glass, J., Friedman, D.P., Green, M.R., Camphausen, K., and Dicker, A.P. (2013). A phase I study of the combination of sorafenib with temozolomide and radiation therapy for the treatment of primary and recurrent high-grade gliomas. Int. J. Radiat. Oncol. Biol. Phys. *85*, 321–328.

Doetsch, F., García-Verdugo, J.M., and Alvarez-Buylla, A. (1997). Cellular composition and three-dimensional organization of the subventricular germinal zone in the adult mammalian brain. J. Neurosci. *17*, 5046–5061.

Dong, J.M., Leung, T., Manser, E., and Lim, L. (1998). cAMP-induced morphological changes are counteracted by the activated RhoA small GTPase and the Rho kinase ROKalpha. J. Biol. Chem. *273*, 22554–22562.

Donsmark, M., Langfort, J., Holm, C., Ploug, T., and Galbo, H. (2004). Contractions induce phosphorylation of the AMPK site Ser565 in hormone-sensitive lipase in muscle. Biochem. Biophys. Res. Commun. *316*, 867–871.

Dulin, N.O., Niu, J., Browning, D.D., Ye, R.D., and Voyno-Yasenetskaya, T. (2001). Cyclic AMP-independent activation of protein kinase A by vasoactive peptides. J. Biol. Chem. *276*, 20827–20830.

Dumaz, N., and Marais, R. (2005). Integrating signals between cAMP and the RAS/RAF/MEK/ERK signalling pathways. Based on the anniversary prize of the Gesellschaft für Biochemie und Molekularbiologie Lecture delivered on 5 July 2003 at the Special FEBS Meeting in Brussels. FEBS J. *272*, 3491–3504.

Duncan, C.G., Killela, P.J., Payne, C.A., Lampson, B., Chen, W.C., Liu, J., Solomon, D., Waldman, T., Towers, A.J., Gregory, S.G., McDonald, K.L., McLendon, R.E., Bigner, D.D., and Yan, H. (2010). Integrated genomic analyses identify ERRFI1 and TACC3 as glioblastoma-targeted genes. Oncotarget *1*, 265–277.

Eekels, J.J.M., Pasternak, A.O., Schut, A.M., Geerts, D., Jeeninga, R.E., and Berkhout, B. (2012). A competitive cell growth assay for the detection of subtle effects of gene transduction on cell proliferation. Gene Ther. *19*, 1058–1064.

Enserink, J.M., Christensen, A.E., de Rooij, J., van Triest, M., Schwede, F., Genieser, H.G., Døskeland, S.O., Blank, J.L., and Bos, J.L. (2002). A novel Epac-specific cAMP analogue demonstrates independent regulation of Rap1 and ERK. Nat. Cell Biol. *4*, 901–906.

Eramo, A., Ricci-Vitiani, L., Zeuner, A., Pallini, R., Lotti, F., Sette, G., Pilozzi, E., Larocca, L.M., Peschle, C., and De Maria, R. (2006). Chemotherapy resistance of glioblastoma stem cells. Cell Death Differ. *13*, 1238–1241.

Fang, X., Yu, S.X., Lu, Y., Bast, R.C., Woodgett, J.R., and Mills, G.B. (2000). Phosphorylation and inactivation of glycogen synthase kinase 3 by protein kinase A. Proc. Natl. Acad. Sci. U.S.A. *97*, 11960–11965.

Fedorov, Y., Anderson, E.M., Birmingham, A., Reynolds, A., Karpilow, J., Robinson, K., Leake, D., Marshall, W.S., and Khvorova, A. (2006). Off-target effects by siRNA can induce toxic phenotype. RNA *12*, 1188–1196.

Fellmann, C., Hoffmann, T., Sridhar, V., Hopfgartner, B., Muhar, M., Roth, M., Lai, D.Y., Barbosa, I.A.M., Kwon, J.S., Guan, Y., Sinha, N., and Zuber, J. (2013). An optimized microRNA backbone for effective single-copy RNAi. Cell Rep *5*, 1704–1713.

Feng, H., Li, Y., Yin, Y., Zhang, W., Hou, Y., Zhang, L., Li, Z., Xie, B., Gao, W.-Q., Sarkaria, J.N., Raizer, J.J., James, C.D., Parsa, A.T., Hu, B., and Cheng, S.-Y. (2015). Protein kinase A-dependent phosphorylation of Dock180 at serine residue 1250 is important for glioma growth and invasion stimulated by platelet derived-growth factor receptor α. Neuro-Oncology *17*, 832–842.

Ferrero, S., Vaira, V., Del Gobbo, A., Vicentini, L., Bosari, S., Beck-Peccoz, P., Mantovani, G., Spada, A., and Lania, A.G. (2015). Different expression of protein kinase A (PKA) regulatory subunits in normal and neoplastic thyroid tissues. Histol. Histopathol. *30*, 473–478.

Fiol, C.J., Mahrenholz, A.M., Wang, Y., Roeske, R.W., and Roach, P.J. (1987). Formation of protein kinase recognition sites by covalent modification of the substrate. Molecular mechanism for the synergistic action of casein kinase II and glycogen synthase kinase 3. J. Biol. Chem. *262*, 14042–14048.

Foss, K.B., Simard, J., Bérubé, D., Beebe, S.J., Sandberg, M., Grzeschik, K.H., Gagné, R., Hansson,V., and Jahnsen, T. (1992). Localization of the catalytic subunit C gamma of the cAMP-dependent protein kinase gene (PRKACG) to human chromosome region 9q13. Cytogenet. Cell Genet. *60*, 22–25.

Frattola, L., Canal, N., Ferrarese, C., Tonini, C., Tonon, G., Villani, R., and Trabucchi, M. (1983). Multiple forms of protein kinase from normal human brain and glioblastoma. Cancer Res. *43*, 1321–1324.

Frosina, G. (2010). The Bright and the Dark Sides of DNA Repair in Stem Cells.

Fukuda, S., Kato, F., Tozuka, Y., Yamaguchi, M., Miyamoto, Y., and Hisatsune, T. (2003). Two distinct subpopulations of nestin-positive cells in adult mouse dentate gyrus. J. Neurosci. *23*, 9357–9366.

Gage, F.H. (2000). Mammalian neural stem cells. Science *287*, 1433–1438.

Galea, I., Bernardes-Silva, M., Forse, P.A., van Rooijen, N., Liblau, R.S., and Perry, V.H. (2007). An antigen-specific pathway for CD8 T cells across the blood-brain barrier. J. Exp. Med. *204*, 2023–2030.

Gallo-Oller, G., Vollmann-Zwerenz, A., Meléndez, B., Rey, J.A., Hau, P., Dotor, J., and Castresana, J.S. (2016). P144, a Transforming Growth Factor beta inhibitor peptide, generates antitumoral effects and modifies SMAD7 and SKI levels in human glioblastoma cell lines. Cancer Lett. *381*, 67–75.

Gao, N., Asamitsu, K., Hibi, Y., Ueno, T., and Okamoto, T. (2008). AKIP1 enhances NF-kappaB-dependent gene expression by promoting the nuclear retention and phosphorylation of p65. J. Biol. Chem. *283*, 7834–7843.

Gao, T., Yatani, A., Dell'Acqua, M.L., Sako, H., Green, S.A., Dascal, N., Scott, J.D., and Hosey, M.M. (1997). cAMP-dependent regulation of cardiac L-type Ca2+ channels requires membrane targeting of PKA and phosphorylation of channel subunits. Neuron *19*, 185–196.

Genßler, S., Burger, M.C., Zhang, C., Oelsner, S., Mildenberger, I., Wagner, M., Steinbach, J.P., and Wels, W.S. (2015). Dual targeting of glioblastoma with chimeric antigen receptor-engineered natural killer cells overcomes heterogeneity of target antigen expression and enhances antitumor activity and survival. Oncoimmunology *5*.

Gerthoffer, W.T., Solway, J., and Camoretti-Mercado, B. (2013). Emerging targets for novel therapy of asthma. Curr Opin Pharmacol *13*, 324–330.

Giard, D.J., Aaronson, S.A., Todaro, G.J., Arnstein, P., Kersey, J.H., Dosik, H., and Parks, W.P. (1973). In vitro cultivation of human tumors: establishment of cell lines derived from a series of solid tumors. J. Natl. Cancer Inst. *51*, 1417–1423.

Gilbert, M.R., Wang, M., Aldape, K.D., Stupp, R., Hegi, M.E., Jaeckle, K.A., Armstrong, T.S., Wefel, J.S., Won, M., Blumenthal, D.T., Mahajan, A., Schultz, C.J., Erridge, S., Baumert, B., Hopkins, K.I., Tzuk-Shina, T., Brown, P.D., Chakravarti, A., Curran, W.J., and Mehta, M.P. (2013). Dose-Dense Temozolomide for Newly Diagnosed Glioblastoma: A Randomized Phase III Clinical Trial. J Clin Oncol *31*, 4085–4091.

Gilbert, M.R., Dignam, J.J., Armstrong, T.S., Wefel, J.S., Blumenthal, D.T., Vogelbaum, M.A., Colman, H., Chakravarti, A., Pugh, S., Won, M., Jeraj, R., Brown, P.D., Jaeckle, K.A., Schiff, D., Stieber, V.W., Brachman, D.G., Werner-Wasik, M., Tremont-Lukats, I.W., Sulman, E.P., Aldape, K.D., Curran, W.J., and Mehta, M.P. (2014). A randomized trial of bevacizumab for newly diagnosed glioblastoma. N. Engl. J. Med. *370*, 699–708.

Goh, G., Scholl, U.I., Healy, J.M., Choi, M., Prasad, M.L., Nelson-Williams, C., Kunstman, J.W., Kuntsman, J.W., Korah, R., Suttorp, A.-C., Dietrich, D., Haase, M., Willenberg, H.S., Stålberg, P., Hellman, P., Akerström, G., Björklund, P., Carling, T., and Lifton, R.P. (2014). Recurrent activating mutation in PRKACA in cortisol-producing adrenal tumors. Nat. Genet. *46*, 613–617.

Gold, M.G., Gonen, T., and Scott, J.D. (2013). Local cAMP signaling in disease at a glance. J. Cell. Sci. *126*, 4537–4543.

Goldfinger, L.E., Han, J., Kiosses, W.B., Howe, A.K., and Ginsberg, M.H. (2003). Spatial restriction of alpha4 integrin phosphorylation regulates lamellipodial stability and alpha4beta1-dependent cell migration. J. Cell Biol. *162*, 731–741.

Gorshkov, K., Mehta, S., Ramamurthy, S., Ronnett, G.V., Zhou, F.-Q., and Zhang, J. (2017). AKAP-mediated feedback control of cAMP gradients in developing hippocampal neurons. Nat. Chem. Biol. *13*, 425–431.

Grandi, P., Peruzzi, P., Reinhart, B., Cohen, J.B., Chiocca, E.A., and Glorioso, J.C. (2009). Design and application of oncolytic HSV vectors for glioblastoma therapy. Expert Rev Neurother *9*, 505–517.

de Groot, J.F., Fuller, G., Kumar, A.J., Piao, Y., Eterovic, K., Ji, Y., and Conrad, C.A. (2010). Tumor invasion after treatment of glioblastoma with bevacizumab: radiographic and pathologic correlation in humans and mice. Neuro-Oncology *12*, 233–242.

Grossauer, S., Koeck, K., and Petritsch, C. (2015). Immunecheckpoint blockage - a promising strategy to overcome glioma stem cell therapy-resistance. Insights in Neurosurgery *1*.

Hadjipanayis, C.G., and Van Meir, E.G. (2009A). Tumor initiating cells in malignant gliomas: biology and implications for therapy. J. Mol. Med. *87*, 363–374.

Hadjipanayis, C.G., and Van Meir, E.G. (2009B). Brain cancer propagating cells: biology, genetics and targeted therapies. Trends Mol Med *15*, 519–530.

Halatsch, M.-E., Löw, S., Mursch, K., Hielscher, T., Schmidt, U., Unterberg, A., Vougioukas, V.I., and Feuerhake, F. (2009). Candidate genes for sensitivity and resistance of human glioblastoma multiforme cell lines to erlotinib. Laboratory investigation. J. Neurosurg. *111*, 211–218.

Hanson, D.A., and Ziegler, S.F. (2004). Fusion of green fluorescent protein to the C-terminus of granulysin alters its intracellular localization in comparison to the native molecule. J Negat Results Biomed. *10*, 3–2.

Harada, H., Becknell, B., Wilm, M., Mann, M., Huang, L.J., Taylor, S.S., Scott, J.D., and Korsmeyer, S.J. (1999). Phosphorylation and inactivation of BAD by mitochondria-anchored protein kinase A. Mol. Cell *3*, 413–422.

Haste, N.M., Talabani, H., Doo, A., Merckx, A., Langsley, G., and Taylor, S.S. (2012). Exploring the Plasmodium falciparum cyclic-adenosine monophosphate (cAMP)-dependent protein kinase (PfPKA) as a therapeutic target. Microbes Infect. *14*, 838–850.

Hayashida, K., Johnston, D.R., Goldberger, O., and Park, P.W. (2006). Syndecan-1 expression in epithelial cells is induced by transforming growth factor beta through a PKA-dependent pathway. J. Biol. Chem. *281*, 24365–24374.

Hegi, M.E., Diserens, A.-C., Gorlia, T., Hamou, M.-F., de Tribolet, N., Weller, M., Kros, J.M., Hainfellner, J.A., Mason, W., Mariani, L., Bromberg, J.E.C., Hau, P., Mirimanoff, R.O., Cairncross, J.G., Janzer, R.C., and Stupp, R. (2005). MGMT gene silencing and benefit from temozolomide in glioblastoma. N. Engl. J. Med. *352*, 997–1003.

Hegi, M.E., Rajakannu, P., and Weller, M. (2012). Epidermal growth factor receptor: a re-emerging target in glioblastoma. Curr. Opin. Neurol. *25*, 774–779.

Hicks, M.J., Chiuchiolo, M.J., Ballon, D., Dyke, J.P., Aronowitz, E., Funato, K., Tabar, V., Havlicek, D., Fan, F., Sondhi, D., Kaminsky, S.M., and Crystal, R.G. (2016). Anti-Epidermal Growth Factor Receptor Gene Therapy for Glioblastoma. PLoS ONE *11*, e0162978.

Hjelmeland, A.B., Wu, Q., Heddleston, J.M., Choudhary, G.S., MacSwords, J., Lathia, J.D., McLendon, R., Lindner, D., Sloan, A., and Rich, J.N. (2011). Acidic stress promotes a glioma stem cell phenotype. Cell Death Differ. *18*, 829–840.

Hoelzinger, D.B., Mariani, L., Weis, J., Woyke, T., Berens, T.J., McDonough, W.S., Sloan, A., Coons, S.W., and Berens, M.E. (2005). Gene expression profile of glioblastoma multiforme invasive phenotype points to new therapeutic targets. Neoplasia *7*, 7–16.

Holz, G.G., Chepurny, O.G., and Schwede, F. (2008). Epac-selective cAMP analogs: new tools with which to evaluate the signal transduction properties of cAMP-regulated guanine nucleotide exchange factors. Cell. Signal. *20*, 10–20.

Honeyman, J.N., Simon, E.P., Robine, N., Chiaroni-Clarke, R., Darcy, D.G., Lim, I.I.P., Gleason, C.E., Murphy, J.M., Rosenberg, B.R., Teegan, L., Takacs, C.N., Botero, S., Belote, R., Germer, S., Emde, A.-K., Vacic, V., Bhanot, U., LaQuaglia, M.P., and Simon, S.M. (2014). Detection of a recurrent DNAJB1-PRKACA chimeric transcript in fibrolamellar hepatocellular carcinoma. Science *343*, 1010–1014.

Hornung, V., Guenthner-Biller, M., Bourquin, C., Ablasser, A., Schlee, M., Uematsu, S., Noronha, A., Manoharan, M., Akira, S., de Fougerolles, A., Endres, S., and Hartmann, G. (2005). Sequence-specific potent induction of IFN-alpha by short interfering RNA in plasmacytoid dendritic cells through TLR7. Nat. Med. *11*, 263–270.

Hottinger, A.F., Aissa, A.B., Espeli, V., Squiban, D., Dunkel, N., Vargas, M.I., Hundsberger, T., Mach, N., Schaller, K., Weber, D.C., Bodmer, A., and Dietrich, P.-Y. (2014). Phase I study of sorafenib combined with radiation therapy and temozolomide as first-line treatment of high-grade glioma. Br. J. Cancer *110*, 2655–2661.

Howe, A.K. (2004). Regulation of actin-based cell migration by cAMP/PKA. Biochim. Biophys. Acta *1692*, 159–174.

Howe, A.K., Baldor, L.C., and Hogan, B.P. (2005). Spatial regulation of the cAMP-dependent protein kinase during chemotactic cell migration. Proc. Natl. Acad. Sci. U.S.A. *102*, 14320–14325.

Hu, Y.-L., Huang, B., Zhang, T.-Y., Miao, P.-H., Tang, G.-P., Tabata, Y., and Gao, J.-Q. (2012). Mesenchymal stem cells as a novel carrier for targeted delivery of gene in cancer therapy based on nonviral transfection. Mol. Pharm. *9*, 2698–2709.

Huse, J.T., Brennan, C., Hambardzumyan, D., Wee, B., Pena, J., Rouhanifard, S.H., Sohn-Lee, C., le Sage, C., Agami, R., Tuschl, T., and Holland, E.C. (2009). The PTEN-regulating microRNA miR-26a is amplified in high-grade glioma and facilitates gliomagenesis in vivo. Genes Dev. *23*, 1327–1337.

Huveldt, D., Lewis-Tuffin, L.J., Carlson, B.L., Schroeder, M.A., Rodriguez, F., Giannini, C., Galanis, E., Sarkaria, J.N., and Anastasiadis, P.Z. (2013). Targeting Src family kinases inhibits bevacizumab-induced glioma cell invasion. PLoS ONE *8*, e56505.

Ichimura, K., Ohgaki, H., Kleihues, P., and Collins, V.P. (2004). Molecular pathogenesis of astrocytic tumours. J. Neurooncol. *70*, 137–160.

Ilouz, R., Lev-Ram, V., Bushong, E.A., Stiles, T.L., Friedmann-Morvinski, D., Douglas, C., Goldberg, G., Ellisman, M.H., and Taylor, S.S. (2017). Isoform-specific subcellular localization and function of protein kinase A identified by mosaic imaging of mouse brain. Elife *6*.

Jackson, A.L., and Linsley, P.S. (2010). Recognizing and avoiding siRNA off-target effects for target identification and therapeutic application. Nat Rev Drug Discov *9*, 57–67.

Jacobs, V.L., Valdes, P.A., Hickey, W.F., and De Leo, J.A. (2011). Current review of in vivo GBM rodent models: emphasis on the CNS-1 tumour model. ASN Neuro *3*.

Jakubowicz-Gil, J., Bądziul, D., Langner, E., Wertel, I., Zając, A., and Rzeski, W. (2017). Temozolomide and sorafenib as programmed cell death inducers of human glioma cells. Pharmacol Rep *69*, 779–787.

Jellinger, K. (1978). Glioblastoma multiforme: morphology and biology. Acta Neurochir (Wien) *42*, 5–32.

Ji, N., Weng, D., Liu, C., Gu, Z., Chen, S., Guo, Y., Fan, Z., Wang, X., Chen, J., Zhao, Y., Zhou, J., Wang, J., Ma, D., and Li, N. (2016). Adenovirus-mediated delivery of herpes simplex virus thymidine kinase administration improves outcome of recurrent high-grade glioma. Oncotarget *7*, 4369–4378.

Jones, B.J., and McTaggart, S.J. (2008). Immunosuppression by mesenchymal stromal cells: from culture to clinic. Exp. Hematol. *36*, 733–741.

Joseph, G.P., McDermott, R., Baryshnikova, M.A., Cobbs, C.S., and Ulasov, I.V. (2017). Cytomegalovirus as an oncomodulatory agent in the progression of glioma. Cancer Lett. *384*, 79–85.

Joseph, J.V., Balasubramaniyan, V., Walenkamp, A., and Kruyt, F.A.E. (2013). TGF-β as a therapeutic target in high grade gliomas - promises and challenges. Biochem. Pharmacol. *85*, 478–485.

Jovčevska, I., Kočevar, N., and Komel, R. (2013). Glioma and glioblastoma - how much do we (not) know? Mol Clin Oncol *1*, 935–941.

Kang, C.-S., Zhang, Z.-Y., Jia, Z.-F., Wang, G.-X., Qiu, M.-Z., Zhou, H.-X., Yu, S.-Z., Chang, J., Jiang, H., and Pu, P.-Y. (2006). Suppression of EGFR expression by antisense or small interference RNA inhibits U251 glioma cell growth in vitro and in vivo. Cancer Gene Ther. *13*, 530–538.

Keunen, O., Johansson, M., Oudin, A., Sanzey, M., Rahim, S.A.A., Fack, F., Thorsen, F., Taxt, T., Bartos, M., Jirik, R., Miletic, H., Wang, J., Stieber, D., Stuhr, L., Moen, I., Rygh, C.B., Bjerkvig, R., and Niclou, S.P. (2011). Anti-VEGF treatment reduces blood supply and increases tumor cell invasion in glioblastoma. Proc. Natl. Acad. Sci. U.S.A. *108*, 3749–3754.

Khan, A.A., Betel, D., Miller, M.L., Sander, C., Leslie, C.S., and Marks, D.S. (2009). Transfection of small RNAs globally perturbs gene regulation by endogenous microRNAs. Nat Biotechnol *27*, 549–555.

Kim, M., and Morshead, C.M. (2003). Distinct populations of forebrain neural stem and progenitor cells can be isolated using side-population analysis. J. Neurosci. *23*, 10703–10709.

Kim, E.S., Kim, J.E., Patel, M.A., Mangraviti, A., Ruzevick, J., and Lim, M. (2016). Immune Checkpoint Modulators: An Emerging Antiglioma Armamentarium. J Immunol Res *2016*, 4683607.

Kim, G., Choe, Y., Park, J., Cho, S., and Kim, K. (2002). Activation of protein kinase A induces neuronal differentiation of HiB5 hippocampal progenitor cells. Brain Res. Mol. Brain Res. *109*, 134–145.

Kim, H., Scimia, M.C., Wilkinson, D., Trelles, R.D., Wood, M.R., Bowtell, D., Dillin, A., Mercola, M., and Ronai, Z.A. (2011). Fine-tuning of Drp1/Fis1 availability by AKAP121/Siah2 regulates mitochondrial adaptation to hypoxia. Mol. Cell *44*, 532–544.

Kim, S.M., Lim, J.Y., Park, S.I., Jeong, C.H., Oh, J.H., Jeong, M., Oh, W., Park, S.-H., Sung, Y.-C., and Jeun, S.-S. (2008). Gene therapy using TRAIL-secreting human umbilical cord blood-derived mesenchymal stem cells against intracranial glioma. Cancer Res. *68*, 9614–9623.

King, C.C., Sastri, M., Chang, P., Pennypacker, J., and Taylor, S.S. (2011). The rate of NF-κB nuclear translocation is regulated by PKA and A kinase interacting protein 1. PLoS ONE *6*, e18713.

Kirschner, L.S., Carney, J.A., Pack, S.D., Taymans, S.E., Giatzakis, C., Cho, Y.S., Cho-Chung, Y.S., and Stratakis, C.A. (2000). Mutations of the gene encoding the protein kinase A type I-alpha regulatory subunit in patients with the Carney complex. Nat. Genet. *26*, 89–92.

Klausner, R.D., Donaldson, J.G., and Lippincott-Schwartz, J. (1992). Brefeldin A: insights into the control of membrane traffic and organelle structure. J. Cell Biol. *116*, 1071–1080.

Klein, R.S., Garber, C., and Howard, N. (2017). Infectious immunity in the central nervous system and brain function. Nat. Immunol. *18*, 132–141.

Komori, T. (2017). The 2016 WHO Classification of Tumours of the Central Nervous System: The Major Points of Revision. Neurol. Med. Chir. (Tokyo) *57*, 301–311.

Koul, D., Wang, S., Wu, S., Saito, N., Zheng, S., Gao, F., Kaul, I., Setoguchi, M., Nakayama, K., Koyama, K., Shiose, Y., Sulman, E.P., Hirota, Y., and Yung, W.K.A. (2017). Preclinical therapeutic efficacy of a novel blood-brain barrier-penetrant dual PI3K/mTOR inhibitor with preferential response in PI3K/PTEN mutant glioma. Oncotarget *8*, 21741–21753.

Kreisl, T.N., McNeill, K.A., Sul, J., Iwamoto, F.M., Shih, J., and Fine, H.A. (2012). A phase I/II trial of vandetanib for patients with recurrent malignant glioma. Neuro-Oncology *14*, 1519–1526.

Ladomersky, E., Genet, M., Zhai, L., Gritsina, G., Lauing, K.L., Lulla, R.R., Fangusaro, J., Lenzen, A., Kumthekar, P., Raizer, J.J., Binder, D.C., James, C.D., and Wainwright, D.A. (2016). Improving vaccine efficacy against malignant glioma. Oncoimmunology *5*.

Laks, D.R., Crisman, T.J., Shih, M.Y.S., Mottahedeh, J., Gao, F., Sperry, J., Garrett, M.C., Yong, W.H., Cloughesy, T.F., Liau, L.M., Lai, A., Coppola, G., and Kornblum, H.I. (2016). Large-scale assessment of the gliomasphere model system. Neuro-Oncology *18*, 1367–1378.

Lamb, J., Ladha, M.H., McMahon, C., Sutherland, R.L., and Ewen, M.E. (2000). Regulation of the functional interaction between cyclin D1 and the estrogen receptor. Mol. Cell. Biol. *20*, 8667–8675.

Lawrence, Y.R., Mishra, M.V., Werner-Wasik, M., Andrews, D.W., Showalter, T.N., Glass, J., Shen, X., Symon, Z., and Dicker, A.P. (2012). Improving prognosis of glioblastoma in the 21st century: who has benefited most? Cancer *118*, 4228–4234.

Lee, E.Q., Kaley, T.J., Duda, D.G., Schiff, D., Lassman, A.B., Wong, E.T., Mikkelsen, T., Purow, B.W., Muzikansky, A., Ancukiewicz, M., Huse, J.T., Ramkissoon, S., Drappatz, J., Norden, A.D., Beroukhim, R., Weiss, S.E., Alexander, B.M., McCluskey, C.S., Gerard, M., Smith, K.H., Jain, R.K., Batchelor, T.T., Ligon, K.L., and Wen, P.Y. (2015). A Multicenter, Phase II, Randomized, Noncomparative Clinical Trial of Radiation and Temozolomide with or without Vandetanib in Newly Diagnosed Glioblastoma Patients. Clin. Cancer Res. *21*, 3610–3618.

Lee, J.K., Choi, M.R., Song, D.K., Huh, S.O., Kim, Y.H., and Suh, H.W. (1999). Activation of adenylate cyclase results in down-regulation of c-jun mRNA expression in rat C6 glioma cells. Neurosci. Lett. *276*, 53–56.

Lefkimmiatis, K., and Zaccolo, M. (2014). cAMP signaling in subcellular compartments. Pharmacol. Ther. *143*, 295–304.

Lerosey, I., Pizon, V., Tavitian, A., and de Gunzburg, J. (1991). The cAMP-dependent protein kinase phosphorylates the rap1 protein in vitro as well as in intact fibroblasts, but not the closely related rap2 protein. Biochem. Biophys. Res. Commun. *175*, 430–436.

Lester, L.B., Langeberg, L.K., and Scott, J.D. (1997). Anchoring of protein kinase A facilitates hormone-mediated insulin secretion. Proc. Natl. Acad. Sci. U.S.A. *94*, 14942–14947.

Li, C.-C., Le, K., Kato, J., Moss, J., and Vaughan, M. (2016). Enhancement of β-catenin activity by BIG1 plus BIG2 via Arf activation and cAMP signals. Proc. Natl. Acad. Sci. U.S.A. *113*, 5946–5951.

Li, F., Tiede, B., Massagué, J., and Kang, Y. (2007A). Beyond tumorigenesis: cancer stem cells in metastasis. Cell Res. *17*, 3–14.

Li, W.-Q., Li, Y.-M., Tao, B.-B., Lu, Y.-C., Hu, G.-H., Liu, H.-M., He, J., Xu, Y., and Yu, H.-Y. (2010). Downregulation of ABCG2 expression in glioblastoma cancer stem cells with miRNA-328 may decrease their chemoresistance. Med. Sci. Monit. *16*, HY27-30.

Li, Y., Yin, W., Wang, X., Zhu, W., Huang, Y., and Yan, G. (2007B). Cholera toxin induces malignant glioma cell differentiation via the PKA/CREB pathway. Proc. Natl. Acad. Sci. U.S.A. *104*, 13438–13443.

Ligon, K.L., Huillard, E., Mehta, S., Kesari, S., Liu, H., Alberta, J.A., Bachoo, R.M., Kane, M., Louis, D.N., Depinho, R.A., Anderson, D.J., Stiles, C.D., and Rowitch, D.H. (2007). Olig2-regulated lineage-restricted pathway controls replication competence in neural stem cells and malignant glioma. Neuron *53*, 503–517.

Liu, G., Yuan, X., Zeng, Z., Tunici, P., Ng, H., Abdulkadir, I.R., Lu, L., Irvin, D., Black, K.L., and Yu, J.S. (2006). Analysis of gene expression and chemoresistance of CD133+ cancer stem cells in glioblastoma. Mol Cancer *5*, 67.

Liu, Y.-J., Ma, Y.-C., Zhang, W.-J., Yang, Z.-Z., Liang, D.-S., Wu, Z.-F., and Qi, X.-R. (2017). Combination therapy with micellarized cyclopamine and temozolomide attenuate glioblastoma growth through Gli1 down-regulation. Oncotarget *8*, 42495–42509.

Louis, D.N., Perry, A., Reifenberger, G., von Deimling, A., Figarella-Branger, D., Cavenee, W.K., Ohgaki, H., Wiestler, O.D., Kleihues, P., and Ellison, D.W. (2016). The 2016 World Health Organization Classification of Tumors of the Central Nervous System: a summary. Acta Neuropathologica *131*, 803–820.

Lu, K.V., Chang, J.P., Parachoniak, C.A., Pandika, M.M., Aghi, M.K., Meyronet, D., Isachenko, N., Fouse, S.D., Phillips, J.J., Cheresh, D.A., Park, M., and Bergers, G. (2012). VEGF inhibits tumor cell invasion and mesenchymal transition through a MET/VEGFR2 complex. Cancer Cell *22*, 21–35.

Maczuga, P., Koornneef, A., Borel, F., Petry, H., van Deventer, S., Ritsema, T., and Konstantinova, P. (2012). Optimization and comparison of knockdown efficacy between polymerase II expressed shRNA and artificial miRNA targeting luciferase and Apolipoprotein B100. BMC Biotechnol. *12*, 42.

Manjunath, N., Wu, H., Subramanya, S., and Shankar, P. (2009). Lentiviral delivery of short hairpin RNAs. Adv. Drug Deliv. Rev. *61*, 732–745.

Mantovani, G., Bondioni, S., Lania, A.G., Rodolfo, M., Peverelli, E., Polentarutti, N., Veliz Rodriguez, T., Ferrero, S., Bosari, S., Beck-Peccoz, P., and Spada, A. (2008A). High expression of PKA regulatory subunit 1A protein is related to proliferation of human melanoma cells. Oncogene *27*, 1834–1843.

Mantovani, G., Lania, A.G., Bondioni, S., Peverelli, E., Pedroni, C., Ferrero, S., Pellegrini, C., Vicentini, L., Arnaldi, G., Bosari, S., Beck-Peccoz, P., and Spada, A. (2008B). Different expression of protein kinase A (PKA) regulatory subunits in cortisol-secreting adrenocortical tumors: relationship with cell proliferation. Exp. Cell Res. *314*, 123–130.

Mantovani, G., Bondioni, S., Alberti, L., Gilardini, L., Invitti, C., Corbetta, S., Zappa, M.A., Ferrero, S., Lania, A.G., Bosari, S., Beck-Peccoz, P., and Spada, A. (2009). Protein kinase A

regulatory subunits in human adipose tissue: decreased R2B expression and activity in adipocytes from obese subjects. Diabetes *58*, 620–626.

Martin, B.R., Deerinck, T.J., Ellisman, M.H., Taylor, S.S., and Tsien, R.Y. (2007). Isoform-specific PKA dynamics revealed by dye-triggered aggregation and DAKAP1alpha-mediated localization in living cells. Chem. Biol. *14*, 1031–1042.

Matsuda, S., Kominato, K., Koide-Yoshida, S., Miyamoto, K., Isshiki, K., Tsuji, A., and Yuasa, K. (2014). PCTAIRE kinase 3/cyclin-dependent kinase 18 is activated through association with cyclin A and/or phosphorylation by protein kinase A. J. Biol. Chem. *289*, 18387–18400.

Matyakhina, L., Lenherr, S.M., and Stratakis, C.A. (2002). Protein kinase A and chromosomal stability. Ann. N. Y. Acad. Sci. *968*, 148–157.

Mavillard, F., Hidalgo, J., Megias, D., Levitsky, K.L., and Velasco, A. (2010). PKA-mediated Golgi remodeling during cAMP signal transmission. Traffic *11*, 90–109.

Mavrakis, M., Lippincott-Schwartz, J., Stratakis, C.A., and Bossis, I. (2006). Depletion of type IA regulatory subunit (RIalpha) of protein kinase A (PKA) in mammalian cells and tissues activates mTOR and causes autophagic deficiency. Hum. Mol. Genet. *15*, 2962–2971.

Mavrakis, M., Lippincott-Schwartz, J., Stratakis, C.A., and Bossis, I. (2007). mTOR kinase and the regulatory subunit of protein kinase A (PRKAR1A) spatially and functionally interact during autophagosome maturation. Autophagy *3*, 151–153.

McBride, J.L., Boudreau, R.L., Harper, S.Q., Staber, P.D., Monteys, A.M., Martins, I., Gilmore, B.L., Burstein, H., Peluso, R.W., Polisky, B., Carter, B.J., and Davidson, B.L. (2008). Artificial miRNAs mitigate shRNA-mediated toxicity in the brain: implications for the therapeutic development of RNAi. Proc. Natl. Acad. Sci. U.S.A. *105*, 5868–5873.

McDaid, H.M., Cairns, M.T., Atkinson, R.J., McAleer, S., Harkin, D.P., Gilmore, P., and Johnston, P.G. (1999). Increased expression of the RIalpha subunit of the cAMP-dependent protein kinase A is associated with advanced stage ovarian cancer. Br. J. Cancer *79*, 933–939.

McKenzie, A.J., Campbell, S.L., and Howe, A.K. (2011). Protein kinase A activity and anchoring are required for ovarian cancer cell migration and invasion. PLoS ONE *6*, e26552.

McLendon, R., Friedman, A., Bigner, D., Meir, E.G.V., Brat, D.J., Mastrogianakis, G.M., Olson, J.J., Mikkelsen, T., Lehman, N., Aldape, K., Yung, W.K.A., Bogler, O., Thomson, E., et al. (2008). Comprehensive genomic characterization defines human glioblastoma genes and core pathways. Nature *455*, 1061–1068.

Meoli, E., Bossis, I., Cazabat, L., Mavrakis, M., Horvath, A., Stergiopoulos, S., Shiferaw, M.L., Fumey, G., Perlemoine, K., Muchow, M., Robinson-White, A., Weinberg, F., Nesterova, M., Patronas, Y., Groussin, L., Bertherat, J., and Stratakis, C.A. (2008). Protein kinase A effects of an expressed PRKAR1A mutation associated with aggressive tumors. Cancer Res. *68*, 3133–3141.

Mesfin, F., and Al-Dhahir, M. (2017). Cancer, Brain, Gliomas. In StatPearls, (Treasure Island (FL): StatPearls Publishing), p.

Millar, J.K., Pickard, B.S., Mackie, S., James, R., Christie, S., Buchanan, S.R., Malloy, M.P., Chubb, J.E., Huston, E., Baillie, G.S., Thomson, P.A., Hill, E.V., Brandon, N.J., Rain, J.-C., Camargo, L.M., Whiting, P.J., Houslay, M.D., Blackwood, D.H.R., Muir, W.J., and Porteous, D.J. (2005). DISC1 and PDE4B are interacting genetic factors in schizophrenia that regulate cAMP signaling. Science *310*, 1187–1191.

Miller, W.R. (2002). Regulatory Subunits of PKA and Breast Cancer. Annals of the New York Academy of Sciences *968*, 37–48.

Miller, R.A., Chu, Q., Xie, J., Foretz, M., Viollet, B., and Birnbaum, M.J. (2013). Biguanides suppress hepatic glucagon signalling by decreasing production of cyclic AMP. Nature *494*, 256–260.

Miranda, A., Blanco-Prieto, M., Sousa, J., Pais, A., and Vitorino, C. (2017). Breaching barriers in glioblastoma. Part I: Molecular pathways and novel treatment approaches. Int J Pharm.

Modrek, A.S., Bayin, N.S., and Placantonakis, D.G. (2014). Brain stem cells as the cell of origin in glioma. World J Stem Cells *6*, 43–52.

Moen, L.V., Ramberg, H., Zhao, S., Grytli, H.H., Sveen, A., Berge, V., Skotheim, R.I., Taskén, K.A., and Skålhegg, B.S. (2017). Observed correlation between the expression levels of catalytic subunit, Cβ2, of cyclic adenosine monophosphate-dependent protein kinase and prostate cancer aggressiveness. Urol. Oncol. *35*, 111.e1-111.e8.

Molenaar, R.J., Botman, D., Smits, M.A., Hira, V.V., van Lith, S.A., Stap, J., Henneman, P., Khurshed, M., Lenting, K., Mul, A.N., Dimitrakopoulou, D., van Drunen, C.M., Hoebe, R.A., Radivoyevitch, T., Wilmink, J.W., Maciejewski, J.P., Vandertop, W.P., Leenders, W.P., Bleeker, F.E., and van Noorden, C.J. (2015). Radioprotection of IDH1-Mutated Cancer Cells by the IDH1-Mutant Inhibitor AGI-5198. Cancer Res. *75*, 4790–4802.

Moschioni C. (2014). Engineered Bovine Herpesvirus type 4: a new tool against glioma stem-like cells? PhD thesis, University of Padova.

Mucignat-Caretta, C., and Caretta, A. (2001). Localization of Triton-insoluble cAMP-dependent kinase type RIbeta in rat and mouse brain. J. Neurocytol. *30*, 885–894.

Mucignat-Caretta, C., and Caretta, A. (2002). Clustered distribution of cAMP-dependent protein kinase regulatory isoform RI alpha during the development of the rat brain. J. Comp. Neurol. *451*, 324–333.

Mucignat-Caretta, C., and Caretta, A. (2004). Regional variations in the localization of insoluble kinase A regulatory isoforms during rodent brain development. J. Chem. Neuroanat. *27*, 201–212.

Mucignat-Caretta, C., and Caretta, A. (2007). Distribution of insoluble cAMP-dependent kinase type RI and RII in the lizard and turtle central nervous system. Brain Res. *1154*, 84–94.

Mucignat-Caretta, C., and Caretta, A. (2011). Aggregates of cAMP-dependent kinase isoforms characterize different areas in the developing central nervous system of the chicken, Gallus gallus. Dev. Neurosci. *33*, 144–158.

Mucignat-Caretta, C., Bondi', M., and Caretta, A. (2004). Animal models of depression: olfactory lesions affect amygdala, subventricular zone, and aggression. Neurobiol. Dis. *16*, 386–395.

Mucignat-Caretta, C., Cavaggioni, A., Redaelli, M., Malatesta, M., Zancanaro, C., and Caretta, A. (2008). Selective distribution of protein kinase A regulatory subunit RII{alpha} in rodent gliomas. Neuro-Oncology *10*, 958–967.

Mucignat-Caretta, C., Denaro, L., D'Avella, D., and Caretta, A. (2018). Protein Kinase A Distribution Differentiates Human Glioblastoma from Brain Tissue. Cancers (Basel) *10*.

Mucignat-Caretta, C., Denaro, L., Redaelli, M., D'Avella, D., and Caretta, A. (2010). Protein kinase A regulatory subunit distribution in medulloblastoma. BMC Cancer *10*, 141.

Mueller, W., Nutt, C.L., Ehrich, M., Riemenschneider, M.J., von Deimling, A., van den Boom, D., and Louis, D.N. (2007). Downregulation of RUNX3 and TES by hypermethylation in glioblastoma. Oncogene *26*, 583–593.

Müller, F.-J., Snyder, E.Y., and Loring, J.F. (2006). Gene therapy: can neural stem cells deliver? Nat. Rev. Neurosci. *7*, 75–84.

Nakamizo, A., Marini, F., Amano, T., Khan, A., Studeny, M., Gumin, J., Chen, J., Hentschel, S., Vecil, G., Dembinski, J., Andreeff, M., and Lang, F.F. (2005). Human bone marrow-derived mesenchymal stem cells in the treatment of gliomas. Cancer Res. *65*, 3307–3318.

Nan, Y., Guo, L., Song, Y., Wang, L., Yu, K., Huang, Q., and Zhong, Y. (2017). Combinatorial therapy with adenoviral-mediated PTEN and a PI3K inhibitor suppresses malignant glioma cell growth in vitro and in vivo by regulating the PI3K/AKT signaling pathway. J. Cancer Res. Clin. Oncol. *143*, 1477–1487.

Narayana, A., Gruber, D., Kunnakkat, S., Golfinos, J.G., Parker, E., Raza, S., Zagzag, D., Eagan, P., and Gruber, M.L. (2012). A clinical trial of bevacizumab, temozolomide, and radiation for newly diagnosed glioblastoma. J. Neurosurg. *116*, 341–345.

Navis, A.C., Bourgonje, A., Wesseling, P., Wright, A., Hendriks, W., Verrijp, K., van der Laak, J.A.W.M., Heerschap, A., and Leenders, W.P.J. (2013). Effects of dual targeting of tumor cells and stroma in human glioblastoma xenografts with a tyrosine kinase inhibitor against c-MET and VEGFR2. PLoS ONE *8*, e58262.

Neary, C.L., Nesterova, M., Cho, Y.S., Cheadle, C., Becker, K.G., and Cho-Chung, Y.S. (2004). Protein kinase A isozyme switching: eliciting differential cAMP signaling and tumor reversion. Oncogene *23*, 8847–8856.

Netland, I.A., Førde, H.E., Sleire, L., Leiss, L., Rahman, M.A., Skeie, B.S., Miletic, H., Enger, P.Ø., and Goplen, D. (2016). Treatment with the PI3K inhibitor buparlisib (NVP-BKM120) suppresses the growth of established patient-derived GBM xenografts and prolongs survival in nude rats. J. Neurooncol. *129*, 57–66.

Network, T.C.G.A.R. (2013). Corrigendum: Comprehensive genomic characterization defines human glioblastoma genes and core pathways. Nature *494*, 506–506.

Ng, W., Pébay, A., Drummond, K., Burgess, A., Kaye, A.H., and Morokoff, A. (2014). Complexities of lysophospholipid signalling in glioblastoma. J Clin Neurosci *21*, 893–898.

Noble, M., and Dietrich, J. (2002). Intersections between neurobiology and oncology: tumor origin, treatment and repair of treatment-associated damage. Trends Neurosci. *25*, 103–107.

Norden, A.D., Young, G.S., Setayesh, K., Muzikansky, A., Klufas, R., Ross, G.L., Ciampa, A.S., Ebbeling, L.G., Levy, B., Drappatz, J., Kesari, S., and Wen, P.Y. (2008). Bevacizumab for recurrent malignant gliomas: efficacy, toxicity, and patterns of recurrence. Neurology *70*, 779–787.

Obeid, J.-P., Zeidan, Y.H., Zafar, N., and El Hokayem, J. (2017). E6-Associated Protein Dependent Estrogen Receptor Regulation of Protein Kinase A Regulatory Subunit R2A Expression in Neuroblastoma. Mol. Neurobiol.

O'Connor, K.L., and Mercurio, A.M. (2001). Protein kinase A regulates Rac and is required for the growth factor-stimulated migration of carcinoma cells. J. Biol. Chem. *276*, 47895–47900.

O'Connor, K.L., Shaw, L.M., and Mercurio, A.M. (1998). Release of cAMP gating by the alpha6beta4 integrin stimulates lamellae formation and the chemotactic migration of invasive carcinoma cells. J. Cell Biol. *143*, 1749–1760.

Odreman, F., Vindigni, M., Gonzales, M.L., Niccolini, B., Candiano, G., Zanotti, B., Skrap, M., Pizzolitto, S., Stanta, G., and Vindigni, A. (2005). Proteomic studies on low- and high-grade human brain astrocytomas. J. Proteome Res. *4*, 698–708.

Ohgaki, H., Dessen, P., Jourde, B., Horstmann, S., Nishikawa, T., Di Patre, P.-L., Burkhard, C., Schüler, D., Probst-Hensch, N.M., Maiorka, P.C., Baeza, N., Pisani, P., Yonekawa, Y., Yasargil, M.G., Lütolf, U.M., and Kleihues, P. (2004). Genetic pathways to glioblastoma: a population-based study. Cancer Res. *64*, 6892–6899.

Oh-hashi, K., Hirata, Y., Koga, H., and Kiuchi, K. (2006). GRP78-binding protein regulates cAMP-induced glial fibrillary acidic protein expression in rat C6 glioblastoma cells. FEBS Lett. *580*, 3943–3947.

Ohka, F., Natsume, A., and Wakabayashi, T. (2012). Current trends in targeted therapies for glioblastoma multiforme. Neurol Res Int *2012*, 878425.

Okuda, T., Tasaki, T., Nakata, S., Yamashita, K., Yoshioka, H., Izumoto, S., Kato, A., and Fujita, M. (2017). Efficacy of Combination Therapy with MET and VEGF Inhibitors for MET-overexpressing Glioblastoma. Anticancer Res. *37*, 3871–3876.

Olar, A., and Aldape, K.D. (2014). Using the molecular classification of glioblastoma to inform personalized treatment. J. Pathol. *232*, 165–177.

Orellana, S.A., and McKnight, G.S. (1992). Mutations in the catalytic subunit of cAMP-dependent protein kinase result in unregulated biological activity. Proc. Natl. Acad. Sci. U.S.A. *89*, 4726–4730.

Palm, D.C., Rohwer, J.M., and Hofmeyr, J.-H.S. (2013). Regulation of glycogen synthase from mammalian skeletal muscle--a unifying view of allosteric and covalent regulation. FEBS J. *280*, 2–27.

Palmer, E., and Freeman, T. (2004). Investigation into the use of C- and N-terminal GFP fusion proteins for subcellular localization studies using reverse transfection microarrays. Comp Funct Genomics. *5*, 342–352.

Palù, G., Cavaggioni, A., Calvi, P., Franchin, E., Pizzato, M., Boschetto, R., Parolin, C., Chilosi, M., Ferrini, S., Zanusso, A., and Colombo, F. (1999). Gene therapy of glioblastoma multiforme via combined expression of suicide and cytokine genes: a pilot study in humans. Gene Ther. *6*, 330–337.

Pan, E., Supko, J.G., Kaley, T.J., Butowski, N.A., Cloughesy, T., Jung, J., Desideri, S., Grossman, S., Ye, X., and Park, D.M. (2016). Phase I study of RO4929097 with bevacizumab in patients with recurrent malignant glioma. J. Neurooncol. *130*, 571–579.

Papanastasiou, L., Fountoulakis, S., Voulgaris, N., Kounadi, T., Choreftaki, T., Kostopoulou, A., Zografos, G., Lyssikatos, C., Stratakis, C.A., and Piaditis, G. (2016). Identification of a novel mutation of the PRKAR1A gene in a patient with Carney complex with significant osteoporosis and recurrent fractures. Hormones (Athens) *15*, 129–135.

Pardal, R., Clarke, M.F., and Morrison, S.J. (2003). Applying the principles of stem-cell biology to cancer. Nat. Rev. Cancer *3*, 895–902.

Parsons, D.W., Jones, S., Zhang, X., Lin, J.C.-H., Leary, R.J., Angenendt, P., Mankoo, P., Carter, H., Siu, I.-M., Gallia, G.L., Olivi, A., McLendon, R., Rasheed, B.A., Keir, S., Nikolskaya, T., Nikolsky, Y., Busam, D.A., Tekleab, H., Diaz, L.A., Hartigan, J., Smith, D.R., Strausberg, R.L., Marie, S.K.N., Shinjo, S.M.O., Yan, H., Riggins, G.J., Bigner, D.D., Karchin, R., Papadopoulos, N., Parmigiani, G., Vogelstein, B., Velculescu, V.E., and Kinzler, K.W. (2008). An integrated genomic analysis of human glioblastoma multiforme. Science *321*, 1807–1812.

Patel, D.M., Foreman, P.M., Nabors, L.B., Riley, K.O., Gillespie, G.Y., and Markert, J.M. (2016). Design of a Phase I Clinical Trial to Evaluate M032, a Genetically Engineered HSV-1 Expressing IL-12, in Patients with Recurrent/Progressive Glioblastoma Multiforme, Anaplastic Astrocytoma, or Gliosarcoma. Hum Gene Ther Clin Dev *27*, 69–78.

Pattabiraman, D.R., Bierie, B., Kober, K.I., Thiru, P., Krall, J.A., Zill, C., Reinhardt, F., Tam, W.L., and Weinberg, R.A. (2016). Activation of PKA leads to mesenchymal-to-epithelial transition and loss of tumor-initiating ability. Science *351*, aad3680.

Paulucci-Holthauzen, A.A., Vergara, L.A., Bellot, L.J., Canton, D., Scott, J.D., and O'Connor, K.L. (2009). Spatial distribution of protein kinase A activity during cell migration is mediated by A-kinase anchoring protein AKAP Lbc. J. Biol. Chem. *284*, 5956–5967.

Perng, P., and Lim, M. (2015). Immunosuppressive Mechanisms of Malignant Gliomas: Parallels at Non-CNS Sites. Front Oncol *5*, 153.

Pistollato, F., Abbadi, S., Rampazzo, E., Persano, L., Della Puppa, A., Frasson, C., Sarto, E., Scienza, R., D'avella, D., and Basso, G. (2010). Intratumoral hypoxic gradient drives stem cells distribution and MGMT expression in glioblastoma. Stem Cells *28*, 851–862.

Pizzato, M., Franchin, E., Calvi, P., Boschetto, R., Colombo, M., Ferrini, S., and Palù, G. (1998). Production and characterization of a bicistronic Moloney-based retroviral vector expressing human interleukin 2 and herpes simplex virus thymidine kinase for gene therapy of cancer. Gene Ther. *5*, 1003–1007.

Plate, K.H., Scholz, A., and Dumont, D.J. (2012). Tumor angiogenesis and anti-angiogenic therapy in malignant gliomas revisited. Acta Neuropathol. *124*, 763–775.

Polyzoidis, S., Tuazon, J., Brazil, L., Beaney, R., Al-Sarraj, S.T., Doey, L., Logan, J., Hurwitz, V., Jarosz, J., Bhangoo, R., Gullan, R., Mijovic, A., Richardson, M., Farzaneh, F., and Ashkan, K. (2015). Active dendritic cell immunotherapy for glioblastoma: Current status and challenges. Br J Neurosurg *29*, 197–205.

Pommepuy, I., Terro, F., Petit, B., Trimoreau, F., Bellet, V., Robert, S., Hugon, J., Labrousse, F., and Yardin, C. (2003). Brefeldin A induces apoptosis and cell cycle blockade in glioblastoma cell lines. Oncology *64*, 459–467.

Pontén, J. (1975). Neoplastic Human Glia Cells in Culture. In Human Tumor Cells in Vitro, (Springer, Boston, MA), pp. 175–206.

Poulsen, H.S., Urup, T., Michaelsen, S.R., Staberg, M., Villingshøj, M., and Lassen, U. (2014). The impact of bevacizumab treatment on survival and quality of life in newly diagnosed glioblastoma patients. Cancer Manag Res *6*, 373–387.

Premsrirut, P.K., Dow, L.E., Kim, S.Y., Camiolo, M., Malone, C.D., Miething, C., Scuoppo, C., Zuber, J., Dickins, R.A., Kogan, S.C., Shroyer, K.R., Sordella, R., Hannon, G.J., and Lowe, S.W. (2011). A rapid and scalable system for studying gene function in mice using conditional RNA interference. Cell *145*, 145–158.

Prymakowska-Bosak, M., Misteli, T., Herrera, J.E., Shirakawa, H., Birger, Y., Garfield, S., and Bustin, M. (2001). Mitotic phosphorylation prevents the binding of HMGN proteins to chromatin. Mol. Cell. Biol. *21*, 5169–5178.

Puxeddu, E., Uhart, M., Li, C.-C., Ahmad, F., Pacheco-Rodriguez, G., Manganiello, V.C., Moss, J., and Vaughan, M. (2009). Interaction of phosphodiesterase 3A with brefeldin A-inhibited guanine nucleotide-exchange proteins BIG1 and BIG2 and effect on ARF1 activity. Proc. Natl. Acad. Sci. U.S.A. *106*, 6158–6163.

Rahman, M., Deleyrolle, L., Vedam-Mai, V., Azari, H., Abd-El-Barr, M., and Reynolds, B.A. (2011). The cancer stem cell hypothesis: failures and pitfalls. Neurosurgery *68*, 531–545; discussion 545.

Rajesh, Y., Pal, I., Banik, P., Chakraborty, S., Borkar, S.A., Dey, G., Mukherjee, A., and Mandal, M. (2017). Insights into molecular therapy of glioma: current challenges and next generation blueprint. Acta Pharmacol. Sin. *38*, 591–613.

Ramezani, S., Vousooghi, N., Kapourchali, F.R., and Joghataei, M.T. (2017). Perifosine enhances bevacizumab-induced apoptosis and therapeutic efficacy by targeting PI3K/AKT pathway in a glioblastoma heterotopic model. Apoptosis *22*, 1025–1034.

Reardon, D.A., Desjardins, A., Vredenburgh, J.J., Herndon, J.E., Coan, A., Gururangan, S., Peters, K.B., McLendon, R., Sathornsumetee, S., Rich, J.N., Lipp, E.S., Janney, D., and Friedman, H.S. (2012). Phase II study of Gleevec plus hydroxyurea in adults with progressive or recurrent low-grade glioma. Cancer *118*, 4759–4767.

Redaelli, M., Franceschi, V., Capocefalo, A., D'Avella, D., Denaro, L., Cavirani, S., Mucignat-Caretta, C., and Donofrio, G. (2012). Herpes simplex virus type 1 thymidine kinase-armed bovine herpesvirus type 4-based vector displays enhanced oncolytic properties in immunocompetent orthotopic syngenic mouse and rat glioma models. Neuro-Oncology *14*, 288–301.

Reddy, A.B.M., Srivastava, S.K., and Ramana, K.V. (2010). Aldose reductase inhibition prevents lipopolysaccharide-induced glucose uptake and glucose transporter 3 expression in RAW264.7 macrophages. Int. J. Biochem. Cell Biol. *42*, 1039–1045.

Rehmann, H., Schwede, F., Døskeland, S.O., Wittinghofer, A., and Bos, J.L. (2003). Ligand-mediated activation of the cAMP-responsive guanine nucleotide exchange factor Epac. J. Biol. Chem. *278*, 38548–38556.

Reissner, K.J. (2013). Proteomic analyses of PKA and AKAP signaling in cocaine addiction. Neuropsychopharmacology *38*, 251–252.

Rello, S., Stockert, J.C., Moreno, V., Gámez, A., Pacheco, M., Juarranz, A., Cañete, M., and Villanueva, A. (2005). Morphological criteria to distinguish cell death induced by apoptotic and necrotic treatments. Apoptosis *10*, 201–208.

Renthal, W., Kumar, A., Xiao, G., Wilkinson, M., Covington, H.E., Maze, I., Sikder, D., Robison, A.J., LaPlant, Q., Dietz, D.M., Russo, S.J., Vialou, V., Chakravarty, S., Kodadek, T.J., Stack, A., Kabbaj, M., and Nestler, E.J. (2009). Genome-wide analysis of chromatin regulation by cocaine reveals a role for sirtuins. Neuron *62*, 335–348.

Reya, T., Morrison, S.J., Clarke, M.F., and Weissman, I.L. (2001). Stem cells, cancer, and cancer stem cells. Nature *414*, 105–111.

Reynolds, B.A., and Weiss, S. (1992). Generation of neurons and astrocytes from isolated cells of the adult mammalian central nervous system. Science *255*, 1707–1710.

Reynolds, B.A., and Weiss, S. (1996). Clonal and population analyses demonstrate that an EGF-responsive mammalian embryonic CNS precursor is a stem cell. Dev. Biol. *175*, 1–13.

Reynolds, B.A., Tetzlaff, W., and Weiss, S. (1992). A multipotent EGF-responsive striatal embryonic progenitor cell produces neurons and astrocytes. J. Neurosci. *12*, 4565–4574.

Rho, H.M., Poiesz, B., Ruscetti, F.W., and Gallo, R.C. (1981). Characterization of the reverse transcriptase from a new retrovirus (HTLV) produced by a human cutaneous T-cell lymphoma cell line. Virology *112*, 355–360.

Rich, J.N. (2008). The Implications of the Cancer Stem Cell Hypothesis for Neuro-Oncology and Neurology. Future Neurol *3*, 265–273.

Richter, S., Gorny, X., Marco-Pallares, J., Krämer, U.M., Machts, J., Barman, A., Bernstein, H.-G., Schüle, R., Schöls, L., Rodriguez-Fornells, A., Reissner, C., Wüstenberg, T., Heinze, H.-J., Gundelfinger, E.D., Düzel, E., Münte, T.F., Seidenbecher, C.I., and Schott, B.H. (2011). A Potential Role for a Genetic Variation of AKAP5 in Human Aggression and Anger Control. Front Hum Neurosci *5*, 175.

Riggle, K.M., Riehle, K.J., Kenerson, H.L., Turnham, R., Homma, M.K., Kazami, M., Samelson, B., Bauer, R., McKnight, G.S., Scott, J.D., and Yeung, R.S. (2016). Enhanced cAMP-stimulated protein kinase A activity in human fibrolamellar hepatocellular carcinoma. Pediatr. Res. *80*, 110–118.

Rohle, D., Popovici-Muller, J., Palaskas, N., Turcan, S., Grommes, C., Campos, C., Tsoi, J., Clark, O., Oldrini, B., Komisopoulou, E., Kunii, K., Pedraza, A., Schalm, S., Silverman, L., Miller, A., Wang, F., Yang, H., Chen, Y., Kernytsky, A., Rosenblum, M.K., Liu, W., Biller, S.A., Su, S.M., Brennan, C.W., Chan, T.A., Graeber, T.G., Yen, K.E., and Mellinghoff, I.K. (2013). An inhibitor of mutant IDH1 delays growth and promotes differentiation of glioma cells. Science *340*, 626–630.

Ropolo, M., Daga, A., Griffero, F., Foresta, M., Casartelli, G., Zunino, A., Poggi, A., Cappedi, E., Zona, G., Spaziante, R., Corte, G., and Frosina, G. (2009). Comparative analysis of DNA repair in stem and nonstem glioma cell cultures. Molecular Cancer Research : MCR *7*, 383–392.

Roth, P., Silginer, M., Goodman, S.L., Hasenbach, K., Thies, S., Maurer, G., Schraml, P., Tabatabai, G., Moch, H., Tritschler, I., and Weller, M. (2013). Integrin control of the transforming growth factor-β pathway in glioblastoma. Brain *136*, 564–576.

Rubinson, D.A., Dillon, C.P., Kwiatkowski, A.V., Sievers, C., Yang, L., Kopinja, J., Rooney, D.L., Zhang, M., Ihrig, M.M., McManus, M.T., Gertler, F.B., Scott, M.L., and Van Parijs, L. (2003). A lentivirus-based system to functionally silence genes in primary mammalian cells, stem cells and transgenic mice by RNA interference. Nat. Genet. *33*, 401–406.

Sakuma, T., Barry, M.A., and Ikeda, Y. (2012). Lentiviral vectors: basic to translational. Biochem. J. *443*, 603–618.

Samaranayake, H., Määttä, A.-M., Pikkarainen, J., and Ylä-Herttuala, S. (2010). Future prospects and challenges of antiangiogenic cancer gene therapy. Hum. Gene Ther. *21*, 381–396.

Sanai, N., Alvarez-Buylla, A., and Berger, M.S. (2005). Neural stem cells and the origin of gliomas. N. Engl. J. Med. *353*, 811–822.

Sandmair, A.M., Loimas, S., Puranen, P., Immonen, A., Kossila, M., Puranen, M., Hurskainen, H., Tyynelä, K., Turunen, M., Vanninen, R., Lehtolainen, P., Paljärvi, L., Johansson, R., Vapalahti, M., and Ylä-Herttuala, S. (2000). Thymidine kinase gene therapy for human malignant glioma, using replication-deficient retroviruses or adenoviruses. Hum. Gene Ther. *11*, 2197–2205.

Sapio, L., Di Maiolo, F., Illiano, M., Esposito, A., Chiosi, E., Spina, A., and Naviglio, S. (2014). Targeting protein kinase A in cancer therapy: an update. EXCLI J *13*, 843–855.

Sasaki, M., Knobbe, C.B., Itsumi, M., Elia, A.J., Harris, I.S., Chio, I.I.C., Cairns, R.A., McCracken, S., Wakeham, A., Haight, J., Ten, A.Y., Snow, B., Ueda, T., Inoue, S., Yamamoto, K., Ko, M., Rao, A., Yen, K.E., Su, S.M., and Mak, T.W. (2012). D-2-hydroxyglutarate produced by mutant IDH1 perturbs collagen maturation and basement membrane function. Genes Dev. *26*, 2038–2049.

Sasaki, R., Aoki, S., Yamato, M., Uchiyama, H., Wada, K., Ogiuchi, H., Okano, T., and Ando, T. (2010). A protocol for immunofluorescence staining of floating neurospheres. Neurosci. Lett. *479*, 126–127.

Sato, Y., Maekawa, S., Ishii, R., Sanada, M., Morikawa, T., Shiraishi, Y., Yoshida, K., Nagata, Y., Sato-Otsubo, A., Yoshizato, T., Suzuki, H., Shiozawa, Y., Kataoka, K., Kon, A., Aoki, K., Chiba, K., Tanaka, H., Kume, H., Miyano, S., Fukayama, M., Nureki, O., Homma, Y., and Ogawa, S.

(2014). Recurrent somatic mutations underlie corticotropin-independent Cushing's syndrome. Science *344*, 917–920.

Savarin, C., Bergmann, C.C., Hinton, D.R., and Stohlman, S.A. (2013). MMP-independent role of TIMP-1 at the blood brain barrier during viral encephalomyelitis. ASN Neuro *5*, e00127.

Schmidt, M., Dekker, F.J., and Maarsingh, H. (2013). Exchange protein directly activated by cAMP (epac): a multidomain cAMP mediator in the regulation of diverse biological functions. Pharmacol. Rev. *65*, 670–709.

Schonberg, D.L., Lubelski, D., Miller, T.E., and Rich, J.N. (2014). Brain tumor stem cells: Molecular characteristics and their impact on therapy. Mol. Aspects Med. *39*, 82–101.

Seidel, S., Garvalov, B.K., Wirta, V., von Stechow, L., Schänzer, A., Meletis, K., Wolter, M., Sommerlad, D., Henze, A.-T., Nistér, M., Reifenberger, G., Lundeberg, J., Frisén, J., and Acker, T. (2010). A hypoxic niche regulates glioblastoma stem cells through hypoxia inducible factor 2 alpha. Brain *133*, 983–995.

Seok, H., Lee, H., Jang, E.-S., and Chi, S.W. (2017). Evaluation and control of miRNA-like off-target repression for RNA interference. Cell. Mol. Life Sci.

Seymour, T., Nowak, A., and Kakulas, F. (2015). Targeting Aggressive Cancer Stem Cells in Glioblastoma. Front Oncol *5*, 159.

Sgubin, D., Wakimoto, H., Kanai, R., Rabkin, S.D., and Martuza, R.L. (2012). Oncolytic herpes simplex virus counteracts the hypoxia-induced modulation of glioblastoma stem-like cells. Stem Cells Transl Med *1*, 322–332.

Shackleton, M., Quintana, E., Fearon, E.R., and Morrison, S.J. (2009). Heterogeneity in cancer: cancer stem cells versus clonal evolution. Cell *138*, 822–829.

Shah, K. (2012). Mesenchymal stem cells engineered for cancer therapy. Adv. Drug Deliv. Rev. *64*, 739–748.

Shaikh, D., Zhou, Q., Chen, T., Ibe, J.C.F., Raj, J.U., and Zhou, G. (2012). cAMP-dependent protein kinase is essential for hypoxia-mediated epithelial-mesenchymal transition, migration, and invasion in lung cancer cells. Cell. Signal. *24*, 2396–2406.

Shir, A., and Levitzki, A. (2002). Inhibition of glioma growth by tumor-specific activation of double-stranded RNA-dependent protein kinase PKR. Nat. Biotechnol. *20*, 895–900.

Sioud, M. (2005). Induction of inflammatory cytokines and interferon responses by double-stranded and single-stranded siRNAs is sequence-dependent and requires endosomal localization. J. Mol. Biol. *348*, 1079–1090.

Sjoberg, T.J., Kornev, A.P., and Taylor, S.S. (2010). Dissecting the cAMP-inducible allosteric switch in protein kinase A RIalpha. Protein Sci. *19*, 1213–1221.

Smith, F.D., Langeberg, L.K., Cellurale, C., Pawson, T., Morrison, D.K., Davis, R.J., and Scott, J.D. (2010). AKAP-Lbc enhances cyclic AMP control of the ERK1/2 cascade. Nat. Cell Biol. *12*, 1242–1249.

Smith, F.D., Reichow, S.L., Esseltine, J.L., Shi, D., Langeberg, L.K., Scott, J.D., and Gonen, T. (2013). Intrinsic disorder within an AKAP-protein kinase A complex guides local substrate phosphorylation. Elife *2*, e01319.

Smith, F.D., Esseltine, J.L., Nygren, P.J., Veesler, D., Byrne, D.P., Vonderach, M., Strashnov, I., Eyers, C.E., Eyers, P.A., Langeberg, L.K., and Scott, J.D. (2017). Local protein kinase A action proceeds through intact holoenzymes. Science *356*, 1288–1293.

Snapp, E. (2005). Design and use of fluorescent fusion proteins in cell biology. Curr Protoc Cell Biol *Chapter 21*, Unit 21.4.

Søberg, K., Moen, L.V., Skålhegg, B.S., and Laerdahl, J.K. (2017). Evolution of the cAMP-dependent protein kinase (PKA) catalytic subunit isoforms. PLoS ONE *12*, e0181091.

Sørensen, M.D., Fosmark, S., Hellwege, S., Beier, D., Kristensen, B.W., and Beier, C.P. (2015). Chemoresistance and chemotherapy targeting stem-like cells in malignant glioma. Adv. Exp. Med. Biol. *853*, 111–138.

Stieber, V.W., and Mehta, M.P. (2007). Advances in radiation therapy for brain tumors. Neurol Clin *25*, 1005–1033, ix.

Stupp, R., Hegi, M.E., Mason, W.P., van den Bent, M.J., Taphoorn, M.J.B., Janzer, R.C., Ludwin, S.K., Allgeier, A., Fisher, B., Belanger, K., Hau, P., Brandes, A.A., Gijtenbeek, J., Marosi, C., Vecht, C.J., Mokhtari, K., Wesseling, P., Villa, S., Eisenhauer, E., Gorlia, T., Weller, M., Lacombe, D., Cairncross, J.G., Mirimanoff, R.-O., European Organisation for Research and Treatment of Cancer Brain Tumour and Radiation Oncology Groups, and National Cancer Institute of Canada Clinical Trials Group (2009). Effects of radiotherapy with concomitant and adjuvant temozolomide versus radiotherapy alone on survival in glioblastoma in a randomised phase III study: 5-year analysis of the EORTC-NCIC trial. Lancet Oncol. *10*, 459–466.

Stupp, R., Hegi, M.E., Neyns, B., Goldbrunner, R., Schlegel, U., Clement, P.M.J., Grabenbauer, G.G., Ochsenbein, A.F., Simon, M., Dietrich, P.-Y., Pietsch, T., Hicking, C., Tonn, J.-C., Diserens, A.-C., Pica, A., Hermisson, M., Krueger, S., Picard, M., and Weller, M. (2010). Phase I/IIa study of cilengitide and temozolomide with concomitant radiotherapy followed by cilengitide and temozolomide maintenance therapy in patients with newly diagnosed glioblastoma. J. Clin. Oncol. *28*, 2712–2718.

Stupp, R., Wong, E.T., Kanner, A.A., Steinberg, D., Engelhard, H., Heidecke, V., Kirson, E.D., Taillibert, S., Liebermann, F., Dbalý, V., Ram, Z., Villano, J.L., Rainov, N., Weinberg, U., Schiff, D., Kunschner, L., Raizer, J., Honnorat, J., Sloan, A., Malkin, M., Landolfi, J.C., Payer, F., Mehdorn, M., Weil, R.J., Pannullo, S.C., Westphal, M., Smrcka, M., Chin, L., Kostron, H., Hofer, S., Bruce, J., Cosgrove, R., Paleologous, N., Palti, Y., and Gutin, P.H. (2012). NovoTTF-100A versus physician's choice chemotherapy in recurrent glioblastoma: a randomised phase III trial of a novel treatment modality. Eur. J. Cancer *48*, 2192–2202.

Stupp, R., Taillibert, S., Kanner, A.A., Kesari, S., Steinberg, D.M., Toms, S.A., Taylor, L.P., Lieberman, F., Silvani, A., Fink, K.L., Barnett, G.H., Zhu, J.-J., Henson, J.W., Engelhard, H.H., Chen, T.C., Tran, D.D., Sroubek, J., Tran, N.D., Hottinger, A.F., Landolfi, J., Desai, R., Caroli, M.,

Kew, Y., Honnorat, J., Idbaih, A., Kirson, E.D., Weinberg, U., Palti, Y., Hegi, M.E., and Ram, Z. (2015). Maintenance Therapy With Tumor-Treating Fields Plus Temozolomide vs Temozolomide Alone for Glioblastoma: A Randomized Clinical Trial. JAMA *314*, 2535–2543.

Stupp, R., Idbaih, A., Steinberg, D.M., Read, W., Toms, S., Barnett, G., Nicholas, G., Kim, C.-Y., Fink, K., Salmaggi, A., Lieberman, F., Zhu, J., Taylor, L., Stragliotto, G., Hottinger, A., Kirson, E.D., Weinberg, U., Palti, Y., Hegi, M.E., and Ram, Z. (2016). LTBK-01: PROSPECTIVE, MULTI-CENTER PHASE III TRIAL OF TUMOR TREATING FIELDS TOGETHER WITH TEMOZOLOMIDE COMPARED TO TEMOZOLOMIDE ALONE IN PATIENTS WITH NEWLY DIAGNOSED GLIOBLASTOMA. Neuro-Oncology *18*, i1–i1.

Sugimoto, N., Miwa, S., Tsuchiya, H., Hitomi, Y., Nakamura, H., Yachie, A., and Koizumi, S. (2013). Targeted activation of PKA and Epac promotes glioblastoma regression in vitro. Mol Clin Oncol *1*, 281–285.

Takahashi, M., Dillon, T.J., Liu, C., Kariya, Y., Wang, Z., and Stork, P.J.S. (2013). Protein kinase A-dependent phosphorylation of Rap1 regulates its membrane localization and cell migration. J. Biol. Chem. *288*, 27712–27723.

Tan, Y., Demeter, M.R., Ruan, H., and Comb, M.J. (2000). BAD Ser-155 phosphorylation regulates BAD/Bcl-XL interaction and cell survival. J. Biol. Chem. *275*, 25865–25869.

Tang, J.-H., Ma, Z.-X., Huang, G.-H., Xu, Q.-F., Xiang, Y., Li, N., Sidlauskas, K., Zhang, E.E., and Lv, S.-Q. (2016). Downregulation of HIF-1a sensitizes U251 glioma cells to the temozolomide (TMZ) treatment. Exp. Cell Res. *343*, 148–158.

Taskén, K., Skålhegg, B.S., Taskén, K.A., Solberg, R., Knutsen, H.K., Levy, F.O., Sandberg, M., Orstavik, S., Larsen, T., Johansen, A.K., Vang, T., Schrader, H.P., Reinton, N.T., Torgersen, K.M., Hansson, V., and Jahnsen, T. (1997). Structure, function, and regulation of human cAMP-dependent protein kinases. Adv. Second Messenger Phosphoprotein Res. *31*, 191–204.

Taylor, D.D., and Gercel-Taylor, C. (2011). Exosomes/microvesicles: mediators of cancer-associated immunosuppressive microenvironments. Semin Immunopathol *33*, 441–454.

Taylor, S.S., Ilouz, R., Zhang, P., and Kornev, A.P. (2012). Assembly of allosteric macromolecular switches: lessons from PKA. Nat. Rev. Mol. Cell Biol. *13*, 646–658.

Taylor, S.S., Zhang, P., Steichen, J.M., Keshwani, M.M., and Kornev, A.P. (2013). PKA: lessons learned after twenty years. Biochim. Biophys. Acta *1834*, 1271–1278.

Tempé, D., Casas, M., Karaz, S., Blanchet-Tournier, M.-F., and Concordet, J.-P. (2006). Multisite protein kinase A and glycogen synthase kinase 3beta phosphorylation leads to Gli3 ubiquitination by SCFbetaTrCP. Mol. Cell. Biol. *26*, 4316–4326.

Tivnan, A., Heilinger, T., Lavelle, E.C., and Prehn, J.H.M. (2017). Advances in immunotherapy for the treatment of glioblastoma. J Neurooncol *131*, 1–9.

Tröger, J., Moutty, M.C., Skroblin, P., and Klussmann, E. (2012). A-kinase anchoring proteins as potential drug targets. Br. J. Pharmacol. *166*, 420–433.

Tseng, I.-C., Huang, W.-J., Jhuang, Y.-L., Chang, Y.-Y., Hsu, H.-P., and Jeng, Y.-M. (2017). Microinsertions in PRKACA cause activation of the protein kinase A pathway in cardiac myxoma. J. Pathol. *242*, 134–139.

Tsujii, M., Kondo, J., Jin, Y., Nishida, T., Hayashi, Y., Ishii, S., Hayashi, Y., Yoshio, T., Egawa, S., Shinzaki, S., Inoue, T., Nakajima, S., Watabe, K., Iijima, H., Tsutsui, S., and Hayashi, N. (2009). S1945 Novel PKA-Targeting Therapy Based On Cancer Stem Cell Biology. Gastroenterology *136*, A-298.

Valenta, T., Hausmann, G., and Basler, K. (2012). The many faces and functions of β-catenin. EMBO J. *31*, 2714–2736.

Van Meir, E.G., Hadjipanayis, C.G., Norden, A.D., Shu, H.-K., Wen, P.Y., and Olson, J.J. (2010). Exciting new advances in neuro-oncology: the avenue to a cure for malignant glioma. CA Cancer J Clin *60*, 166–193.

Wakimoto, H., Kesari, S., Farrell, C.J., Curry, W.T., Zaupa, C., Aghi, M., Kuroda, T., Stemmer-Rachamimov, A., Shah, K., Liu, T.-C., Jeyaretna, D.S., Debasitis, J., Pruszak, J., Martuza, R.L., and

Rabkin, S.D. (2009). Human glioblastoma-derived cancer stem cells: establishment of invasive glioma models and treatment with oncolytic herpes simplex virus vectors. Cancer Res. *69*, 3472–3481.

Wallner, K.E., Galicich, J.H., Krol, G., Arbit, E., and Malkin, M.G. (1989). Patterns of failure following treatment for glioblastoma multiforme and anaplastic astrocytoma. Int. J. Radiat. Oncol. Biol. Phys. *16*, 1405–1409.

Walsh, D.A., Perkins, J.P., and Krebs, E.G. (1968). An adenosine 3',5'-monophosphate-dependant protein kinase from rabbit skeletal muscle. J. Biol. Chem. *243*, 3763–3765.

Wang, P., Ye, J.-A., Hou, C.-X., Zhou, D., and Zhan, S.-Q. (2016). Combination of lentivirus-mediated silencing of PPM1D and temozolomide chemotherapy eradicates malignant glioma through cell apoptosis and cell cycle arrest. Oncol. Rep. *36*, 2544–2552.

Wang, W., Liu, F., Xiang, B., Xiang, C., and Mou, X. (2015). Stem cells as cellular vehicles for gene therapy against glioblastoma. Int J Clin Exp Med *8*, 17102–17109.

Wang, Y., Wang, X., Zhang, J., Sun, G., Luo, H., Kang, C., Pu, P., Jiang, T., Liu, N., and You, Y. (2012). MicroRNAs involved in the EGFR/PTEN/AKT pathway in gliomas. J. Neurooncol. *106*, 217–224.

Weigand, I., Ronchi, C.L., Rizk-Rabin, M., Dalmazi, G.D., Wild, V., Bathon, K., Rubin, B., Calebiro, D., Beuschlein, F., Bertherat, J., Fassnacht, M., and Sbiera, S. (2017). Differential expression of the protein kinase A subunits in normal adrenal glands and adrenocortical adenomas. Sci Rep *7*, 49.

Weiswald, L.-B., Guinebretière, J.-M., Richon, S., Bellet, D., Saubaméa, B., and Dangles-Marie, V. (2010). In situ protein expression in tumour spheres: development of an immunostaining protocol for confocal microscopy. BMC Cancer *10*, 106.

Weller, M., van den Bent, M., Tonn, J.C., Stupp, R., Preusser, M., Cohen-Jonathan-Moyal, E., Henriksson, R., Le Rhun, E., Balana, C., Chinot, O., Bendszus, M., Reijneveld, J.C., Dhermain, F., French, P., Marosi, C., Watts, C., Oberg, I., Pilkington, G., Baumert, B.G., Taphoorn, M.J.B., Hegi, M., Westphal, M., Reifenberger, G., Soffietti, R., Wick, W., and European Association for Neuro-

Oncology (EANO) Task Force on Gliomas (2017). European Association for Neuro-Oncology (EANO) guideline on the diagnosis and treatment of adult astrocytic and oligodendroglial gliomas. Lancet Oncol. *18*, e315–e329.

Westphal, M., Ylä-Herttuala, S., Martin, J., Warnke, P., Menei, P., Eckland, D., Kinley, J., Kay, R., Ram, Z., and ASPECT Study Group (2013). Adenovirus-mediated gene therapy with sitimagene ceradenovec followed by intravenous ganciclovir for patients with operable high-grade glioma (ASPECT): a randomised, open-label, phase 3 trial. Lancet Oncol. *14*, 823–833.

Wick, W. (2016). TTFields: where does all the skepticism come from? Neuro Oncol *18*, 303–305.

Wong, T.H., Chiu, W.Z., Breedveld, G.J., Li, K.W., Verkerk, A.J.M.H., Hondius, D., Hukema, R.K., Seelaar, H., Frick, P., Severijnen, L.-A., Lammers, G.-J., Lebbink, J.H.G., van Duinen, S.G., Kamphorst, W., Rozemuller, A.J., Netherlands Brain Bank, Bakker, E.B., International Parkinsonism Genetics Network, Neumann, M., Willemsen, R., Bonifati, V., Smit, A.B., and van Swieten, J. (2014). PRKAR1B mutation associated with a new neurodegenerative disorder with unique pathology. Brain *137*, 1361–1373.

Workman, P., Clarke, P.A., Raynaud, F.I., and van Montfort, R.L.M. (2010). Drugging the PI3 kinome: from chemical tools to drugs in the clinic. Cancer Res. *70*, 2146–2157.

Wu, J., Dent, P., Jelinek, T., Wolfman, A., Weber, M.J., and Sturgill, T.W. (1993). Inhibition of the EGF-activated MAP kinase signaling pathway by adenosine 3',5'-monophosphate. Science *262*, 1065–1069.

Xu, P., Zhang, A., Jiang, R., Qiu, M., Kang, C., Jia, Z., Wang, G., Han, L., Fan, X., and Pu, P. (2013). The different role of Notch1 and Notch2 in astrocytic gliomas. PLoS ONE *8*, e53654.

Xu, R., Shimizu, F., Hovinga, K., Beal, K., Karimi, S., Droms, L., Peck, K.K., Gutin, P., Iorgulescu, J.B., Kaley, T., DeAngelis, L., Pentsova, E., Nolan, C., Grommes, C., Chan, T., Bobrow, D., Hormigo, A., Cross, J.R., Wu, N., Takebe, N., Panageas, K., Ivy, P., Supko, J.G., Tabar, V., and Omuro, A. (2016). Molecular and Clinical Effects of Notch Inhibition in Glioma Patients: A Phase 0/I Trial. Clin. Cancer Res. *22*, 4786–4796.

Yahyanejad, S., King, H., Iglesias, V.S., Granton, P.V., Barbeau, L.M.O., van Hoof, S.J., Groot, A.J., Habets, R., Prickaerts, J., Chalmers, A.J., Eekers, D.B.P., Theys, J., Short, S.C., Verhaegen, F., and Vooijs, M. (2016). NOTCH blockade combined with radiation therapy and temozolomide prolongs survival of orthotopic glioblastoma. Oncotarget *7*, 41251–41264.

Yang, H., Lee, C.J., Zhang, L., Sans, M.D., and Simeone, D.M. (2008). Regulation of transforming growth factor beta-induced responses by protein kinase A in pancreatic acinar cells. Am. J. Physiol. Gastrointest. Liver Physiol. *295*, G170–G178.

Yang, X., Boehm, J.S., Yang, X., Salehi-Ashtiani, K., Hao, T., Shen, Y., Lubonja, R., Thomas, S.R., Alkan, O., Bhimdi, T., Green, T.M., Johannessen, C.M., Silver, S.J., Nguyen, C., Murray, R.R., Hieronymus, H., Balcha, D., Fan, C., Lin, C., Ghamsari, L., Vidal, M., Hahn, W.C., Hill, D.E., and Root, D.E. (2011). A public genome-scale lentiviral expression library of human ORFs. Nat. Methods *8*, 659–661.

Yu, J.-B., Jiang, H., and Zhan, R.-Y. (2016). Aberrant Notch signaling in glioblastoma stem cells contributes to tumor recurrence and invasion. Mol Med Rep *14*, 1263–1268.

Yu, S., Cheng, Q., Li, L., Liu, M., Yang, Y., and Ding, F. (2014). 2-(4-Methoxyphenyl)ethyl-2-acetamido-2-deoxy-β-d-pyranoside confers neuroprotection in cell and animal models of ischemic stroke through calpain1/PKA/CREB-mediated induction of neuronal glucose transporter 3. Toxicol. Appl. Pharmacol. *277*, 259–269.

Zagzag, D., Friedlander, D.R., Margolis, B., Grumet, M., Semenza, G.L., Zhong, H., Simons, J.W., Holash, J., Wiegand, S.J., and Yancopoulos, G.D. (2000). Molecular events implicated in brain tumor angiogenesis and invasion. Pediatr Neurosurg *33*, 49–55.

Zeppernick, F., Ahmadi, R., Campos, B., Dictus, C., Helmke, B.M., Becker, N., Lichter, P., Unterberg, A., Radlwimmer, B., and Herold-Mende, C.C. (2008). Stem cell marker CD133 affects clinical outcome in glioma patients. Clin. Cancer Res. *14*, 123–129.

Zhang, L., Duan, C.J., Binkley, C., Li, G., Uhler, M.D., Logsdon, C.D., and Simeone, D.M. (2004). A transforming growth factor beta-induced Smad3/Smad4 complex directly activates protein kinase A. Mol. Cell. Biol. *24*, 2169–2180.

Zheng, X., Ou, Y., Shu, M., Wang, Y., Zhou, Y., Su, X., Zhu, W., Yin, W., Li, S., Qiu, P., Yan, G., Zhang, J., Hu, J., and Xu, D. (2014). Cholera toxin, a typical protein kinase A activator, induces G1 phase growth arrest in human bladder transitional cell carcinoma cells via inhibiting the c-Raf/MEK/ERK signaling pathway. Mol Med Rep *9*, 1773–1779.

Zhong, H., SuYang, H., Erdjument-Bromage, H., Tempst, P., and Ghosh, S. (1997). The transcriptional activity of NF-kappaB is regulated by the IkappaB-associated PKAc subunit through a cyclic AMP-independent mechanism. Cell *89*, 413–424.

Zhou, Y., Wu, S., Liang, C., Lin, Y., Zou, Y., Li, K., Lu, B., Shu, M., Huang, Y., Zhu, W., Kang, Z., Xu, D., Hu, J., and Yan, G. (2015). Transcriptional upregulation of microtubule-associated protein 2 is involved in the protein kinase A-induced decrease in the invasiveness of glioma cells. Neuro-Oncology *17*, 1578–1588.

Ziegler, U., and Groscurth, P. (2004). Morphological features of cell death. News Physiol. Sci. *19*, 124–128.

Zorzan M. (2012). Interferenza con la via della PKA nei gliomi umani mediante molecole attivanti ed inibenti ed un approccio di silenziamento genico. Thesis in Biotecnologie Sanitarie, University of Padova.

Zorzan M. (2014). Functional effects of PKA modulation in glioma cells: a multi-focus approach. Master thesis in Medical Biotechnologies, University of Padova.

Zorzan, M., Redaelli, M., Caretta, A., and Mucignat-Caretta, C. (2013). Molecular interference with cAMP-dependent Protein Kinase activity in human glioma cells. P01.44. XV National Congress of the Italian Society of Neuroscience, 2013, Rome, Italy.

Zorzan, M., Redaelli, M., Mucignat, C., and Caretta, A. (2014). Protein kinase A silencing in human glioma: role of regulatory subunit RIIalpha. C092-113. IX Forum of the European Neuroscience Societies, 2014, Milan, Italy.

Zorzan, M., Giordan, E., Redaelli, M., Caretta, A., and Mucignat-Caretta, C. (2015). Molecular targets in glioblastoma. Future Oncol *11*, 1407–1420.

Zuker, M. (2003). Mfold web server for nucleic acid folding and hybridization prediction. Nucleic Acids Res. *31*, 3406–3415.

Zynda, E.R., Matveev, V., Makhanov, M., Chenchik, A., and Kandel, E.S. (2014). Protein kinase A type II-α regulatory subunit regulates the response of prostate cancer cells to taxane treatment. Cell Cycle *13*, 3292–3301.

Web sites (accessed on August-October 2017):

www.braintumourresearch.org - report-on-national-research-funding-2016

www. clinicaltrials.gov

http://unafold.rna.albany.edu/?q=mfold

https://www.genscript.com/ssl-bin/app/scramble

http://projects.insilico.us/SpliceCenter/siRNACheck.jsp

https://blast.ncbi.nlm.nih.gov/Blast.cgi?PROGRAM=blastn&PAGE_TYPE=BlastSearch&LINK_LOC=blasthome

Appendix A1

A1.1 PKA R2A subunit in human glioblastoma

Summary of previous data from the Laboratory of Neurophysiology, Department of Molecular Medicine, University of Padova, on PKA R2A subunit in human GBM are reported in Figure S1.

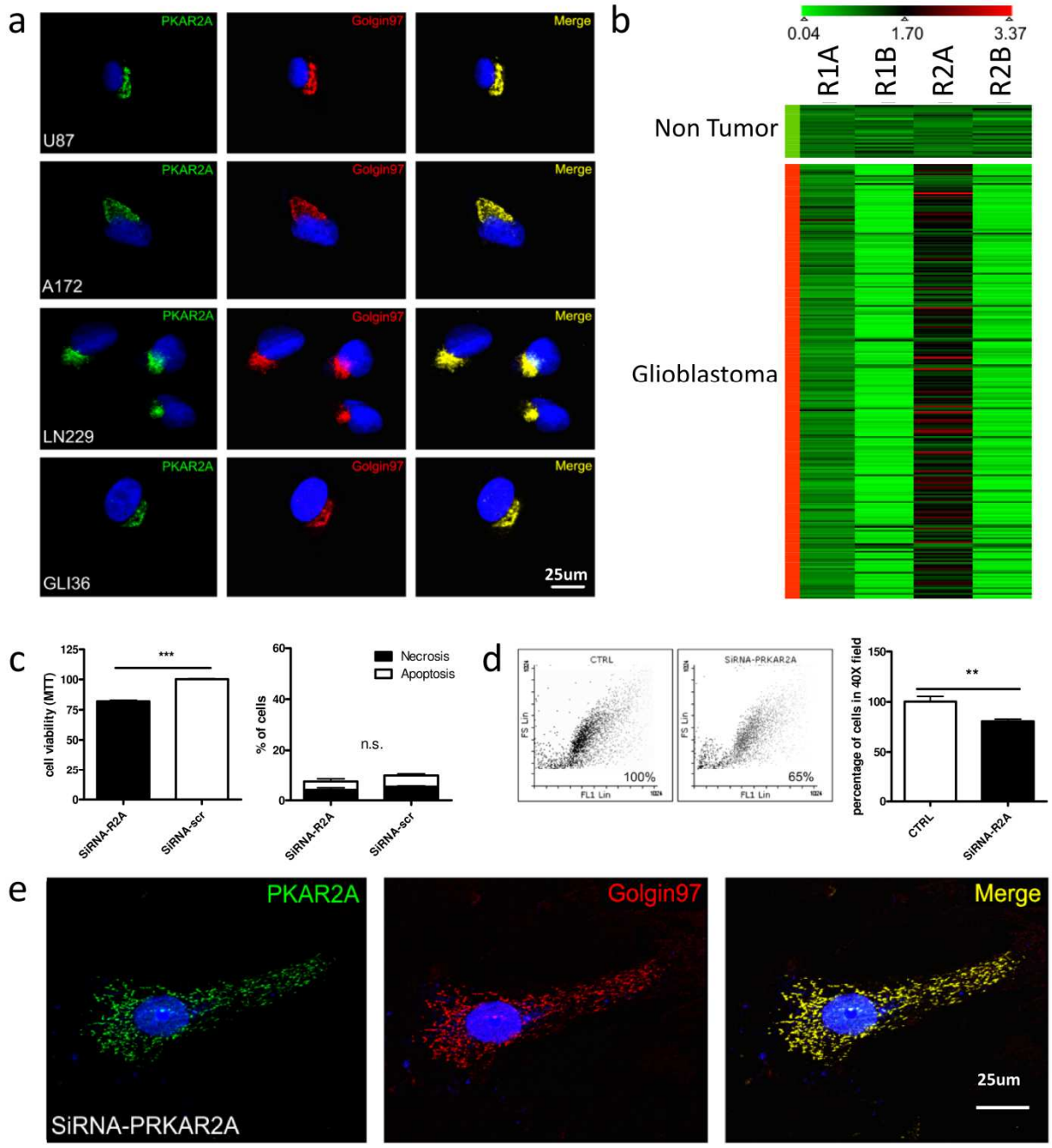

Figure S1 - Summary of previous data on PKA R2A subunit in human GBM (Zorzan et al. 2014; Zorzan 2014). **a.** Immunofluorescence on U87, A172, LN229 and GLI36 human GBM cells. Green: PKA R2A; red: Golgin97; blue: DRAQ5 nuclear staining. Confocal 63x, bar 25 µm. **b.** Heatmap of

PKA subunits expression according to REMBRANDT database. GB: glioblastoma; NT: non-tumor brain tissue. **c.** Citotoxicity assays on U87 cells transfected with siRNA-PRKAR2A. Left: MTT assay revealed a decrease in cell viability of siRNA-PRKAR2A-transfected cells. Right: morphological analysis did not reveal an increase in cell death of siRNA-PRKAR2A-transfected cells. t-test, *p<0.05, **p<0.01, ***p<0.001. scr: scrambled sequence. **d.** Left: cytofluorimetric cell counting detected a lower cell number in the siRNA-PRKAR2A-transfected cell population compared to untransfected cell culture after 72 hours. Right: manual counting of Wright-stained cells revealed a significant decrease in cell number in the siRNA-PRKAR2A-transfected cells compared to untransfected cells. t-test, *p<0.05, **p<0.01, ***p<0.001. **e.** Immunofluorescence on U87 cells transfected with siRNA-PRKAR2A. Green: PKA R2A; red: Golgin97; blue: DRAQ5 nuclear staining. Confocal 63x, bar 25 μm.

A1.2 Previously generated PKA overexpression plasmids

Recombinant pLX303 plasmids for overexpression of PKA subunits (pLX303-PRKACG, pLX303-PRKACA, pLX303-PRKAR2A, pLX303-PRKAR2B) were generated through clonase LR-mediated recombination of the empty backbone pLX303 (Addgene, cat. n° 25897) with entry plasmids containing PKA subunit coding sequences. For PKA R2B, pDONR223-PRKAR2B (Addgene, cat. n° 23667) was used as entry vector. For PKA R2A and PKA CG, DNA sequences coding for PKA subunits were PCR amplified from pWLZ-Neo-Myr-Flag-PRKAR2A (Addgene, cat. n° 20601) and HeLa cDNA respectively, and subsequently cloned in the pENTR-3C entry vector. After Sanger sequencing verification, pENTR-3C-PRKAR2A and pENTR-3C-PRKACG plasmids were used as entry vectors for recombination with pLX303. Cloning details are reported in Zorzan 2014. For PKA CA overexpression plasmid, cDNA coding for CA subunit was PCR amplified from HeLa cDNA and cloned in pENTR-3C plasmid for following recombination with pLX303 vector.

Ringraziamenti

Ringrazio il mio tutor la Prof.ssa Carla Mucignat, la Prof.ssa Arianna Calistri e la Dott.ssa Claudia Del Vecchio per avermi seguito nel corso del mio dottorato: consigli, suggerimenti, critiche, osservazioni e confronti sono stati per me importanti stimoli per approfondire e migliorare continuamente il lavoro svolto in questi anni.

Ringrazio il Dott. Marco Redaelli, che con grande passione ed entusiasmo mi ha fatto scoprire e apprezzare per la prima volta il mondo della ricerca.

Ringrazio di cuore tutta la mia famiglia: mamma, papà, Néné e in modo particolare il mio compagno di vita. Grazie infinite per i vostri indispensabili consigli, per aver sopportato tutte le mie ansie e preoccupazioni, per avermi ascoltato e supportato in ogni momento. Senza di voi e senza il vostro aiuto non sarei riuscita ad arrivare alla fine di questo percorso.

Ringrazio gli studenti e le studentesse che ho avuto l'opportunità di seguire nel corso del loro internato di tesi: aiutarvi e insegnarvi è stata per me una delle più grandi soddisfazioni del mio dottorato. Tra loro, dedico un ringraziamento particolare a Maria Chiara e Mariarita per il rapporto di amicizia che abbiamo insaturato nei mesi di lavoro insieme.

Ringrazio infine Adriana, Mattia, Lorena, Elisa, Valentina e tutti i colleghi della sede di Microbiologia del Dipartimento di Medicina Molecolare che in vari momenti e occasioni mi hanno dato una mano.